IN VIVO AND IN VITRO METHODS TO DETERMINE BILIARY CLEARANCE OF DRUGS IN HUMANS

by
Giulia Ghibellini

A dissertation submitted to the faculty of the University of North Carolina at Chapel Hill in partial fulfillment of the requirements for the degree of Doctor of Philosophy in the School of Pharmacy

Chapel Hill
2006

Approved by:

Advisor: Kim L.R. Brouwer, Pharm.D., Ph.D.

Reader: William D. Heizer, M.D.

Reader: Richard J. Kowalsky, Pharm.D.

Reader: Gary M. Pollack, Ph.D.

Reader: Joseph W. Polli, Ph.D.

ABSTRACT

Giulia Ghibellini

IN VIVO AND IN VITRO METHODS TO DETERMINE BILIARY CLEARANCE OF DRUGS IN HUMANS

(Under the direction of Kim L.R. Brouwer, Pharm.D., Ph.D.)

Biliary excretion is an important route of hepatic elimination of drugs and metabolites that is investigated commonly using *in vitro* or *in vivo* animal models. However, changes in biliary clearance due to drug-drug interactions, genetic polymorphisms and/or disease state may be species-specific, and animal data may be difficult to extrapolate to humans. This dissertation research focused on the development and refinement of a specialized clinical protocol and novel oroenteric tube to accurately quantify biliary clearance of drugs in humans and the comparison of these values with predicted biliary clearance values determined in sandwich-cultured human hepatocytes. Hepatocytes cultured between two layers of extracellular matrix express and correctly localize functional transport proteins on the canalicular as well as the basolateral domains, and enable determination of drug excretion into bile by quantifying accumulation within the hepatocyte and bile canalicular networks. Experiments were devised and performed to establish the utility of this model to predict hepatobiliary drug disposition in humans. The biliary clearance of three model probes, Tc-99m mebrofenin, Tc-99m sestamibi, and piperacillin, was evaluated in healthy humans. These model compounds exhibited high, intermediate and low biliary clearance, respectively. Pharmacokinetic

modeling and simulations of the disposition of Tc-99m mebrofenin in humans, combined with results of *in vitro* systems transfected with hepatic transport proteins, revealed that disease states and drug interactions would impact the hepatobiliary disposition of this probe. Moreover, the recovery of piperacillin metabolites in bile samples obtained during the clinical studies suggested that the clinical methodology developed is useful for the identification of metabolites unique to the human species. Finally, the biliary clearance values obtained *in vivo* were compared to those calculated using sandwich-cultured human hepatocytes. The *in vitro* system proved to be a reliable model for predicting biliary clearance of xenobiotics in humans.

Collectively, the results of this research provide new tools, both *in vivo* and *in vitro*, to study and characterize biliary clearance of drugs in the most relevant species, humans.

ACKNOWLEDGEMENTS

I want to thank Dr. Kim Brouwer for the opportunity to work on this exciting project and for guiding my personal and scientific development.

I also want to thank all the members of my doctoral committee who have been instrumental in the progression of this project: Dr. William H. Heizer for his help and suggestions in the execution and design of the clinical studies, Dr. Dick J. Kowalsky who patiently taught me the principles of nuclear medicine, Dr. Gary M. Pollack who has been a wonderful chair of this committee and helped me with the mathematical modeling and Dr. Joe Polli who found time for me in his busy schedule and inspired me for my future career.

I am very grateful to the support of my family: my parents Mario and Daniela and my brothers Luca and Michele who always believed in me and even from such a distance showed unconditional love and support. Lastly and even more importantly to my husband Matthew who supported and helped me in the day to day quest for my PhD and made my life so fulfilling and wonderful.

TABLE OF CONTENTS

LIST OF TABLES

LIST OF FIGURES

LIST OF ABBREVIATIONS

ABC	ATP-binding cassette
ASBT	apical sodium-dependent bile salt transporter
AUC	area under the curve
BCA	bicinchoninic acid
BCRP	breast cancer resistance protein
BEI	biliary excretion index
BSEP	bile salt export pump
CCK	cholecystokinin
CDF	5-carboxy-2’-7’-dichloro fluorescein
CysA	cyclosporine A
DEP	desethyl piperacillin
DEX	dexamethasone
DMEM	Dulbecco’s modified Eagle’s medium
DPEG	desethyl piperacillin glucuronide
DTT	dithriothretol
EF	ejection fraction
ERCP	endoscopic retrograde cholangiopancreatography
FBS	fetal bovine serum
HBSS	Hank’s balanced salts solution
HEK	human embryonic kidney cells
IBAT	ileal bile salt transporter
IPL	isolated perfused liver

IS	internal standard
ITLS-SA	instant thin layer chromatography-polysilicic acid
LDH	Lactate dehydrogenase
MANOVA	multivariate analysis of variance
MDCK	Madin-Darby canine kidney epithelial cells
MEB	Tc-99m mebrofenin
MIBI	Tc-99m sestamibi
MRP	multidrug resistance-associated protein
NEAA	non essential amino acids
OATP	organic anion transport polypeptide
OST	ileocyte basolateral organic solute transporter
PB	phenobarbital
P-gp	P-glycoprotein
PIP	piperacillin
PVDF	polyvinylidene fluoride
PXR	pregnane X receptor
SCHH	sandwich-cultured human hepatocytes
SCRH	sandwich-cultured rat hepatocytes
SDS	sodium dodecyl sulfate
SLC	solute carrier protein
SLCO	solute carrier protein
TFA	trifluoroacetic acid
TJ	tight junction

TLC	thin layer chromatography
t-SIE	transformed spectral index
TR^-	transport deficient
WT	wild type

CHAPTER 1

INTRODUCTION

A portion of this Chapter is in press in *Molecular Pharmaceutics* Volume 3, Issue 3, 2006.

ABSTRACT:

Determining the biliary clearance of drugs in humans is very challenging because bile in not readily accessible due to the anatomy of the hepatobiliary tract. The collection of bile usually is limited to post-surgical patients with underlying hepatobiliary disease. In healthy subjects, feces typically are used as a surrogate to quantify the amount of drug excreted via non-urinary pathways. Nevertheless, it is very important to characterize hepatobiliary elimination because this is a potential site of drug interactions that might result in significant alterations in systemic or hepatic exposure. In addition to the determination of *in vivo* biliary clearance values of drugs, the availability of *in vitro* models that can predict the extent of biliary excretion of drugs in humans may be a powerful tool in the pre-clinical stages of drug development. In this review, recent advances in the most commonly used *in vivo* methods to estimate biliary excretion of drugs in humans are outlined. Additionally, *in vitro* models that can be employed to investigate the molecular processes involved in biliary excretion are discussed to present an updated picture of the new tools and techniques that are available to study the complex processes involved in hepatic drug transport.

KEYWORDS: bile, excretion, biliary clearance, hepatic transport, hepatobiliary transport

INTRODUCTION:

With the advent of combinatorial chemistry, an increasing number of new chemical entities that are more lipophilic and characterized by high molecular weight are being synthesized and screened during the drug discovery process.[1] Drugs with these physicochemical characteristics often are associated with significant hepatic metabolism and/or excretion via the biliary route.[2,3] The threshold molecular weight for drugs and metabolites to be excreted preferentially into bile varies between species, ranging from ~235 in rats up to 500-600 in humans. Biliary excretion of compounds can significantly impact the systemic exposure, pharmacological effect and toxicity of certain drugs. Drugs excreted into bile often undergo some degree of reabsorption along the gastrointestinal tract (e.g., mycophenolic acid[4], warfarin[5], and digoxin[3]). Enterohepatic recycling is also a very important physiological process for bile salt homeostasis. In humans, the intestinal reabsorption of bile salts is very efficient; more than 95% of the bile salt pool is reabsorbed in the distal ileum.[6,7] So far, limited *in vivo* information has been available regarding the extent of biliary elimination of drugs and metabolites in humans, primarily due to the difficulty in obtaining bile samples from healthy human subjects. An accurate measure of biliary clearance and of the extent of biliary excretion of compounds would be extremely valuable in evaluating the contribution of biliary clearance to total systemic clearance, elucidating potential mechanisms of hepatobiliary toxicity, predicting drug-drug interactions, and identifying enterohepatic versus enteroenteric recirculation. Several clinical studies have shown that drug-drug interactions can result in changes in drug absorption due to inhibition of transport proteins [increased exposure to talinolol after P-glycoprotein (P-gp, gene symbol *ABCB1*) inhibition[8], or inhibition of intestinal secretion resulting in improved therapeutic efficacy of paclitaxel[9]].

Important modifications in the pharmacokinetics/pharmacodynamics of digoxin, another P-gp substrate, have been observed with co-administration of other P-gp substrates/inhibitors, which are thought to cause interactions in intestinal[10], biliary[11,12] and/or renal[13,14] levels. However, drug-drug interactions influencing biliary clearance of compounds have not been investigated systematically due to technical difficulties in performing these experiments in humans. The inhibition of hepatobiliary transport processes can affect the ability of the liver to extract bile salts from the bloodstream or, potentially more importantly, can affect the metabolism and biliary excretion of bile salts. Although mechanisms of hepatotoxicity are believed to be multifactorial, it has been demonstrated that inhibition of bile salt biliary excretion by drugs (e.g., troglitazone[15] and bosentan[16]) can affect hepatocyte viability due to the accumulation and direct toxicity of detergent-like bile salts.[17]

The contribution of biliary excretion to the overall disposition and pharmacological effect of some drugs has been underestimated due to the lack of methodologies to accurately quantify the amount of drug subjected to enterohepatic recirculation, and a poor understanding of the processes involved in hepatic excretion and reabsorption of drugs from the canalicular space, bile ducts and intestine. Several animal models, primarily rodent, have been used to study genetic diseases affecting biliary clearance and drug-drug interactions. Mouse and rat isolated perfused liver experiments and bile duct cannulated animals are useful tools for studying biliary disposition of drugs in the early phases of drug development. The availability of rodent models genetically deficient in specific transport proteins has improved understanding of the complex molecular processes involved in excretion of endogenous and exogenous compounds into bile.[18-22] However, accumulating evidence suggests that significant inter-species differences exist in the function and regulation of

transport proteins, in addition to the already thoroughly characterized species differences in metabolism; these findings complicate the direct extrapolation of animal data to humans.[23-25] Enterohepatic recirculation of drugs has been studied extensively in experimental animals where cannulation of the bile duct allows for interruption of bile flow into the intestine. The importance of enterohepatic recirculation also has been investigated with a similar study design in humans. The pharmacokinetic profiles of drugs have been compared in patients with bile duct obstruction, before and after removal of nasobiliary drainage. This design allows complete collection of bile and interruption of enterohepatic recirculation while the drainage is in place.[26] However, since the subjects studied in this type of experimental design are affected by hepatobiliary disease, it is not possible to account for changes in the hepatobiliary tract that might have followed the resolution of bile duct obstruction.

Mechanisms for Excretion of Endogenous and Exogenous Compounds into Bile:

Several recent reviews have been published on the transporters involved in hepatobiliary disposition of drugs and bile salts.[27-31] The liver (Figure 1.1) plays a central role in the biotransformation and removal of xenobiotics and endogenous compounds from the blood. While the majority of small, lipophilic compounds enter the hepatocyte from the Space of Disse on the basolateral membrane by simple passive diffusion, more polar and bulky molecules require transport systems to cross the sinusoidal membrane (Figure 1.2 A). Once inside the hepatocyte, compounds can be transported into bile either unchanged or as more hydrophilic metabolites after phase I and/or phase II biotransformations, or can be excreted into blood by basolateral transport proteins (Figure 1.2 B). The presence of several transport proteins on the canalicular domain of hepatocytes results in the excretion of solutes into the bile canaliculi, which are dilated intercellular spaces. One of the many functions of the liver

is the synthesis of bile acids from cholesterol[32]. The major bile acids present in human bile are cholic and chenodeoxycholic acids conjugated with glycine and taurine.[33] Bile salts are excreted into bile by the bile salt export pump (BSEP/*ABCB11*, Figure 1.2 B). Bile salts facilitate the absorption of nutrients in the intestine by emulsifying lipophilic molecules due to their surfactant characteristics.[34] Once this function is served, bile salts are very efficiently reabsorbed into the cells of the distal ileum by the apical sodium-dependent bile salt transport protein (ASBT/IBAT/*SLC10A2* [35]) and excreted across the basolateral membrane into portal blood by the recently identified organic solute transport proteins OST α and β.[36,37] In addition to bile salt transport, hepatic transport proteins facilitate excretion of end-products of metabolism, such as bilirubin and/or xenobiotics, into bile for subsequent removal via the intestine, and thus act as an important clearance mechanism.

Bile Formation and Excretion:

Bile formation includes uptake of bile components from the sinusoidal blood and secretion of these substances into the canalicular space. Water and other small ions also diffuse into bile due to the differential osmotic pressure between bile and the hepatocyte cytoplasm. Subsequently, bile is drained into the biliary tree along the liver lobules and reaches the hepatic ducts. In humans, a fraction of this hepatic bile is secreted continuously into the duodenum while the majority of the ~800 mL of bile secreted per day is concentrated and stored in the gallbladder (Figure 1.1). Bile freely flows into the gallbladder, because this organ has a much lower internal pressure than the intra-hepatic ducts, common bile duct and the Sphincter of Oddi (Figure 1.1). The gallbladder fills to its maximum capacity (40-70 mL) in approximately 6 hours, while re-absorbing water and electrolytes from hepatic bile.[3,38-40] After ingestion of a meal, fats, proteins and acid reach the duodenum and

endogenous neurohormones such as cholecystokinin (CCK) and secretin are released by endocrine cells in the small intestine.[41] CCK, acting on the CCK-A type receptors of smooth muscle fibers, contracts the gallbladder and relaxes the Sphincter of Oddi. A similar effect can be obtained by intravenous infusion of physiological amounts of CCK analogs (e.g., CCK-8).[42,43] CCK blood concentrations are decreased to minimal values during fasting, which promotes contraction of the Sphincter of Oddi and relaxation of the gallbladder walls, facilitating storage of bile in the gallbladder. CCK also delays gastric emptying in order to coordinate the digestive postprandial process. In the blood of humans and animals, CCK-33, 8 and 58 are the predominant active forms of this polypeptide [44] generated by differential post-translational modifications of the same gene; functional activity is dependent upon the last seven amino acids at the carboxyl terminus. In addition to the role of CCK in gallbladder contraction, CCK also functions as a neurotransmitter in the cerebral cortex to regulate satiety, and on the peripheral nerves of the GI tract to regulate bowel movement.[45,46]

Methods Used to Determine *In Vivo* Biliary Clearance:

Several preclinical tools involving *in vivo* or *ex vivo* rodent models can be utilized to evaluate the extent of biliary excretion of drugs and the interaction of xenobiotics with bile salt transport proteins. These tools employ animal species with well characterized differences from humans, making the prediction/extrapolation to humans less accurate.[47] Determination of the extent of biliary excretion can be attained in human subjects with different methodologies as described in detail below. However, only a few studies have been performed *in vivo* in humans to evaluate biliary clearance of drugs, and little is known about the contribution of biliary clearance to the overall systemic clearance for most drugs. Table

1.1 summarizes those studies published in the literature along with the techniques used for the determination of the amount of drug and metabolites excreted into bile.

I. Patients as Study Subjects

Historically, there has been little success in the development of valid and reliable techniques to quantify biliary excretion of drugs or endogenous compounds in healthy human volunteers. Such data is obtained more easily from patients diagnosed with diseases of the gallbladder and biliary tract who require medical procedures that allow measurements of drug concentrations in bile. Usually these patients suffer from cholestasis and/or occlusion of the biliary or cystic ducts, and some may have undergone liver transplantation.

i. Cholecystectomy

Several groups have investigated gallbladder bile concentrations and disposition of drugs into bile by administering the compound of interest to patients prior to cholecystectomy. Drug concentrations in the gallbladder bile and tissue after removal are quantified and compared to the plasma concentrations. Although this approach only allows the determination of drug content in bile and tissue at a single time point, it is still very useful and has been employed to establish whether an antibiotic reaches the necessary therapeutic concentrations to treat bacterial infections of the gallbladder and biliary tract.[48,49]

ii. T-tube

Patients that require a temporary bile shunt (T-tube) that diverts part of the bile flowing from the liver to a transcutaneous port for external collection have been employed commonly to study biliary excretion of drugs. T-tubes are used primarily in patients with cholangitis, distal bile duct obstruction or edema, and often are inserted after cholecystectomy and choledochotomy. T-tubes allow for partial collection of liver bile, and

provide an estimate of the biliary excretion of administered drugs during the time that the shunt is in place.[50-55] A limitation of this technique is that bile collection in these patients is not complete. Furthermore, the composition of bile may be very different in patients due to underlying hepatobiliary disease.[56]

iii. Nasobiliary Drainage

Patients with bile duct stenosis can be treated with the temporary insertion of a nasobiliary tube. This patient population has been recruited less frequently for drug disposition studies, probably due to the fact that this procedure is relatively new. This intervention theoretically allows for complete collection of bile while the tube is in place. The nasobiliary drainage interrupts delivery of bile into the duodenum and can be used to evaluate the influence of enterohepatic recirculation on the plasma concentration-time profile for the drug of interest. In these studies, the same patients have been used as their own control when the stricture has resolved and the tube has been removed thus restoring the enterohepatic recycling process.[26,50]

Less commonly, bile has been collected from patients equipped with other types of drainage devices such as biliary-enteric diversions or percutaneous transhepatic cholangiodrainage.[51] Although the details of the surgical procedures are beyond the scope of this review, all these techniques allow free access to partial or complete collection of hepatic bile from patients.

In recent years laparoscopic cholecystectomy with duct exploration and endoscopic retrograde cholangiopancreatography (ERCP) have largely replaced more invasive methods for removing common duct stones. As a result, many fewer patients with T-tubes have been available to enroll in studies examining the biliary excretion of drugs. The relatively few

patients who are treated with nasobiliary drainage are seldom well enough or maintain the tube long enough to be suitable study candidates.

II. Healthy Volunteers as Study Subjects

One of the major limitations of the techniques described above is the use of subjects with significant hepatobiliary disease. Disease status may significantly influence transport protein expression, function, localization and/or bile flow, thereby altering drug excretion and reabsorption patterns.[57,58] It is well known that biliary obstruction decreases the expression of BSEP and MRP2 (*ABCC2*) in hepatocytes, and increases P-gp, MDR3 (*ABCB4*) and MRP3 (*ABCC3*) expression.[59,60] Moreover, cholestatic syndromes may be associated with genetic polymorphisms in transport proteins.[61,62] More relevant information may be obtained by enrolling healthy volunteers as study subjects. In this case, the physiology of the hepatobiliary tract is intact and healthy. However, the collection of bile from the gallbladder or upon immediate secretion into the intestine is more challenging, due to the difficulty of accessing the gallbladder and the anatomy of the human hepatobiliary tract.

i. Fecal Recovery

The approach most commonly used in the determination of biliary excretion as a route for drug elimination is the quantification of the drug of interest in feces. Often these studies are performed with a radiolabeled compound in order to increase the selectivity and the recovery of drug and unknown metabolites, resulting in good mass balance.[63-69] More recently, sensitive analytical techniques such as HPLC coupled with mass spectrometry have been applied widely to the analysis of biological matrices to identify the excretion routes of parent drugs and metabolites. Several drawbacks are associated with the quantification of drugs in feces. Most importantly, this method does not distinguish between biliary excretion

and intestinal secretion processes. For orally administered drugs, this method does not distinguish between unabsorbed drug and that secreted by the liver and/or gut back into the intestinal lumen, thus, the percentage of the dose in feces does not necessarily reflect the dose excreted into bile. Moreover, relatively unstable drugs, or compounds that are transformed into unstable metabolites, may not be recovered in feces due to the long exposure to the intestinal contents and colonic flora. Finally, drugs subjected to entero-hepatic or entero-enteric recycling, such as glucuronide conjugates, can be reabsorbed in the colon upon intestinal degradation by β-glucuronidases of the microbial flora, and will not be recovered in the feces.

ii. Aspiration of Duodenal Fluids

An ideal methodology would provide information on the amount of parent drug and metabolites excreted into bile, and would be flexible enough to allow for studies examining potential drug-drug interactions. This type of information can be obtained by sampling duodenal fluids to collect bile upon discharge from the biliary tract into the small intestine.[11,12,70,71] Duodenal bile is representative of gallbladder bile in terms of bile composition, although it is more dilute.[72] The use of oroenteric tubes to withdraw pancreatico-biliary secretions from the duodenum is a common practice in the medical field, and has been used to study the biliary excretion of endogenous compounds such as radiolabeled bile acids.[35,73] Some of these investigations have utilized occlusive balloons to facilitate more complete bile collection, along with the perfusion of a marker to evaluate leakage of bile or duodenal fluids distal to the balloon seal.[74] Other groups have corrected for any incomplete bile collection by perfusing non-absorbable markers, such as polyethylene glycol or sulphobromophthalein, into the duodenum.[71,75,76] Modified versions of these

methodologies have been applied successfully to the determination of intestinal absorption and secretion of drugs, thus enhancing the knowledge regarding intestinal processes, which complements information acquired regarding biliary excretion of drugs.[77-82] All the methods cited are particularly sophisticated, and the execution of these studies is not trivial. These clinical studies often require custom-made catheters, specialized personnel and equipment, and they need to be approved by local Institutional Review Boards and Research Ethics Committees. For these reasons, these methods are not used widely. Although a direct comparison of methods has not been published, it is reasonable to believe that the information obtained is, in many cases, an estimate of the amount of drug excreted via the biliary route. Nevertheless, many of the studies conducted in healthy human volunteers have resulted in incomplete and highly variable recovery of compounds excreted in bile. This is primarily due to the difficulty in obtaining and assessing the completeness of bile collection, and an inherent lack of control over gallbladder contraction.

A novel method to increase the recovery of biliary secretions and correct for the degree of gallbladder contraction, with the intention of reducing the level of complexity of the procedure, has been developed recently by our group.[83] This method assures the quantitative collection of bile secreted into the duodenum by temporary occlusion of the intestine with an inflatable balloon. At the same time, the administration of a hepatobiliary imaging agent (e.g. Tc-99m mebrofenin) is used to evaluate the degree of gallbladder contraction in response to pharmacological stimulation, and to detect any leakage of bile due to partial occlusion of the intestine. One of the major factors affecting the variability in the determination of biliary excretion in humans is related to differences in the amount of bile and drug delivered into the duodenum during the collection interval. Partial spontaneous

contractions of the gallbladder during fasting are not uncommon, and can deliver over 25% of total gallbladder bile into the intestine. To obtain more complete gallbladder contraction, CCK-8 can be administered intravenously to pharmacologically stimulate gallbladder emptying. CCK-8 administered at a low dose (0.02 μg/Kg) infused slowly over 30-60 min has been reported to provide the most complete gallbladder contraction[43]; however, inter-individual response is variable, and possibly influenced by the collection procedure. Therefore, it is important to assess the degree of gallbladder contraction in each subject. The administration of trace amounts of a gamma-emitting probe that accumulates quickly in bile, such as Tc-99m mebrofenin, can assist in the determination of the overall gallbladder response, and indicate when intestinal occlusion is not complete. Alternatively, ultrasound may be used to determine the extent of gallbladder contraction together with perfusion of the occluded tract with a non-absorbable marker to identify leakages. A gallbladder ejection fraction (EF) can be calculated from the abdominal gamma images of the volunteers during gallbladder contraction, and this number can be incorporated as a correction factor when determining the amount of bile (containing drug) excreted into the duodenum and collected by aspiration.[83] This method has been shown to correct reasonably well for the high variability in the gallbladder contraction which influences the amount of drug excreted into the duodenum.[84] Quantification of parent drug and metabolites in bile aspirated directly from the duodenum rather than in feces can be extremely advantageous in the identification of unknown metabolites, uniquely formed in humans, that are unstable and would not be found after prolonged contact with intestinal enzymes (such as unstable glucuronides).

Finally, the possibility of repeating a pharmacokinetic study in the same volunteers with and without the balloon inflated enables an evaluation of the importance of biliary

excretion in systemic drug exposure, and in studying the enterohepatic recirculation process.[85] Biliary excretion and intestinal reabsorption may be one explanation for multiple peaks in the plasma concentration-time profiles of some drugs.[86,87] Often, pharmacokinetic modeling of these data with a model that incorporates enterohepatic recycling has been used to explain these experimental observations.[88] Unfortunately, this approach does not provide direct evidence for biliary excretion, and does not allow for precise quantification of the biliary clearance parameter. Experimentally, the pharmacokinetic disposition of drugs and glucuronide conjugates have been compared in patients before and, upon removal of nasobiliary drainage, after the restoration of enterohepatic recirculation.[26] Other studies have interrupted enterohepatic recirculation with antibiotics, to eliminate the colonic flora, and/or cholestyramine, a resin that prevents the availability of lipophilic compounds for absorption in the gut lumen.[4,89] Improved methods for studying drug disposition in healthy volunteers in the presence or absence of enterohepatic recirculation should enable the investigation of hepatobiliary disposition mechanisms in much more depth than what has been attempted to date.

Methods Used to Determine *In Vitro* Biliary Excretion

Several *in vitro* models are available to investigate the processes governing biliary excretion and potential interactions of drugs with the hepatic uptake and excretion of bile salts and other endogenous and exogenous substances. These tools span from the whole hepatocyte to membrane vesicles prepared from cell lines transfected with specific transport proteins. Such techniques complement human and animal *in vivo* studies, and allow characterization of transport processes at the molecular level. Unfortunately, the results obtained with *in vitro* models are difficult to compare to human *in vivo* data. This is primarily due to the fact that

the data generated *in vitro* are used to determine values for the intrinsic biliary clearance of a drug. In contrast, *in vivo* studies often are designed to obtain more crude estimates such as the percentage of the dose excreted into bile rather than pharmacokinetic parameters. The *in vivo* biliary clearance values in humans usually are not reported (Table 1.1). Whole liver perfusion, a common technique in rodent models to obtain biliary clearance values, is rarely possible in humans due to limited availability of viable whole human livers.

i. Sandwich-Cultured Hepatocytes

Primary hepatocytes isolated from humans and animals are useful tools for studying hepatic metabolism and transport due to the expression of the full array of proteins involved in these processes. In conventional culture, a rapid decline in expression of both metabolizing enzymes and transport proteins occurs over time after cell isolation.[90] In addition, collagenase digestion of liver, required for hepatocyte isolation results in the disruption of the canalicular membrane and consequently, the cellular internalization of transport proteins expressed at this membrane.[91] A novel *in vitro* model system using primary hepatocytes from various species, including rat and human, cultured in a collagen-sandwich configuration (SC) has several distinct advantages over conventional hepatocyte culture. For example, SC hepatocytes develop functional and extensive bile canalicular networks, acquire and maintain normal cell polarity, and allow direct access to the hepatocyte and adjacent biliary compartment.[92-96] Thus, hepatocytes maintained under these culture conditions offer a unique opportunity to study basolateral uptake and canalicular efflux transport processes. Using simple alterations in buffer components, accumulation of substrates of interest can be measured in hepatocytes alone, or in hepatocytes plus canalicular networks. This allows determination of the *in vitro* intrinsic biliary clearance. To date, most

SC experiments have been conducted using rat hepatocytes. [93,96-100] Recently, SC human hepatocytes also have been characterized; uptake and efflux transport proteins are expressed, properly localized on the apical and basolateral membranes and functional.[91,101] Since SC human hepatocytes also retain metabolic capabilities, this model allows for investigation of the interplay between many of the processes that take place *in vivo*. Additionally, these cells can be maintained in culture for several days allowing for the study of drug interactions involving induction mechanisms. Human hepatocytes are not readily available and are associated with high costs. Furthermore, each culture is performed with cells from a single donor reflecting the inherent variability among donors in protein expression, function, and canalicular network formation. SC human hepatocytes serve as a unique, comprehensive tool to investigate hepatobiliary transport mechanisms.

ii. Suspended Hepatocytes

Viability of primary hepatocytes can be maintained for several hours in suspension when supplemented with appropriate culture media and oxygen. Fresh or cryopreserved rat and human hepatocytes have been used extensively to determine the hepatic metabolic clearance of drugs. [102,103] Suspended hepatocytes are a useful tool to characterize hepatic uptake and metabolism processes and inhibition studies can be perfomed with this system. However, due to the limited viability of these cells, it is not possible to study induction processes.[104-106] Additionally, internalization of canalicular transport proteins during collagenase perfusion limits the use of suspended hepatocytes to predict an overall value for biliary clearance when transport into bile is important.

iii. Vectorial Transport Using Polarized Cell Lines

The Madin Darby Canine Kidney, strain II (MDCKII) cells are polarized cells that have been used extensively to express various combinations of recombinant uptake and efflux transport proteins. Initially, MDCKII cells transfected with different combinations of a single basolateral uptake and a single canalicular efflux pump were established.[107-109] More recently, MDCKII cells transfected with a single efflux pump (MRP2/*ABCC2*) and three basolateral uptake transport proteins (OATP1B1/*SLCO1B1*, OATP1B3/*SLCO1B3* and OATP2B1/*SLCO2B1*) have been established in an attempt to mimic vectorial transport processes in human liver.[110] The combination of quadruple, double and single transfected cells is very useful for determining the contribution of individual transport proteins to vectorial transport processes. These cell lines can be transfected with transport proteins of interest, grown on a permeable membrane, and used to study the transcellular passage of selected substrates. Many model substrates have been studied using MDCK cells, and correlated with biliary clearance values obtained from rats *in vivo*.[108] Although the polarized transfected cell systems are powerful tools for studying vectorial transport, they lack a full complement of transport proteins, metabolic enzymes and co-factors present in hepatocytes, and expression levels of transport proteins may not be comparable to hepatocytes *in vivo*. These issues must be considered in data interpretation and when extrapolating to *in vivo* hepatic or biliary clearance values. Nevertheless, transfected systems are simple to use and more readily available than primary human hepatocytes and are useful as a high-throughput screening tool.

iv. Whole Cells and Membrane Vesicles

Whole cell expression systems such as *Xenopus laevis* oocytes or immortalized cell lines transfected with the transporter of interest are ideal tools when functional studies of the kinetics of transport for individual transport proteins are needed.[111] Such expression systems have been used extensively in the literature to demonstrate substrate specificity and for functional characterization of mutant proteins, such as genetic polymorphisms.[112,113] Although oocytes are a transient expression system and need to be injected individually with cRNA of the protein of interest, oocytes often are used to study uptake processes. The commercial availability of this model facilitates their use for transport studies.[114] These expression systems are more applicable to studying the effect of genetic diseases and the molecular mechanisms of transport than for the determination of hepatobiliary clearance.[115] Because of technical difficulties in loading whole cells with a substrate of interest prior to measuring efflux, these models are more suitable for the study of uptake transport proteins. To circumvent this issue, the double transfected MDCKII cells have been used, or more commonly, efflux transport processes have been studied with inside-out membrane vesicles. Such vesicles can be prepared from primary hepatocytes or from cell lines transfected with a transport protein of interest. Basolateral and apical membrane vesicles prepared from polarized cells such as primary hepatocytes can be isolated through various centrifugation steps and membrane fractions enriched in basolateral or canalicular transporters can be used to investigate drug transport and transport inhibition.[116,117] Canalicular vesicles .are more commonly prepared from rat than human hepatocytes due to limited human tissue availability. However, several recent studies have used canalicular membrane vesicles isolated from human hepatocytes.[117-119] Membrane vesicles prepared from primary

hepatocytes have distinct advantages over transfected systems: the native membrane environment is in place during isolation from the other cellular components, and all the hepatic transport systems are present. Membrane vesicles can be prepared, stored frozen, and used as needed; however, isolation of basolateral and canalicular fractions is labor intensive and complete purity is never achieved.

Membrane vesicles prepared from cell lines transiently and stably expressing membrane proteins of interest have been used extensively to characterize polymorphisms, substrate specificity and structure-function relationships of efflux transport proteins.[120-122] The expression systems used are many (insect cells: e.g., Sf9 cells [123,124]; mammalian cells: e.g. HEK293 cell line [125]) and expression of endogenous transporters may vary. The background activity of membrane vesicles must be accounted for by performing control experiments in untransfected cells; moreover, post-translational protein modifications may be different depending on the host cells and may affect the affinity of the transport protein for the substrate of interest.

CONCLUSIONS:

Novel and important technologies for evaluation of biliary excretion and the related toxicological/pharmacological issues derived from drug-drug interactions at the hepatobiliary transport level are under development. Currently, several *in vitro* models are used as screening tools in drug discovery and early development to eliminate molecules that present challenges in this particular aspect of disposition.[126-128] Comparison of results obtained using *in vitro* systems to data generated *in vivo* in humans would be extremely beneficial to substantiate *in vitro* observations. Unfortunately, information on *in vivo* biliary excretion of drugs is not readily available, and studies in volunteers will continue to be challenging and limited to few subjects. However, the findings of these studies can be extremely valuable, not only to explain results obtained using *in vitro* systems, but also to determine the importance of biliary excretion and enterohepatic recirculation in the overall disposition of drugs.

In the future, it is possible that a more systematic comparison between *in vivo* and *in vitro* hepatobiliary clearance will confirm the accuracy of *in vitro* scaled predictions, and allow the development of accurate models to predict drug disposition in humans with a higher degree of confidence. We believe that this combination of tools, together with extensive use of mathematical modeling and simulations, will not only improve our understanding of drug disposition, but will also help predict drug-drug interactions and/or the impact of genetic polymorphisms on drug exposure and toxicity.

ACKNOWLEDGMENTS

The authors are grateful to Dr. William Heizer for helpful scientific discussions and to Mr. Robert Kelly for assistance with figure preparation. This work was supported by National Institutes of Health grant R01 GM41935 and grant RR00046 from the GCRC program of the Division of Research Resources. Giulia Ghibellini is an American Foundation for Pharmaceutical Education predoctoral fellow. Dr. Elaine M. Leslie is the recipient of a Canadian Institutes of Health Research postdoctoral fellowship.

PROJECT RATIONALE AND SPECIFIC AIMS

This project is part of a long-term research effort to develop a method to accurately predict from *in vitro* data the biliary clearance of drugs measured *in vivo* in humans. This type of correlation is lacking in the current literature despite the extensive use of *in vitro* systems to predict disposition and metabolism of drugs in humans. One of the major obstacles encountered in studying the biliary excretion of drugs is the difficulty in accessing the gallbladder and collecting bile from healthy volunteers. This is why, for many drugs, very little is known about the actual fraction of the dose excreted in bile, and the portion of total clearance that can be attributed to the biliary route. The development and validation of a technique to determine biliary clearance in healthy human volunteers would provide novel *in vivo* information which could be compared to biliary clearance values generated *in vitro*. Several *in vitro* models have been used to examine mechanisms of biliary clearance. The most physiologically relevant *in vitro* system, which is characterized by the presence of both metabolic enzymes and transport proteins, is the sandwich-cultured human hepatocyte model. This *in vitro* system could be employed for moderate- to high-throughput screening of human hepatic clearance mechanisms, and perhaps more importantly, for investigating and predicting drug associated hepatotoxicity and drug-drug interactions.

In summary, the first aim of this research project was to develop a method to quantitatively collect bile in healthy volunteers after administration of probe compounds. These probes were specifically selected to exhibit various degrees of biliary excretion, in order to generate a range of *in vivo* biliary clearance values for these compounds. A second objective was to utilize pharmacokinetic modeling and simulations, as well as *in vitro* systems expressing specific transport proteins, to elucidate the mechanisms involved in the hepatobiliary

disposition of the model compound Tc-99m mebrofenin, and to explore the effects of pathophysiological changes due to disease states or drug interactions on the disposition of this compound. Additionally, the versatility of the clinical technique was demonstrated by collecting previously unknown metabolites that were excreted in bile, in addition to quantifying the biliary excretion of drugs. Finally, the sandwich-cultured human hepatocyte model was used to investigate the *in vitro* biliary clearance of the model compounds previously studied *in vivo*, in order to evaluate the accuracy of the *in vitro* predictions. These Aims are described briefly in the next few pages and in depth results, analyses and discussion are reported in Chapters 2-5 and in Appendices A-D.

HYPOTHESES: A method to quantitatively estimate biliary clearance of drugs in healthy human volunteers can be developed and applied to model compounds exhibiting a wide range of biliary excretion (Aim #1). Pharmacokinetic modeling and simulation studies with Tc-99m mebrofenin can explain *in vivo* observations in health and disease; information obtained with the aid of *in vitro* tools concerning the mechanisms underlying Tc-99m mebrofenin biliary excretion can be incorporated into the pharmacokinetic model (Aim #2). The clinical methodology developed in Aim #1 can be applied to the collection of labile metabolites in bile that are unique to the human species (Aim #3). The biliary clearance of the model compounds obtained in sandwich-cultured human hepatoyctes, once properly scaled, can accurately predict *in vivo* biliary clearance in humans (Aim #4).

Specific Aim #1 Hypothesis: It is possible to quantitatively collect bile secreted into the duodenum in healthy volunteers and obtain reliable estimates of biliary clearance for drugs that exhibit various degrees of biliary excretion.

1.a. Design an oroenteric tube and a clinical protocol to quantitatively collect duodenal secretions in humans.

1.b. Validate the oroenteric tube and clinical protocol in a study involving healthy human volunteers using Tc-99m mebrofenin.

1.c. Utilize the technique developed in 1.a and 1.b to obtain biliary clearance values in healthy volunteers for piperacillin, Tc-99m sestamibi and Tc-99m mebrofenin, compounds expected to exhibit low, intermediate and high biliary clearance, respectively.

Specific Aim #2 Hypothesis: The disposition of Tc-99m mebrofenin observed in the clinical studies can be characterized with the aid of pharmacokinetic modeling. The mechanisms of hepatobiliary transport of this probe can be clarified with the use of *in vitro* tools.

2.a. Use pharmacokinetic modeling as an approach to evaluate the disposition of Tc-99m mebrofenin (a model compound that undergoes high biliary clearance) in humans and simulate alterations in disposition caused by drug interactions or disease states.

2.b. Identify the human transport proteins involved in the hepatic basolateral uptake of Tc-99m mebrofenin using *Xenopus leavis* oocytes transfected with OATP1B1 and OATP1B3.

2.c. Elucidate the mechanism of canalicular and basolateral excretion of Tc-99m mebrofenin using inside-out membrane vesicles prepared from HEK293 cells transfected with MRP2 or MRP3.

2.d. Evaluate the contribution of Mrp2 in the biliary excretion of Tc-99m mebrofenin in the sandwich-cultured rat hepatocyte model using cells from control (Wistar) and TR^- (Mrp2-deficient) rats.

Specific Aim #3 Hypothesis: The collection of bile as soon as it is secreted into the human intestine by utilizing the oroenteric tube and clinical protocol developed in Aim #1 allows for identification of labile metabolites unique to the human species.

3.a. Use LC-MS-MS to analyze bile and urine obtained from healthy volunteers after administration of piperacillin in order to investigate the formation and excretion of Phase I and Phase II metabolites.

3.b. Demonstrate that the formation of labile metabolites identified *in vivo* can be generated *in vitro*.

Specific Aim #4 Hypothesis: The sandwich-cultured human hepatocyte model is a useful tool for predicting biliary clearance values in humans.

4.a. Customize experimental conditions for studying the cellular accumulation of model compounds in sandwich-cultured human hepatocytes.

4.b. Determine the biliary excretion index (BEI) and *in vitro* biliary clearance parameters for Tc-99m mebrofenin, Tc-99m sestamibi and piperacillin in sandwich-cultured hepatocytes.

4.c. Investigate the predictive capabilities of the sandwich-cultured human hepatoycte model by comparing *in vitro* data with *in vivo* data obtained in humans.

REFERENCES

(1) Lipinski, C. A.; Lombardo, F.; Dominy, B. W.; Feeney, P. J. Experimental and computational approaches to estimate solubility and permeability in drug discovery and development settings. *Adv Drug Deliv Rev* **2001**, *46* (1-3), 3-26.

(2) Fleck, C.; Braunlich, H. Factors determining the relationship between renal and hepatic excretion of xenobiotics. *Arzneimittelforschung* **1990**, *40* (8), 942-946.

(3) Roberts, M. S.; Magnusson, B. M.; Burczynski, F. J.; Weiss, M. Enterohepatic circulation: physiological, pharmacokinetic and clinical implications. *Clin Pharmacokinet* **2002**, *41* (10), 751-790.

(4) Bullingham, R. E.; Nicholls, A. J.; Kamm, B. R. Clinical pharmacokinetics of mycophenolate mofetil. *Clin Pharmacokinet* **1998**, *34* (6), 429-455.

(5) Jahnchen, E.; Meinertz, T.; Gilfrich, H. J.; Kersting, F.; Groth, U. Enhanced elimination of warfarin during treatment with cholestyramine. *Br J Clin Pharmacol* **1978**, *5* (5), 437-440.

(6) Pauli-Magnus, C.; Stieger, B.; Meier, Y.; Kullak-Ublick, G. A.; Meier, P. J. Enterohepatic transport of bile salts and genetics of cholestasis. *J Hepatol* **2005**, *43* (2), 342-357.

(7) Kullak-Ublick, G. A.; Stieger, B.; Meier, P. J. Enterohepatic bile salt transporters in normal physiology and liver disease. *Gastroenterology* **2004**, *126* (1), 322-342.

(8) Schwarz, U. I.; Gramatte, T.; Krappweis, J.; Oertel, R.; Kirch, W. P-glycoprotein inhibitor erythromycin increases oral bioavailability of talinolol in humans. *Int J Clin Pharmacol Ther* **2000**, *38* (4), 161-167.

(9) Chico, I.; Kang, M. H.; Bergan, R.; Abraham, J.; Bakke, S.; Meadows, B.; Rutt, A.; Robey, R.; Choyke, P.; Merino, M.; Goldspiel, B.; Smith, T.; Steinberg, S.; Figg, W. D.; Fojo, T.; Bates, S. Phase I study of infusional paclitaxel in combination with the P-glycoprotein antagonist PSC 833. *J Clin Oncol* **2001**, *19* (3), 832-842.

(10) Johne, A.; Brockmoller, J.; Bauer, S.; Maurer, A.; Langheinrich, M.; Roots, I. Pharmacokinetic interaction of digoxin with an herbal extract from St John's wort (Hypericum perforatum). *Clin Pharmacol Ther* **1999**, *66* (4), 338-345.

(11) Angelin, B.; Arvidsson, A.; Dahlqvist, R.; Hedman, A.; Schenck-Gustafsson, K. Quinidine reduces biliary clearance of digoxin in man. *Eur J Clin Invest* **1987**, *17* (3), 262-265.

(12) Hedman, A.; Angelin, B.; Arvidsson, A.; Beck, O.; Dahlqvist, R.; Nilsson, B.; Olsson, M.; Schenck-Gustafsson, K. Digoxin-verapamil interaction: reduction of biliary but not renal digoxin clearance in humans. *Clin Pharmacol Ther* **1991**, *49* (3), 256-262.

(13) Hedman, A.; Angelin, B.; Arvidsson, A.; Dahlqvist, R. Digoxin-interactions in man: spironolactone reduces renal but not biliary digoxin clearance. *Eur J Clin Pharmacol* **1992**, *42* (5), 481-485.

(14) Ding, R.; Tayrouz, Y.; Riedel, K. D.; Burhenne, J.; Weiss, J.; Mikus, G.; Haefeli, W. E. Substantial pharmacokinetic interaction between digoxin and ritonavir in healthy volunteers. *Clin Pharmacol Ther* **2004**, *76* (1), 73-84.

(15) Funk, C.; Pantze, M.; Jehle, L.; Ponelle, C.; Scheuermann, G.; Lazendic, M.; Gasser, R. Troglitazone-induced intrahepatic cholestasis by an interference with the hepatobiliary export of bile acids in male and female rats. Correlation with the gender difference in troglitazone sulfate formation and the inhibition of the canalicular bile salt export pump (Bsep) by troglitazone and troglitazone sulfate. *Toxicology* **2001**, *167* (1), 83-98.

(16) Fattinger, K.; Funk, C.; Pantze, M.; Weber, C.; Reichen, J.; Stieger, B.; Meier, P. J. The endothelin antagonist bosentan inhibits the canalicular bile salt export pump: a potential mechanism for hepatic adverse reactions. *Clin Pharmacol Ther* **2001**, *69* (4), 223-231.

(17) Rolo, A. P.; Palmeira, C. M.; Wallace, K. B. Interactions of combined bile acids on hepatocyte viability: cytoprotection or synergism. *Toxicol Lett* **2002**, *126* (3), 197-203.

(18) Hoffmaster, K. A.; Zamek-Gliszczynski, M. J.; Pollack, G. M.; Brouwer, K. L. Hepatobiliary disposition of the metabolically stable opioid peptide [D-Pen2, D-Pen5]-enkephalin (DPDPE): pharmacokinetic consequences of the interplay between multiple transport systems. *J Pharmacol Exp Ther* **2004**, *311* (3), 1203-1210.

(19) Patel, N. J.; Zamek-Gliszczynski, M. J.; Zhang, P.; Han, Y. H.; Jansen, P. L.; Meier, P. J.; Stieger, B.; Brouwer, K. L. Phenobarbital alters hepatic Mrp2 function by direct and indirect interactions. *Mol Pharmacol* **2003**, *64* (1), 154-159.

(20) Manautou, J. E.; de Waart, D. R.; Kunne, C.; Zelcer, N.; Goedken, M.; Borst, P.; Elferink, R. O. Altered disposition of acetaminophen in mice with a disruption of the Mrp3 gene. *Hepatology* **2005**, *42* (5), 1091-1098.

(21) Zelcer, N.; van de Wetering, K.; Hillebrand, M.; Sarton, E.; Kuil, A.; Wielinga, P. R.; Tephly, T.; Dahan, A.; Beijnen, J. H.; Borst, P. Mice lacking multidrug resistance protein 3 show altered morphine pharmacokinetics and morphine-6-glucuronide antinociception. *Proc Natl Acad Sci U S A* **2005**, *102* (20), 7274-7279.

(22) Nezasa, K.; Tian, X.; Zamek-Gliszczynski, M. J.; Patel, N. J.; Raub, T. J.; Brouwer, K. L. Altered Hepatobiliary Disposition of 5 (and 6)-carboxy-2',7'dichlorofluorescein in Abcg2 (Bcrp1) and Abcc2 (Mrp2) Knockout Mice. *Drug Metab Dispos* **2006**.

(23) Wang, H.; LeCluyse, E. L. Role of orphan nuclear receptors in the regulation of drug-metabolising enzymes. *Clin Pharmacokinet* **2003**, *42* (15), 1331-1357.

(24) Ishizuka, H.; Konno, K.; Shiina, T.; Naganuma, H.; Nishimura, K.; Ito, K.; Suzuki, H.; Sugiyama, Y. Species differences in the transport activity for organic anions across the bile canalicular membrane. *J Pharmacol Exp Ther* **1999**, *290* (3), 1324-1330.

(25) Zhang, P.; Swift, B. D.; Tian, X.; Brouwer, K. R. Interspecies variability of transport protein functions in sandwich-cultured (B-ClearTM) rat, dog and human hepatocytes. *Drug Metab Rev* **2005**, *37* (supplement 2), 307-307.

(26) Hellstern, A.; Hildebrand, M.; Humpel, M.; Hellenbrecht, D.; Saller, R.; Madetzki, C. Minimal biliary excretion and enterohepatic recirculation of lormetazepam in man as investigated by a new nasobiliary drainage technique. *Int J Clin Pharmacol Ther Toxicol* **1990**, *28* (6), 256-261.

(27) Faber, K. N.; Müller, M.; Jansen, P. L. M. Drug transport proteins in the liver. *Adv Drug Deliv Rev* **2003**, *55* (1), 107-124.

(28) Meier, P. J.; Stieger, B. Bile salt transporters. *Annu Rev Physiol* **2002**, *64*, 635-661.

(29) Kullak-Ublick, G. A.; Becker, M. B. Regulation of drug and bile salt transporters in liver and intestine. *Drug Metab Rev* **2003**, *35* (4), 305-317.

(30) van Montfoort, J. E.; Hagenbuch, B.; Groothuis, G. M.; Koepsell, H.; Meier, P. J.; Meijer, D. K. Drug uptake systems in liver and kidney. *Curr Drug Metab* **2003**, *4* (3), 185-211.

(31) Chandra, P.; Brouwer, K. L. The complexities of hepatic drug transport: current knowledge and emerging concepts. *Pharm Res* **2004**, *21* (5), 719-735.

(32) Eloranta, J. J.; Kullak-Ublick, G. A. Coordinate transcriptional regulation of bile acid homeostasis and drug metabolism. *Arch Biochem Biophys* **2005**, *433* (2), 397-412.

(33) Chiang, J. Y. Regulation of bile acid synthesis: pathways, nuclear receptors, and mechanisms. *J Hepatol* **2004**, *40* (3), 539-551.

(34) Mithani, S. D.; Bakatselou, V.; TenHoor, C. N.; Dressman, J. B. Estimation of the increase in solubility of drugs as a function of bile salt concentration. *Pharm Res* **1996**, *13* (1), 163-167.

(35) Galatola, G.; Jazrawi, R. P.; Bridges, C.; Joseph, A. E. A.; Northfield, T. C. Direct measurement of first-pass ileal clearance of a bile acid in humans. *Gastroenterology* **1991**, *100* (4), 1100-1105.

(36) Ballatori, N.; Hammond, C. L.; Cunningham, J. B.; Krance, S. M.; Marchan, R. Molecular mechanisms of reduced glutathione transport: role of the MRP/CFTR/ABCC and OATP/SLC21A families of membrane proteins. *Toxicol Appl Pharmacol* **2005**, *204* (3), 238-255.

(37) Dawson, P. A.; Hubbert, M.; Haywood, J.; Craddock, A. L.; Zerangue, N.; Christian, W. V.; Ballatori, N. The heteromeric organic solute transporter alpha-beta, Ostalpha-Ostbeta, is an ileal basolateral bile acid transporter. *J Biol Chem* **2005**, *280* (8), 6960-6968.

(38) Svanvik, J. In *Hepatic Transport and Bile Secretion: Physiology and Pathophysiology* Tavoloni, N., Berk, P. D., Eds.; Raven Press: New York, 1993, pp 607-618.

(39) LaRusso, N. F. *Gallbaldder and Bile Ducts*; Churchill Livingstone: Philadelphia, 1997; Vol. 6.

(40) Krishnamurthy G. T., K. S. *Nuclear Hepatology: a textbook of hepatobiliary diseases*; Springer: Berlin, New York, 2000.

(41) Jazrawi, R. P. Review article: measurement of gall-bladder motor function in health and disease. *Aliment Pharmacol Ther* **2000**, *14 Suppl 2*, 27-31.

(42) Yamamura, T.; Takahashi, T.; Kusunoki, M.; Kantoh, M.; Seino, Y.; Utsunomiya, J. Gallbladder dynamics and plasma cholecystokinin responses after meals, oral water, or sham feeding in healthy subjects. *Am J Med Sci* **1988**, *295* (2), 102-107.

(43) Ziessman, H. A.; Muenz, L. R.; Agarwal, A. K.; ZaZa, A. A. Normal values for sincalide cholescintigraphy: comparison of two methods. *Radiology* **2001**, *221* (2), 404-410.

(44) Rehfeld, J. F.; Sun, G.; Christensen, T.; Hillingso, J. G. The predominant cholecystokinin in human plasma and intestine is cholecystokinin-33. *J Clin Endocrinol Metab* **2001**, *86* (1), 251-258.

(45) Beglinger, C.; Degen, L. Fat in the intestine as a regulator of appetite--role of CCK. *Physiol Behav* **2004**, *83* (4), 617-621.

(46) Wank, S. A. Cholecystokinin receptors. *Am J Physiol* **1995**, *269* (5 Pt 1), G628-646.

(47) Lave, T.; Portmann, R.; Schenker, G.; Gianni, A.; Guenzi, A.; Girometta, M. A.; Schmitt, M. Interspecies pharmacokinetic comparisons and allometric scaling of napsagatran, a low molecular weight thrombin inhibitor. *J Pharm Pharmacol* **1999**, *51* (1), 85-91.

(48) Westphal, J. F.; Brogard, J. M.; Caro-Sampara, F.; Adloff, M.; Blickle, J. F.; Monteil, H.; Jehl, F. Assessment of biliary excretion of piperacillin-tazobactam in humans. *Antimicrob Agents Chemother* **1997**, *41* (8), 1636-1640.

(49) Edmiston, C. E., Jr.; Suarez, E. C.; Walker, A. P.; Demeure, M. P.; Frantzides, C. T.; Schulte, W. J.; Wilson, S. D. Penetration of ciprofloxacin and fleroxacin into biliary tract. *Antimicrob Agents Chemother* **1996**, *40* (3), 787-791.

(50) Brune, K.; Nuernberg, B.; Schneider, H. T. Biliary elimination of aspirin after oral and intravenous administration in patients. *Agents Actions Suppl* **1993**, *44*, 51-57.

(51) Schneider, H. T.; Nuernberg, B.; Dietzel, K.; Brune, K. Biliary elimination of non-steroidal anti-inflammatory drugs in patients. *Br J Clin Pharmacol* **1990**, *29* (1), 127-131.

(52) Siegers, C. P.; Loeser, W.; Gieselmann, J.; Oltmanns, D. Biliary and renal excretion of paracetamol in man. *Pharmacology* **1984**, *29* (5), 301-303.

(53) Cheng, H.; Schwartz, M. S.; Vickers, S.; Gilbert, J. D.; Amin, R. D.; Depuy, B.; Liu, L.; Rogers, J. D.; Pond, S. M.; Duncan, C. A.; et al. Metabolic disposition of simvastatin in patients with T-tube drainage. *Drug Metab Dispos* **1994**, *22* (1), 139-142.

(54) Verho, M.; Luck, C.; Stelter, W. J.; Rangoonwala, B.; Bender, N. Pharmacokinetics, metabolism and biliary and urinary excretion of oral ramipril in man. *Curr Med Res Opin* **1995**, *13* (5), 264-273.

(55) Jackson, D. V., Jr.; Castle, M. C.; Bender, R. A. Biliary excretion of vincristine. *Clin Pharmacol Ther* **1978**, *24* (1), 101-107.

(56) Pattinson, N. R.; Willis, K. E.; Frampton, C. M. Comparative analysis of cholesterol transport in bile from patients with and without cholesterol gallstones. *J Lipid Res* **1991**, *32* (2), 205-214.

(57) Lecureur, V.; Courtois, A.; Payen, L.; Verhnet, L.; Guillouzo, A.; Fardel, O. Expression and regulation of hepatic drug and bile acid transporters. *Toxicology* **2000**, *153* (1-3), 203-219.

(58) Keitel, V.; Nies, A. T.; Brom, M.; Hummel-Eisenbeiss, J.; Spring, H.; Keppler, D. A common Dubin-Johnson syndrome mutation impairs protein maturation and transport activity of MRP2 (ABCC2). *Am J Physiol Gastrointest Liver Physiol* **2003**, *284* (1), G165-G174.

(59) Trauner, M.; Wagner, M.; Fickert, P.; Zollner, G. Molecular regulation of hepatobiliary transport systems: clinical implications for understanding and treating cholestasis. *J Clin Gastroenterol* **2005**, *39* (4 Suppl 2), S111-124.

(60) Shoda, J.; Kano, M.; Oda, K.; Kamiya, J.; Nimura, Y.; Suzuki, H.; Sugiyama, Y.; Miyazaki, H.; Todoroki, T.; Stengelin, S.; Kramer, W.; Matsuzaki, Y.; Tanaka, N. The expression levels of plasma membrane transporters in the cholestatic liver of patients undergoing biliary drainage and their association with the impairment of biliary secretory function. *Am J Gastroenterol* **2001**, *96* (12), 3368-3378.

(61) Pratt, D. S. Cholestasis and cholestatic syndromes. *Curr Opin Gastroenterol* **2005**, *21* (3), 270-274.

(62) Pauli-Magnus, C.; Meier, P. J. Hepatocellular transporters and cholestasis. *J Clin Gastroenterol* **2005**, *39* (4 Suppl 2), S103-110.

(63) Cook, C. S.; Berry, L. M.; Bible, R. H.; Hribar, J. D.; Hajdu, E.; Liu, N. W. Pharmacokinetics and metabolism of [14C]eplerenone after oral administration to humans. *Drug Metab Dispos* **2003**, *31* (11), 1448-1455.

(64) Tse, F. L.; Jaffe, J. M.; Troendle, A. Pharmacokinetics of fluvastatin after single and multiple doses in normal volunteers. *J Clin Pharmacol* **1992**, *32* (7), 630-638.

(65) Anggard, E.; Gunne, L. M.; Homstrand, J.; McMahon, R. E.; Sandberg, C. G.; Sullivan, H. R. Disposition of methadone in methadone maintenance. *Clin Pharmacol Ther* **1975**, *17* (3), 258-266.

(66) Karim, A.; Zagarella, J.; Hribar, J.; Dooley, M. Spironolactone. I. Disposition and metabolism. *Clin Pharmacol Ther* **1976**, *19* (2), 158-169.

(67) Slatter, J. G.; Schaaf, L. J.; Sams, J. P.; Feenstra, K. L.; Johnson, M. G.; Bombardt, P. A.; Cathcart, K. S.; Verburg, M. T.; Pearson, L. K.; Compton, L. D.; Miller, L. L.; Baker, D. S.; Pesheck, C. V.; Lord, R. S., 3rd Pharmacokinetics, metabolism, and excretion of irinotecan (CPT-11) following I.V. infusion of [(14)C]CPT-11 in cancer patients. *Drug Metab Dispos* **2000**, *28* (4), 423-433.

(68) Martin, P. D.; Warwick, M. J.; Dane, A. L.; Hill, S. J.; Giles, P. B.; Phillips, P. J.; Lenz, E. Metabolism, excretion, and pharmacokinetics of rosuvastatin in healthy adult male volunteers. *Clin Ther* **2003**, *25* (11), 2822-2835.

(69) Moller, A.; Iwasaki, K.; Kawamura, A.; Teramura, Y.; Shiraga, T.; Hata, T.; Schafer, A.; Undre, N. A. The disposition of 14C-labeled tacrolimus after intravenous and oral administration in healthy human subjects. *Drug Metab Dispos* **1999**, *27* (6), 633-636.

(70) Maudgal, D. P.; Lanzini, A.; Northfield, T. C.; Bridges, C.; Joseph, A. E. Quantification of temocillin biliary excretion and gallbladder bile concentration in healthy subjects. *Drugs* **1985**, *29 Suppl 5*, 146-150.

(71) Gundert-Remy, U.; Frohnapfel, F.; Jourdan, W.; Weber, E.; Stiehl, A. Estimation of biliary excretion of ureidopenicillins in healthy volunteers using marker dilution technique. *Br J Clin Pharmacol* **1982**, *13* (6), 795-801.

(72) Janowitz, P.; Swobodnik, W.; Wechsler, J. G.; Zöller, A.; Kuhn, K.; Ditschuneit, H. Comparison of gall bladder bile and endoscopically obtained duodenal bile. *Gut* **1990**, *31* (12), 1407-1410.

(73) Northfield, T. C.; Hofmann, A. F. Biliary lipid output during three meals and an overnight fast. I. Relationship to bile acid pool size and cholesterol saturation of bile in gallstone and control subjects. *Gut* **1975**, *16* (1), 1-11.

(74) Ryde, M.; Gustavsson, S. Biliary excretion of olsalazine sodium in humans. *Eur J Drug Metab Pharmacokinet* **1987**, *12* (1), 17-24.

(75) Lanzini, A.; Pigozzi, M. G.; Wuhrer, A.; Facchinetti, D.; Castellano, M.; Bettini, L.; Guerra, U. P.; Beschi, M.; Muiesan, G. Quantitative measurement of biliary excretion and of gall bladder concentration of drugs under physiological conditions in man. *Gut* **1989**, *30* (1), 104-109.

(76) Caldwell, J. H.; Cline, C. T. Biliary excretion of digoxin in man. *Clin Pharmacol Ther* **1976**, *19* (4), 410-415.

(77) von Richter, O.; Greiner, B.; Fromm, M. F.; Fraser, R.; Omari, T.; Barclay, M. L.; Dent, J.; Somogyi, A. A.; Eichelbaum, M. Determination of in vivo absorption, metabolism, and transport of drugs by the human intestinal wall and liver with a novel perfusion technique. *Clin Pharmacol Ther* **2001**, *70* (3), 217-227.

(78) Drescher, S.; Glaeser, H.; Murdter, T.; Hitzl, M.; Eichelbaum, M.; Fromm, M. F. P-glycoprotein-mediated intestinal and biliary digoxin transport in humans. *Clin Pharmacol Ther* **2003**, *73* (3), 223-231.

(79) Glaeser, H.; Drescher, S.; Hofmann, U.; Heinkele, G.; Somogyi, A. A.; Eichelbaum, M.; Fromm, M. F. Impact of concentration and rate of intraluminal drug delivery on absorption and gut wall metabolism of verapamil in humans. *Clin Pharmacol Ther* **2004**, *76* (3), 230-238.

(80) Tannergren, C.; Petri, N.; Knutson, L.; Hedeland, M.; Bondesson, U.; Lennernas, H. Multiple transport mechanisms involved in the intestinal absorption and first-pass extraction of fexofenadine. *Clin Pharmacol Ther* **2003**, *74* (5), 423-436.

(81) Petri, N.; Tannergren, C.; Holst, B.; Mellon, F. A.; Bao, Y.; Plumb, G. W.; Bacon, J.; O'Leary, K. A.; Kroon, P. A.; Knutson, L.; Forsell, P.; Eriksson, T.; Lennernas, H.; Williamson, G. Absorption/metabolism of sulforaphane and quercetin, and regulation of phase II enzymes, in human jejunum in vivo. *Drug Metab Dispos* **2003**, *31* (6), 805-813.

(82) Takamatsu, N.; Kim, O. N.; Welage, L. S.; Idkaidek, N. M.; Hayashi, Y.; Barnett, J.; Yamamoto, R.; Lipka, E.; Lennernas, H.; Hussain, A.; Lesko, L.; Amidon, G. L. Human jejunal permeability of two polar drugs: cimetidine and ranitidine. *Pharm Res* **2001**, *18* (6), 742-744.

(83) Ghibellini, G.; Johnson, B. M.; Kowalsky, R. J.; Heizer, W. D.; Brouwer, K. L. A novel method for the determination of biliary clearance in humans. *AAPS J* **2004**, *6* (4), e33.

(84) Ghibellini, G.; Vasist, L. S.; Hill, T. E.; Bridges, A. S.; Heizer, W. D.; Brouwer, K. L. Determination of Piperacillin Biliary Clearance in Humans and Identification of Its Metabolites in Bile and Urine. *AAPS J* **2005**, *7* (S2), M1293.

(85) Reynolds, K. S.; Song, M. H.; Heizer, W. D.; Burns, C. B.; Sica, D. A.; Brouwer, K. L. Effect of pancreatico-biliary secretions and GI transit time on the absorption and pharmacokinetic profile of ranitidine in humans. *Pharm Res* **1998**, *15* (8), 1281-1285.

(86) Colburn, W. A.; Vane, F. M.; Bugge, C. J.; Carter, D. E.; Bressler, R.; Ehmann, C. W. Pharmacokinetics of 14C-isotretinoin in healthy volunteers and volunteers with biliary T-tube drainage. *Drug Metab Dispos* **1985**, *13* (3), 327-332.

(87) Ezzet, F.; Krishna, G.; Wexler, D. B.; Statkevich, P.; Kosoglou, T.; Batra, V. K. A population pharmacokinetic model that describes multiple peaks due to enterohepatic recirculation of ezetimibe. *Clin Ther* **2001**, *23* (6), 871-885.

(88) Hoglund, P.; Ohlin, M. Effect modelling for drugs undergoing enterohepatic circulation. *Eur J Drug Metab Pharmacokinet* **1993**, *18* (4), 333-338.

(89) Herman, R. J.; Van Pham, J. D.; Szakacs, C. B. Disposition of lorazepam in human beings: enterohepatic recirculation and first-pass effect. *Clin Pharmacol Ther* **1989**, *46* (1), 18-25.

(90) LeCluyse, E. L.; Bullock, P. L.; Parkinson, A.; Hochman, J. H. Cultured rat hepatocytes. *Pharm Biotechnol* **1996**, *8*, 121-159.

(91) Hoffmaster, K. A.; Turncliff, R. Z.; LeCluyse, E. L.; Kim, R. B.; Meier, P. J.; Brouwer, K. L. P-glycoprotein expression, localization, and function in sandwich-cultured primary rat and human hepatocytes: relevance to the hepatobiliary disposition of a model opioid peptide. *Pharm Res* **2004**, *21* (7), 1294-1302.

(92) Hamilton, G. A.; Jolley, S. L.; Gilbert, D.; Coon, D. J.; Barros, S.; LeCluyse, E. L. Regulation of cell morphology and cytochrome P450 expression in human hepatocytes by extracellular matrix and cell-cell interactions. *Cell Tissue Res* **2001**, *306* (1), 85-99.

(93) Annaert, P. P.; Turncliff, R. Z.; Booth, C. L.; Thakker, D. R.; Brouwer, K. L. P-glycoprotein-mediated in vitro biliary excretion in sandwich-cultured rat hepatocytes. *Drug Metab Dispos* **2001**, *29* (10), 1277-1283.

(94) Liu, X.; LeCluyse, E. L.; Brouwer, K. R.; Lightfoot, R. M.; Lee, J. I.; Brouwer, K. L. Use of Ca2+ modulation to evaluate biliary excretion in sandwich-cultured rat hepatocytes. *J Pharmacol Exp Ther* **1999**, *289* (3), 1592-1599.

(95) Dunn, J. C.; Yarmush, M. L.; Koebe, H. G.; Tompkins, R. G. Hepatocyte function and extracellular matrix geometry: long-term culture in a sandwich configuration. *FASEB J* **1989**, *3* (2), 174-177.

(96) Turncliff, R. Z.; Meier, P. J.; Brouwer, K. L. Effect of dexamethasone treatment on the expression and function of transport proteins in sandwich-cultured rat hepatocytes. *Drug Metab Dispos* **2004**, *32* (8), 834-839.

(97) Liu, X.; LeCluyse, E. L.; Brouwer, K. R.; Gan, L. S.; Lemasters, J. J.; Stieger, B.; Meier, P. J.; Brouwer, K. L. Biliary excretion in primary rat hepatocytes cultured in a collagen-sandwich configuration. *Am J Physiol* **1999**, *277* (1 Pt 1), G12-21.

(98) Liu, X.; Brouwer, K. L.; Gan, L. S.; Brouwer, K. R.; Stieger, B.; Meier, P. J.; Audus, K. L.; LeCluyse, E. L. Partial maintenance of taurocholate uptake by adult rat hepatocytes cultured in a collagen sandwich configuration. *Pharm Res* **1998**, *15* (10), 1533-1539.

(99) Liu, X.; Chism, J. P.; LeCluyse, E. L.; Brouwer, K. R.; Brouwer, K. L. Correlation of biliary excretion in sandwich-cultured rat hepatocytes and in vivo in rats. *Drug Metab Dispos* **1999**, *27* (6), 637-644.

(100) Chandra, P.; Lecluyse, E. L.; Brouwer, K. L. Optimization of culture conditions for determining hepatobiliary disposition of taurocholate in sandwich-cultured rat hepatocytes. *In Vitro Cell Dev Biol Anim* **2001**, *37* (6), 380-385.

(101) Kostrubsky, V. E.; Strom, S. C.; Hanson, J.; Urda, E.; Rose, K.; Burliegh, J.; Zocharski, P.; Cai, H.; Sinclair, J. F.; Sahi, J. Evaluation of hepatotoxic potential of drugs by inhibition of bile-acid transport in cultured primary human hepatocytes and intact rats. *Toxicol Sci* **2003**, *76* (1), 220-228.

(102) McGinnity, D. F.; Soars, M. G.; Urbanowicz, R. A.; Riley, R. J. Evaluation of fresh and cryopreserved hepatocytes as in vitro drug metabolism tools for the prediction of metabolic clearance. *Drug Metab Dispos* **2004**, *32* (11), 1247-1253.

(103) Ito, K.; Houston, J. B. Comparison of the use of liver models for predicting drug clearance using in vitro kinetic data from hepatic microsomes and isolated hepatocytes. *Pharm Res* **2004**, *21* (5), 785-792.

(104) Hoffmaster, K. A.; Zamek-Gliszczynski, M. J.; Pollack, G. M.; Brouwer, K. L. Multiple transport systems mediate the hepatic uptake and biliary excretion of the metabolically stable opioid peptide [D-penicillamine2,5]enkephalin. *Drug Metab Dispos* **2005**, *33* (2), 287-293.

(105) Kemp, D. C.; Zamek-Gliszczynski, M. J.; Brouwer, K. L. Xenobiotics inhibit hepatic uptake and biliary excretion of taurocholate in rat hepatocytes. *Toxicol Sci* **2005**, *83* (2), 207-214.

(106) Blanchard, N.; Alexandre, E.; Abadie, C.; Lave, T.; Heyd, B.; Mantion, G.; Jaeck, D.; Richert, L.; Coassolo, P. Comparison of clearance predictions using primary cultures and suspensions of human hepatocytes. *Xenobiotica* **2005**, *35* (1), 1-15.

(107) Cui, Y.; Konig, J.; Keppler, D. Vectorial transport by double-transfected cells expressing the human uptake transporter SLC21A8 and the apical export pump ABCC2. *Mol Pharmacol* **2001**, *60* (5), 934-943.

(108) Sasaki, M.; Suzuki, H.; Aoki, J.; Ito, K.; Meier, P. J.; Sugiyama, Y. Prediction of in vivo biliary clearance from the in vitro transcellular transport of organic anions across a double-transfected Madin-Darby canine kidney II monolayer expressing both rat organic

anion transporting polypeptide 4 and multidrug resistance associated protein 2. *Mol Pharmacol* **2004**, *66* (3), 450-459.

(109) Matsushima, S.; Maeda, K.; Kondo, C.; Hirano, M.; Sasaki, M.; Suzuki, H.; Sugiyama, Y. Identification of the hepatic efflux transporters of organic anions using double-transfected Madin-Darby canine kidney II cells expressing human organic anion-transporting polypeptide 1B1 (OATP1B1)/multidrug resistance-associated protein 2, OATP1B1/multidrug resistance 1, and OATP1B1/breast cancer resistance protein. *J Pharmacol Exp Ther* **2005**, *314* (3), 1059-1067.

(110) Kopplow, K.; Letschert, K.; Konig, J.; Walter, B.; Keppler, D. Human hepatobiliary transport of organic anions analyzed by quadruple-transfected cells. *Mol Pharmacol* **2005**, *68* (4), 1031-1038.

(111) Pritchard, J. B.; Miller, D. S. Expression systems for cloned xenobiotic transporters. *Toxicol Appl Pharmacol* **2005**, *204* (3), 256-262.

(112) Urban, T. J.; Sebro, R.; Hurowitz, E. H.; Leabman, M. K.; Badagnani, I.; Lagpacan, L. L.; Risch, N.; Giacomini, K. M. Functional genomics of membrane transporters in human populations. *Genome Res* **2005**.

(113) Lee, W.; Glaeser, H.; Smith, L. H.; Roberts, R. L.; Moeckel, G. W.; Gervasini, G.; Leake, B. F.; Kim, R. B. Polymorphisms in human organic anion-transporting polypeptide 1A2 (OATP1A2): implications for altered drug disposition and central nervous system drug entry. *J Biol Chem* **2005**, *280* (10), 9610-9617.

(114) Bourdet, D. L.; Pritchard, J. B.; Thakker, D. R. Differential substrate and inhibitory activities of ranitidine and famotidine toward human organic cation transporter 1 (hOCT1; SLC22A1), hOCT2 (SLC22A2), and hOCT3 (SLC22A3). *J Pharmacol Exp Ther* **2005**, *315* (3), 1288-1297.

(115) Nozawa, T.; Minami, H.; Sugiura, S.; Tsuji, A.; Tamai, I. Role of organic anion transporter OATP1B1 (OATP-C) in hepatic uptake of irinotecan and its active metabolite, 7-ethyl-10-hydroxycamptothecin: in vitro evidence and effect of single nucleotide polymorphisms. *Drug Metab Dispos* **2005**, *33* (3), 434-439.

(116) Zamek-Gliszczynski, M. J.; Brouwer, K. R. L. In *Pharmaceutical profiling in drug discovery for lead selection*; Borchardt, R. T., Kerns, E. H., Lipinski, C. A., Thakker, D. R., Wang, B., Eds.; AAPS Press: Arlington, 2004, pp 259-292.

(117) Horikawa, M.; Kato, Y.; Tyson, C. A.; Sugiyama, Y. Potential cholestatic activity of various therapeutic agents assessed by bile canalicular membrane vesicles isolated from rats and humans. *Drug Metab Pharmacokinet* **2003**, *18* (1), 16-22.

(118) Shilling, A. D.; Azam, F.; Kao, J.; Leung, L. Use of canalicular membrane vesicles (CMVs) from rats, dogs, monkeys and humans to assess drug transport across the canalicular membrane. *J Pharmacol Toxicol Methods* **2005**.

(119) Nakagomi-Hagihara, R.; Nakai, D.; Kawai, K.; Yoshigae, Y.; Tokui, T.; Abe, T.; Ikeda, T. Oatp1b1, Oatp1b3 and Mrp2 Are Involved in Hepatobiliary Transport of Olmesartan, a Novel Angiotensin Ii Blocker. *Drug Metab Dispos* **2006**.

(120) Kondo, C.; Suzuki, H.; Itoda, M.; Ozawa, S.; Sawada, J.; Kobayashi, D.; Ieiri, I.; Mine, K.; Ohtsubo, K.; Sugiyama, Y. Functional analysis of SNPs variants of BCRP/ABCG2. *Pharm Res* **2004**, *21* (10), 1895-1903.

(121) Letourneau, I. J.; Deeley, R. G.; Cole, S. P. Functional characterization of non-synonymous single nucleotide polymorphisms in the gene encoding human multidrug resistance protein 1 (MRP1/ABCC1). *Pharmacogenet Genomics* **2005**, *15* (9), 647-657.

(122) Leslie, E. M.; Bowers, R. J.; Deeley, R. G.; Cole, S. P. Structural requirements for functional interaction of glutathione tripeptide analogs with the human multidrug resistance protein 1 (MRP1). *J Pharmacol Exp Ther* **2003**, *304* (2), 643-653.

(123) Zelcer, N.; Huisman, M. T.; Reid, G.; Wielinga, P.; Breedveld, P.; Kuil, A.; Knipscheer, P.; Schellens, J. H.; Schinkel, A. H.; Borst, P. Evidence for two interacting ligand binding sites in human multidrug resistance protein 2 (ATP binding cassette C2). *J Biol Chem* **2003**, *278* (26), 23538-23544.

(124) Ozvegy, C.; Varadi, A.; Sarkadi, B. Characterization of drug transport, ATP hydrolysis, and nucleotide trapping by the human ABCG2 multidrug transporter. Modulation of substrate specificity by a point mutation. *J Biol Chem* **2002**, *277* (50), 47980-47990.

(125) Leslie, E. M.; Mao, Q.; Oleschuk, C. J.; Deeley, R. G.; Cole, S. P. Modulation of multidrug resistance protein 1 (MRP1/ABCC1) transport and atpase activities by interaction with dietary flavonoids. *Mol Pharmacol* **2001**, *59* (5), 1171-1180.

(126) Song, S.; Suzuki, H.; Kawai, R.; Sugiyama, Y. Effect of PSC 833, a P-glycoprotein modulator, on the disposition of vincristine and digoxin in rats. *Drug Metab Dispos* **1999**, *27* (6), 689-694.

(127) Watanabe, T.; Miyauchi, S.; Sawada, Y.; Iga, T.; Hanano, M.; Inaba, M.; Sugiyama, Y. Kinetic analysis of hepatobiliary transport of vincristine in perfused rat liver. Possible roles of P-glycoprotein in biliary excretion of vincristine. *J Hepatol* **1992**, *16* (1-2), 77-88.

(128) Watanabe, T.; Suzuki, H.; Sawada, Y.; Naito, M.; Tsuruo, T.; Inaba, M.; Hanano, M.; Sugiyama, Y. Induction of hepatic P-glycoprotein enhances biliary excretion of vincristine in rats. *J Hepatol* **1995**, *23* (4), 440-448.

(129) Karachalios, G.; Charalabopoulos, K. Biliary excretion of antimicrobial drugs. *Chemotherapy* **2002**, *48* (6), 280-297.

(130) Balant, L.; Dayer, P.; Auckenthaler, R. Clinical pharmacokinetics of the third generation cephalosporins. *Clinical Pharmacokinetics* **1985**, *10* (2), 101-143.

(131) Brogard, J. M.; Jehl, F.; Blickle, J. F.; Dorner, M.; Arnaud, J. P.; Monteil, H. Biliary pharmacokinetic profile of piperacillin: experimental data and evaluation in man. *Int J Clin Pharmacol Ther Toxicol* **1990**, *28* (11), 462-470.

(132) Raber, M. N.; Newman, R. A.; Newman, B. M.; Gaver, R. C.; Schacter, L. P. Phase I trial and clinical pharmacology of elsamitrucin. *Cancer Res* **1992**, *52* (6), 1406-1410.

(133) Mathijssen, R. H.; van Alphen, R. J.; Verweij, J.; Loos, W. J.; Nooter, K.; Stoter, G.; Sparreboom, A. Clinical pharmacokinetics and metabolism of irinotecan (CPT-11). *Clin Cancer Res* **2001**, *7* (8), 2182-2194.

(134) Walle, T.; Walle, U. K.; Kumar, G. N.; Bhalla, K. N. Taxol metabolism and disposition in cancer patients. *Drug Metab Dispos* **1995**, *23* (4), 506-512.

(135) Gidding, C. E.; Kellie, S. J.; Kamps, W. A.; de Graaf, S. S. Vincristine revisited. *Crit Rev Oncol Hematol* **1999**, *29* (3), 267-287.

(136) Ghibellini, G.; Vasist, L. S.; Heizer, W. D.; Kowalsky, R. J.; Brouwer, K. L. Quantitation of Tc-99m Sestamibi Biliary Excretion in Humans. *Clin Pharmacol Ther* **2006**, *79* (2), PI-48.

(137) Jayasinghe, K. S.; Roberts, C. J.; Read, A. E. Is biliary excretion of paracetamol significant in man? *Br J Clin Pharmacol* **1986**, *22* (3), 363-366.

(138) Kosoglou, T.; Statkevich, P.; Johnson-Levonas, A. O.; Paolini, J. F.; Bergman, A. J.; Alton, K. B. Ezetimibe: a review of its metabolism, pharmacokinetics and drug interactions. *Clin Pharmacokinet* **2005**, *44* (5), 467-494.

(139) Hatanaka, T. Clinical pharmacokinetics of pravastatin: mechanisms of pharmacokinetic events. *Clin Pharmacokinet* **2000**, *39* (6), 397-412.

(140) Molimard, M.; Diquet, B.; Benedetti, M. S. Comparison of pharmacokinetics and metabolism of desloratadine, fexofenadine, levocetirizine and mizolastine in humans. *Fundam Clin Pharmacol* **2004**, *18* (4), 399-411.

(141) Simons, F. E.; Simons, K. J. Clinical pharmacology of new histamine H1 receptor antagonists. *Clin Pharmacokinet* **1999**, *36* (5), 329-352.

(142) Brookman, L. J.; Rolan, P. E.; Benjamin, I. S.; Palmer, K. R.; Wyld, P. J.; Lloyd, P.; Flesch, G.; Waldmeier, F.; Sioufi, A.; Mullins, F. Pharmacokinetics of valsartan in patients with liver disease. *Clin Pharmacol Ther* **1997**, *62* (3), 272-278.

(143) Cox, P. J.; Ryan, D. A.; Hollis, F. J.; Harris, A. M.; Miller, A. K.; Vousden, M.; Cowley, H. Absorption, disposition, and metabolism of rosiglitazone, a potent thiazolidinedione insulin sensitizer, in humans. *Drug Metab Dispos* **2000**, *28* (7), 772-780.

(144) Rozman, B. Clinical pharmacokinetics of leflunomide. *Clin Pharmacokinet* **2002**, *41* (6), 421-430.

(145) Wallemacq, P. E.; Verbeeck, R. K. Comparative clinical pharmacokinetics of tacrolimus in paediatric and adult patients. *Clin Pharmacokinet* **2001**, *40* (4), 283-295.

(146) Hellstern, A.; Hellenbrecht, D.; Saller, R.; Gatzen, M.; Achtert, G.; Brockmann, P.; Hausleiter, H. J. Minimal biliary excretion and enterohepatic recirculation of metoclopramide in patients with extrahepatic cholestasis. *Eur J Clin Pharmacol* **1993**, *45* (5), 415-418.

(147) Hedman, A.; Angelin, B.; Arvidsson, A.; Dahlqvist, R. No effect of probenecid on the renal and biliary clearances of digoxin in man. *Br J Clin Pharmacol* **1991**, *32* (1), 63-67.

(148) DeVane, C. L.; Nemeroff, C. B. Clinical pharmacokinetics of quetiapine: an atypical antipsychotic. *Clin Pharmacokinet* **2001**, *40* (7), 509-522.

(149) Hucker, H. B.; Stauffer, S. C.; Balletto, A. J.; White, S. D.; Zacchei, A. G.; Arison, B. H. Physiological disposition and metabolism of cyclobenzaprine in the rat, dog, rhesus monkey, and man. *Drug Metab Dispos* **1978**, *6* (6), 659-672.

(150) Daneshmend, T. K.; Warnock, D. W. Clinical pharmacokinetics of ketoconazole. *Clin Pharmacokinet* **1988**, *14* (1), 13-34.

(151) Verebely, K.; Volavka, J.; Mule, S.; Resnick, R. Methadone in man: pharmacokinetic and excretion studies in acute and chronic treatment. *Clin Pharmacol Ther* **1975**, *18* (2), 180-190.

(152) Balani, S. K.; Xu, X.; Pratha, V.; Koss, M. A.; Amin, R. D.; Dufresne, C.; Miller, R. R.; Arison, B. H.; Doss, G. A.; Chiba, M.; Freeman, A.; Holland, S. D.; Schwartz, J. I.; Lasseter, K. C.; Gertz, B. J.; Isenberg, J. I.; Rogers, J. D.; Lin, J. H.; Baillie, T. A. Metabolic profiles of montelukast sodium (Singulair), a potent cysteinyl leukotriene1 receptor antagonist, in human plasma and bile. *Drug Metab Dispos* **1997**, *25* (11), 1282-1287.

(153) Kumar, G. N.; Jayanti, V. K.; Johnson, M. K.; Uchic, J.; Thomas, S.; Lee, R. D.; Grabowski, B. A.; Sham, H. L.; Kempf, D. J.; Denissen, J. F.; Marsh, K. C.; Sun, E.; Roberts, S. A. Metabolism and disposition of the HIV-1 protease inhibitor lopinavir (ABT-378) given in combination with ritonavir in rats, dogs, and humans. *Pharm Res* **2004**, *21* (9), 1622-1630.

(154) Denissen, J. F.; Grabowski, B. A.; Johnson, M. K.; Buko, A. M.; Kempf, D. J.; Thomas, S. B.; Surber, B. W. Metabolism and disposition of the HIV-1 protease inhibitor ritonavir (ABT-538) in rats, dogs, and humans. *Drug Metab Dispos* **1997**, *25* (4), 489-501.

(155) Arvidsson, A.; Alvan, G.; Angelin, B.; Borga, O.; Nord, C. E. Ceftriaxone: renal and biliary excretion and effect on the colon microflora. *J Antimicrob Chemother* **1982**, *10* (3), 207-215.

(156) Bearden, D. T. Clinical pharmacokinetics of quinupristin/dalfopristin. *Clin Pharmacokinet* **2004**, *43* (4), 239-252.

(157) Vincent, J.; Teng, R.; Dalvie, D. K.; Friedman, H. L. Pharmacokinetics and metabolism of single oral doses of trovafloxacin. *Am J Surg* **1998**, *176* (6A Suppl), 8S-13S.

TABLES

Table 1.1: Summary of human studies that report the amount of parent drug and/or metabolites excreted via the biliary route.

The percentages of the dose excreted into bile and/or feces as parent drug or total radioactivity are summarized where possible. The administration route and methods used to obtain this information, the particular population of subjects studied, and systemic and biliary clearance values, if published also are listed. Antibiotics are a therapeutic class that has been studied in particular detail in terms of biliary excretion and distribution within the gallbladder tissue. In addition to the studies reported here, the reader is referred to comprehensive reviews on this topic.[71,122-124]

Therapeutic Class	Compound	Administration route	Population studied	Bile collection methodology (number of subjects)	% of dose excreted in bile or feces (collection interval)	Clearance parameters	Reference
Antineoplastic Agent	Elsamitrucin	IV	Cancer patients	Indwelling biliary catheter (n=1)	~22 unchanged (51 hr)	Cl_{total}=10-19 L/h/m^2	132
	Irinotecan	IV (^{14}C)	Cancer patients	Feces (n=7); T-tube bile and feces (n=1)	54-75 total in feces, 30 total in bile; 32.3 unchanged, 14 total in feces	Cl_{total}=13.5 L/h/m^2	67 133
	Taxol	IV	Cancer patients	Feces (n=5)	5 and 71.1 unchanged and total (4-5 days)	N.D.	134
	Vincristine	[a]IV (^{3}H)	Cancer patients	T-Tube bile and feces (n=1)	[a]49.6 total in bile and 4.2 in feces (72 hr), 46.5 of bile radioactivity at 2 hr as unchanged	[b]Cl_{total}=189 mL/min/m^2	a, 55 b, 135
Hepatobiliary Imaging Agent	Tc-99m Mebrofenin	IV	Healthy volunteers	Duodenal aspiration (n=4)	67.1/84.2 unchanged/ corrected by EF (3 hr)	Cl_{total}=17.3 $Cl_{biliary}$=12.5 *in vivo* $Cl_{biliary}$ =16.1 mL/min/Kg	83
Cardiac Imaging Agent	Tc-99m Sestamibi	IV	Healthy volunteers	Duodenal aspiration (n=7)	14.7/ 21.5 unchanged/ corrected by EF (3 hr)	Cl_{total}=25.8 $Cl_{biliary}$=3.9 *in vivo* $Cl_{biliary}$=6.0 mL/min/Kg	136
NSAID	Aspirin	PO and IV	Patients	T-tube bile (n=3); nasobiliary tube bile (n=2)	0.02-1.89 primarily conjugated (24 hr)	N.D.	50

	Diclofenac	PO	Patients	Percutaneous transhepatic cholangiodrainage (n=2)	4.6 total (24 hr), 1.1 unchanged and active phase II metabolites	N.D.	[51]
	Indomethacin	PO	Patients	Percutaneous transhepatic cholangiodrainage (n=3)	0.23-15 (24 hr)	N.D.	[51]
	Ibuprofen	PO	Patients	Percutaneous transhepatic cholangiodrainage (n=3)	0.82 (24 hr), 0.15 unchanged and active phase II metabolites	N.D.	[51]
Analgesic, Antipyretic	Paracetamol/ Acetaminophen	PO	[c]Patients; [d]healthy volunteers	[c]T-tube bile (n=6); [d]duodenal aspiration for 15 min post CCK administration(n=10)	[c]2.6 total and [c]0.57 unchanged; [d]7.3 total	N.D.	[c,52] [d, 137]
Antihyperlipidemic	Ezetimibe	PO (^{14}C)	Healthy males	Feces (n=8)	78 mostly unchanged (10 days)	N.D.	[138]
	Fluvastatin	IV/PO (^{3}H)	Healthy volunteers	Feces (n=6)	86-92 total (120 hr), 1.8 of total radioactivity as unchanged	Cl_{total}=0.97 L/hr/Kg	[64]
	Pravastatin	IV	Healthy volunteers	Feces	34 total and 23 unchanged	Cl_{total}=13.5 mL/min/Kg	[139]
	Rosuvastatin	PO (^{14}C)	Healthy volunteers	Feces (n=6)	90 total at 10 days (~70 at 72hr); 78.8 as unchanged (10 days)	N.D.	[68]

	Simvastatin	PO (^{14}C)	Patients	T-tube bile and feces (n=4)	25 total in bile and 20 in feces	N.D.	53
Antihistamine	Desloratadine	PO (^{14}C)	Healthy volunteers	Feces	47 primarily metabolites	N.D.	140
	Ebastine	PO	Healthy volunteers	Feces	6 total (24hr), 28 total (312 hr)	N.D.	141
	Fexofenadine	PO (^{14}C)	Healthy volunteers	Feces	80 total (~95 of radioactivity as unchanged)	Cl/F=1.10 L/hr/Kg	140,141
	Levocetrizine	PO (^{14}C)	Healthy volunteers	Feces	13 total and 86 unchanged	N.D.	140
	Mizolastine	PO (^{14}C)	Healthy volunteers	Feces	84-95 primarily glucuronidated	Cl/F=0.69 L/hr/Kg	140,141
Antihypertensive	Eplerenone	PO (^{14}C)	Healthy volunteers	Feces (n=8)	32.0 primarily metabolites (96 hr)	N.D.	63
	Ramipril	PO	Patients	T-tube bile (n=8)	~17 total and 0.1 unchanged (24 hr)	N.D.	54
	Spironolactone	PO (^{3}H)	Healthy males	Feces (n=5)	22.7 total (5 days)	N.D.	66
	Valsartan	IV	Patients	Biliary-enteric diversion (n=1)	89 mostly unchanged	N.D.	142
Antidiabetic	Rosiglitazone	PO/IV (^{14}C)	Healthy volunteers	Feces (n=4)	21.6 from PO, 25.2 from IV (21 days) mostly metabolites	N.D.	143
Immuno Suppressant/ Modulator	Leflunomide	PO (^{14}C)	Healthy volunteers	Feces (n=4)	48 (28 days) as methylhydroxy-metabolite (M1)	Cl_{total} for M1=0.051 L/h	144

Immunosuppressant	Mycophenolic acid	PO	Healthy volunteers; patients	Feces (n=4); T-tube bile (n=17)	5.5 in feces; 16.5-26 in bile as glucuronide conjugate, <0.1 unchanged in bile	Cl_{total}=8.5-11.6 L/min	[4]
	Tacrolimus	[e]IV /PO (^{14}C) [f]IV	[e]Healthy males; [f]patients	[e]Feces (n=6)	[e]0.29 (IV) and 0.12 (PO) unchanged, [e]5.4 (IV) and 92.6 (PO) total (11 days)	[f]Cl_{total}= 0.3-5.4 L/hr/Kg	[e, 69] [f, 145]
Gastrointestinal Stimulant	Metoclopramide	PO	Patients	Nasobiliary tube (n=10), repeated with restored enterohepatic recirculation	<1 as unchanged and conjugated metabolites	Cl/F= 0.5 L/hr/Kg	[146]
Antiarrhythmic	Digoxin	PO	[g]Healthy Males; [h]patients	Intestinal perfusion (n=6)		[g]Cl_{total}=255 Cl_{bile}= [g]72-163 or [h]79-343 or [i]58-142 mL/min	[g, 147] [h, 12] [i, 11]
Antipsychotic	Quetiapine	PO		Feces	21 total, < 1 of total radioactivity as unchanged (168 hr)	Cl/F=86-105 L/hr	[148]
Skeletal Muscle Relaxant	Cyclobenzaprine	IV and PO (^{14}C)	Healthy volunteers	Feces (n=5, PO) (n=3, IV)	13.5 (PO) and 15.1 (IV) primarily as glucuronide (120 hr)	N.D.	[149]
Antifungal	Ketoconazole	PO (^{3}H)	Healthy males	Feces (n=3)	57 total, 20-65 of total radioactivity as unchanged (4 days)	N.D.	[150]

Benzodiazepine	Lormetazepam	PO	Patients	Nasobiliary drainage bile (n=5)	0.3-2.8 total (24 hr)	Cl_{total}=1.9-6.2 mL/min/Kg	[26]
Analgesic Opioid	Methadone	PO (acute, intermediate, chronic administration)	Post-addict volunteers	Feces (n=12)	3.0, 7.4, 20.1 total and 0.14, 0.47, 1.2 unchanged (acute, intermediate, chronic, respectively)	N.D.	[151]
Anti-asthma	Montelukast	PO (^{14}C)	Healthy volunteers	Duodenal secretions suction at 2-8 and 8-12 hr post dose (n=6)	3-20 total	N.D.	[152]
Antiretroviral	Lopinavir	PO (^{14}C in combination with ritonavir)	Healthy volunteers	Feces (n=5)	82.6 total, 19.8 unchanged (0-8 days)	N.D.	[153]
	Ritonavir	PO (^{14}C)	Healthy males	Feces (n=5)	86.3 total, 33.8 unchanged (6 days)	N.D.	[154]
Antibiotic	Azlocillin	IV	Healthy volunteers	Duodenal perfusion (n=5)	3.4 as unchanged	Cl_{total}=173-375 Cl_{bile}=1.4-25.9 mL/min	[71]
	Ceftriaxone	IV	Healthy males	Duodenal perfusion for 6-8 hr (n=5)	11-65 total	Cl_{total}=9-20 Cl_{bile}=1-13 mL/min	[155]
	Mezlocillin	IV	Healthy volunteers	Duodenal perfusion (n=5)	29.9 unchanged	Cl_{total}=187-477 Cl_{bile}=45.8-122.8 mL/min	[71]

	Piperacillin	IV	[j]Cholecystectomy patients; [k]healthy volunteers	[j]T-tube (n=5); [k]duodenal aspiration (n=3)	[j]0.7 as total (12 hr); [k]0.41/1.1 unchanged/corrected by EF (6 hr)	[j]Cl_{total}=276 [j]Cl_{bile}=1.74 mL/min [k]Cl_{total}=2.9 [k]$Cl_{biliary}$=0.012 [k] *in vivo* $Cl_{biliary}$= 0.032 mL/min/Kg	j, 48 k, 84
	Quinupristin/ Dalfopristin	IV	Healthy volunteers	Feces (n=24)	74.4-77.5 total, <15 unchanged	Cl_{total}=0.83-0.87 Cl_{total}=0.85-0.82 L/hr/Kg	156
	Temocillin	IV	Healthy volunteers	Duodenal perfusion (n=6)	2.2 unchanged (6 hr)	N.D.	70
	Trovafloxacin	PO (^{14}C)	Healthy volunteers	Feces (n=4)	63.3 total, 43.2 of total radioactivity as unchanged	N.D.	157

IV= intravenous administration
PO= oral administration
EF= gallbladder ejection fraction
in vivo $Cl_{biliary}$= biliary clearance corrected for EF

FIGURES

Fig 1.1: Macro-anatomy of the hepatobiliary system.

Bile flow into the gallbladder is facilitated by lower internal pressure when compared to the rest of the biliary tract (pressure values are in parenthesis[40]). Water and solutes are reabsorbed within the gallbladder.

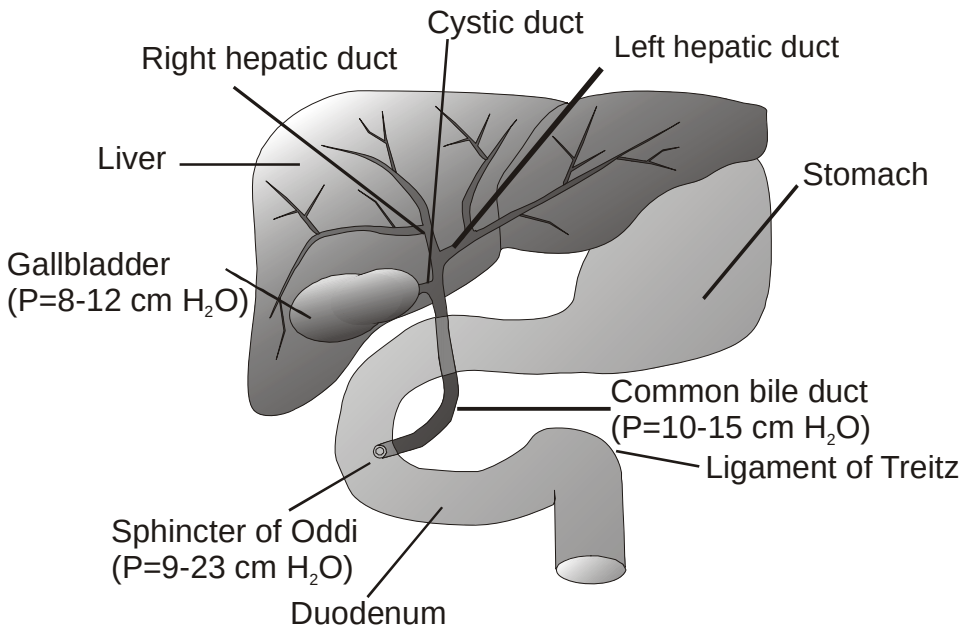

Fig 1.2: Micro-anatomy of the hepatobiliary tract.

(A) At the cellular level, hepatocytes are organized in cords and bathed by sinusoidal blood from the basolateral side; the canalicular membranes form the bile canaliculi. Bile flows in the opposite direction to blood and drains into bile ducts.

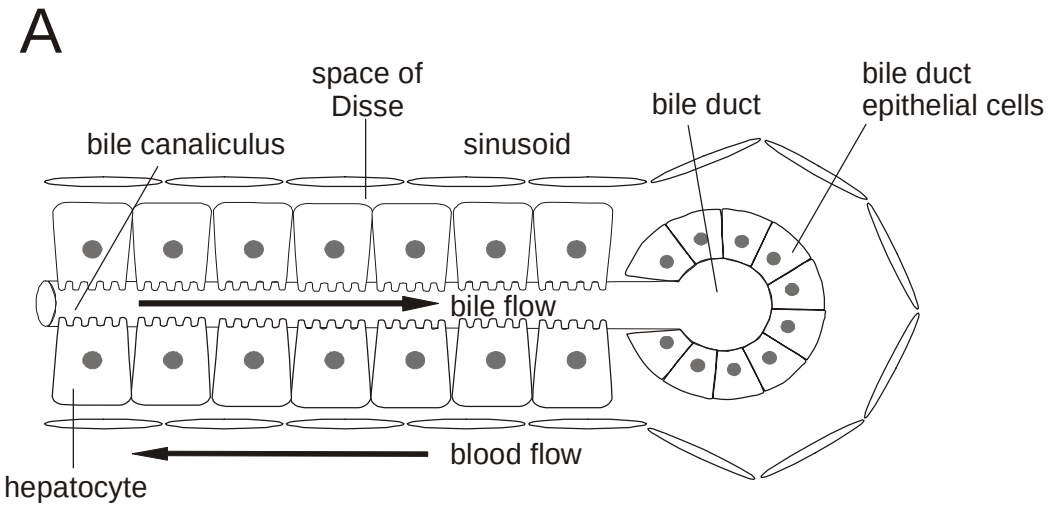

(B) An enlarged view of two hepatocytes from Figure A. Transport proteins are involved in the uptake and excretion of endogenous substances and xenobiotics into blood and bile. Filled symbols represent unidirectional primary active transport by ATP-binding cassette (ABC) transport proteins (Pgp, *ABCB1*; BSEP, *ABCB11*; BCRP, *ABCG2*; MRP2, *ABCC2*; MRP3, *ABCC3*; MRP4, *ABCC4*; MRP5, *ABCC5*; MRP6, *ABCC6*; ABCG5, *ABCG5*; ABCG8, *ABCG8*). Open symbols represent transport by members of the solute carrier protein families including the SLC family (OAT2, *SLC22A7*; OCT1, *SLC22A1*; NTCP, *SLC10A1*) and the SLCO family (OATP1B1, *SLCO1B1*; OATP1B3, *SLCO1B3*; OATP1A2, *SLC01A2*; OATP2B1, *SLCO2B1*). Each functional hepatocyte contains all the transport proteins depicted in this figure. Adjacent hepatocytes form tight junctions (TJ) to seal the canalicular domain from the basolateral domain.

B

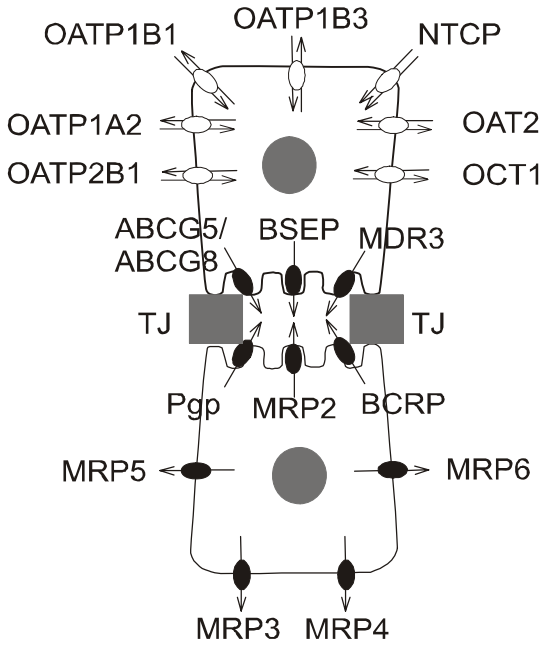

CHAPTER 2

A NOVEL METHOD FOR THE DETERMINATION OF BILIARY CLEARANCE IN HUMANS

This chapter was published in *The AAPS Journal* Volume 6, Issue 4, 33, 2004

ABSTRACT

Biliary excretion is an important route of elimination and the biliary tract is a potential site of toxicity for many drugs and xenobiotics. Quantification of biliary excretion in healthy human volunteers is logistically challenging and is rarely defined during drug development. The current study uses a novel oroenteric tube coupled with a specialized clinical protocol to examine the pharmacokinetics of ^{99m}Technetium (Tc-99m) mebrofenin, a compound that undergoes rapid hepatic uptake and extensive biliary excretion. A custom-made multi-lumen oroenteric tube was positioned in the duodenum of healthy human volunteers. Subjects were positioned under a gamma camera and 2.5 mCi of Tc-99m mebrofenin was administered intravenously. Duodenal aspirates, blood samples, and urine were collected periodically for 3 hours. Two hours after Tc-99m mebrofenin administration, the gallbladder was contracted with an intravenous infusion of cholecystokinin-8. Gamma scintigraphy was used to determine the gallbladder ejection fraction in each subject. Total systemic clearance of Tc-99m mebrofenin approximated liver blood flow (Cl_{total} 17.3 ± 1.7 mL/min/kg) and 35 to 84% of the Tc-99m mebrofenin dose was recovered in bile. However, when the data were corrected for the gallbladder ejection fraction, 71 to 92% of the *excreted* Tc-99m mebrofenin dose was recovered. This novel oroenteric tube and clinical protocol provide a useful method to quantify biliary excretion of xenobiotics in healthy human volunteers.

Keywords: oroenteric tube, gallbladder, Tc-99m mebrofenin, biliary excretion, biliary clearance

INTRODUCTION

With the advent of combinatorial chemistry, an increasing number of new chemical entities characterized by high molecular weight and lipophilicity are being synthesized and screened during the drug discovery process.[1] Drugs with these physicochemical characteristics often are associated with significant hepatic metabolism and excretion via the biliary route.[2] Therefore, new tools and techniques are needed to investigate and predict biliary excretion of investigational drugs in healthy human volunteers. Currently, limited information is available regarding the extent of biliary elimination of drugs and metabolites, primarily due to the difficulty in obtaining bile samples from healthy human subjects. Biliary excretion data would be extremely valuable in evaluating the contribution of biliary clearance to total systemic clearance, elucidating potential mechanisms of hepatobiliary toxicity, and examining enterohepatic recirculation. In addition, the FDA recently published guidelines detailing the requirements for drug-drug interaction studies necessary in New Drug Application submissions. These guidelines suggest that mechanisms of interactions should be explored, rather than simply performing observational studies.[3] Therefore, a method to investigate drug interactions that may occur during biliary elimination may increase the quality of information provided to registration agencies and help avoid the withdrawal of drugs from the market due to a serious, but foreseeable, drug interaction.

One valuable preclinical tool to investigate biliary clearance of drugs is the sandwich-cultured hepatocyte model. This model has been developed using rat and human hepatocytes to examine biliary excretion *in vitro*, and has been validated with *in vivo* data collected from rats.[4] However, the human *in vivo* data required to develop *in vitro-in vivo* correlation in biliary clearance for humans is lacking. This shortcoming is primarily a result of the

difficulty in obtaining biliary excretion data in humans, particularly in healthy human volunteers.

Historically, there has been little success in the development of valid and reliable techniques to quantify biliary excretion of drugs or endogenous compounds in humans. Such data may be obtained from patients suffering from gallbladder disease requiring removal of the gallbladder. Typically, patients are administered the drug of interest prior to surgery, and the amount of drug found in the gallbladder after removal is quantified.[5, 6] This approach only allows a single time point determination of drug content in bile. More commonly, studies employ patients that require a temporary bile shunt (T-tube) that diverts bile from the liver to a transcutaneous port for external collection.[7, 8] With this method, biliary excretion may be determined over time while the shunt is in place.

The major limitation of both of the above techniques is the use of patients with significant hepatobiliary disease as study subjects. Several studies have employed healthy human volunteers and oroenteric tubes to withdraw pancreatic-biliary secretions from the duodenum.[9] These studies have utilized occlusive balloons to facilitate more complete bile collection,[10] or have perfused non-absorbable markers into the duodenum to evaluate recovery.[11, 12] A significant advantage of these techniques is the ability to conduct studies in healthy human volunteers, particularly in light of the role of hepatobiliary transport proteins in hepatic drug disposition. Certain disease states may significantly influence transport protein expression, function, localization and/or bile flow along the bile canaliculi and bile ducts, thereby altering drug secretion and excretion patterns.[13-15]

Previous studies conducted in healthy human volunteers have resulted in incomplete and highly variable recovery of compounds excreted in bile.[10, 16] This is primarily a result of difficulties in obtaining and assessing the completeness of bile collection, and a lack of control over gallbladder contraction. Described here is a method using a novel oroenteric tube and specialized clinical protocol that facilitates efficient recovery of biliary secretions and optimal gallbladder refilling status and contractibility. The use of the gamma emitter ^{99m}Technetium (Tc-99m) mebrofenin as a probe compound in this study allowed real-time assessment of biliary excretion, gallbladder ejection fraction, and the efficiency of bile collection. This compound is available for intravenous administration, is not significantly metabolized, and is principally excreted unchanged in bile.

MATERIALS AND METHODS

Catheter design: A commercially available oroenteric catheter extrusion was modified according to the design in Figure 2.1 to aspirate secretions from the gastric and duodenal regions of the human gastrointestinal tract (Dentsleeve, Wayville, Australia). Briefly, the tube is a silicone multi-lumen extrusion 4.5 mm in diameter, 128 cm long, with 3 tungsten tip weights to facilitate passage of the tube through the pyloric sphincter. The distal/terminal end of the tube was fitted with a welded polyethylene balloon to facilitate migration of the tube during placement, and to ensure occlusion of the intestine during the bile collection period. The balloon (9 cm long x 4.7 cm wide uninflated) was single use and fitted to metal balloon attachment rings using 1.0 silk suture. Two of the large lumens of the extrusion (Figure 2.1, Panel A, lumens A and C) were dedicated to aspiration of secretions from the duodenal region, while lumen E was used for aspiration from the gastric region. Aspiration vacuum relief was provided by lumens B, D, and F. Lumen G was used to inflate/deflate the polyethylene balloon and lumen H provided a saline flush to reduce viscosity of the duodenal secretions. A radio-opaque pyloric marker was positioned 100 cm from the syringe connectors to facilitate correct placement of the tube under fluoroscopy.

Clinical Protocol: Four non-smoking volunteers (20-24 years of age; 3 male, 1 female) within 20% of ideal body weight (64.5-84.4 kg) completed the study. All procedures were approved by the Clinical Research Advisory Committee and the Committee on the Protection of the Rights of Human Subjects of the University of North Carolina (UNC) at Chapel Hill School of Medicine. Subjects provided written informed consent prior to participation in the study, and were healthy as indicated by their medical history, physical examination, routine laboratory tests, and electrocardiogram. Subjects were asked to abstain from any medication

(with the exception of oral contraceptives) for 2 weeks prior to the study, and to abstain from caffeine and alcohol during the study. Subjects were admitted to the General Clinical Research Center of UNC Hospitals the evening before the study and given a high fat meal (~55 grams of fat) at 18:00 hours and a high fat snack (~45 grams of fat) at 23:00 hours. Subjects then remained fasted until the end of the study. At 06:00 the following morning, the oroenteric tube was passed through the mouth and positioned with the aid of dynamic fluoroscopic radiography (ICONOS R200, Siemens, Hoffman Estates, IL). Correct placement of the tube was judged by the position of the pyloric marker (right hand margin of spine) and the tip weights (immediately distal to the Ligament of Treitz) (Figure 2.2). Subjects were then positioned supine under a gamma camera (E-CAM Dual Head Gamma Camera, Siemens), baseline blood, urine and bile samples were collected; and the occlusive polyethylene balloon was inflated with ~ 20 mL of air until the subjects experienced mild discomfort. Subjects were then administered a 2.5 mCi IV bolus dose of Tc-99m mebrofenin (Squibb Diagnostics, Princeton, NJ) via a forearm vein indwelling catheter (specific activity 0.8-1.1 mCi/mg at time of preparation). Blood samples (3 mL) were collected at 1, 2.5, 5, 7.5, 10, 20, 40, 60, 80, 100, 120, 140, 165 and 180 minutes post-dose from the contralateral arm. Biliary secretions collected from the occluded duodenal region were continuously aspirated and pooled over the following intervals: 0-5, 5-10, 10-30, 30-50, 50-70, 70-90, 90-110, 110-120, 120-130, 130-150, 150-180 minutes post-dose. Anterior gamma scintigraphic images of the abdomen were acquired under dynamic mode at 1-minute intervals and analyzed using ESOFT 2.5 software (Siemens). Two hours post Tc-99m mebrofenin administration, cholecystokinin-8 (sincalide, 0.02 μg/kg, Bracco Diagnostics, Princeton, NJ) was administered as an IV infusion over 30 minutes to facilitate contraction of

the gallbladder. Cholecystokinin-8 is an octa-peptide derived from cholecystokinin and has a very short duration of action (half-life in blood of 2.5 minutes).[17, 18] Urine was collected at the conclusion of the sampling period (180 minutes).

Whole blood radioactivity was determined by gamma scintillation counting (Quantum-8 Multichannel Analyzer, Oak Ridge, TN). Bile collected over each interval, and an aliquot of urine, were analyzed by a CRC-15R dose calibrator (Capintec, Ramsay, NJ). All samples were corrected for decay based on the Tc-99m half-life of 6.01 hours. Linearity of the gamma camera response was assessed utilizing 250 mL saline bags injected with pre-determined amounts of radioactivity (0.5 - 3 mCi) measured with a CRC-15R dose calibrator.

Data Analysis: A duplicate dose of Tc-99m mebrofenin was prepared at the same time as the dose administered to the subject and used for calculation of the "theoretical dose". This reference standard also was used to convert the units of the whole blood radioactivity from counts per minute (cpm) to nCi, in order to obtain a more quantitative measurement of the amount of radioactivity present in blood. After assessing the radioactivity remaining in the syringe, IV tubing, and catheter, the "administered dose" was then calculated by difference. Biliary recovery and urinary recovery were calculated as the percentage of the administered dose that accumulated in bile and urine, respectively, 180 minutes after dosing. A gallbladder ejection fraction (EF) was calculated from planar scintigraphic images using the following equation:

$$Ejection\ Fraction = \frac{\left(GB^{120\,\min}\right) - \left(GB^{150\,\min}\right)}{\left(GB^{120\,\min}\right)} \qquad (1)$$

where *GB* represents the counts per minute in the gallbladder region of the image pre- (time=120 minutes) and post- (time=150 minutes) infusion of cholecystokinin-8.

In order to account for the variable contractile response of the gallbladder, the total amount of radioactivity collected from the duodenal region during the 30 minute infusion of cholecystokinin-8 was divided by the ejection fraction. This correction accounted for the Tc-99m mebrofenin remaining in the gallbladder after contraction. Addition of this value to the cumulative amount of Tc-99m mebrofenin collected in the first 120 minutes of the study represented the total amount of Tc-99m mebrofenin transported from the liver into bile, and the amount that would have been collected if the gallbladder were to contract completely.

$$\%\ Recovery\ of\ Excreted\ Dose = \frac{100\%}{X^{0}} \times \left(X_{Bile}^{0-120\,min} + \frac{X_{Bile}^{120-150\,min}}{EF} \right) \qquad (2)$$

where X^0 represents the administered dose; X_{Bile} the amount of Tc-99m mebrofenin recovered in biliary secretions collected over the time interval specified; and EF is the ejection fraction. Therefore, $\frac{X_{Bile}^{120\text{-}150\,min}}{EF}$ estimates the total amount of Tc-99m mebrofenin that would have been collected from the duodenal region if the *EF*=1. This corrected amount, expressed as a percentage of the administered dose, represented the recovery of Tc-99m mebrofenin *excreted* from the gallbladder during the study, and assumes that no additional Tc-99m mebrofenin remains to be excreted into the duodenum from 150 to 180 minutes. Therefore this value can therefore provide an estimate of recovery efficiency and performance of the oroenteric tube.

Pharmacokinetic data analysis: Blood activity-time profiles were analyzed by non-compartmental analysis using WinNonlin (version 4.1, Pharsight Corp., Mountain View, CA). The frequency of the blood sampling at the beginning of the experiment and the slow clearance of radioactivity from the injection site allowed the characterization of Tc-99m mebrofenin distribution into the systemic circulation. Therefore, the kinetics of

administration were modeled as an IV infusion of duration T_{max} to account for this observation. The area under the blood concentration time curve (AUC) was calculated using the linear trapezoidal rule, and where appropriate, extrapolated to infinity using the slope obtained from linear regression of the last 5 to 6 time points. Total blood clearance of Tc-99m mebrofenin was determined as the ratio of the administered dose and the AUC extrapolated through infinite time. Biliary clearance was determined as the ratio of the cumulative amount of Tc-99m mebrofenin recovered in bile from 0 to 180 minutes (not corrected for EF) and the AUC from 0 to 180 minutes.

RESULTS

Proper positioning of the oroenteric tube required between 0.5 and 2 hours. However, 1 subject failed to pass the tube through the pylorus and into the duodenum in the allocated time and, therefore, did not complete the study. Correct positioning of the oroenteric tube was confirmed by fluoroscopic radiography. A representative image of the tube located in the correct anatomical position is shown in Figure 2.2. The marker at the pyloric sphincter and the tungsten tip weights just beyond the Ligament of Treitz (immediately preceded by the 2 balloon attachment rings) are clearly visible.

As expected, rapid and extensive biliary excretion of Tc-99m mebrofenin was observed. As evident in animated Figure 2.3 (Panels A, B, C and D), after IV administration Tc-99m mebrofenin was rapidly taken up into the liver, secreted into the canalicular space, and collected in the common bile duct and gallbladder. Despite the consistency in the rate and extent of Tc-99m mebrofenin accumulation in the gallbladder, each subject exhibited a different pattern of bile secretion into the intestine, presumably due to differing spontaneous contraction patterns of the gallbladder.[19] These differing release patterns of Tc-99m mebrofenin in bile are evident in animated Figure 2.3 and in the profiles shown in Figure 2.4. Subject 1 did not expel Tc-99m mebrofenin from the gallbladder until administration of cholecystokinin-8 at 120 minutes, whereas subjects 2 and 4 exhibited partial spontaneous contraction of the gallbladder prior to cholecystokinin-8. Of interest, Subject 3 immediately ejected bile and Tc-99m mebrofenin into the intestine before accumulation in the gallbladder, and did not respond to cholecystokinin-8 as quickly or to the same extent as the other subjects.

The gamma camera images obtained during the study allow a visual, subjective assessment of tube performance and indicate that the biliary and duodenal secretions were efficiently and entirely removed via the duodenal aspiration ports. Specifically, Tc-99m mebrofenin and bile accumulated in a small segment of the duodenum and were not visible in more distal regions of the intestinal tract (Figure 2.3, Panels B, C, and D). At times, Tc-99m mebrofenin was recovered as quickly as it was expelled from the gallbladder, resulting in little accumulation of radioactivity in the duodenal region (Figure 2.3, Panel D). In subject 1, the scintigraphic images also allowed visualization of a small amount of Tc-99m mebrofenin that leaked beyond the occlusive balloon after cholecystokinin-8 administration (Figure 2.3, Panel A). This observation corresponded with a lower recovery of Tc-99m mebrofenin in subject 1 (Table 2.1). Static gamma camera images of subject 2 pre-cholecystokinin-8 and post-cholecystokinin-8 (Figure 2.5) clearly illustrate the efficiency of the oroenteric tube in removing Tc-99m mebrofenin and bile from the duodenum.

At the conclusion of the sampling period (180 minutes post dose), residual radioactivity was evident in the gallbladder, consistent with incomplete emptying of the gallbladder after contraction.[18, 20] Using planar images obtained before and after cholecystokinin-8 administration, the gallbladder ejection fraction was determined (Table 2.1). With the exception of subject 3, remarkably large and consistent ejection fractions were obtained. The extent of Tc-99m mebrofenin recovered in aspirated bile exhibited high inter-subject variability (35-84% of the administered dose); however, once corrected for the gallbladder ejection fraction, the recovery of *excreted* Tc-99m mebrofenin was consistently high (84.2 ± 9.3%, Table 2.1).

The blood concentration-time profiles, bile amount-time profiles and the amount in urine at 180 minutes for subjects 1, 2, 3, and 4 are shown in Figure 2.4, Panels A, B, C, and D, respectively. The blood profiles are similar in all subjects; C_{max} was followed by a rapid distributional phase and polyexponential decay. A terminal monoexponential decay phase was not clearly evident after 3 hours of sampling. Table 2.1 summarizes the pharmacokinetic parameters obtained. Systemic exposure and total body clearance were comparable in all subjects, and biliary clearance ranged from 7.8 to 15.6 mL/min/kg (Table 2.1). The fraction of total clearance that can be attributed to biliary excretion is numerically equivalent to the biliary recovery (expressed as percentage of dose) of Tc-99m mebrofenin reported in Table 2.1, averaging 78% in subjects that responded to cholecystokinin-8 (subjects 1, 2, and 4). The variability in biliary clearance was due primarily to incomplete excretion of Tc-99m mebrofenin from the gallbladder during the collection period. The total amount of Tc-99m mebrofenin recovered in urine 3 hours post dose was very low (0.6 % ± 0.2%).

DISCUSSION

This study used a customized oroenteric tube and tailored clinical protocol to validate successfully an experimental procedure that allowed efficient collection of biliary secretions from healthy human volunteers. In a previous pilot study, only modest outcomes were obtained: gallbladder ejection fractions after cholecystokinin-8 administration were abnormally low, and the oroenteric tube utilized failed to completely collect biliary secretions. It was hypothesized that the lack of response to cholecystokinin-8 in the pilot study was a result of the prolonged fasting period required by the protocol (the intubation procedure took place the night before the study), while the incomplete biliary recovery was due to the design of the tube and the absence of an occlusive balloon. The clinical protocol designed in the present study sought to maintain a more physiologically normal gallbladder refilling state, thereby maximizing the response to cholecystokinin-8. With the exception of subject 3, subjects responded to the infusion of cholecystokinin-8 in a manner typical for healthy volunteers, with gallbladder ejection fractions greater than 0.8.[17] To optimize the filling status of the gallbladder during the study, subjects received a high fat evening meal and snack ~ 15 and 9 hours, respectively, prior to Tc-99m mebrofenin administration. This proved to be a successful method to ensure refilling of the gallbladder the following day, as evidenced by the rapid accumulation of Tc-99m mebrofenin in the gallbladder. These results suggested that the gallbladder was not overfilled, a state often associated with reduced bile flow, poor accumulation of cholecystographic agents in the gallbladder, and in some cases, significant spontaneous contraction of the gallbladder in inter-digestive states.[21]

The oroenteric tube design utilized in the current study, and the presence of an occlusive balloon, allowed for more complete recovery of biliary secretions; a high percentage of the

administered dose was collected in bile in subjects 1, 2, and 4 (Table 2.1). Unfortunately, only the theoretical dose was determined for subject 1, and a small amount of bile containing Tc-99m mebrofenin leaked past the occlusive balloon (Figure 2.3), thus a lower than expected recovery of Tc-99m mebrofenin was determined for this subject (Table 2.1).

The calculated ejection fraction theoretically represents the fraction of gallbladder content that is expelled into the intestine following infusion of cholecystokinin-8. Radioactivity remaining in the gallbladder after contraction, therefore, represents the amount of Tc-99m mebrofenin irreversibly removed from the systemic circulation that has not yet been excreted into the intestine. By correcting the amount of Tc-99m mebrofenin collected in the bile during the infusion of cholecystokinin-8 by the ejection fraction, and adding this value to the biliary recovery from 0 to 120 minutes, the subsequent recovery of Tc-99m mebrofenin represents the proportion of the administered dose that was collected by the oroenteric tube and is defined as *excreted* dose. The recovery of *excreted* Tc-99m mebrofenin was high and exhibited less variability, ranging from 70.9% to 91.9% of the administered dose across all subjects. These results are consistent with the extent of biliary excretion of Tc-99m mebrofenin in humans (98% in 24 hours).[22] The correction for incomplete gallbladder ejection takes into account a poor or incomplete response to cholecystokinin-8 (as observed for subject 3), and demonstrates the efficiency of the oroenteric tube to collect *excreted* Tc-99m mebrofenin from the duodenal region.

The Tc-99m mebrofenin blood concentration-time profiles exhibited polyexponential decay (Figure 2.4), and a non-compartmental approach was employed to obtain primary pharmacokinetic parameters (Table 2.1). The total systemic clearance of Tc-99m mebrofenin (17.3 ± 1.7 mL/min/kg) approximated liver blood flow in humans (21 mL/min/kg)[23], and was

in agreement with previously published animal and human data.[24] The calculated biliary clearance for subjects 1, 2, and 4 was 14.0 ± 2.2 mL/min/kg, consistent with the high biliary excretion of Tc-99m mebrofenin, and represented over 66% of the total body clearance observed in these subjects. The poor ejection fraction observed in subject 3 resulted in a lower recovery of Tc-99m mebrofenin, and subsequently, a lower biliary clearance (7.8 mL/min/kg), representing only 35% of the total body clearance for this subject. It is clear that if bile could be collected for a longer time period, eventually all but a fraction of the dose would be recovered in bile. However, owing to practical constraints, it is not possible to keep the balloon inflated for more than 3 to 4 hours. Therefore, quantitative assessment of the gallbladder ejection fraction is vital to the correct interpretation of the biliary clearance value obtained in time-constrained studies such as those described here. Similarly, although samples were collected only for 180 minutes, the cumulative amount of Tc-99m mebrofenin excreted in the urine (0.6 % ± 0.2%) was consistent with that reported in the literature (2% over 24 hours).[22]

In conclusion, the oroenteric tube and clinical protocol developed in this study represent a useful method to investigate the biliary excretion of the probe drug Tc-99m mebrofenin. The custom-made oroenteric tube fitted with an occlusive balloon allowed extremely efficient recovery of biliary secretions from the duodenum. The approach described in this study uses a combination of gamma scintigraphy and a carefully designed clinical protocol to overcome variability in biliary excretion and gallbladder responsiveness to cholecystokinin-8 observed in previous studies.[10, 16] A similar experimental design may be used to investigate the biliary excretion of a variety of endogenous compounds and xenobiotics (including investigational

drugs) and to calculate biliary clearance, a pharmacokinetic parameter that previously has been difficult to estimate or predict in healthy human subjects.

AKNOWLEDGEMENTS

The authors would like to acknowledge the technical assistance of Mrs. Ann Whitlow, Mr. Jonathan Simpson, Ms. Jennifer Barner and Professor C. Barry Burns. This work was supported in part by an R01 grant (GM41935) National Institutes of Health from (Bethesda,MD) and a grant (RR00046) from the General Clinical Research Centers program of the Division of Research Resources, National Institutes of Health. Brendan M. Johnson was supported by a Clinical Pharmacokinetic/Pharmacodynamics fellowship sponsored by the University of North Carolina in collaboration with GlaxoSmithKline, research Triangle Park, NC.

REFERENCES

1. Lipinski CA, Lombardo F, Dominy BW, and Feeney PJ. Experimental and computational approaches to estimate solubility and permeability in drug discovery and development settings. Adv. Drug Deliv. Rev. 2001; 46:3-26.

2. Fleck C and Braunlich H. Factors determining the relationship between renal and hepatic excretion of xenobiotics. Arzneimittelforschung. 1990; 40:942-946.

3. US Food and Drug Administration Center for Drug Evaluation and Research, Information Guidance for Industry: In Vivo Drug Metabolism/Drug Interaction Studies-Study Design, Data Analysis, and Recommendations for Dosing and Labeling Drug, Rockville,MD: FDA information branch. November 1999

4. Liu X, Chism JP, LeCluyse EL, Brouwer KR, and Brouwer KL. Correlation of biliary excretion in sandwich-cultured rat hepatocytes and in vivo in rats. *Drug Metab. Dispos.* 1999; 27:637-644.

5. Acocella G, Mattiussi R, Nicolis FB, Pallanza R, and Tenconi LT. Biliary excretion of antibiotics in man. *Gut* 1968; 9:536-545.

6. Westphal JF, Brogard JM, Caro-Sampara F, Adloff M, Blickle JF, Monteil H, and Jehl F. Assessment of biliary excretion of piperacillin-tazobactam in humans. *Antimicrob. Agents Chemother.* 1997; 41:1636-1640.

7. Lorenz D, Lucker PW, Mennicke WH, and Wetzelsberger N. Pharmacokinetic studies with silymarin in human serum and bile. *Methods Find. Exp. Clin. Pharmacol.* 1984; 6:655-661.

8. Brookman LJ, Rolan PE, Benjamin IS, et al Pharmacokinetics of valsartan in patients with liver disease. *Clin. Pharmacol. Ther.* 1997; 62:272-278.

9. Strasberg SM, Harvey PR, and Hofmann AF. Bile sampling, processing and analysis in clinical studies. *Hepatology.* 1990; 12:176S-180S; discussion 180S-182S.

10. Ryde M and Gustavsson S. Biliary excretion of olsalazine sodium in humans. *Eur. J. Drug Metab. Pharmacokinet.* 1987; 12:17-24.

11. Gundert-Remy U, Frohnapfel F, Jourdan W, Weber E, and Stiehl A. Estimation of biliary excretion of ureidopenicillins in healthy volunteers using marker dilution technique. *Br. J. Clin. Pharmacol.* 1982; 13:795-801.

12. Caldwell JH and Cline CT. Biliary excretion of digoxin in man. *Clin. Pharmacol. Ther.* 1976; 19:410-415.

13. Keitel V, Nies AT, Brom M, Hummel-Eisenbeiss J, Spring H, and Keppler D. A common Dubin-Johnson syndrome mutation impairs protein maturation and transport activity of MRP2 (ABCC2). *Am. J. Physiol. Gastrointest. Liver Physiol.* 2003; 284:G165-G174.

14. Lecureur V, Courtois A, Payen L, Verhnet L, Guillouzo A, and Fardel O. Expression and regulation of hepatic drug and bile acid transporters. *Toxicology.* 2000; 153:203-219.

15. Simons FE, Watson WTA, Minuk GY, and Simons KJ. Cetirizine pharmacokinetics and pharmacodynamics in primary biliary cirrhosis. *J. Clin. Pharmacol.* 1993; 33:949-954.

16. Lanzini A, Pigozzi MG, Wuhrer A, Facchinetti D, Castellano M, Bettini L, Guerra UP, Beschi M, and Muiesan G. Quantitative measurement of biliary excretion and of gall bladder concentration of drugs under physiological conditions in man. *Gut.* 1989; 30:104-109.

17. Ziessman HA, Muenz LR, Agarwal AK, and ZaZa AA. Normal values for sincalide cholescintigraphy: comparison of two methods. *Radiology*. 2001; 221:404-410.

18. Ziessman HA. Cholecystokinin cholescintigraphy: clinical indications and proper methodology. *Radiol. Clin. North Am.* 2001; 39:997-1006.

19. Jazrawi RP. Review article: measurement of gall-bladder motor function in health and disease. *Aliment. Pharmacol. Ther.* 2000; 14:27-31.

20. Lanzini A, Jazrawi RP, and Northfield TC. Simultaneous quantitative measurements of absolute gallbladder storage and emptying during fasting and eating in humans. *Gastroenterology.* 1987; 92:852-861.

21. Choletec package insert. Bracco Diagnostic, Inc. Princeton (NJ); 1994.

22. Krishnamurthy S and Krishnamurthy GT. Technetium-99m-iminodiacetic acid organic anions: review of biokinetics and clinical application in hepatology. *Hepatology*. 1989; 9:139-153.

23. Gibaldi MP, Perrier D. *Pharmacokinetics*. New York: Marcel Dekker Inc.; 1982.

24. Daniel GB, Bahr A, Dykes JA, DeNovo R, Young K, and Smith GT. Hepatic extraction efficiency and excretion rate of technetium-99m-mebrofenin in dogs. *J. Nuclear Med.* 1996; 37:1846-1849.

TABLES

Table 2.1: Summary of Tc-99m mebrofenin dose, recovery, gallbladder ejection fraction, and pharmacokinetic parameters for Subjects 1, 2, 3, and 4.

	Subject 1	Subject 2	Subject 3	Subject 4	Mean	S.D.
Theoretical Dose (μCi)	2188	2498	2500	2497	2421	155
Administered Dose (μCi)	-[a]	2072	2282	2476	2277	202
Biliary Recovery (% of dose[b])	65.5	84.3	35.2	83.5	67	23
Urinary Recovery (% of dose[b])	0.7	0.5	0.8	0.5	0.6	0.2
Total Recovery (% of dose[b])	66.2	84.8	36	84	67.8	22.8
Ejection Fraction (EF)	0.82	0.86	0.03	0.86	0.64	0.4
Recovery of *Excreted* Dose (% of dose[b])	70.9	89.1	91.9	-84.9	84.2	9.3
$AUC_{0-\infty}$ (nCi.min/mL)	1466	1613	1422	2305	1701	410
Cl_{total} (mL/min/kg)	16.4	16.2	19.9	16.7	17.3	1.7
AUC_{0-180} (nCi.min/mL)	1371	1462	1279	2054	1542	350
$Cl_{biliary}$ (mL/min/kg)	11.5	15.0	7.8	15.6	12.5	3.6

[a]Not determined, all calculations based on theoretical dose.

[b]Administered dose, where available.

FIGURES

Figure 2.1: (A) Cross-sectional diagram of the oroenteric tube. Lumen labels correspond to the following functions: A, duodenal aspiration 1; B, duodenal aspiration 1 vacuum relief; C, duodenal aspiration 2; D, duodenal aspiration 2 vacuum relief; E, gastric aspiration; F, gastric aspiration vacuum relief; G, balloon inflation; H, saline flush.

A

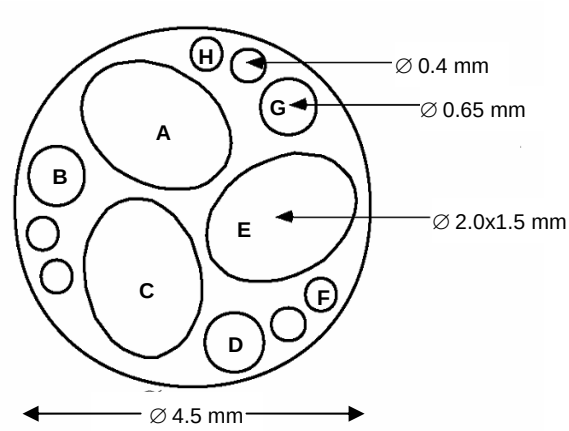

(B) Schematic of oroenteric tube. Syringe connector labels correspond to the following channels: I, duodenal aspiration 1 and 2; II, gastric aspiration; III, duodenal aspiration 1 and 2 vacuum relief; IV, gastric aspiration vacuum relief; V, balloon inflation/deflation; VI, saline flush.

B

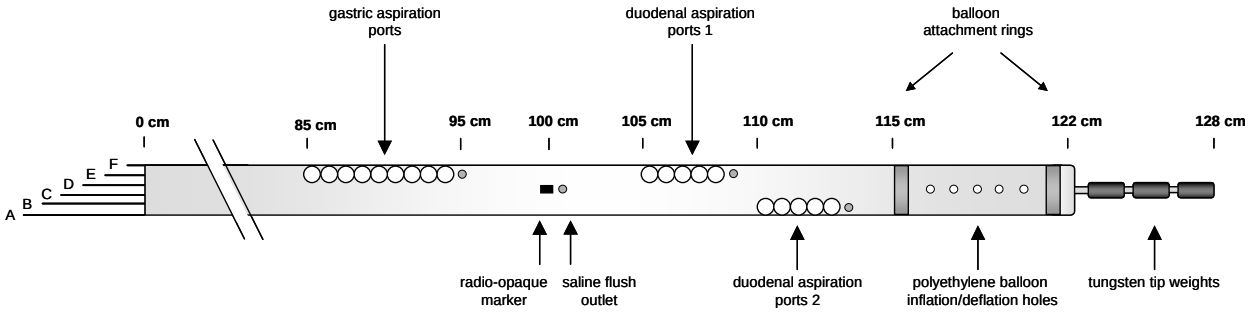

Figure 2.2: A representative fluoroscopic image of the oroenteric tube correctly positioned. Arrows indicate the following: A, radio-opaque marker at the pyloric sphincter; B, balloon attachment rings; C, tungsten tip weights positioned at the Ligament of Treitz.

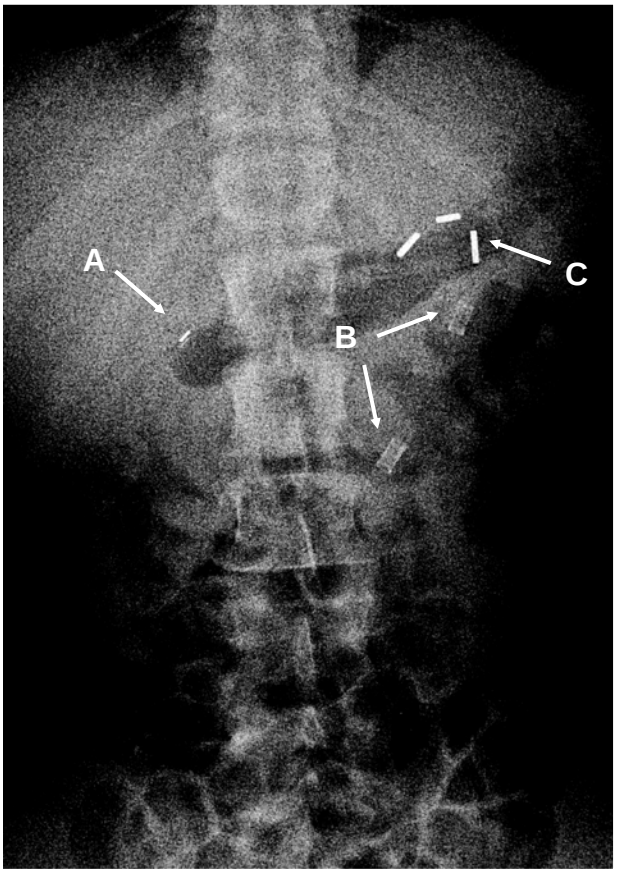

Figure 2.3: Animated gamma scintigraphic images of Tc-99m mebrofenin disposition (from 0 to 180 minutes): A, subject 1; B, subject 2; C, subject 3; D, subject 4. Hepatic uptake of Tc-99m mebrofenin was rapid, followed by excretion into the canalicular space and accumulation in the gallbladder. Gallbladder contraction, facilitated by cholecystokinin-8 IV infusion at 120 minutes, resulted in expulsion of bile containing Tc-99m mebrofenin from the gallbladder into the duodenum and subsequent aspiration via the oroenteric tube. Online link to animation: http://www.aapsj.org/articles/aapsj0604/aapsj060433/aapsj060433_figure3.htm

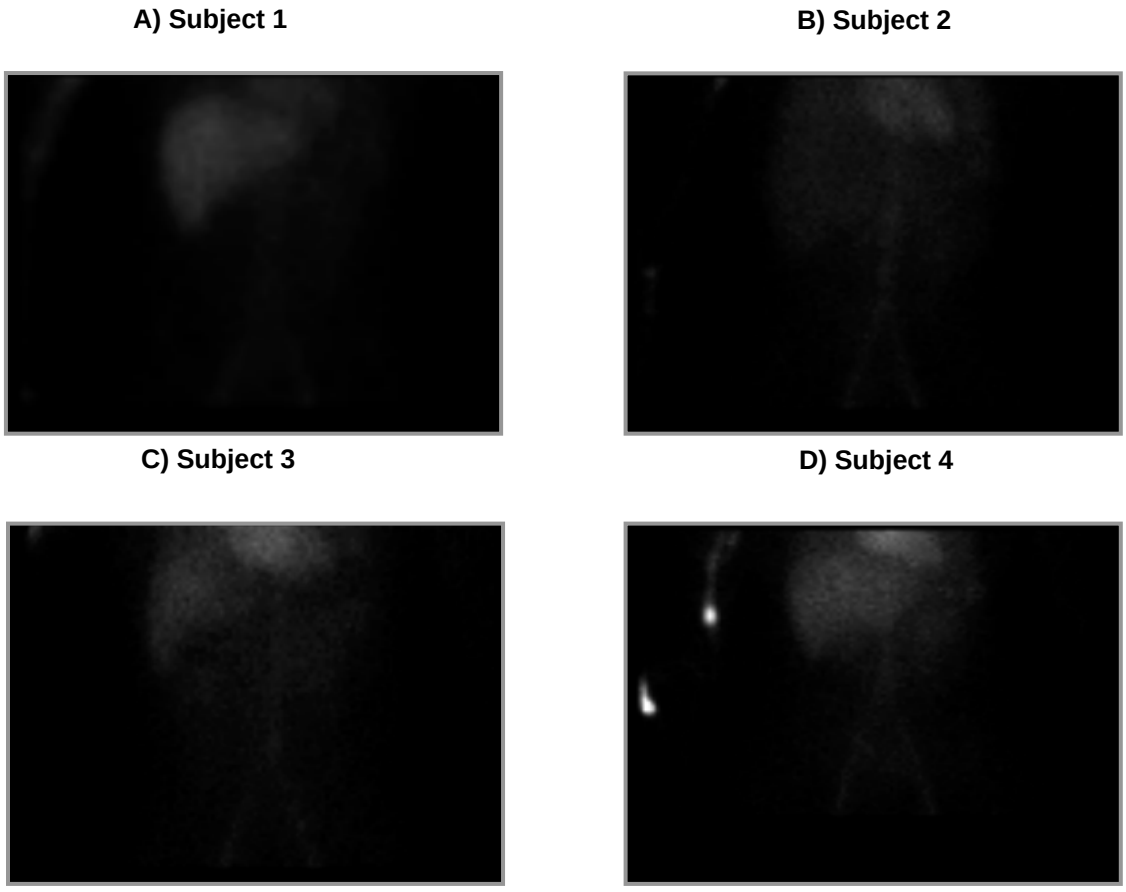

Figure 2.4: Tc-99m mebrofenin blood concentration (circles) and amount in bile (triangles) vs. time profiles, and the amount in urine at 180 minutes (diamonds): A, Subject 1; B, Subject 2; C, Subject 3; D, Subject 4. Cholecystokinin-8 was administered at 120 minutes as a 30 minute IV infusion to facilitate contraction of the gallbladder

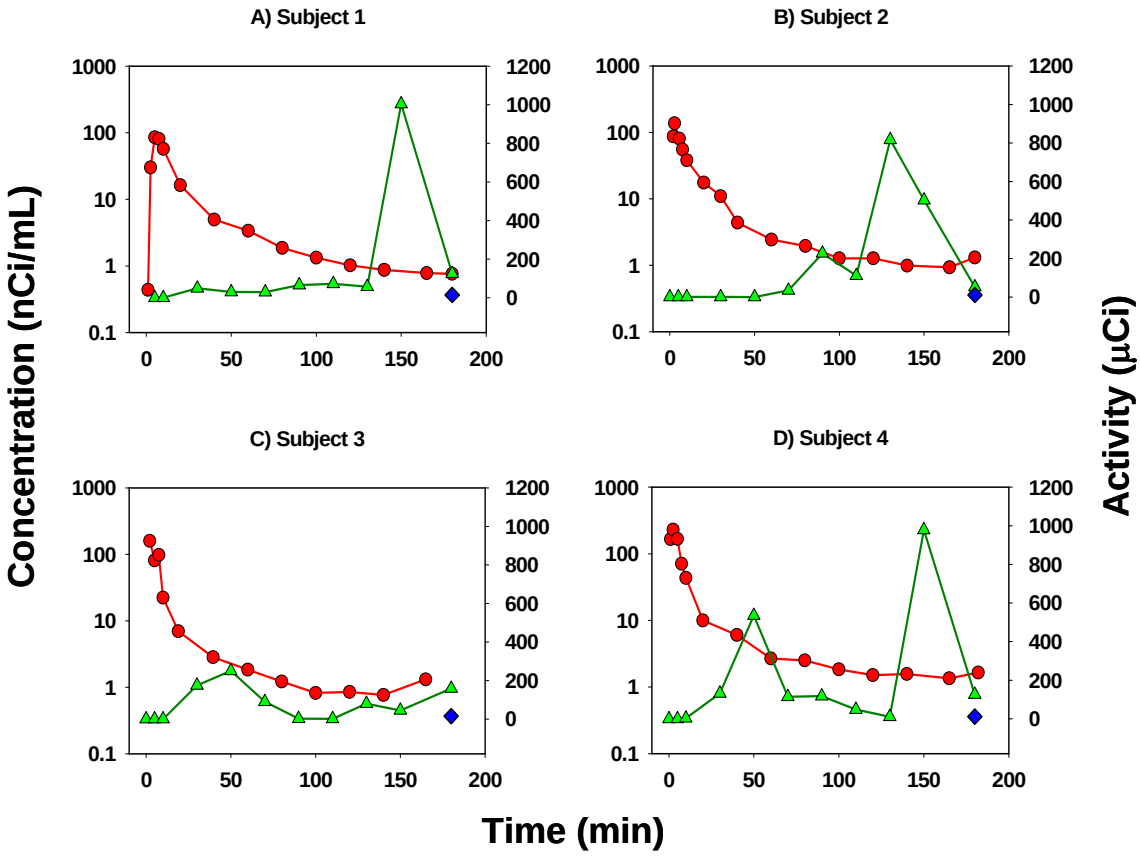

Figure 2.5: Static gamma camera images of Subject 2 at 80 and 160 minutes after administration of Tc-99m mebrofenin. Tc-99 mebrofenin accumulation in the intestine after 80 minutes was aspirated efficiently via the oroenteric tube as limited radioactivity was present in the intestine by 160 minutes.

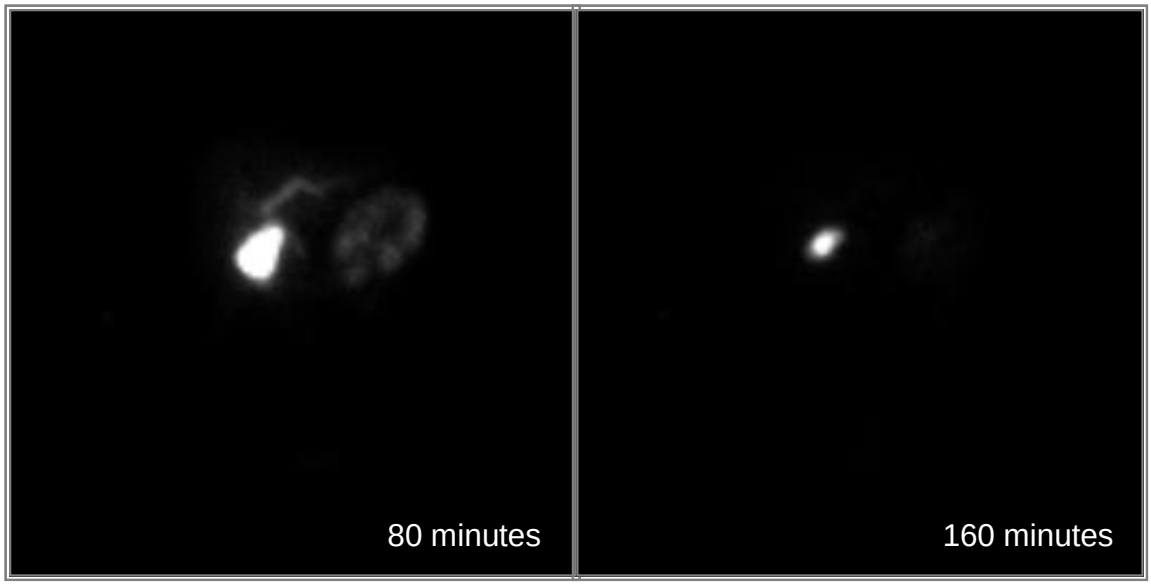

CHAPTER 3

IN VITRO CHARACTERIZATION AND PHARMACOKINETIC MODELING OF TC-99m MEBROFENIN HEPATOBILIARY DISPOSITION IN HUMANS AND RELEVANCE IN DISEASE STATES

This Chapter will be submitted to *Pharmaceutical Research* and is presented in the style of that journal.

ABSTRACT

Purpose: This study was conducted to characterize the disposition of the hepatobiliary scintigraphy agent Tc-99m mebrofenin in humans using *in vitro* tools and pharmacokinetic modeling.

Methods: Four healthy volunteers received 2.5 mCi of Tc-99 mebrofenin intravenously and blood, urine and bile were collected over time. *Xenopus laevis* oocytes and membrane vesicles prepared from HEK293 cells were used to identify transport proteins involved in Tc-99m mebrofenin transport. Several compartmental pharmacokinetic models were developed to describe the clinical data. The pharmacokinetic model was used to simulate patho-physiological changes in drug disposition due to drug interactions and disease states.

Results: *In vitro* studies demonstrated that Tc-99m mebrofenin is a substrate for OATP1B1, OATP1B3, MRP2 and MRP3. These data support the hypothesis that OATPs are involved in the hepatic uptake of Tc-99m mebrofenin while MRP2 and MRP3 are responsible for excretion into bile and blood, respectively. Systemic and hepatic exposure to Tc-99m mebrofenin would be influenced markedly by hyperbilirubinemia, or altered canalicular or basolateral excretion based on simulations of disease states (e.g., Dubin-Johnson syndrome) or drug interactions at the level of the transport protein (e.g., inhibition or induction).

Conclusions: The pharmacokinetic model developed to describe Tc-99m mebrofenin disposition in humans can be used to predict drug interactions and alterations associated with disease states in Tc-99m mebrofenin disposition.

Keywords: Tc-99m mebrofenin, hepatobiliary disposition, pharmacokinetic modeling, Dubin-Johnson syndrome, OATP1B1, OATP1B3, MRP2, MRP3

INTRODUCTION

Tc-99m mebrofenin is an imino diacetic acid derivative (HIDA) commonly used in hepatobiliary scintigraphy (Fig 3.1). This class of agents was developed to couple selective liver uptake and rapid transit into bile with the gamma emitting properties of technetium-99m (1). Tc-99m mebrofenin is used commonly in nuclear medicine to evaluate hepatobiliary dysfunction associated with the gallbladder, although broader uses, such as the evaluation of hepatocyte viability *in vivo* (2, 3) and the detection of genetic diseases that could affect excretion of compounds into bile (4, 5), have been proposed by several investigators. The kinetics of hepatic uptake, secretion into bile and systemic disposition of Tc-99m mebrofenin and analogs have been studied using invasive techniques in animals (6, 7). However, only gamma images have been used to derive these kinetic parameters in clinical studies, typically performed in patients undergoing a hepatobiliary scan for diagnostic reasons. Thus, these data may not reflect normal disposition of these compounds (1, 8, 9). During the development of a clinical protocol to determine biliary excretion of drugs in humans, Tc-99m mebrofenin was administered as a model high biliary clearance compound to healthy volunteers (10).

Dubin-Johnson syndrome is an autosomal recessive genetic disease. Although generally asymptomatic, these patients present with mild icterus, bilirubinuria and an elevated serum bilirubin concentration with half of the serum bilirubin in the conjugated form (mainly as diglucuronide) (11, 12). Dubin-Johnson syndrome is caused by mutations in the MRP2 (ABCC2) gene, including several in the region coding for the nucleotide binding domains (13-16) and in other domains affecting expression, maturation and appropriate localization of the protein (17, 18). In these patients, MRP3 (ABCC3), an ABC transport

protein which is closely related to MRP2 and expressed on the basolateral membrane of hepatocytes, is present at higher levels than normal (19). Upregulation of MRP3 compensates for the lack of MRP2, and protects the liver from bilirubin conjugates and other organic anions that cannot be excreted into bile. TR^- rats are a naturally occurring strain of Mrp2-deficient Wistar rat that have impaired bilirubin excretion (absence of canalicular Mrp2) and enhanced basolateral expression of Mrp3 (20, 21).

Despite the extensive diagnostic use of Tc-99m mebrofenin, its hepatobiliary disposition has not been investigated fully. The involvement of MRP2/Mrp2 in the biliary excretion of Tc-99m mebrofenin and analogs is suggested by case reports indicating lack of visualization of the hepatobiliary tree after Tc-99m mebrofenin injection in Dubin-Johnson patients (4, 5, 22), and by reduced biliary excretion of Tc-99m HIDA in TR^- rats (23). The implication of OATP family members in the hepatic uptake of Tc-99m mebrofenin is supported by the finding that Tc-99m disofenin, an analog of mebrofenin, is taken up actively into the liver by a sodium-independent transport protein (24, 25).

The purpose of the current study was to characterize the mechanisms of hepatic uptake and excretion of Tc-99m mebrofenin using *in vitro* systems such as *Xenopus laevis* oocytes expressing OATP1B1 or 1B3, and membrane vesicles prepared from HEK293 cells transfected with MRP2 or MRP3. Moreover a pharmacokinetic model was developed to describe the kinetics of distribution and elimination of Tc-99m mebrofenin in healthy subjects, and to simulate changes in Tc-99m mebrofenin disposition that are associated with disease states such as hyperbilirubinemia and Dubin-Johnson syndrome. Changes in disposition of this agent that might occur due to drug-drug interactions also were simulated.

MATERIALS AND METHODS

Chemicals

Tc-99m mebrofenin (Choletec®, Bracco Diagnostics, Princeton, NJ) was prepared at the Nuclear Medicine pharmacy, UNC Hospital, and radiochemical purity was evaluated by TLC using instant thin layer chromatography with polysilicic acid (ITLS-SA) as a the stationary phase and 20% sodium chloride as the mobile phase. Solutions employed in the *in vitro* experiments had a radiochemical purity ≥ 90% (26). β-Estradiol 17-β-D-glucuronide ($E_2$17βG), rifampicin, AMP, ATP, pyruvic acid and gentamicin sulfate were purchased from Sigma Chemical Co (St. Louis, MO), creatine phosphate, creatine kinase, protease inhibitor cocktail (Complete™) were purchased from Roche Diagnostics (Indianapolis, IN), MK571 was purchased from Cayman Chemical Co (Ann Arbor, MI), [^{3}H]$E_2$17βG (39.8 Ci/mmol, purity > 97%) was obtained from Perkin Elmer Life Sciences (Boston, MA, USA), all other chemicals were of reagent grade and were readily available from commercial sources.

Oocyte Uptake Studies

Xenopus laevis oocytes injected with hOATP1B1 and hOATP1B3 cRNA were acquired from BD Bioscience (Transportocytes, BD Gentest™, Woburn, MA). In preliminary experiments, the suitability of uninjected oocytes versus water injected oocytes as controls was established. Upon receipt, oocytes were inspected visually and the viable cells were maintained for 24 hr at 18°C in oocyte Ringer's 2 buffer (OR-2: 82.5 mM NaCl, 2.5 mM KCl, 1 mM Na_2HPO_4, 3 mM NaOH, 1 mM $CaCl_2$, 1 mM $MgCl_2$, 1 mM pyruvic acid, and 5 mM HEPES, pH 7.6) supplemented with 0.05 mg/ml gentamicin sulfate, 1.5 mM sodium pyruvate and 5% heat-inactivated horse serum. Uptake was determined according to the method described in Bow et al. (27). In brief, oocytes were incubated at 18 to 22°C over 60

min in OR-2 containing Tc-99m mebrofenin (9-10 μCi/ml). Subsequently, the oocytes were rinsed three times in ice-cold OR-2 and placed into individual vials for immediate analysis of associated radioactivity by gamma scintillation counting using a TN-1750 Multichannel Analyzer (Tracor Northen, Middleton, WI). Tc-99m mebrofenin uptake was calculated in picoCi per oocyte. The effect of rifampicin (50 μM), a well-characterized inhibitor of OATP proteins, on Tc-99m mebrofenin uptake was measured at the 60-min time point.

MRP2 and MRP3 Expression Vectors and Transfections in HEK293 Cells

The construction of vectors containing MRP2 [pcDNA3.1(-)MRP2] and MRP3 [pcDNA3.1(+)MRP3] has been described previously (28, 29). pcDNA3.1(-)MRP2 and pcDNA3.1(+)MRP3 were a kind gift of Dr. Susan P.C. Cole (Queen's University, Kingston, ON, Canada) and were transfected into SV40 transformed human embryonic kidney cells (HEK293). HEK293 cells were seeded at $5.8x10^6$ cells per 162 cm^2 flask and transfected 24 hrs later with 16.8 μg of plasmid DNA using FuGENE 6 (Roche Diagnostics) according to the manufacturer's instructions. After 72 hr, cells were harvested as described previously (30).

Membrane Vesicle Preparation and Immunoblotting

Plasma membrane vesicles from MRP2 and MRP3 transfected HEK293 cells were prepared as described, with modifications (30). Briefly, cells were homogenized in buffer containing 250 mM sucrose, 50 mM Tris pH 7.5, 0.25 mM $CaCl_2$ and protease inhibitor cocktail tablets. Cells were disrupted by N_2 cavitation (5 min equilibration at 200 psi) and then released to atmospheric pressure and EDTA was added to 1 mM. The suspension was centrifuged at 800x*g* at 4˚C for 10 min and the supernatant was layered onto 10 ml of a 35% (w/w) sucrose, 50 mM Tris pH 7.4 cushion. After centrifugation at 10,000x*g* at 4˚C for 1 h, the interface

was removed and placed in a 25 mM sucrose, 50 mM Tris, pH 7.4 solution and centrifuged at 100,000x*g* at 4˚C for 30 min. The membranes were washed with Tris sucrose buffer (250 mM sucrose, 50 mM Tris, pH 7.4) and then resuspended by vigorous syringing with a 27-gauge needle. Protein concentrations were determined using a BCA protein assay (Pierce Chemical, Rockford, IL) and aliquots of membrane vesicles were stored at –80˚C.

[^{3}H]$E_2$17βG and Tc-99m mebrofenin Transport Studies

Transport assays were carried out by a rapid filtration method as described previously (31). Membrane vesicles (8 μg of protein per time point) were incubated at 37 ˚C in a final volume of 60 μl. The transport assay buffer used was Tris (50 mM, pH 7.5)/sucrose (250 mM), and contained ATP or AMP (4 mM), $MgCl_2$ (10 mM), creatine phosphate (10 mM), creatine kinase (100 μg/ml), and $E_2$17βG (120 nCi, 400 nM) or Tc-99m mebrofenin (2 μCi). At the indicated time points, 19 μl (for time courses) or 60 μl (single time points) of transport reaction mixture was removed and placed in 800 μl of Tris sucrose buffer and filtered through glass fiber filters (type A/E; Pall Life Sciences, East Hills, NY), washed twice, and radioactivity was quantitated by liquid scintillation counting (Packard Tricarb, Packard Corp., Meriden, CT,). Transport in the presence of AMP was subtracted from transport in the presence of ATP and reported as ATP-dependent $E_2$17βG or Tc-99m mebrofenin transport. The effects of potential modulators of Tc-99m mebrofenin transport [MK571 (50 μM) and $E_2$17βG (100 μM)] were measured at a single time point of 3 min.

In vitro Tc-99m mebrofenin protein binding

Plasma samples containing a range of concentrations of Tc-99m mebrofenin between 1 and 160 nCi/mL were obtained from a healthy subject participating in the clinical study described below. Samples were centrifuged (1000xg) at room temperature using Centrifree®

ultrafiltration devices equipped with YMT membranes (Millipore Corporation, Bedford, MA). Centrifugation in a fixed angle rotor varied from 3 to 5 min, depending on the time required to yield approximately 10% of the sample volume as ultrafiltrate. Initial studies were conducted to validate that Tc-99m mebrofenin did not bind to the device or the membrane.

Clinical study

Details on the study design and results have been reported previously (10). In brief, four healthy non-smoking volunteers within 20% of ideal body weight participated in this study. All procedures were approved by the Clinical Research Advisory Committee and the Committee on the Protection of the Rights of Human Subjects of the University of North Carolina at Chapel Hill School of Medicine. Subjects provided written informed consent prior to participation in the study. After an overnight fast, a custom-made oroenteric tube was passed through the mouth and positioned in the upper portion of the duodenum with the aid of dynamic fluoroscopic radiography. The oroenteric tube used in these studies was a silicone multi-lumen extrusion fitted at the distal end with a polyethylene balloon to occlude the intestine during bile collection; this tube has been described in detail previously (10). Subjects received a 2.5-mCi IV bolus dose of Tc-99m mebrofenin (Squibb Diagnostics, Princeton, NJ). Blood samples were collected at predetermined time points up to 180 min post dose. Biliary secretions were aspirated continuously and pooled over predetermined intervals up to 180 min post dose. Urine was collected at 180 min. Anterior gamma scintigraphic images of the abdomen were acquired under dynamic mode at 1-min intervals using a gamma camera (E-CAM Dual Head Gamma Camera, Siemens), and analyzed using ESOFT 2.5 software (Siemens, Hoffman Estates, IL). Two hr post Tc-99m mebrofenin

administration, cholecystokinin-8 (CCK-8; sincalide; 0.02 μg/kg; Bracco Diagnostics, Princeton, NJ) was administered as an IV infusion over 30 min to facilitate contraction of the gallbladder. A gallbladder ejection fraction (EF) value was calculated from the abdominal images.

Whole blood radioactivity was determined by gamma scintillation counting (Quantum-8 Multichannel Analyzer, Oak Ridge, TN). Bile and urine were analyzed by a CRC-15R dose calibrator (Capintec, Ramsay, NJ). All samples were corrected for decay based on the Tc-99m half-life of 6.01 hr.

Biliary and urinary recovery were calculated as the percentage of the administered dose that accumulated in bile and urine, respectively, 180 min after dosing. The biliary recovery of Tc-99m mebrofenin was corrected by EF to obtain the percentage of the excreted dose. This corrected value was used in the modeling to minimize inter-subject variability among volunteers associated with gallbladder response to CCK-8.

Pharmacokinetic modeling

A series of multicompartmental models was developed using the concentration- and mass-time profiles from subject 4, who had the most complete data set, to describe Tc-99m mebrofenin hepatobiliary disposition in healthy volunteers. The final model is shown in Fig 3.2. This model included a central compartment (V_c, C_c) that described the blood activity-time profiles, a peripheral compartment that represented the liver (X_{liver}), from which unidirectional elimination into bile (collected in the duodenum) was characterized by k_{20}. Urinary elimination was described by unidirectional elimination from the central compartment (k_{10}). k_{21} described the egress of Tc-99m mebrofenin from the liver into the central compartment. All processes were assumed to be linear and were represented by first-

order rate constants. Tc-99m mebrofenin was administered as a single IV bolus; although intense blood sampling at early time points captured the distribution into the systemic circulation, initial data points up to C_{max} were not considered in development of the pharmacokinetic model. The terminal elimination phase of the plasma profiles was truncated at 140 min because inclusion of concentrations beyond this time point in the regression analysis resulted in decreased values of R-square and the slope of the fitted line. Differential equations describing the mass balance of the compound in the compartments depicted in Fig 3.2 were fit simultaneously to blood, urine and bile activity time profiles using nonlinear least-squares regression (WinNonlin Pro version 4.2; Pharsight, Mountain View, CA). Model selection was based on Akaike's Information Criterion, the residual sum of squares, visual inspection of the residual plots and of model fitting to the concentration- and mass-time profiles. A weighting scheme was developed to account for the relative contribution of each data set to the overall number of data points, due to the disparity in the number of observations among the data-supported functions. Each data point was assigned a weight of $\frac{1}{y} \times (1-n)$ where n is the fraction of total number of data points that support a particular function. The following differential equations described Tc-99m mebrofenin disposition in healthy volunteers:

$$\frac{dC_c}{dt} = -k_{10} \times C_c - k_{12} \times C_c + k_{21} \times \frac{X_{liver}}{V_c} \qquad C_c^0 = \frac{X_0}{V_c}$$

$$\frac{dX_{liver}}{dt} = k_{12} \times V_c \times C_c - k_{20} \times X_{liver} - k_{21} \times X_{liver} \qquad X_{liver}^0 = 0$$

$$\frac{dX_{urine}}{dt} = k_{10} \times V_c \times C_c \qquad X_{urine}^0 = 0$$

$$\frac{dX_{bile}}{dt} = k_{20} \times X_{liver} \qquad X^{0}_{bile} = 0$$

Pharmacokinetic Simulations

Simulations were performed to explore the potential effect of disease states such as hyperbilirubinemia and Dubin-Johnson syndrome on the disposition of trace amounts of Tc-99m mebrofenin. Moreover, several potential clinical interactions with other xenobiotics at the hepatic uptake or efflux level were simulated. Using transfected *in vitro* systems, transport proteins that may play a role in the Tc-99m mebrofenin hepatobiliary disposition were identified. However, it was not possible to characterize the transport kinetic parameters (V_{max} and K_m values) with increasing concentrations of Tc-99m mebrofenin because of the amount of radioactivity that would be required to conduct these studies. For the simulations it was assumed that the rate constant k_{12} was associated with OATP-mediated hepatic uptake, k_{20} described MRP2-dependent canalicular efflux, and k_{21} was associated with hepatic basolateral efflux of Tc-99m mebrofenin. The effect of high blood levels of bilirubin and its conjugates on Tc-99m mebrofenin hepatobiliary disposition in the presence and absence of physiologic changes associated with Dubin-Johnson syndrome or extra-hepatic cholestasis was simulated through changes in the first-order rate constants obtained from pharmacokinetic modeling of the data from healthy subjects. Additionally, the potential effects of alterations in uptake and biliary excretion of Tc-99m mebrofenin in healthy subjects due to drug-drug interaction were investigated in cases in which agents such as cyclosporin A (MRP2 and OATP inhibitor), gemfibrozil (OATP1B1 inhibitor) and phenobarbital (Mrp3 inducer and Mrp2 inhibitor in the rat) would be co-administered with Tc-99m mebrofenin. The renal excretion of Tc-99m mebrofenin was assumed to be due only

to glomerular filtration. Therefore, k_{10} was not expected to be modified by the disease states or drug interactions investigated in these simulations.

In order to simulate the effect of the described pathologies or co-treatments on the disposition of Tc-99m mebrofenin, the following alterations were made:

1) Elevated plasma bilirubin may be associated with elevated Tc-99m mebrofenin plasma concentrations at 10 min, resulting in increased renal excretion at 3 and 24 hr (32). To describe competitive inhibition of Tc-99m mebrofenin uptake in the liver, $k_{12,}$ the rate constant associated with hepatic uptake, was lowered 10-, 5- and 2.5-fold.
2) MRP3 protein expression is induced in patients with Dubin-Johnson syndrome (19). Additionally, a 7-fold induction in Mrp3 has been observed in TR^- rats (20). The mean estimate for k_{21} (reflecting MRP3 basolateral efflux) was increased 7-fold to simulate expected alterations in Tc-99m mebrofenin disposition in patients with Dubin-Johnson syndrome. To account for the absence of functional MRP2 at the canalicular membrane, as well as the delayed gallbladder and intestinal visualization that has been observed in Dubin-Johnson patients' scans after Tc-99m mebrofenin analogs administration, k_{20} (reflecting canalicular efflux) was diminished 100-fold. Jaundice is observed in most patients with Dubin-Johnson syndrome. Additional simulations were conducted for these patients incorporating mild hyperbilirubinimia (k_{12} lowered by 2.5-fold) in addition to impaired MRP2 function (k_{20} lowered of 100-fold) and induction of MRP3 (k_{21} increased 7-fold).
3) Extra-hepatic or obstructive cholestasis can cause changes in hepatic transport proteins similar to Dubin-Johnson syndrome. Mrp2 expression has been reported to

be reduced and Mrp3 enhanced in response to stasis of bile in bile-duct ligated rats (33). Similar changes in patients affected by obstructive cholestasis were simulated by diminishing k_{20} 3-fold and increasing k_{21} 5-fold.

4) Finally, the effect of drug interactions at the level of the transport proteins on blood and hepatic concentration of Tc-99m mebrofenin were investigated. Cyclosporin A is known to inhibit Oatps (34) and to inhibit modestly Mrp2-dependent transport in rats (35). Acute co-administration of Tc-99m mebrofenin and cyclosporine A was simulated by lowering k_{20} 2-fold and k_{12} 5-fold. Inhibition of Tc-99m mebrofenin uptake might be observed with xenobiotics that are known to inhibit OATP1B1 [e.g. gemfibrozil (36)], this scenario was simulated by decreasing k_{12} 5-fold. Phenobarbital treatment increases Mrp3 expression (>10-fold induction) without altering the expression of Mrp2 in rats (37). A similar scenario was simulated to investigate changes in the disposition of Tc-99m mebrofenin in patients chronically treated with phenobarbital (k_{21} was increased 10- and 100-fold).

RESULTS

Tc-99m mebrofenin transport by OATP1B1 and OATP1B3

Published *in vitro* studies have implicated a Na^+-independent process in the uptake of Tc-99m mebrofenin analogs into hepatocytes (25). Additionally, elevated bilirubinemia enhances Tc-99m mebrofenin urinary excretion (32). Since OATP1B1 and OATP1B3 are responsible for the hepatic uptake of bilirubin and its glucuronide metabolites, these clinical observations might be due an interaction in hepatic uptake between bilirubin and Tc-99m mebrofenin (38). For these reasons, *Xenopus laevis* oocytes expressing OATP1B1 and OATP1B3 were utilized to investigate the potential role of these transport proteins in the hepatic uptake of Tc-99m mebrofenin. Tc-99m mebrofenin uptake by uninjected, OATP1B1- and OATP1B3- expressing oocytes was measured over 60 min (Fig 3.3A). Transport was linear up to 30 min in oocytes expressing OATPs. After 30 min, OATP1B1 transport reached a plateau. Uninjected oocytes did not show any significant transport of Tc-99m mebrofenin. Rifampicin is used commonly as a potent inhibitor of OATP-dependent transport (39). Co-incubation of the oocytes with 50 μM rifampicin inhibited Tc-99m mebrofenin uptake over 60 min to ~90% and ~96% of untreated control values in OATP1B1- and OATP1B3- expressing oocytes, respectively (Fig 3.3B).

Tc-99m mebrofenin transport by MRP2 and MRP3

Previously reported clinical observations in patients with Dubin-Johnson syndrome, and experiments using TR^- rats, have suggested that Tc-99m mebrofenin is transported into bile by MRP2/Mrp2. Thus, to determine whether Tc-99m mebrofenin is a substrate for MRP2, and for another important hepatic transport protein, MRP3, ATP-dependent uptake of Tc-99m mebrofenin by inside-out membrane vesicles prepared from HEK293 cells transiently

transfected with MRP2 or MRP3 was measured (Fig. 3.4). Control experiments to measure the uptake of [^{3}H]$E_2$17βG, a well-characterized substrate for both MRP2 and MRP3, were performed at a single time point (3 min) to ensure that membrane vesicles were functional (Fig. 3.4A). Consistent with previously published observations, uptake of [^{3}H]$E_2$17βG in membrane vesicles prepared from untransfected, MRP2 and MRP3 transfected HEK293 cells was 6.2, 16.1 and 102.3 pmol/mg protein, respectively (28). Tc-99m mebrofenin uptake in inside-out membrane vesicles from MRP2 transfected HEK293 cells was linear for up to 3 min (Fig 3.4B); uptake was more extensive than in vesicles from MRP3 transfected HEK293 cells at 3 min (~23 vs. 5 nCi/μg protein) as shown in Fig. 3.4B. Transport of Tc-99m mebrofenin by MRP3 was linear for up to 3 min, at which time 5 nCi/μg protein had accumulated and uptake began to plateau. No significant transport activity was detected for membrane vesicles prepared from untransfected HEK293 cells.

Several MRP2 and MRP3 substrates have been shown to be competitive inhibitors of MRP2 and MRP3 transport. $E_2$17βG (100 μM) inhibited ATP-dependent MRP3-mediated transport of Tc-99m mebrofenin ~95% (Fig. 3.4C). Unexpectedly, MRP2-dependent transport of Tc-99m mebrofenin was not inhibited by the same concentration of $E_2$17βG, possibly due to a higher affinity of MRP2 for Tc-99m mebrofenin than $E_2$17βG. MRP2 transport of Tc-99m mebrofenin was inhibited (~88% of control) by MK571 (50 μM), an LTD_4 receptor antagonist commonly used as an MRP family inhibitor.

Pharmacokinetic modeling of the disposition of Tc-99m mebrofenin in healthy subjects; disease state and drug interaction simulations:

The model depicted in Fig 3.2 was suitable for describing Tc-99m mebrofenin disposition in all subjects. The goodness of fit of this model to representative data from subject 4 is shown

in Fig 3.5. The parameter estimates and associated coefficients of variation for k_{10}, k_{12}, k_{21}, k_{20} and V_c are reported in Table 3.1 together with the administered dose and the amounts of Tc-99m mebrofenin excreted into bile and urine, which were used as input for the pharmacokinetic modeling studies (10). The model clearly supports the hypothesis that a fraction of hepatic Tc-99m mebrofenin is effluxed back into sinusoidal blood and is available for urinary excretion or reuptake by the liver. In all subjects, the ratio between the canalicular (k_{20}) and basolateral (k_{21}) efflux rate constants exceeded 2 (k_{20}/k_{21} = 3.5±0.8, mean ± SD), suggesting that once in the liver, the predominant process that determines Tc-99m mebrofenin fate is excretion into bile. The small volume of distribution for the central compartment (V_c) suggests that this represents the blood pool; differences in the V_c among subjects were reduced when volumes were weight-normalized (0.09-0.15 L/kg).

Simulations were performed using the mean values for the rate constants obtained from modeling the data from the four healthy (Fig 3.6). The percentage of the dose predicted to remain in blood and to be excreted into urine was very similar to clinical data reported for Tc-99m mebrofenin (32). Based on these simulations, ~22% of the dose remained in blood 10 min after dose administration, which was consistent with a mean value of 17% reported in the literature. The simulated percentage of the dose recovered in urine at 3 hr was ~0.6 %, which was similar to the average urinary excretion of 0.4-2.0% of the dose reported in previous clinical studies.

Alterations in the disposition of Tc-99m mebrofenin due to pathophysiological abnormalities occurring in hyperbilirubinemia, Dubin-Johnson syndrome, cholestatic patients and possible drug-drug interactions were examined using mathematical simulations.

In the four healthy subjects enrolled in this clinical study, Tc-99m mebrofenin renal clearance was 5-13 mL/min. *In vitro* protein binding studies revealed that the unbound fraction of Tc-99m mebrofenin in plasma was ~10%. For a compound with these characteristics, the expected renal clearance would be 12 mL/min if glomerular filtration was the predominant process determining renal elimination. Therefore, it can be concluded that Tc-99m mebrofenin elimination into urine is a passive process driven primarily by filtration. Since Tc-99m mebrofenin renal excretion is minimal and due to glomerular filtration, only liver uptake and efflux processes were assumed to be modified by pathologies and interactions with other drugs.

Fig 3.7 depicts the changes in blood Tc-99m mebrofenin concentrations in the presence of pathologies affecting liver transport processes or drug interactions. Impaired hepatic uptake of Tc-99m mebrofenin due to either elevated plasma bilirubin (Fig 3.7A) or drug-interactions (Fig 3.7C gemfibrozil, cyclosporin A), caused an elevation in Tc-99m mebrofenin blood concentrations, with slow removal by the kidneys; elevation in blood concentration also was predicted when hepatic basolateral efflux was induced by phenobarbital treatment (Fig 3.7C, PB x10 and PB x100). For pathologies in which biliary excretion processes were obliterated, however, the concentrations in blood remained elevated for a much more prolonged period of time (Fig 3.7B) because of the extensive hepatic accumulation of Tc-99m mebrofenin increased the driving force for excretion of Tc-99m mebrofenin back into blood via MRP3.

Hepatic accumulation is depicted in Fig 3.8. Impaired hepatic uptake of Tc-99m mebrofenin would, as expected, lower the exposure of this organ to the drug (Fig 3.8A and 3.8C). Induction of MRP3 transport due to phenobarbital treatment also diminished hepatic exposure. Inhibition of the hepatic uptake rate constant due to drug interactions delayed the

C_{max} in the liver (Fig 3.8C). On the other hand, impaired biliary excretion due to absence or downregulation of MRP2 resulted in sustained hepatic accumulation of Tc-99m mebrofenin over time (Fig 3.8B).

The renal and biliary excretion of Tc-99m mebrofenin predicted from these simulations varied greatly in response to elevated blood and liver concentrations, as well as changes in hepatic transport protein expression and function. The cumulative Tc-99m mebrofenin excretion in urine at 3 hr was predicted to be 0.6% of the dose in normal subjects; this value increased to 1.5, 2.9 and 5.3 % of the dose when hepatic uptake (k_{12}) was decreased 2.5-, 5- and 10-fold, respectively. Cumulative urinary excretion at 3 hr was predicted to be high in cholestasis (1.5% of the Tc-99m mebrofenin dose), and in patients with Dubin-Johnson syndrome (2.2% and 4.6% when accompanied by hyperbilirubinemia). Finally, all drug-drug interactions examined in the simulations enhanced urinary excretion (cyclosporin A, 3.1%; phenobarbital x10, 1.6%; phenobarbital x100, 7.4%; gemfibrozil, 2.9%). Simulated cumulative amounts of Tc-99m mebrofenin excreted into bile decreased: hyperbilirubinemia decreased biliary excretion from 86% to 83%, 77% and 65% of the dose. As expected in patients with Dubin-Johnson syndrome, less than 2% of the dose was predicted to be excreted into bile. Cholestasis decreased the biliary excretion of Tc-99m mebrofenin to 46% of the dose. Cyclosporine A and the highest dose of phenobarbital significantly changed the cumulative biliary excretion of Tc-99m mebrofenin to 54% and 48% of the dose.

DISCUSSION

This series of studies was designed to develop a model to describe the polyexponential disposition of Tc-99 mebrofenin in blood as observed during a clinical study in healthy volunteers. An integral part of the study was the characterization of the transport proteins involved in liver uptake and excretion of this compound. Since changes in expression of hepatic transport proteins are common in hepatobiliary disease, pharmacokinetic modeling and simulations were employed to investigate the effects of disease states and drug interactions on Tc-99m mebrofenin disposition.

The OATP family is responsible for the uptake of a very broad range of substrates, preferentially anionic amphipathic compounds such as bile acids, bilirubin and other compounds/metabolites with high molecular weight that bind to plasma albumin and are ultimately excreted into bile (40, 41). Tc-99m mebrofenin has a high molecular weight and a negative charge, accordingly it was not surprising to find that OATP1B1 and OATP1B3 are involved in the transport of this compound. In the liver, OATP1B1 also is responsible for basolateral uptake of bilirubin and its glucuronide metabolites (38, 42), elevated plasma bilirubin concentrations may impair hepatic uptake and enhance urinary excretion of Tc-99m mebrofenin by competing for OATP-mediated transport into the liver. The finding that Tc-99m mebrofenin can be excreted into bile by MRP2 and effluxed from the liver into blood by MRP3 is in good agreement with clinical observations in patients with Dubin-Johnson syndrome, as well as experiments in TR^- rats. In the liver, MRP2 mediates the efflux of endogenous and exogenous organic anions and conjugates into bile (12, 43, 44). The basolateral transport protein MRP3 shares tissue distribution and substrate specificity with MRP2, and these transporters have a complementary role in hepatic detoxification so that, in

disease states where MRP2 is absent or down-regulated, MRP3 is induced several fold (12, 43, 45).

The findings from the *in vitro* experiments, coupled with the results of the pharmacokinetic modeling, were used in simulation studies to predict the effect of disease states or drug interaction on Tc-99m mebrofenin disposition due to alterations of expression or activity of hepatic transport proteins. The pharmacokinetic model described all data sets from the four healthy subjects well. There was low variability associated with parameter estimates in all subjects. Data sets from Subjects 1 and 3 were most affected by experimental error and, as expected, the model performed slightly worse in fitting these data sets when compared to the remaining subjects. In Subject 1, the actual administered dose was not known, and a small leak of Tc-99m mebrofenin, below the balloon occluding the intestine, prevented complete quantitative recovery of the probe over the 3 hr study period. Subject 3 did not respond completely to CCK-8 and, for this reason, the amount of the Tc-99m mebrofenin dose excreted into bile was the least certain, since it was based primarily on the mathematical correction for EF. As previously demonstrated in dogs (6), Tc-99m mebrofenin is transported into bile and can be excreted from the hepatocyte back into blood. The terminal phase of the Tc-99m mebrofenin blood activity-time profile may be due to egress into blood by the efflux transport protein MRP3, located on the basolateral membrane of hepatocytes. This excretory process is required in the pharmacokinetic model (k_{21}). The *in vitro* findings in this study demonstrated that OATP1B1, 1B3 and MRP2 and MRP3 play a role for the hepatobiliary disposition of Tc-99m mebrofenin in humans. *In vitro* observations together with the predictions from the simulation exercise support the clinical observation that high

bilirubin concentrations in blood would cause, at least in part, the elimination route of this compound to shift from biliary to urinary excretion.

Drug elimination by the kidney is the result of glomerular filtration, active secretion and active reabsorption (when transport processes are involved). This differs from hepatic elimination of drugs that relies heavily on the uptake (active or passive) of compounds into the hepatocyte. The renal clearance in the four subjects enrolled in this study was within the range of normal glomerular filtration when Tc-99m mebrofenin plasma protein binding was taken into account. Therefore, modifications of active tubular secretion and reabsorption as a consequence of disease states or drug interactions would play a minor role in Tc-99m mebrofenin urinary excretion.

Tc-99m mebrofenin simulated blood mass-time profiles, revealed that patients affected by Dubin-Johnson syndrome and obstructive cholestasis would exhibit significant differences in the blood pharmacokinetics of this agent, compared to patients with hyperbilirubinemia caused by other diseases. In addition, simulations indicated that Tc-99m mebrofenin blood concentrations change minimally over the first hour post administration in patients lacking MRP2, therefore, sparse blood sampling coupled with gamma scintigraphy scans might be sufficient to diagnose Dubin-Johnson syndrome. This diagnostic tool could be especially useful in children in whom liver biopsy would be considered very invasive. Additionally, the pharmacokinetic modeling and simulations provided important information on the distribution of Tc-99m mebrofenin within the liver. Typically, it is not possible to quantify liver exposure to drugs in humans, but changes in hepatic accumulation due to disease state or drug interactions could be an important cause of hepatotoxicity. The simulations were particularly useful in examining the impact of impaired hepatic uptake and

biliary efflux processes and in appreciating the differences when both processes are inhibited. The liver exposure to Tc-99m mebrofenin in the presence of cyclosporin A (k_{12} diminished 5-fold and k_{20} diminished 2-fold) differed considerably from the predicted hepatic exposure in the presence of gemfibrozil (k_{12} diminished 5-fold). These differences in hepatic accumulation may be relevant in cases where the drug affected by this interaction has hepatotoxic potential when liver exposure is prolonged. Additionally, hepatotoxicants that are handled by the liver in a manner similar to Tc-99m mebrofenin may cause significant toxicity in patients with impaired MRP2 function or in patients with cholestasis.

The importance of changes in systemic and hepatic exposure illustrated by these pharmacokinetic simulations may be considerable for drugs that are administered in larger doses and have toxic potential. For example, cases of fatal rhabdomyolysis caused the withdrawal of cerivastatin from the market (46); these adverse events were related later to concomitant administration of gemfibrozil. Other studies have shown that cerivastatin hepatic uptake can be inhibited by cyclosporin A (47), resulting in increased systemic exposure, as predicted for Tc-99m mebrofenin (48). These data suggest that this compound could be used as an *in vivo* probe to investigate potential drug-drug interactions due to hepatic transport proteins.

In conclusion, these studies identified the transport proteins involved in the hepatobiliary disposition of Tc-99m mebrofenin. Utilizing pharmacokinetic modeling and simulations, the impact of changes in the hepatic uptake or excretion on the systemic and liver exposure, as well as the biliary and renal excretion of Tc-99m mebrofenin was demonstrated. Pharmacokinetic studies with Tc-99m mebrofenin may be a useful *in vivo*

clinical tool to identify genetic polymorphisms and assess the potential impact of drug-drug interactions at the hepatic transport level as well as mechanisms of liver toxicity.

AKNOWLEDGEMENTS

This work was supported by National Institutes of Health grant R01 GM41935 and grant RR00046 from the GCRC program of the Division of Research Resources. Drs. Daniel Bow, Joe Polli and Brendan Johnson are gratefully acknowledged for their expertise and help in the execution of the *in vitro* and *in vivo* studies. Dr Susan P.C. Cole (Queen's University) kindly provided the MRP2 and MRP3 vectors. Giulia Ghibellini is an American Foundation for Pharmaceutical Education Predoctoral Fellow. Dr Elaine Leslie is the recipient of a Postdoctoral Fellowship from the Canadian Institutes of Health Research (CIHR).

REFERENCES

1. S. Krishnamurthyand G. T. Krishnamurthy. Technetium-99m-iminodiacetic acid organic anions: review of biokinetics and clinical application in hepatology. *Hepatology* **9**: 139-153 (1989).

2. E. Gencoglu, H. Karakayali, G. Moray, A. Aktas, and M. Haberal. Evaluation of pediatric liver transplant recipients using quantitative hepatobiliary scintigraphy. *Transplant Proc* **34**: 2160-2 (2002).

3. M. Koruk, S. Ozkilic, M. C. Savas, Z. Celen, A. Kadayifci, and C. Ozkilic. Evaluation of hepatic functions and biliary dynamics in patients with liver cirrhosis by quantitative scintigraphy. *Hepatogastroenterology* **50**: 1803-5 (2003).

4. Y. Bujanover, S. Bar-Meir, I. Hayman, and J. Baron. 99mTc-HIDA cholescintigraphy in children with Dubin-Johnson syndrome. *J Pediatr Gastroenterol Nutr* **2**: 311-2 (1983).

5. T. Pinos, J. M. Constansa, A. Palacin, and C. Figueras. A new diagnostic approach to the Dubin-Johnson syndrome. *The American Journal of Gastroenterology* **85**: 91-93 (1990).

6. A. M. Peters, M. J. Myers, S. Mohammadtaghi, M. Mubashar, and R. T. Mathie. Bidirectional transport of iminodiacetic organic anion analogues between plasma and hepatocyte. *Eur J Nucl Med* **25**: 766-73 (1998).

7. G. B. Daniel, A. Bahr, J. A. Dykes, R. DeNovo, K. Young, and G. T. Smith. Hepatic extraction efficiency and excretion rate of technetium-99m-mebrofenin in dogs. *J Nucl Med* **37**: 1846-9 (1996).

8. E. Doo, G. T. Krishnamurthy, M. J. Eklem, S. Gilbert, and P. H. Brown. Quantification of hepatobiliary function as an integral part of imaging with technetium-99m-mebrofenin in health and disease. *J Nucl Med* **32**: 48-57 (1991).

9. S. Araikum, T. Mdaka, J. D. Esser, and M. Zuckerman. Hepatobiliary kinetics of technetium-99m-IDA analogs: quantification by linear systems theory. *Journal of Nuclear Medicine* **37**: 1323-1330 (1996).

10. G. Ghibellini, B. M. Johnson, R. J. Kowalsky, W. D. Heizer, and K. L. Brouwer. A novel method for the determination of biliary clearance in humans. *AAPS J* **6**: e33 (2004).

11. I. N. Dubinand F. B. Johnson. Chronic idiopathic jaundice with unidentified pigment in liver cells; a new clinicopathologic entity with a report of 12 cases. *Medicine (Baltimore)* **33**: 155-97 (1954).

12. D. Kepplerand J. Konig. Hepatic secretion of conjugated drugs and endogenous substances. *Semin Liver Dis* **20**: 265-72 (2000).

13. J. Kartenbeck, U. Leuschner, R. Mayer, and D. Keppler. Absence of the canalicular isoform of the MRP gene-encoded conjugate export pump from the hepatocytes in Dubin-Johnson syndrome. *Hepatology* **23**: 1061-1066 (1996).

14. S. Toh, M. Wada, T. Uchiumi, A. Inokuchi, Y. Makino, Y. Horie, Y. Adachi, S. Sakisaka, and M. Kuwano. Genomic structure of the canalicular multispecific organic anion-transporter gene (MRP2/cMOAT) and mutations in the ATP-binding-cassette region in Dubin-Johnson syndrome. *Am J Hum Genet* **64**: 739-46 (1999).

15. H. Tsujii, J. Konig, D. Rost, B. Stockel, U. Leuschner, and D. Keppler. Exon-intron organization of the human multidrug-resistance protein 2 (MRP2) gene mutated in Dubin-Johnson syndrome. *Gastroenterology* **117**: 653-60 (1999).

16. C. C. Paulusma, M. Kool, P. J. Bosma, G. L. Scheffer, F. ter Borg, R. J. Scheper, G. N. Tytgat, P. Borst, F. Baas, and R. P. Oude Elferink. A mutation in the human canalicular multispecific organic anion transporter gene causes the Dubin-Johnson syndrome. *Hepatology* **25**: 1539-42 (1997).

17. S. Kajihara, A. Hisatomi, T. Mizuta, T. Hara, I. Ozaki, I. Wada, and K. Yamamoto. A splice mutation in the human canalicular multispecific organic anion transporter gene causes Dubin-Johnson syndrome. *Biochem Biophys Res Commun* **253**: 454-7 (1998).

18. V. Keitel, A. T. Nies, M. Brom, J. Hummel-Eisenbeiss, H. Spring, and D. Keppler. A common Dubin-Johnson syndrome mutation impairs protein maturation and transport activity of MRP2 (ABCC2). *Am J Physiol Gastrointest Liver Physiol* **284**: G165-G174 (2003).

19. J. Konig, D. Rost, Y. Cui, and D. Keppler. Characterization of the human multidrug resistance protein isoform MRP3 localized to the basolateral hepatocyte membrane. *Hepatology* **29**: 1156-63 (1999).

20. B. M. Johnson, P. Zhang, J. D. Schuetz, and K. L. Brouwer. Characterization of transport protein expression in multidrug resistance-associated protein (mrp) 2-deficient rats. *Drug Metab Dispos* (2005).

21. T. Kitamura, P. Jansen, C. Hardenbrook, Y. Kamimoto, Z. Gatmaitan, and I. M. Arias. Defective ATP-dependent bile canalicular transport of organic anions in mutant (TR-) rats with conjugated hyperbilirubinemia. *Proc Natl Acad Sci U S A* **87**: 3557-61 (1990).

22. T. Pinos, C. Figueras, and R. Herranz. Scintigraphic diagnosis of Dubin-Johnson syndrome: DISIDA is also useful. *Am J Gastroenterol* **86**: 1687-8 (1991).

23. N. H. Hendrikse, F. Kuipers, C. Meijer, R. Havinga, C. M. Bijleveld, W. T. van der Graaf, W. Vaalburg, and E. G. de Vries. In vivo imaging of hepatobiliary transport function mediated by multidrug resistance associated protein and P-glycoprotein. *Cancer Chemother Pharmacol* **54**: 131-8 (2004).

24. J. A. Lan, L. R. Chervu, K. L. Johansen, and A. W. Wolkoff. Uptake of technetium 99m hepatobiliary imaging agents by cultured rat hepatocytes. *Gastroenterology* **95**: 1625-1631 (1988).

25. H. Okuda, R. Nunes, S. Vallabhajosula, A. Strashun, S. J. Goldsmith, and P. D. Berk. Studies of the hepatocellular uptake of the hepatobiliary scintiscanning agent 99mTc-DISIDA. *J Hepatol* **3**: 251-9 (1986).

26. R. J. Kowalskyand S. W. Falen. *Radiopharmaceuticals in Nuclear Pharmacy and Nuclear Medicine*, American Pharmacists Association, Washington, D.C., 2004.

27. D. A. Bow, J. L. Perry, J. D. Simon, and J. B. Pritchard. The impact of plasma protein binding on the renal transport of organic anions. *J Pharmacol Exp Ther* **316**: 349-55 (2006).

28. K. Ito, C. J. Oleschuk, C. Westlake, M. Z. Vasa, R. G. Deeley, and S. P. Cole. Mutation of Trp1254 in the multispecific organic anion transporter, multidrug resistance protein 2 (MRP2) (ABCC2), alters substrate specificity and results in loss of methotrexate transport activity. *J Biol Chem* **276**: 38108-14 (2001).

29. C. J. Oleschuk, R. G. Deeley, and S. P. Cole. Substitution of Trp1242 of TM17 alters substrate specificity of human multidrug resistance protein 3. *Am J Physiol Gastrointest Liver Physiol* **284**: G280-9 (2003).

30. D. W. Loe, K. C. Almquist, R. G. Deeley, and S. P. Cole. Multidrug resistance protein (MRP)-mediated transport of leukotriene C4 and chemotherapeutic agents in membrane vesicles. Demonstration of glutathione-dependent vincristine transport. *J Biol Chem* **271**: 9675-82 (1996).

31. E. M. Leslie, Q. Mao, C. J. Oleschuk, R. G. Deeley, and S. P. Cole. Modulation of multidrug resistance protein 1 (MRP1/ABCC1) transport and atpase activities by interaction with dietary flavonoids. *Mol Pharmacol* **59**: 1171-80 (2001).

32. Choletec. Kit for the Preparation of Technetium Tc 99m Mebrofenin, Bracco Diagnostic, Inc., Princeton (NJ).

33. M. G. Donnerand D. Keppler. Up-regulation of basolateral multidrug resistance protein 3 (Mrp3) in cholestatic rat liver. *Hepatology* **34**: 351-9 (2001).

34. A. Treiber, R. Schneiter, S. Delahaye, and M. Clozel. Inhibition of organic anion transporting polypeptide-mediated hepatic uptake is the major determinant in the

pharmacokinetic interaction between bosentan and cyclosporin A in the rat. *J Pharmacol Exp Ther* **308**: 1121-9 (2004).

35. I. S. Westley, L. R. Brogan, R. G. Morris, A. M. Evans, and B. C. Sallustio. Role of Mrp2 in the hepatic disposition of mycophenolic acid and its glucuronide metabolites: effect of cyclosporine. *Drug Metab Dispos* **34**: 261-6 (2006).

36. M. Yamazaki, B. Li, S. W. Louie, N. T. Pudvah, R. Stocco, W. Wong, M. Abramovitz, A. Demartis, R. Laufer, J. H. Hochman, T. Prueksaritanont, and J. H. Lin. Effects of fibrates on human organic anion-transporting polypeptide 1B1-, multidrug resistance protein 2- and P-glycoprotein-mediated transport. *Xenobiotica* **35**: 737-53 (2005).

37. H. Xiong, H. Suzuki, Y. Sugiyama, P. J. Meier, G. M. Pollack, and K. L. Brouwer. Mechanisms of impaired biliary excretion of acetaminophen glucuronide after acute phenobarbital treatment or phenobarbital pretreatment. *Drug Metab Dispos* **30**: 962-9 (2002).

38. Y. Cui, J. Konig, I. Leier, U. Buchholz, and D. Keppler. Hepatic uptake of bilirubin and its conjugates by the human organic anion transporter SLC21A6. *J Biol Chem* **276**: 9626-30 (2001).

39. S. R. Vavricka, J. Van Montfoort, H. R. Ha, P. J. Meier, and K. Fattinger. Interactions of rifamycin SV and rifampicin with organic anion uptake systems of human liver. *Hepatology* **36**: 164-72 (2002).

40. B. Hagenbuch and P. J. Meier. The superfamily of organic anion transporting polypeptides. *Biochim Biophys Acta* **1609**: 1-18 (2003).

41. B. Hagenbuch and P. J. Meier. Organic anion transporting polypeptides of the OATP/ SLC21 family: phylogenetic classification as OATP/ SLCO superfamily, new nomenclature and molecular/functional properties. *Pflugers Arch* **447**: 653-65 (2004).

42. A. Ayrton and P. Morgan. Role of transport proteins in drug absorption, distribution and excretion. *Xenobiotica* **31**: 469-497 (2001).

43. J. Konig, A. T. Nies, Y. Cui, I. Leier, and D. Keppler. Conjugate export pumps of the multidrug resistance protein (MRP) family: localization, substrate specificity, and MRP2-mediated drug resistance. *Biochim Biophys Acta* **1461**: 377-94 (1999).

44. P. Chandr and K. L. Brouwer. The complexities of hepatic drug transport: current knowledge and emerging concepts. *Pharm Res* **21**: 719-35 (2004).

45. B. Stockel, J. Konig, A. T. Nies, Y. Cui, M. Brom, and D. Keppler. Characterization of the 5'-flanking region of the human multidrug resistance protein 2 (MRP2) gene

and its regulation in comparison with the multidrug resistance protein 3 (MRP3) gene. *Eur J Biochem* **267**: 1347-1358 (2000).

46. A. A. Alsheikh-Ali, J. T. Kuvin, and R. H. Karas. Risk of adverse events with fibrates. *Am J Cardiol* **94**: 935-8 (2004).

47. Y. Shitara, T. Itoh, H. Sato, A. P. Li, and Y. Sugiyama. Inhibition of transporter-mediated hepatic uptake as a mechanism for drug-drug interaction between cerivastatin and cyclosporin A. *J Pharmacol Exp Ther* **304**: 610-6 (2003).

48. W. Muck, I. Mai, L. Fritsche, K. Ochmann, G. Rohde, S. Unger, A. Johne, S. Bauer, K. Budde, I. Roots, H. H. Neumayer, and J. Kuhlmann. Increase in cerivastatin systemic exposure after single and multiple dosing in cyclosporine-treated kidney transplant recipients. *Clin Pharmacol Ther* **65**: 251-61 (1999).

TABLES

Table 3.1: Biliary and urinary recovery of Tc-99m mebrofenin after IV administration to 4 healthy human volunteers (10). The biliary recovery was corrected for the degree of gallbladder contraction in response to pharmacological stimulation, thereby correcting the amount of drug recovered in bile for the residual amount remaining in the gallbladder. The individual parameter estimates and associated variability for the first-order rate constants (see Fig. 3.2 legend for parameter definitions) and the volume of the central compartment (V_c) were obtained from pharmacokinetic modeling of Tc-99m mebrofenin disposition data.

Table 3.1

	Subject 1	Subject 2	Subject 3	Subject 4	Mean	S.D.
*Dose (μCi)	2188[a]	2072	2282	2476	2255	171
*Urinary Recovery (% of dose)	0.7	0.5	0.8	0.5	0.6	0.2
*Biliary Recovery corrected for EF (% of dose)	70.9	89.1	91.9	84.9	84.2	9.3
	Parameter Estimate (CV%)					
K_{12} (min^{-1})	0.11 (10.1)	0.17 (10.9)	0.22 (17.0)	0.23 (7.9)	0.18	0.06
K_{21} (min^{-1})	0.0019 (26.5)	0.0051 (21.9)	0.0034 (64.6)	0.0032 (25.5)	0.0034	0.0013
K_{20} (min^{-1})	0.0073 (0.75)	0.013 (0.91)	0.015 (1.3)	0.011 (0.55)	0.012	0.003
K_{10} (min^{-1})	0.00065 (11.8)	0.00063 (17.4)	0.0015 (21.8)	0.00087 (18.5)	0.0009	0.0004
V_c (L)	13.6 (9.84)	10.1 (10.8)	8.73 (18.7)	5.79 (9.27)	9.56	3.25
Ratio K_{20}/K_{21}	3.8	2.6	4.5	3.5	3.5	0.8

[a] Only theoretical dose available
* From (10)

FIGURES

Fig 3.1: Structure of Tc-99m mebrofenin. This hepatobiliary imaging agent consists of two molecules of mebrofenin chelating a central atom of Tc-99m.

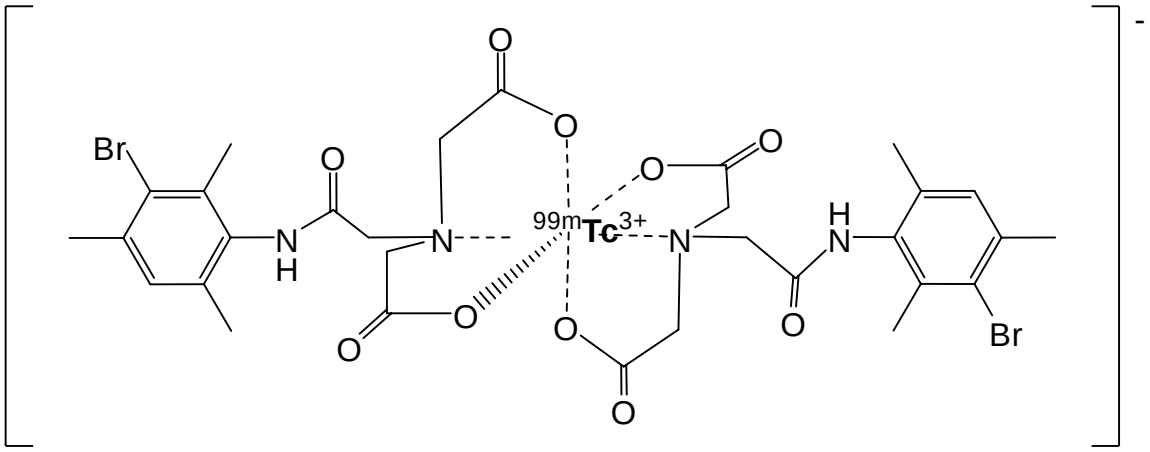

Fig 3.2: Scheme of the pharmacokinetic model describing the disposition and elimination of Tc-99m mebrofenin in humans. X_0 represents the IV bolus dose. C_c is the concentration of Tc-99m mebrofenin in the central compartment (blood) and V_c the central compartment volume. All other compartments were modeled as amounts [in urine (X_{urine}), in liver (X_{liver}) and in duodenal bile corrected by EF (X_{bile})]. All rate constants were assumed to be first-order: k_{12} represents hepatic basolateral uptake, k_{21} hepatic basolateral egress, k_{20} hepatic canalicular excretion, and k_{10} represents the rate constant for renal elimination.

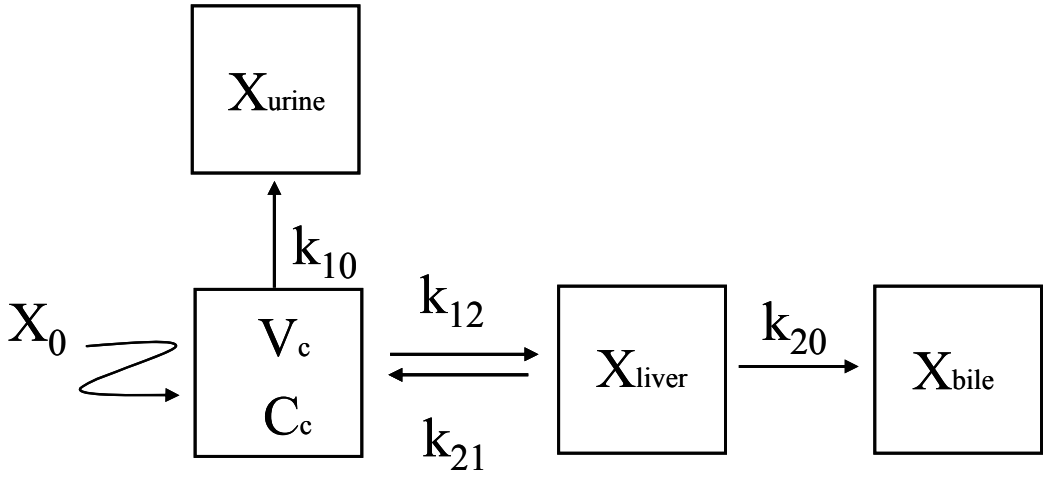

Fig 3.3: Tc-99m mebrofenin uptake in *Xenopus laevis* oocytes expressing human OATP1B1 and 1B3. Uptake was measured at room temperature with a Tc-99m mebrofenin concentration of 9-10 μCi/mL. Results are expressed as a percentage of untreated oocytes expressing the same protein. Bars and data points represent mean (± SEM) of 5-8 oocytes in a single experiment. Similar results were obtained in an additional independent experiment.

(A) Time course of Tc-99m mebrofenin uptake by uninjected oocytes (control, ●), OATP1B1 (▽) and OATP1B3 (■) expressing oocytes.

(B) Inhibition of OATP1B1 and OATP1B3 uptake of Tc-99m mebrofenin by rifampicin. Oocytes expressing OATP1B1 and OATP1B3 were incubated for 60 min with Tc-99m mebrofenin in the presence (open bar) and absence (closed bar) of rifampicin (50 μM).

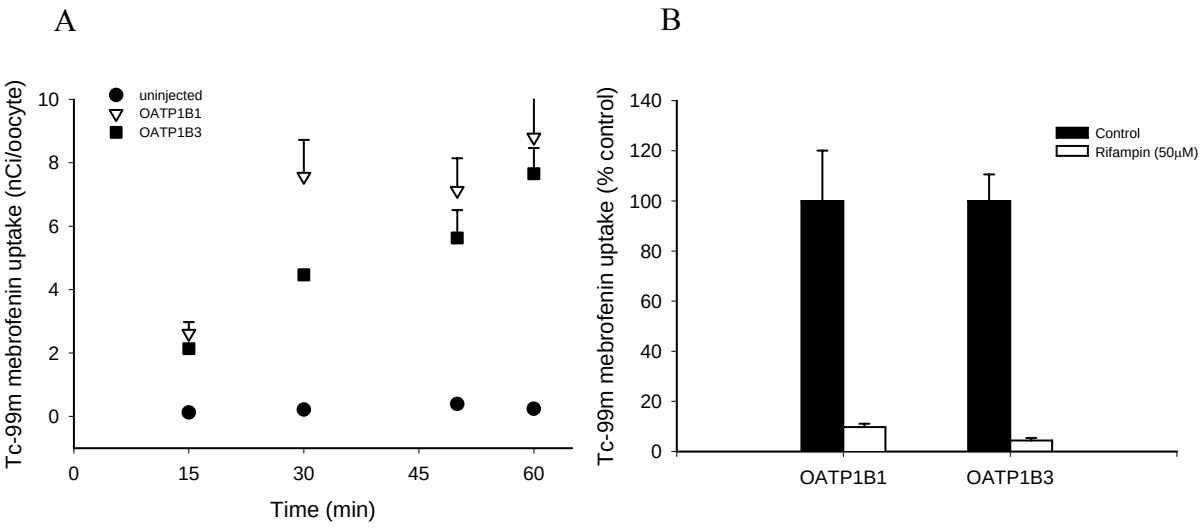

Fig 3.4: Tc-99m mebrofenin uptake in inside-out membrane vesicles prepared from HEK293 cells transiently transfected with MRP2 or MRP3.

(A) [^{3}H]$E_2$17βG uptake by membrane vesicles prepared from untransfected, MRP2 and MRP3 transfected HEK293 cells. ATP-dependent uptake was measured at 3 min after incubating the membrane vesicles with [^{3}H]$E_2$17βG (0.4 μM, 120 nCi). Bars represent mean (± SD) of a triplicate incubation in a single experiment.

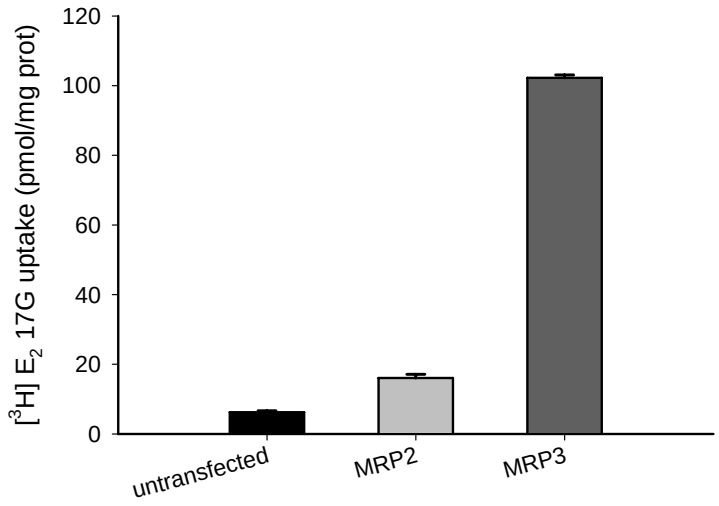

(B) A time course of Tc-99m mebrofenin ATP-dependent transport by control (●), MRP2(▽) and MRP3 (■) vesicles. Uptake was measured at 37°C with a Tc-99m mebrofenin concentration of 50 μCi/mL. Data points represent mean (± SD) of a triplicate incubation in a single experiment.

(C) Inhibition of MRP2- and MRP3-mediated ATP-dependent transport of Tc-99m mebrofenin. Membrane vesicles were incubated for 3 min with Tc-99m mebrofenin in the presence (open bar) and absence (closed bar) of $E_2$17βG (100 μM) for MRP3 inhibition, and MK571 (50 μM) for MRP2 inhibition. Results are expressed as a percentage of untreated membrane expressing the same protein. Bars represent mean (± SD) of a triplicate incubation in a single experiment.

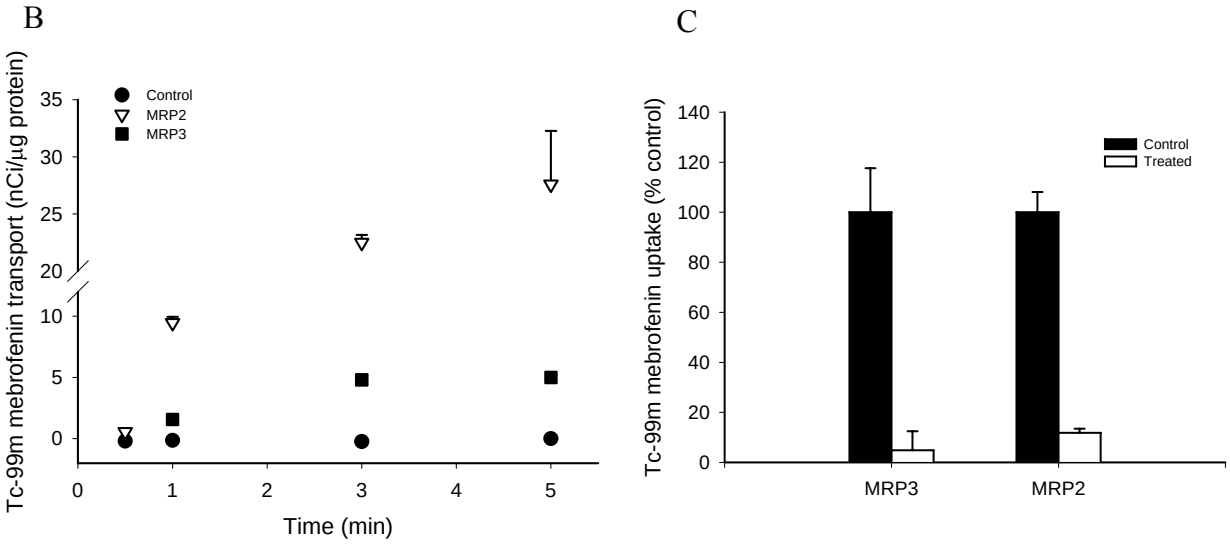

Fig 3.5: Tc-99m mebrofenin disposition in Subject # 4. The solid curve represents the fit of the pharmacokinetic model depicted in Fig 3.2 to the data. The blood concentration-time profile (◆) is shown on a log-linear scale (left axes), while bile (●) and urine (▲) amount vs. time profiles are plotted on a Cartesian scale (right axes). Symbols represent actual data points while lines represent fit of the model to the clinical observations.

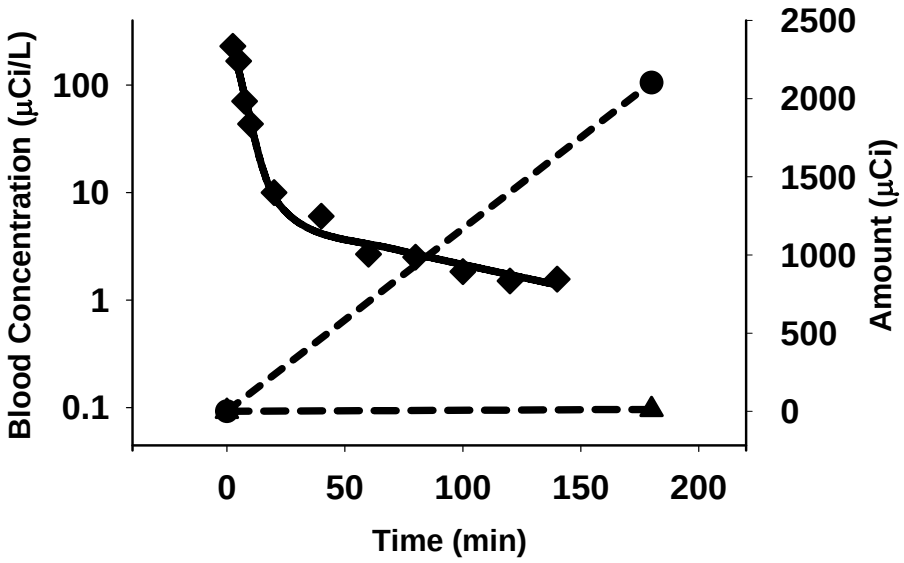

Fig 3.6: Simulation of blood, liver, bile and urine mass-time profiles for an "average" healthy subject after administration of an IV bolus of Tc-99m mebrofenin.

The blood mass-time profile is plotted on a log-linear scale on the left axis, while liver, bile and urine mass-time profiles are plotted on a Cartesian scale on the right axis.

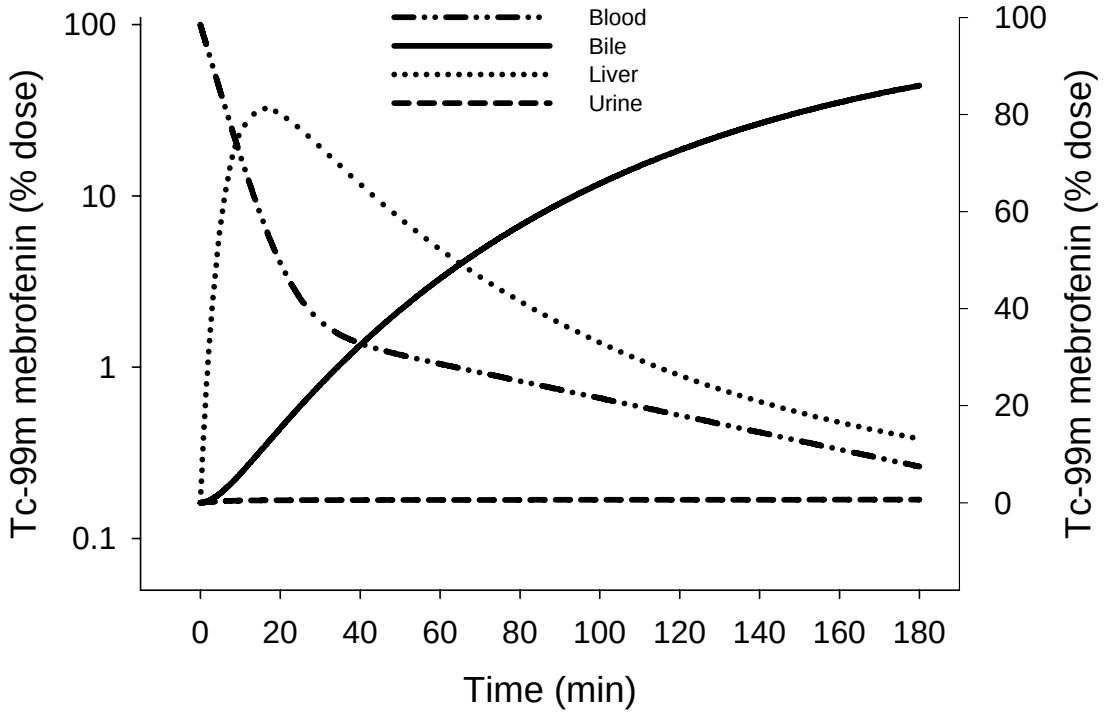

Fig 3.7: Effects of modifications in hepatic uptake and efflux processes on the blood concentrations of Tc-99m mebrofenin. Solid line represents the simulated profile in normal healthy volunteers in all panels.

(A) Inhibition of hepatic uptake of Tc-99m mebrofenin with a 2.5-, 5- and 10-fold impairment in k_{12} (mild, intermediate and severe bili). These simulations predict modifications due to elevated plasma bilirubin concentrations.

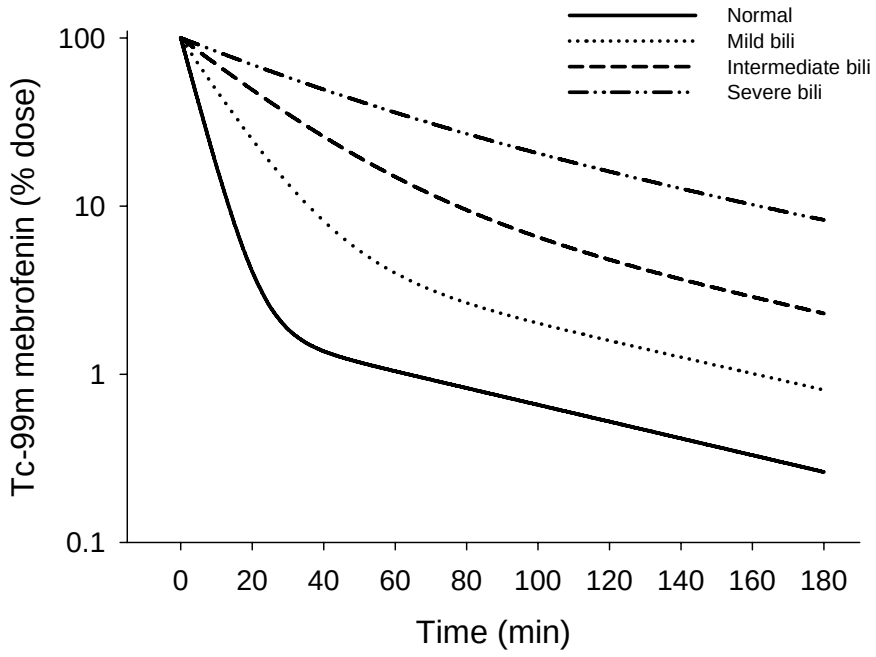

(B) Simulation of changes in MRP2 and MRP3 caused by Dubin-Johnson syndrome (k_{21} induced 7-fold and k_{20} reduced 100-fold, DJ), in the presence of elevated plasma bilirubin (k_{12} reduced 2.5-fold, DJ bili) are compared to normal volunteers and simulations of patients with obstructive cholestasis (k_{21} induced 5-fold and k_{20} reduced 3-fold, cholestasis).

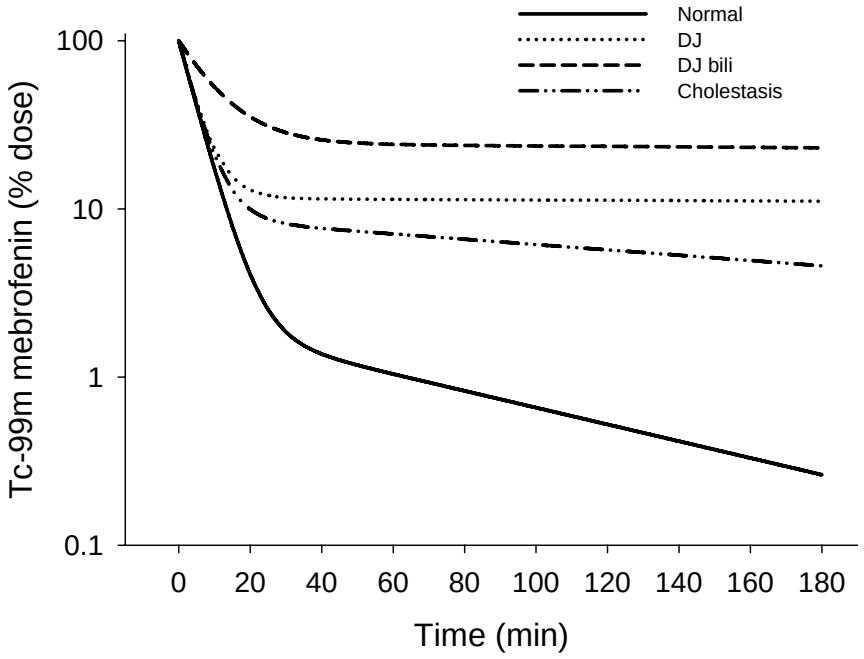

(C) Simulated alterations in the disposition of Tc-99m mebrofenin in blood caused by drug-drug interactions with concomitant administration of cyclosporin A (CsA, k_{12} reduced 5-fold and k_{20} reduced 2-fold), chronic administration of phenobarbital (PB x10 and x100, induction of k_{21} 10- and 100-fold) and acute administration of gemfibrozil (k_{12} reduced 5-fold).

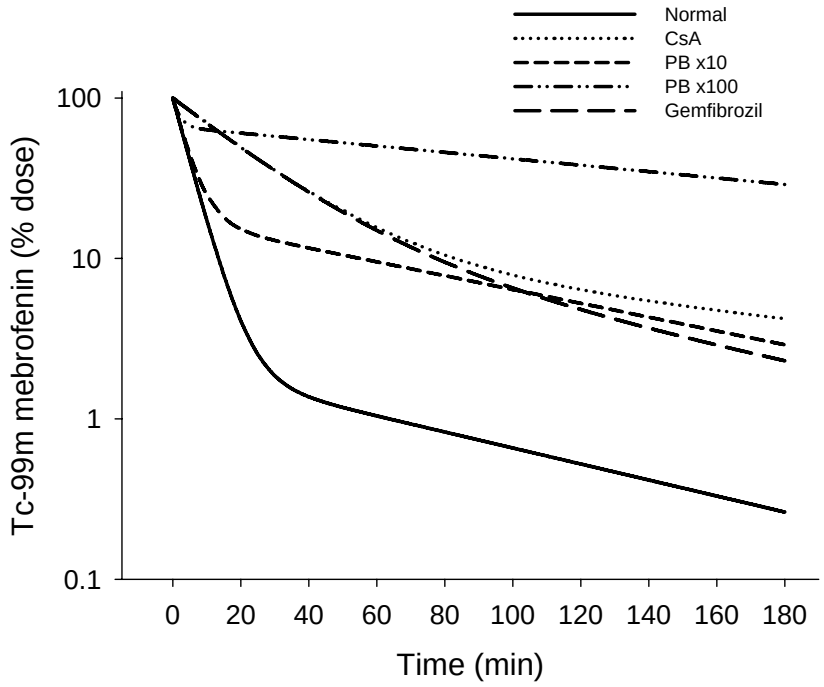

Fig 3.8: Effects of modifications in hepatic uptake and efflux processes on the hepatic accumulation of Tc-99m mebrofenin. Solid line represents the simulated profile in normal healthy volunteers in all panels.

(A) Inhibition of hepatic uptake of Tc-99m mebrofenin with a 2.5-, 5- and 10-fold impairment in k_{12} (mild, intermediate and severe bili). These simulations predict modifications due to elevated plasma bilirubin concentrations.

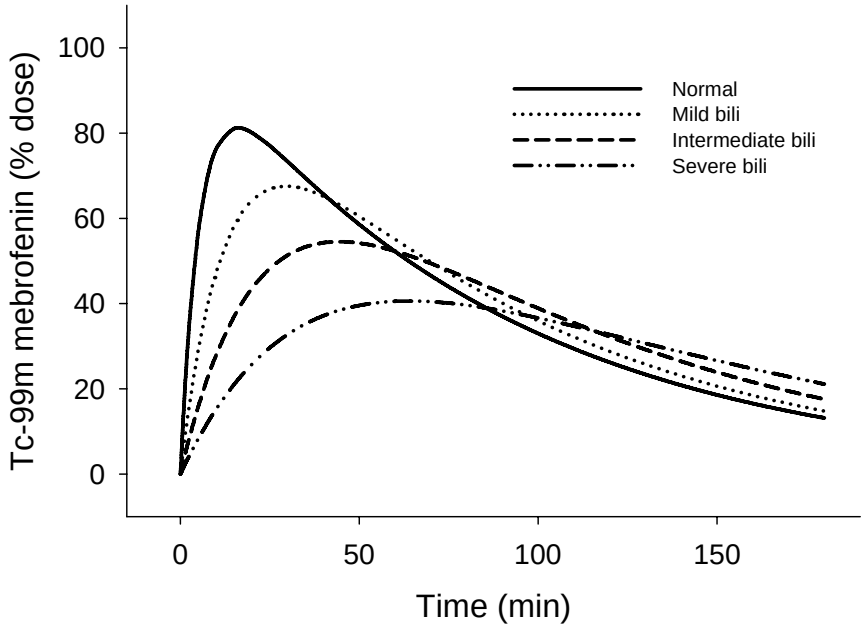

(B) Simulation of changes in MRP2 and MRP3 caused by Dubin-Johnson syndrome (k_{21} induced 7-fold and k_{20} reduced 100-fold, DJ), in the presence of elevated plasma bilirubin (k_{12} reduced 2.5-fold, DJ bili) are compared to normal volunteers and simulations of patients with obstructive cholestasis (k_{21} induced 5-fold and k_{20} reduced 3-fold, cholestasis).

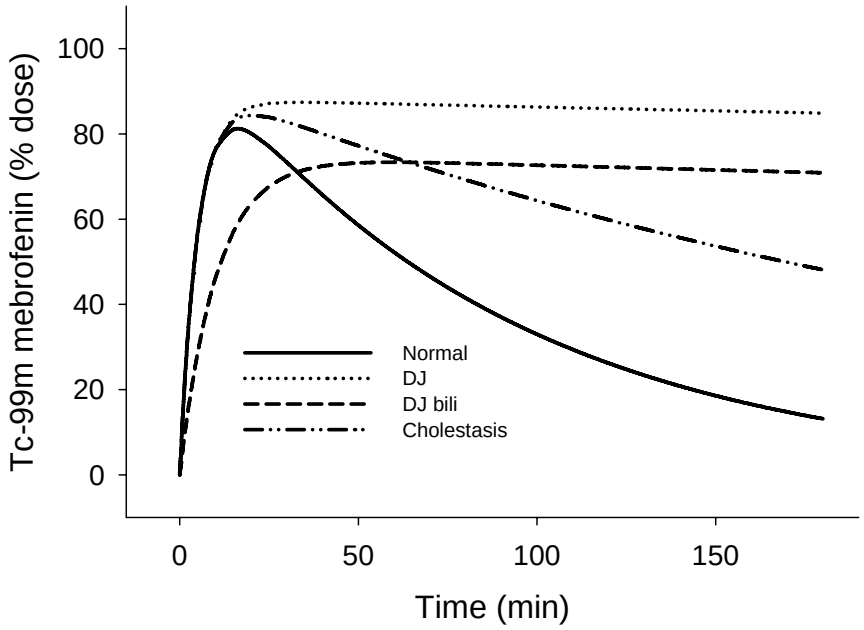

(C) Simulated alterations in the disposition of Tc-99m mebrofenin in liver tissue caused by drug-drug interactions with concomitant administration of cyclosporin A (CsA, k_{12} reduced 5-fold and k_{20} reduced 2-fold), chronic administration of phenobarbital (PB x10 and x100, induction of k_{21} 10- and 100-fold) and acute administration of gemfibrozil (k_{12} reduced 5-fold).

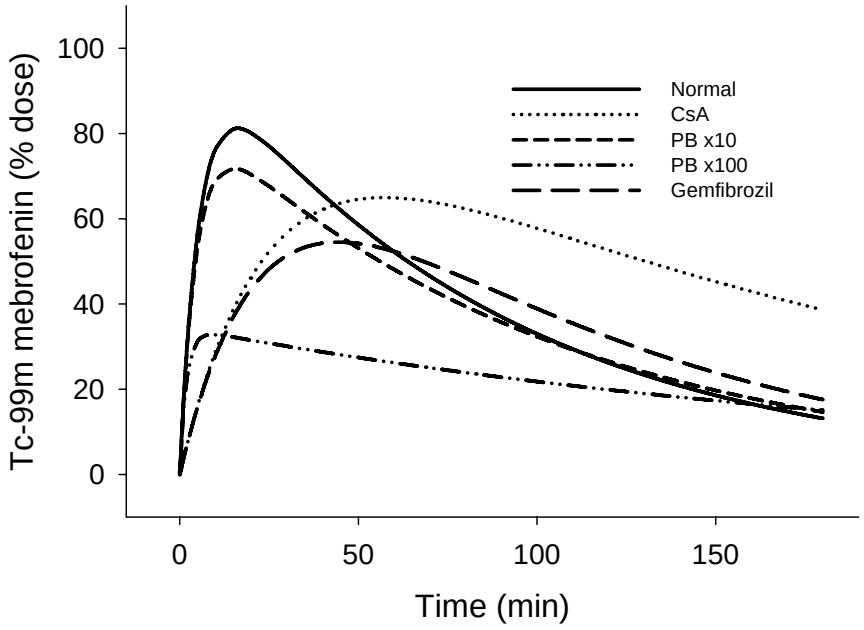

CHAPTER 4

DETERMINATION OF THE BILIARY EXCRETION OF PIPERACILLIN AND METABOLITES IN HUMANS USING A NOVEL METHOD

This Chapter was submitted to *The British Journal of Clinical Pharmacology* and is presented in the style of that journal.

INTRODUCTION

The biliary clearance of drugs in healthy human volunteers has been evaluated by several groups with varying degrees of success [1-4]. Major challenges in developing an accurate method to quantify biliary clearance include the complex anatomy of the human hepatobiliary system, as well as the intermittent and incomplete expulsion of bile from the gallbladder. Pharmacological contraction of the gallbladder has been employed in an attempt to collect as much bile stored within the gallbladder as possible [4]. However, gallbladder response to pharmacological contraction can vary considerably among human subjects, and is influenced by a variety of factors, including prolonged fasting [5]. Unless the degree of gallbladder contraction is considered, the estimated extent of biliary excretion of the drug of interest may be inaccurately low and inter-subject variability may be exaggerated [5, 6].

Recently, we developed a technique to quantify biliary clearance of compounds in humans that couples gamma scintigraphy with a specially designed oroenteric catheter [7]. This catheter is equipped with an inflatable occlusive balloon that facilitates periodic collection of duodenal fluids and bile. The gallbladder ejection fraction (EF) is determined by administering a hepatobiliary imaging agent (Tc-99m mebrofenin). Tc-99m mebrofenin is a gamma emitting diagnostic agent used in nuclear medicine to evaluate the patency of the hepatobiliary tract. Tc-99m mebrofenin is taken up in a rapid and selective manner by the hepatocyte and excreted into bile unchanged [8]. In humans, the majority of the Tc-99m mebrofenin administered dose is found in bile three hours after administration [7]. This imaging agent allows visualization of the gallbladder before, during and after pharmacological contraction. Administration of a gamma emitter that is excreted into bile also aids in the identification of bile leakage beyond the occlusive balloon in the duodenum.

ABSTRACT

Aims: To evaluate the applicability of a novel method to determine the biliary excretion of piperacillin, a low biliary clearance drug, and metabolites in healthy volunteers.

Methods: Healthy volunteers were administered 2 g piperacillin IV. Duodenal aspirates were collected via a custom-made oroenteric catheter; blood and urine also were collected. Gallbladder ejection fraction (EF) was determined by gamma scintigraphy using Tc-99m mebrofenin as an imaging agent. Piperacillin and metabolites were quantified by LC-UV and LC-MS. Relevant pharmacokinetic parameters were calculated using noncompartmental analysis. Formation of metabolites also was investigated *in vitro* using human liver microsomes.

Results: The fraction of the piperacillin dose excreted unchanged into bile was 1.1±0.3% (biliary clearance corrected for EF=0.032±0.008 mL/min/kg). Desethylpiperacillin and its glucuronide conjugate were detected in bile and urine; these metabolites also were formed in human liver microsomal incubates. This is the first report of glucuronidation of piperacillin.

Conclusions: This methodology can be used to determine biliary clearance of drugs and to identify metabolites as soon as they are excreted from the gallbladder, thereby minimizing the exposure of labile compounds to the intestinal environment. Although a prolonged intubation influences negatively gallbladder contractility, normalization of biliary clearance for EF significantly reduces inter-subject variability of this parameter.

The primary goal of the present series of investigations was to assess the versatility of our approach by applying it to piperacillin, a drug expected to exhibit low biliary clearance. Piperacillin is a third-generation, broad-spectrum, penicillin derivative. This bactericidal drug is used commonly in the treatment of intra-abdominal infections and prophylactically for gastrointestinal and biliary tract procedures [9]. Studies performed in patients with bile duct drainage reported recovery of 0.7-2% of the administered piperacillin dose in bile and 43-53% in urine, [10, 11] while only 0.08% of the dose was recovered in duodenal fluids of healthy volunteers [10].

A second goal was to evaluate the effect of prolonged intubation on gallbladder contractility and on the biliary clearance of drugs. The recovery of Tc-99m mebrofenin in this study was compared to the recovery of this probe in our previous study [7] to evaluate the effect of the intubation time and prolonged presence of the inflated balloon in the duodenum on the variability of gallbladder response to CCK-8.

The characterization of metabolic pathways that are unique to humans is very important in the drug development process. Accordingly, a third goal was to use mass spectrometry to evaluate whether sampling bile immediately upon secretion into the intestine would enable identification of potentially unstable drug metabolites. Although the metabolite desethylpiperacillin has been recovered in human urine and is formed in human liver homogenates [12, 13], the enzymes involved in the formation of this metabolite have not been elucidated and excretion of desethylpiperacillin into bile or faeces has not been demonstrated to date. Therefore, the excretion pattern of piperacillin metabolites was evaluated *in vivo* and compared to metabolites generated *in vitro*.

This work demonstrated the utility of a novel clinical protocol and oroenteric tube to directly quantify drug and metabolites in bile of healthy subjects. Results established that incorporation of the EF factor in the biliary clearance calculation provides a method to account for inherent variability associated with the determination of this parameter in healthy volunteers.

METHODS

Clinical Studies:

Clinical Protocol: Three male volunteers (23-40 years of age) within 20% of their ideal body weight completed the study. All study subjects were in good health as documented by medical history, physical examination, EKG and routine laboratory testing. Subjects were asked to abstain from any medications for 2 weeks prior to the study, and to abstain from caffeine and alcohol during the study. The Clinical Research Advisory Committee and the Committee on the Protection of the Rights of Human Subjects at the University of North Carolina (UNC) at Chapel Hill School of Medicine approved all procedures. Subjects provided written informed consent prior to participation in the study.

Subjects were admitted to the General Clinical Research Centre at UNC Hospitals 12 hr prior to the procedure. To stimulate gallbladder contraction, subjects were given a high-fat, caffeine-free meal consisting of ~1150 kcal (45% fat, 16% protein) upon admission and a high-fat snack (48% fat, 18% protein) 5 hr later. After an overnight fast, a custom-made oroenteric tube was passed through the mouth and positioned in the upper portion of the duodenum with the aid of dynamic fluoroscopic radiography. The oroenteric tube used in these studies was a silicone multi-lumen extrusion (4.5 mm diameter; 128 cm length, Dentsleeve, Wayville, Australia) and was described in detail previously [7]. The distal end of the tube was fitted with a polyethylene balloon, which was inflated to occlude the intestine during bile collection.

To determine relevant pharmacokinetic parameters for piperacillin, subjects were administered 2 g of piperacillin (generous gift of American Pharmaceutical Partners) as a 15-min IV infusion via an arm vein, and blood samples were collected at 15, 30, 45, 60, 75, 90,

120, 150, 180, 210, 240, 270, 300, 330, 360, 480, 600 min. To visualize the gallbladder, 2.5 mCi of Tc-99m mebrofenin (Choletec®, Bracco Diagnostics, Princeton, NJ) was administered as an IV bolus 2 hr post piperacillin, to allow time for hepatic uptake and accumulation of piperacillin. At this time, subjects were positioned under a gamma camera (E-CAM Dual Head Gamma Camera, Siemens) and anterior planar gamma scintigraphic images of the abdomen were acquired at 1-min intervals for the remaining 4 hr of the study. Gallbladder contraction was induced with cholecystokinin-8 (CCK-8, Sincalide, Kinevac®, 0.02 μg/kg) administered as an IV infusion over 30 min, 4 hr after piperacillin administration. If CCK-8 failed to contract the gallbladder, 10-20 mL of half milk/half cream were delivered into the stomach ports of the catheter to stimulate endogenous CCK secretion with the presence of partially digested proteins and fats in the small intestine [14, 15]. In one case, orange zest was used as an olfactory stimulant to promote gallbladder contraction upon failure of the previously described methods. Duodenal aspirates and continuous images of the abdominal region were collected for a total of 6 hr. Urine and blood samples were collected for a total of 10 hr. Piperacillin was quantified in plasma, bile and urine as described under *Analytical Methods*. Radioactivity was quantified in blood, bile and urine as described previously [7].

Analytical Methods:

Bilirubin Determination: Bilirubin was quantified in the duodenal aspirates to demonstrate the presence of bile. The Total Bilirubin Kit (CATACHEM, Bridgeport, CT) was used with modifications. Bilirubin (Sigma-Aldrich, St. Luis, MO) was dissolved in 0.01 M NaOH and 25 μL of samples or standards (range 1.4-35 mg/dL) were added with 200 μL of Total Bilirubin Working Reagent. Following incubation at 22°C for 4 hr, samples were analyzed

at 540 nm using a microplate reader FL600 (Bio-Tek Instruments Inc., Winooski, VT). Preliminary kinetic studies demonstrated that the colorimetric reaction reached a plateau after 240 min.

Piperacillin quantification in plasma and urine: Piperacillin was quantified in plasma and urine by HPLC-UV using an HP1050 HPLC-UV system (Agilent, Germany) equipped with a Phenomenex Luna column (C_{18}, particle size 5 μm, 250 x 4.60 mm). The flow rate was 1.5 mL/min, detection wavelength 254 nm, and dynamic range 1-200 μg/mL. Samples were analyzed with a 14-min reverse phase gradient using sodium acetate 10 mM, pH 5.2, and acetonitrile. For plasma, the gradient started at 18% acetonitrile and increased to 25% over 7 min. For urine, the gradient started at 13% acetonitrile and increased to 25% over 9 min. Prior to analysis by HPLC, the internal standard cefoxitin (final concentration 20 μg/mL) was added to 300 μL of plasma. Proteins were precipitated with 100 μL of saturated solution of ammonium sulphate. Samples were then added to 600 μL of acetonitrile, incubated at room temperature for 15 min, centrifuged at 15,000 g for 10 min, and the supernatant was collected, evaporated, and reconstituted in sodium acetate (10 mM pH 5.2). Urine samples were diluted with mobile phase containing internal standard. The method was evaluated in both matrices in terms of accuracy, intra-day and inter-day variability (coefficient of variation, CV%). Accuracy ranged between 83 and 119% for the plasma and urine assays. The inter-day and intra-day CV% was ≤ 11% for both matrices.

Determination of Piperacillin and metabolites in bile and urine: Bile and urine were analyzed for piperacillin and metabolites using HPLC-MS-MS. Bile and urine samples were diluted 1:7 with methanol containing cefazolin (4.5 μg/mL) or cimetidine (0.5 μg/mL) as the internal standards. The HPLC system was an HP1100 (Agilent, Germany), it was coupled to an

Applied Biosystems API4000 mass spectrometer with a TurboIonSpray source (Foster City, CA). All components were controlled by Analyst software (version 1.3, Foster City, CA). Mobile phases consisted of water and methanol with 0.5% formic acid in each. A methanol gradient was used to elute the analytes from an Aquasil (C_{18}, particle size 5.0 μm, 50x2.1 mm) analytical column (ThermoElectron, West Palm Beach, FL) at room temperature with a flow rate of 0.75 mL/min. The gradient was held at 95% water for 0.5 min, then water was decreased to 10% over 2 min and was held for 1 min. The system was returned to 100% water at 3.5 min. The total run time was 4 min. The dynamic range of this method was 1-100 μM. Accuracy was in the range of 89-99% and the inter-day and intra-day CV% was ≤17.2%. An analytical standard was available only for piperacillin; therefore desethylpiperacillin and desethylpiperacillin glucuronide concentrations were estimated qualitatively and expressed as internal standard peak area ratios.

User controlled parameters were optimized for the detection of the parent-to-product transitions when analytical standards were available (piperacillin, cefazolin and cimetidine). For desethylpiperacillin and glucuronides, the most likely transitions were monitored. For positive ion multiple reaction monitoring (MRM), the following transitions were used: piperacillin, 518.2→143.3; desethylpiperacillin, 490.0→115.0 and cefazolin, 455.0→156.2. For negative ion MRM, the following transitions were used: piperacillin, 516.0→141.0; desethylpiperacillin, 488.0→113.0; piperacillin glucuronide, 692.0→516.0; desethylpiperacillin glucuronide, 664→488 and cimetidine 250.9→165.9. For negative MRM, the relative concentrations of piperacillin, desethylpiperacillin, piperacillin glucuronide and desethylpiperacillin glucuronide were estimated by analyte: internal

standard peak-area ratio and amounts were expressed as the product of the area ratio and the volume collected.

To confirm the presence of piperacillin and desethylpiperacillin glucuronides, samples prepared as described for the triple quadrupole analysis were injected onto an Agilent 1100MSD ion trap mass spectrometer. Analysis was conducted in negative mode using autoMS^n in which parent ions of sufficient intensity were subjected to fragmentation. All product ions were scanned; since both parent and glucuronidated compounds contained similar structural elements, they were expected to form similar fragments.

Pharmacokinetic analysis: A gallbladder EF was calculated from anterior planar scintigraphic images obtained after Tc-99m mebrofenin administration, using ESOFT 2.5 software (Siemens) [16]. EF was determined as described below where GB represents the counts over the gallbladder region and the time in all formulas refers to the minutes after piperacillin administration. The amount of piperacillin (X_{bile}) collected in bile during the time period used for the EF calculation was normalized by EF to account for the drug excreted into bile, yet remaining in the gallbladder due to incomplete contraction (X_{GB}= Excreted dose).

$$\text{EF}= \left(\frac{GB^{240\,\text{min}} - GB^{360\,\text{min}}}{GB^{240\,\text{min}}} \right)$$

$$\text{Piperacillin } X_{GB} = X_{bile}^{0-240\,\text{min}} + \left(\frac{X_{bile}^{240-360\,\text{min}}}{EF} \right)$$

The amount of Tc-99m mebrofenin (X_{GB}) collected in bile over 4 hrs was calculated and corrected by EF as follows in order to compare the recovery obtained in this study to results obtained previously with this technique [7].

$$\text{Tc-99m mebrofenin } X_{GB} = X_{bile}^{120-240\,\text{min}} + \left(\frac{X_{bile}^{240-360\,\text{min}}}{EF} \right)$$

Noncompartmental analysis was used to calculate pharmacokinetic parameters using WinNonlin (Pro version 4.2; Pharsight, Mountain View, CA). The area under the plasma concentration-time curves (AUC) was calculated using the linear trapezoidal rule, and where appropriate, extrapolated to infinity using the slope obtained from linear regression of the last 3 to 6 time points; $AUC_{0\text{-}Tlast}$ was calculated up to 6 hr. Total clearance (Cl_{total}) was calculated as the ratio of the administered dose to $AUC_{0\text{-}\infty}$. Biliary clearance ($Cl_{biliary}$) was calculated as the ratio of the cumulative amount of drug recovered in bile at the end of the experiment and the $AUC_{0\text{-}Tlast}$. The biliary clearance corrected by gallbladder EF (*in vivo* $Cl_{biliary}$) was calculated as the ratio of the Excreted Dose (X_{GB}) and the $AUC_{0\text{-}Tlast}$.

***In vitro* metabolism studies:**

Phase I metabolism of piperacillin: To determine whether piperacillin was metabolized by microsomal enzymes, incubations were performed in triplicate using human liver microsomes [17]. Human liver microsomal proteins (2.5 mg/mL mixed-gender pooled human liver microsomes from XenoTech, LLC, Lenexa, KS) were incubated with a concentration of piperacillin (Sigma-Aldrich) within the range of the observed clinical C_{max} (200 μM) in 100 mM potassium phosphate buffer (pH 7.4) and 3.3 mM $MgCl_2$. After pre-warming for 5 min at 37°C the reactions were initiated by the addition of 1 mM β-NADPH (Sigma-Aldrich); a control incubation without β-NADPH was included. Aliquots of incubation mixtures were removed at 0, 5, 15, 30, 60 and 90 min and the reaction was stopped with an equal volume of ice-cold acetonitrile containing internal standard (0.5 μg/mL cimetidine). Samples were centrifuged (3500xg for 5 min) to precipitate the protein, and the supernatant was analyzed immediately by positive ion HPLC/MS triple quadrupole

mass spectrometry, as described for bile and urine. The same experiments also were performed using human liver S9 and cytosolic fractions (XenoTech, LLC, Lenexa, KS).

Phase II metabolism of piperacillin: To demonstrate piperacillin and desethylpiperacillin glucuronidation *in vitro*, piperacillin was subjected to microsomal incubations in the presence of UDPGA. Microsomal incubations, performed in duplicate, contained human liver microsomal protein (2.5 mg/mL mixed-gender pooled human liver microsomes from XenoTech, LLC, Lenexa, KS), 100 mM potassium phosphate buffer (pH 7.4), 3.3 mM $MgCl_2$, 50 μg alamethicin/mg protein, 5 mM saccharolactone and 500 μM piperacillin. Samples were pre-warmed for 5 min at 37°C and the reactions were initiated by the addition of 2 mM β-NADPH (to allow for the formation of desethylpiperacillin) and 5 mM UDPGA. Reactions were terminated at 0, 5, 15, 30, 60, and 90 min by removing 50 μL of the incubation mixture and quenching with an equal volume of ice-cold 80:20 (v/v) acetonitrile: 1% acetic acid containing internal standard (0.5 μg/mL cimetidine). Samples were centrifuged to precipitate the protein, and the supernatant was analyzed immediately by negative ion HPLC triple quadrupole mass spectrometry, as described for bile and urine. Appearance of an analyte with an exact mass 176 amu greater than either piperacillin or desethylpiperacillin confirmed the glucuronidation of these compounds.

RESULTS

Evaluation of gallbladder contractility and recovery of Tc-99m mebrofenin:

The overall duration of intubation and the fasting time between the intubation and the administration of Tc-99m mebrofenin and CCK-8 in this study were modified from the design adopted previously [7] to account for the longer elimination half-life of piperacillin. These modifications seemed to affect the gallbladder contractility. The gallbladder ejection fraction of the 4 subjects enrolled in the previous study (where three out four subjects had an EF $\geq$ 0.82, [7]) differed considerably from the healthy volunteers enrolled in this study (Table 4.1). As expected, all subjects reported intestinal cramping in response to CCK-8. However, only four out of the seven healthy volunteers enrolled in these two studies demonstrated normal gallbladder contraction by the end of the study [18]. Since CCK-8 did not completely contract the gallbladder of any of the subjects enrolled in the current study, these volunteers were administered 10-20mL half milk/half cream at approximately 160 min post Tc-99m mebrofenin administration. Subject A demonstrated satisfactory gallbladder contraction (EF=0.82) following fatty food (milk/cream) administration, while Subjects B and C did not. Due to complete lack of response to both CCK-8 and half milk/half cream, Subject C was asked to smell orange zest at 200 min post Tc-99m mebrofenin administration in an attempt to stimulate gallbladder discharge. Regardless of differences in gallbladder contraction, the overall Tc-99m mebrofenin dose recovered in bile corrected for EF was very high, and comparable to our previous results [7] (84.2 $\pm$ 9.3% versus 60.9 $\pm$ 14.9% in the current study, mean $\pm$ SD). Urinary recovery of Tc-99m mebrofenin was extremely low in both studies as well (0.6 $\pm$ 0.2% versus 0.8 $\pm$ 0.2% in the current study, mean $\pm$ SD).

To further demonstrate that Tc-99m mebrofenin accumulation and excretion into bile was not affected by the study design, but that the gallbladder contractility in response to CCK-8 administration was adversely affected by prolonged intubation, gamma scintigraphic images of representative subjects from the previous and current studies are shown in Figure 4.1. These images were captured at the times specified in the figure, which refers to the time after administration of the radiotracer Tc-99m mebrofenin. Images and duodenal secretions were collected for an extra hour post CCK-8 administration during the current piperacillin study (Subject B). Tc-99m mebrofenin rapidly accumulated in the liver, hepatobiliary tree and gallbladder of both subjects (Figure 4.1, 10 and 45 or 43 min). Within 60 minutes, the radiotracer was cleared out of the liver and excreted into bile. At the time of CCK-8 administration (120 min), both subjects displayed similar Tc-99m mebrofenin disposition, with almost all radioactivity contained within the gallbladder. However, the gallbladder response to CCK-8 differed between subjects. In Subject 2, who was representative of other subjects from the Tc-99m mebrofenin study, CCK-8 stimulated almost complete contraction of the gallbladder (total EF=0.86) and expulsion of radioactive bile into the intestine (Fig 4.1). However, CCK-8 failed to completely contract the gallbladder in Subject B and the partial EF calculated from 120-150 min after Tc-99m mebrofenin administration was only 0.21. Additionally, Subject B exhibited only a minimal response to fatty food administration (partial EF calculated from 160-240 min after Tc-99m mebrofenin administration was 0.08). As visible in Figure 4.1, at the end of the imaging time, more radioactivity remained within the gallbladder of Subject B. The duodenal region was effectively isolated and occluded by the terminal balloon in both cases, as demonstrated by the confinement of radioactive bile within the hepatobiliary tree and duodenum. Regardless of these differences, use of EF to

correct for incomplete gallbladder contraction improved the estimate of the amount of Tc-99m mebrofenin excreted into bile by decreasing inter-subject variability.

Piperacillin pharmacokinetics and biliary excretion:

Piperacillin pharmacokinetics in all subjects in this study were similar to previously published data [19, 20]. The mean plasma concentration-time profile and individual cumulative biliary excretion plots for Subjects A, B and C are presented in Fig 4.2, and pharmacokinetic parameters are listed in Table 4.1. Piperacillin biliary recovery was minimal (0.41 ± 0.32% of the dose), with the majority of the dose excreted as unchanged drug in urine (72 ± 13%). Correction for incomplete contraction of the gallbladder decreased inter-subject variability improving the estimate of the amount of piperacillin excreted in bile (1.1 ± 0.3% of the dose) by accounting for the amount that would have been excreted in bile if the EF had been complete. Likewise, the calculated biliary clearance of piperacillin was less variable among subjects when corrected for the gallbladder EF ($Cl_{biliary}$ 0.012 ± 0.011 mL/min/kg vs. *in vivo* $Cl_{biliary}$ 0.032 ± 0.008 mL/min/kg).

To establish whether the appearance of piperacillin in the duodenum coincided with bile discharge, the time-course of piperacillin and bilirubin in the duodenal aspirates was plotted (Figure 4.3). To normalize for inter-individual variability, these values were expressed as a percentage of the maximal amounts recovered in the aspirates. The majority of piperacillin was excreted upon gallbladder contraction, as illustrated by simultaneous peaks of maximal piperacillin and bilirubin commencing at 240 min post piperacillin administration (the time of CCK-8 administration) for Subjects A and B. Subject C did not have gallbladder contraction until olfactory stimulation with orange zest at 300 min; a peak in both piperacillin and bilirubin was detected readily in the duodenal samples at this time. Interestingly, some

piperacillin was found in duodenal secretions at early time points, especially in Subjects A and C. These duodenal aspirates did not contain bilirubin, supporting the hypothesis that piperacillin is not only excreted into bile, but also is secreted actively into the intestinal lumen.

Characterization of piperacillin metabolism in humans:

Piperacillin is excreted primarily unchanged in urine and bile. However, a metabolite unique to humans has been identified in human urine and in incubates of human liver homogenates [13, 21]. The comparison of samples from a clinical study analyzed using a bioassay and an HPLC method revealed that an active metabolite of piperacillin was detected in bile and urine [10]. Mass spectrometric detection allowed for structural identification of two metabolites of piperacillin in the clinical samples obtained in the present study. Desethylpiperacillin and the glucuronide conjugate of desethylpiperacillin were identified in urine and bile of all subjects. No measurable concentrations of piperacillin glucuronide were detected. While dealkylation of piperacillin has been observed previously [12, 22], the conjugated metabolite is a novel finding of the present study. The relative amounts of piperacillin, desethylpiperacillin and desethylpiperacillin glucuronide, expressed as the peak area ratios corrected for the volume of aspirate collected in the duodenal aspirates and in urine fractions analyzed by LC-MS-MS in negative ionization mode, are plotted in Figure 4.4. The presence of desethylpiperacillin glucuronide was investigated further. Bile samples were incubated with bovine β-glucuronidase (Sigma-Aldrich 4000 units/mL, pH 5, 37°C, over 24 hours). As expected, the desethylpiperacillin glucuronide peak was sensitive to enzymatic degradation (results not shown). Secondly, the structure of the phase II metabolite (Figure 4.5, Panel A) was verified by HPLC-MS-MS, as shown in Figure 4.5 (Panel B). The

fragmentation pattern of the desethylpiperacillin glucuronide peak (pseudomolecular ions of 664 amu) was the same as that of the desethylpiperacillin peak.

The products of phase I and II metabolism subsequently were examined *in vitro* using pooled human microsomes, liver cytosol and S9 fractions. There was no turnover of piperacillin in the cytosolic fractions of human liver (data not shown), while metabolites were formed readily in microsomal incubations. Panel A in Figure 4.6 depicts *in vitro* formation of desethylpiperacillin by incubation of piperacillin with pooled human liver microsomes in the presence of β-NADPH; the lack of desethylpiperacillin formation in the absence of β-NADPH confirmed that this oxidation is most likely a cytochrome P450-mediated reaction. The determination of the extent of metabolism *in vitro* through substrate depletion was not possible due to the low turnover of piperacillin. Nevertheless, it was feasible to demonstrate that glucuronidation also took place *in vitro,* once the microsomes were made permeable with alamethicin. Figure 4.6 (Panel B) illustrates that both piperacillin glucuronide and desethylpiperacillin glucuronide were formed over time upon incubation of the liver microsomes with piperacillin in the presence of β-NADPH and UDPGA. Since desethylpiperacillin glucuronide formation was dependent upon the initial turnover of the parent drug into the phase I metabolite, the amount of this glucuronide formed *in vitro* was extremely small, yet detectable after a 15-min incubation, as shown in Figure 4.6 (Panel B insert).

DISCUSSION

Investigating the mechanisms of biliary clearance of drugs in humans presents a number of challenges, some of which are impossible to overcome, such as complete bile collection utilizing a non-invasive technique. However, as demonstrated in this study, a combination of tools can be used to obtain a reliable estimate of the biliary clearance of a drug in healthy humans. Determination of the gallbladder ejection fraction and correction of the amount of Tc-99m mebrofenin excreted into bile by this value, diminishes the variability of the biliary clearance parameter. For example, if this corrected amount is used for the calculation of the corrected biliary clearance of Tc-99m mebrofenin obtained in our previous study, 93% of the systemic clearance for this probe (17.3 ± 1.7 mL/min/kg, [7]) can be accounted for by biliary elimination (*in vivo* $Cl_{biliary}$ =16.1 ± 3.2 mL/min/kg vs $Cl_{biliary}$ 12.5 ± 3.5 mL/min/kg) **.**

Inconsistent contraction of the gallbladder in healthy volunteers after CCK-8 administration has not been extensively reported in the literature, but has been observed by our group during the development of the current methodology [23]. The lack of responsiveness to CCK-8 for two of the three subjects involved in the present study may be attributed to prolonged fasting, which was 4 hours longer than in the previous study [7], or to the prolonged presence of the tube and the inflated balloon in the duodenum, which may have altered gastrointestinal motility. It is well documented in animals that the duodenum is important in maintaining sphincter of Oddi response to CCK [24]. In the present study, the pressure exerted by the inflated balloon in the intestinal lumen may have modified response to CCK-8 and gallbladder emptying.

Piperacillin biliary excretion estimates in this study are highly consistent with Westphal and Brogard's published results [10, 11], and clearly demonstrate that piperacillin is only marginally eliminated into bile in humans. The correction of the excreted dose of piperacillin for the gallbladder ejection fraction greatly diminished inter-subject variability and yielded estimates for the fraction of dose excreted into bile similar to previously reported values in T-tube patients [10]. In contrast, the biliary excretion of piperacillin in animal models is extensive, making the extent of biliary elimination in humans more difficult to predict from preclinical studies; ~15% of the piperacillin dose was recovered in rat bile after single-pass isolated perfused liver experiments, [25] and 37% of the dose was recovered in recirculating rabbit isolated perfused livers [26]. The importance of biliary clearance and the difficulty in predicting this value from preclinical species, has been recognized recently [27]. The present clinical data establish the utility of this oroenteric tube and clinical protocol to accurately quantify the biliary clearance of drugs that exhibit low biliary clearance values in humans, in addition to drugs like Tc-99m mebrofenin, which are extensively excreted into human bile.

Interestingly, upon administration of CCK-8, duodenal aspirates were collected through the more proximal ports of the oroenteric catheter indicating that either the tube slipped further along the GI tract or that the intestinal segment contracted. This phenomenon was observed in all subjects and corresponded to CCK-8 administration, suggesting that it could be related to CCK-8 action on the gastrointestinal tract. The pH of the duodenal aspirates was variable (results not shown), and secretions with a pH of 7 or more were obtained upon discharge of gallbladder bile, perhaps due to stimulation of bicarbonate secretion [28]. The observation that the pH varied greatly among fractions collected was not

unexpected, although this should be taken into consideration when drugs sensitive to pH are studied, given that compound degradation could occur, confounding final results.

The lack of complete overlap between piperacillin and bilirubin appearance patterns in the duodenal aspirates provides evidence that, in addition to biliary excretion, piperacillin may be secreted actively into the gastrointestinal lumen. Previous studies of piperacillin distribution and excretion suggest that intestinal secretion may explain the lack of mass balance observed [11]. Piperacillin intestinal excretion could account for a percentage of the dose found in the duodenum, while hepatic metabolism explains the lack of mass balance at the end of our studies. The quantification of bilirubin in the duodenal aspirates can therefore be used to overcome a limitation of the current methodology in discriminating between intestinal and biliary secretion.

Quantification of desethylpiperacillin and desethylpiperacillin glucuronide was not possible because analytical standards of these metabolites were not available. Thus, only relative amounts of piperacillin and its metabolites, as determined by LC-MS-MS in negative ionization mode, were expressed as the internal standard area ratio multiplied by the volume of urine or duodenal aspirates collected. As analyte ionization also can be affected by the biological matrix analyzed, the trend in the excretion pattern in urine and bile was examined, rather than a strict comparison. From the quantitative analysis (Table 4.1), as well as from this comparison of relative amounts, piperacillin was primarily excreted into urine. In fact, piperacillin was the most abundant analyte in urine; the opposite held true for the duodenal aspirates, where the trend showed that desethylpiperacillin and desethylpiperacillin glucuronide were the more prevalent analytes found (Figure 4.4). This observation could be explained by differential affinities for transport proteins in the liver [e.g. the apical and

basolateral members of the MRP (multidrug resistance associated protein) family], which may determine the major route of hepatic elimination of each species.

The liver specific metabolism of piperacillin into desethylpiperacillin has been reported previously [13], however, no mechanistic details were elucidated. *In vitro* studies demonstrated that this N-dealkylation reaction is a microsomal, NADPH-dependent pathway, most likely involving a cytochrome P450 enzyme. Additional studies in the presence of UPDGA and β-NADPH demonstrated that piperacillin and its metabolite, desethylpiperacillin, undergo glucuronidation *in vitro*. The *in vitro* glucuronidation reaction in the present studies relied on the initial conversion of piperacillin by phase I metabolism into desethylpiperacillin, because the purified metabolite was not available. Piperacillin has been reported to inhibit AZT glucuronidation [29]; however, no literature reports document phase II metabolism of this antibiotic *in vitro* or *in vivo*. Although piperacillin glucuronide was detected in the *in vitro* incubations, it was not detected in the clinical samples, perhaps due to degradation of this labile metabolite in bile and urine. The identification of these glucuronides leads to an intriguing hypothesis that other drugs (e.g. penicillin G [30]), that have been shown to "activate" Mrp2, but are not transported directly, may be metabolized to glucuronide conjugates. It is well known that MRP2 generally transports phase II metabolites, such as glucuronides, into bile. Due to the relative instability of these metabolites, the conjugates could degrade immediately and only the parent drug would be detected in bile. If this hypothesis is correct, the contribution of phase II metabolism as a clearance mechanism may be underestimated for numerous drugs.

In conclusion, the results of this study extend the applicability of this technique to drugs that exhibit a low biliary clearance. This approach also could be useful to characterize

metabolic processes for new chemical entities in development, in particular when the metabolic pathways are exclusive to humans. This study led to the identification of a novel metabolite of piperacillin in duodenal aspirates and urine, and illustrated the potential use of this method to compare the relative importance of different excretion routes for specific compounds. Although these findings are not likely to have any impact on the clinical use of piperacillin, the experimental design developed in the present study could be applied to other drugs in development, not only to determine the extent of biliary clearance, but also to identify and thoroughly characterize drug metabolism. This information could be obtained with a small number of healthy volunteers, and may be a strategic tool in the early stages of clinical research to unveil elimination pathways unique to humans.

AKNOWLEDGEMENTS

This work was supported by National Institutes of Health grant R01 GM41935, and by a grant (RR00046) from the General Clinical Research Centers program of the Division of Research Resources. The authors are grateful for the technical assistance of Dr. Brendan Johnson, Dr. J. Ed Hall, Jonathan Simpson, Ann Whitlow and Jennifer Barner. Drs. Elaine Leslie and Mary Paine are gratefully acknowledged for their helpful comments in the preparation of this manuscript. Giulia Ghibellini is an American Foundation for Pharmaceutical Education Predoctoral Fellow. Dr. Lakshmi Vasist was supported by a Clinical Pharmacokinetics/Pharmacodynamics Fellowship sponsored by the University of North Carolina, Chapel Hill and GlaxoSmithKline, RTP, NC.

REFERENCES

1 Angelin B, Arvidsson A, Dahlqvist R, Hedman A, Schenck-Gustafsson K. Quinidine reduces biliary clearance of digoxin in man. Eur. J. Clin. Invest1987;17(3):262-265.

2 Strasberg SM, Harvey PR, Hofmann AF. Bile sampling, processing and analysis in clinical studies. Hepatology 1990;12(3 Pt 2):176S-180S; discussion 180S-182S.

3 Brookman LJ, Rolan PE, Benjamin IS, Palmer KR, Wyld PJ, Lloyd P, Flesch G, Waldmeier F, Sioufi A, Mullins F. Pharmacokinetics of valsartan in patients with liver disease. Clin Pharmacol Ther 1997;62(3):272-278.

4 Ryde M, Gustavsson S. Biliary excretion of olsalazine sodium in humans. Eur J Drug Metab Pharmacokinet 1987;12(1):17-24.

5 Zillmann M, Schentke KU. Ultrasonography studies on spontaneous and pharmacologically modified gallbladder motility. Gastroenterol J 1991;51(2):66-72.

6 Schiedermaier P, Neubrand M, Hansen S, Sauerbruch T. Variability of gallbladder emptying after oral stimulation. Scand J Gastroenterol 1997;32(7):719-24.

7 Ghibellini G, Johnson BM, Kowalsky RJ, Heizer WD, Brouwer KL. A novel method for the determination of biliary clearance in humans. AAPS J 2004;6(4):e33.

8 Krishnamurthy S, Krishnamurthy GT. Technetium-99m-iminodiacetic acid organic anions: review of biokinetics and clinical application in hepatology. Hepatology 1989;9(1):139-153.

9 Holmes B, Richards DM, Brogden RN, Heel RC. Piperacillin. A review of its antibacterial activity, pharmacokinetic properties and therapeutic use. Drugs 1984;28(5):375-425.

10 Brogard JM, Jehl F, Blickle JF, Dorner M, Arnaud JP, Monteil H. Biliary pharmacokinetic profile of piperacillin: experimental data and evaluation in man. Int J Clin Pharmacol Ther Toxicol 1990;28(11):462-70.

11 Westphal JF, Brogard JM, Caro-Sampara F, Adloff M, Blickle JF, Monteil H, Jehl F. Assessment of biliary excretion of piperacillin-tazobactam in humans. Antimicrob Agents Chemother 1997;41(8):1636-40.

12 Komuro M, Maeda T, Hayakawa H, Allen KL, Green CE. The formation of desethyl-piperacillin from piperacillin by human liver S9 in vitro. Biopharm Drug Dispos 1997;18(3):185-90.

13 Minami Y, Komuro M, Sakawa K, Ishida N, Matsumoto K, Oishi K. Desethyl piperacillin, a new active metabolite of piperacillin in human. J Antibiot (Tokyo) 1991;44(2):256-8.

14 Krishnamurthy GT, Brown PH. Comparison of fatty meal and intravenous cholecystokinin infusion for gallbladder ejection fraction. J Nucl Med 2002;43(12):1603-10.

15 Ziessman HA, Jones DA, Muenz LR, Agarval AK. Cholecystokinin cholescintigraphy: methodology and normal values using a lactose-free fatty-meal food supplement. J Nucl Med 2003;44(8):1263-6.

16 Krishnamurthy GT, Bobba VR, McConnell D, Turner F, Mesgarzadeh M, Kingston E. Quantitative biliary dynamics: introduction of a new noninvasive scintigraphic technique. J Nucl Med 1983;24(3):217-23.

17 Ansede JH, Voyksner RD, Ismail MA, Boykin DW, Tidwell RR, Hall JE. In vitro metabolism of an orally active O-methyl amidoxime prodrug for the treatment of CNS trypanosomiasis. Xenobiotica 2005;35(3):211-26.

18 Ziessman HA, Muenz LR, Agarwal AK, ZaZa AA. Normal values for sincalide cholescintigraphy: comparison of two methods. Radiology 2001;221(2):404-410.

19 Tjandramaga TB, Mullie A, Verbesselt R, De Schepper PJ, Verbist L. Piperacillin: human pharmacokinetics after intravenous and intramuscular administration. Antimicrob Agents Chemother 1978;14(6):829-37.

20 Viollier AF SH, Drusano GL, Tatem BA, Moody MR, Schimpff SC. Comparative pharmacokinetics and serum bactericidal activity of mezlocillin, ticarcillin and piperacillin, with and without gentamicin. J Antimicrob Chemother 1985;15(5):597-606.

21 Fujii R, Okuno A, Fujita K, Yoshikawa M, Inyaku F, Takimoto M, et al. Comprehensive evaluation of pharmacokinetic and clinical studies on tazobactam/piperacillin in pediatric field. Jpn J Antibiot 1995;48(3):311-45.

22 Toyonaga Y, Ishihara T, Tezuka T, Nakamura H. Pharmacokinetic and clinical evaluation of tazobactam/piperacillin in the pediatric field. Jpn J Antibiot 1998;51(5):325-45.

23 Ford SL, Kowalsky RJ, Heizer WD, Falen SW and Brouwer KL. Evaluation of a novel method to quantify biliary excretion in humans. Clin Pharmacol Ther 2002;71(P26):MPI-85.

24 Dong M, Sonoda Y, Kawamoto M, Konomi H, Kobayashi K, Yamaguchi K, Tanaka M. Duodenum is important for the sphincter of Oddi motor response to cholecystokinin octapeptide in conscious dogs. J Gastroenterol 2005;40(4):389-95.

25 Calhoun P, Brown KB, Strunk R, Krusch DA, Scheld WM, Hanks JB. Experimental studies of biliary excretion of piperacillin. Ann Surg 1987;205(4):420-7.

26 Brogard JM, Caro-Sampara F, Westphal JF, Blickle JF, Jehl F. Biliary elimination and hepatic disposition of an association of piperacillin and tazobactam: experimental evaluation. Drugs Exp Clin Res 1994;20(6):247-55.

27 Mahmood I. Interspecies scaling of biliary excreted drugs: a comparison of several methods. J Pharm Sci 2005;94(4):883-92.

28 Owyang C, Williams, J. A. Pancreatic Secretion. In: Yamada T, editor. Textbook of Gastroenterology. 4 ed. Philadelphia: Lippincott Williams and Wilkins; 2003. p. 340-348.

29 Rajaonarison JF, Lacarelle B, Catalin J, Placidi M, Rahmani R. 3'-azido-3'-deoxythymidine drug interactions. Screening for inhibitors in human liver microsomes. Drug Metab Dispos 1992;20(4):578-84.

30 Ito K, Koresawa T, Nakano K, Horie T. Mrp2 is involved in benzylpenicillin-induced choleresis. Am J Physiol Gastrointest Liver Physiol 2004;287(1):G42-9.

TABLES

Table 4.1: Summary of individual and mean pharmacokinetic parameters, biliary recovery and urinary recovery of piperacillin and ejection fraction for Subjects A, B and C.

Parameter	Subject A	Subject B	Subject C	Mean	SD
Administered Dose (mg)	1700	1764	1586	1683	90
Biliary Recovery (% dose)	0.77	0.32	0.14	0.41	0.32
Urinary Recovery (% dose)	72	85	60	72	13
Ejection Fraction	0.82	0.28	0.07	0.39	0.39
Recovery of Excreted Dose (% dose)	0.87	1.1	1.4	1.1	0.3
CL_{total} (mL/min/kg)	3.2	2.5	2.9	2.9	0.3
$CL_{biliary}$ (mL/min/kg)	0.025	0.008	0.004	0.012	0.011
in vivo $CL_{biliary}$ (mL/min/kg)	0.028	0.028	0.041	0.032	0.008

Fig 4.1: Planar gamma scintigraphic frontal images from Subject 2 and Subject B.

Images illustrate Tc-99m mebrofenin accumulation in the liver, hepatobiliary tree and discharge into the duodenum after CCK-8 administration (specified time refers to the min post Tc-99m mebrofenin administration in both subjects). Radioactive bile was collected from the portion of the intestine occluded by the distal balloon, which prevented visualization of lower parts of the gastrointestinal tract.

Subject 2 in [7] (total EF=0.86)

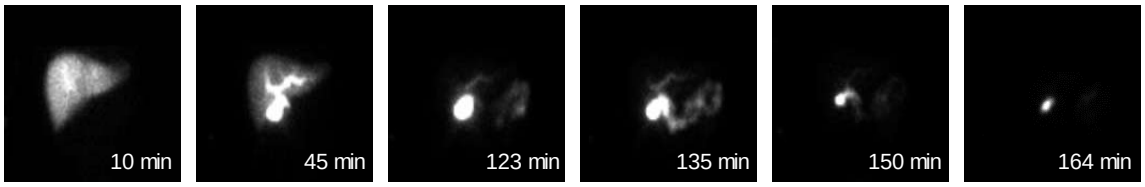

Subject B (total EF=0.28)

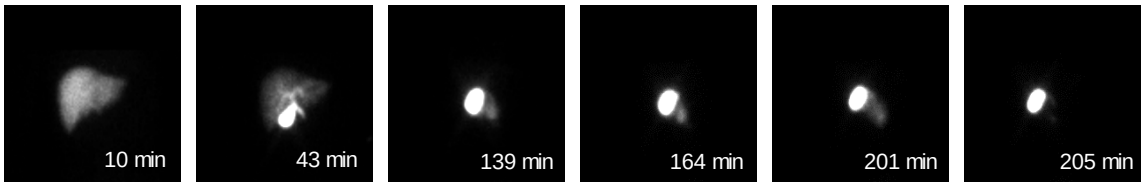

Fig. 4.2: Piperacillin plasma concentration-time profile for Subjects A, B and C and individual piperacillin cumulative biliary recoveries.

Piperacillin plasma concentration-time profile for Subjects A, B and C are plotted on the left axis (mean ± SD). Individual piperacillin cumulative biliary recoveries expressed as a percentage of the maximum recovery are plotted on the right axis. CCK-8, fatty food (milk) and orange zest were administered at 240, 280 and 320 min post piperacillin administration (arrows).

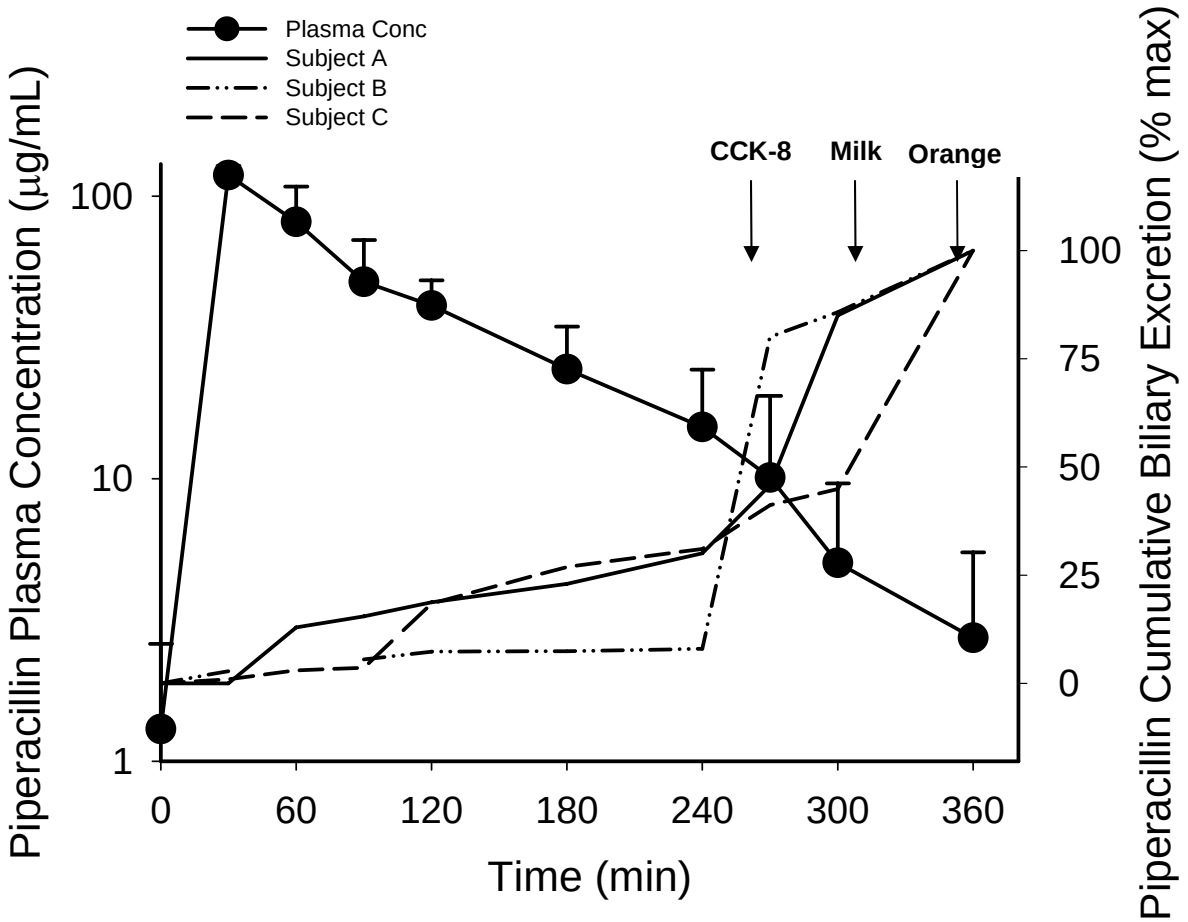

Fig 4.3: **Time-course of bilirubin and piperacillin excretion in duodenal aspirates.**

The amounts of bilirubin and piperacillin recovered in the duodenal aspirates are expressed as a percentage of maximum recovery. CCK-8, fatty food (milk) and orange zest (to Subject C only) were administered at 240, 280 and 320 min post piperacillin administration (arrows).

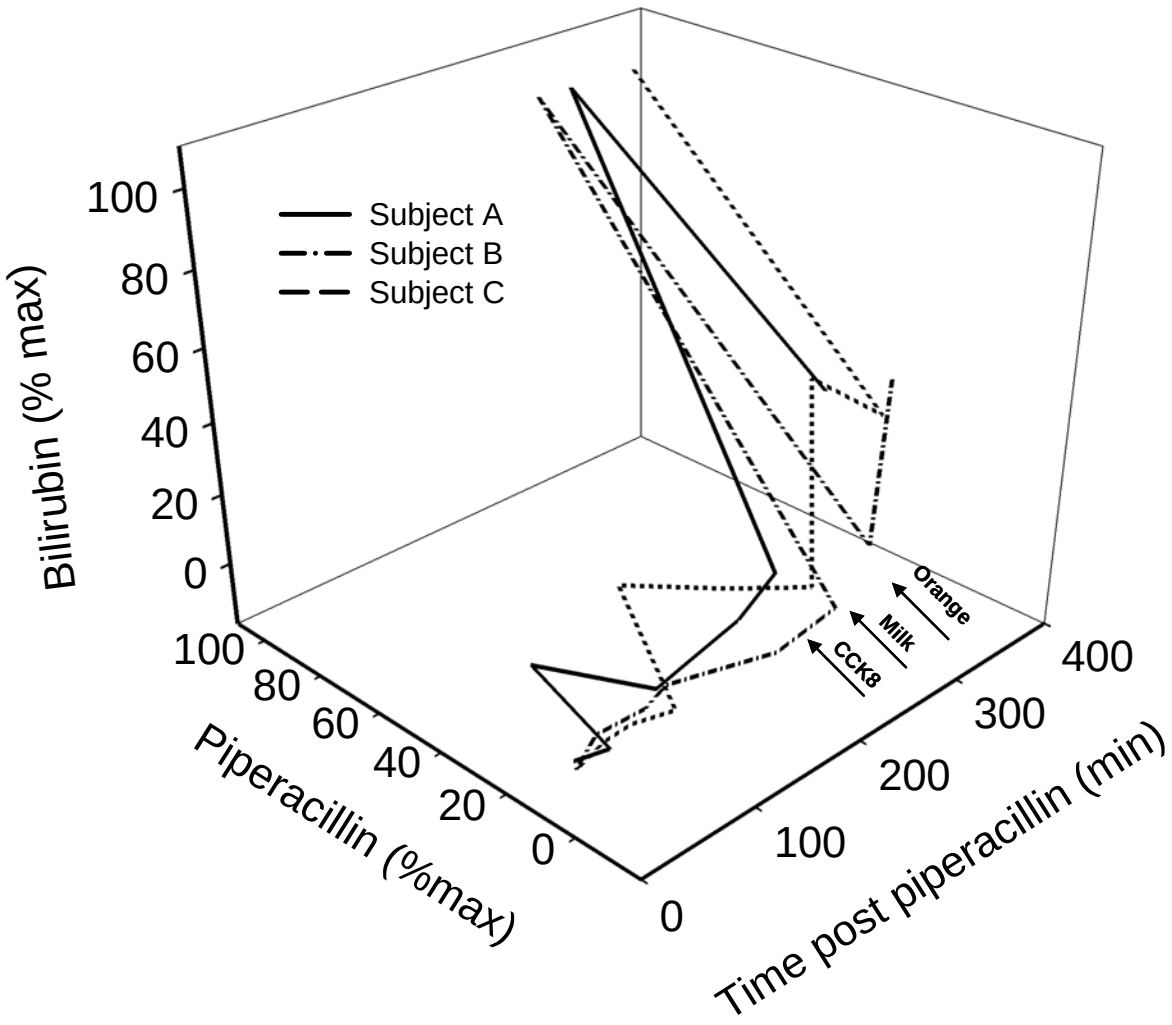

Fig 4.4: Relative amounts of piperacillin, desethylpiperacillin and desethylpiperacillin glucoronide in urine and duodenal aspirates.

Relative amounts of piperacillin (PIP), desethylpiperacillin (DEP) and desethylpiperacillin glucuronide (DEPG) in urine (left ordinate axis) and duodenal aspirates (right ordinate axis). Relative amounts are expressed as the mean ± SD of the internal standard (IS) area ratio multiplied by the collected volume.

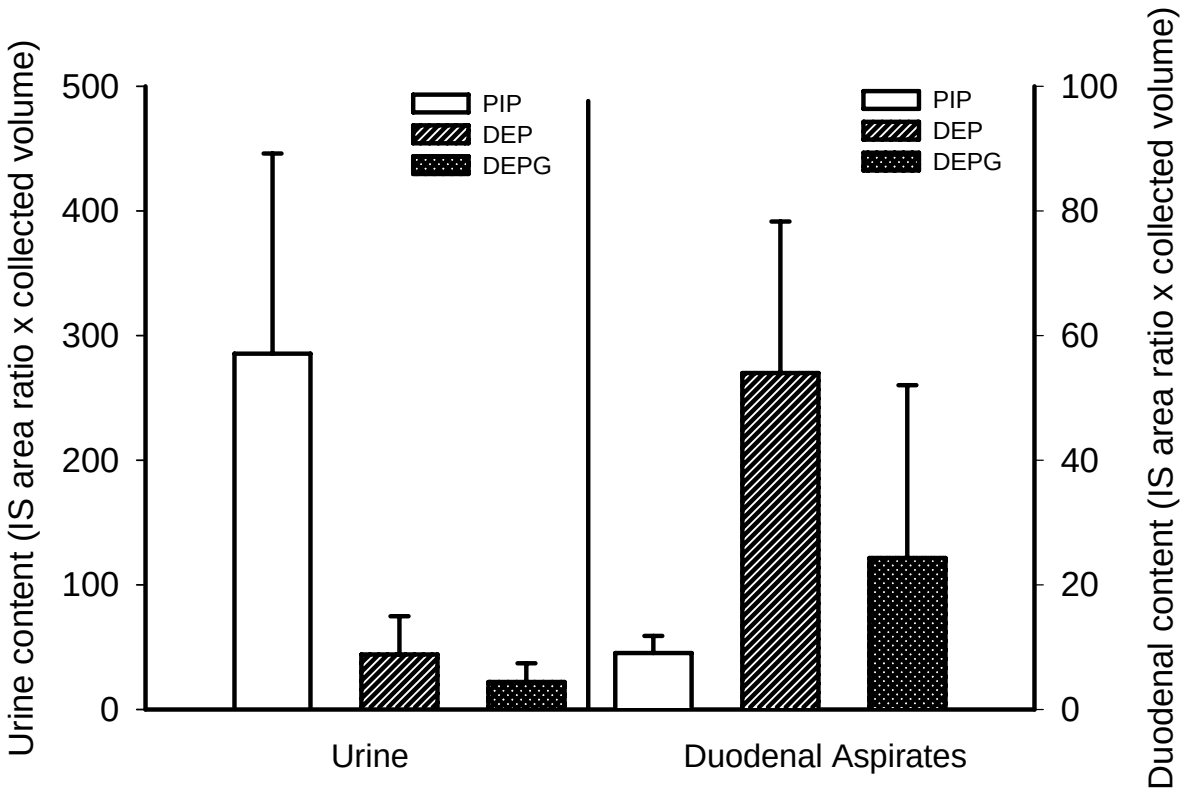

Fig 4.5: Structure and Structural identification of piperacillin and metabolites.

A) Structure of piperacillin, desethylpiperacillin and desethylpiperacillin glucuronide.

B) Auto MS^n of [M+H] = 664, the predicted pseudomolecular ion of desethylpiperacillin glucuronide, and Auto MS^n of [M+H] = 488, the pseudomolecular ion of desethylpiperacillin. A glucuronide specific neutral loss of 176 amu was observed

A

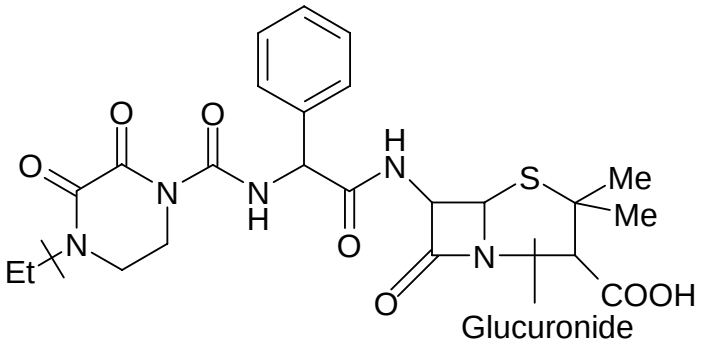

B

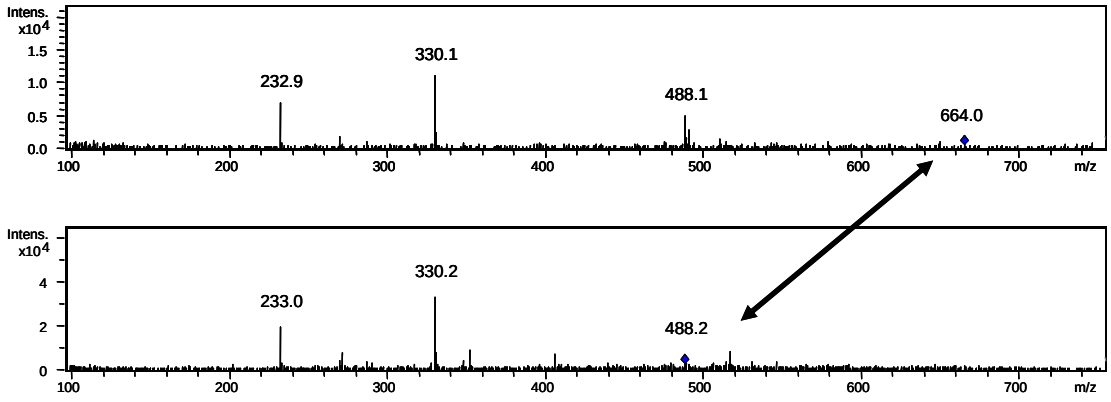

Fig 4.6: Piperacillin metabolism in human liver microsomal incubations.

A) Desethylpiperacillin formation (mean ± SD) over time in the presence and absence of NADPH. NADPH incubations were performed in triplicate.

B) Desethylpiperacillin (DEP), desethylpiperacillin glucuronide (DEPG) and piperacillin glucuronide (PIPG) formation over time in the presence of NADPH and UDPGA. All incubations were performed in duplicate and the mean value is reported. Insert shows the formation of desethylpiperacillin glucuronide over time on an enlarged scale.

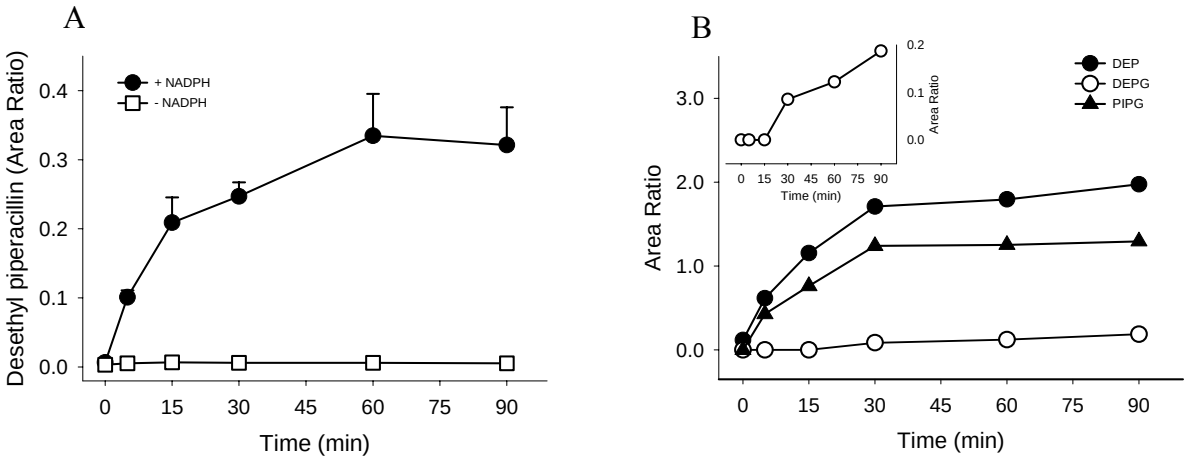

CHAPTER 5

UTILITY OF SANDWICH-CULTURED HUMAN HEPATOCYTES TO PREDICT HEPATOBILIARY DRUG DISPOSITION IN HUMANS

This Chapter will be submitted to *The Journal of Clinical Investigation* and is presented in the style of that journal.

ABSTRACT

The complexities of hepatobiliary drug disposition, coupled with species-dependent differences in metabolism and transport of drugs, make predictions regarding the extent of hepatobiliary clearance and interactions with endogenous and exogenous substances in humans very challenging. Sandwich-cultured human hepatocytes are an *in vitro* tool used to estimate the biliary clearance of drugs ($Cl_{biliary}$). However, information on the predictive capabilities of this model are lacking due to the absence of systematic *in vivo* studies in healthy volunteers. Recently, a reliable method was developed to quantify the $Cl_{biliary}$ of drugs in healthy humans. Using this methodology, Tc-99m mebrofenin (MEB) and piperacillin (PIP) were determined to exhibit high and low $Cl_{biliary}$, respectively. In the present study, the $Cl_{biliary}$ of Tc-99m sestamibi (MIBI), calculated as the ratio of the mass in bile corrected for gallbladder ejection fraction, to the area under the blood concentration-time profile was determined in healthy subjects (5.5±1.2 mL/min/kg). Additionally, *in vivo* $Cl_{biliary}$ values were compared to predicted $Cl_{biliary}$ values obtained in sandwich-cultured human hepatocytes. The rank order of predicted $Cl_{biliary}$ corresponded well with measured *in vivo* $Cl_{biliary}$ values for MEB (7.44 vs 16.1 mL/min/kg), MIBI (1.2 vs 5.5 mL/min/kg) and PIP (0.0028 vs 0.0032 mL/min/kg), indicating that sandwich-cultured human hepatocytes may be a useful model to predict hepatobiliary drug clearance.

INTRODUCTION

The prominent role of the liver in the biotransformation and elimination of xenobiotics in animals and humans is well recognized. Many *in vitro* tools as well as animal models have been established to study processes involved in the metabolism and hepatobiliary disposition of drugs (1, 2). Despite the availability of *in vitro* models to estimate the biliary clearance of compounds *in vivo*, there is little information on the predictive accuracy of these methods due to the absence of systematic studies measuring the biliary clearance of xenobiotics in humans. These values are needed to compare *in vitro* and *in vivo* systems (3, 4). However, due to the complexities of the procedures needed to measure hepatobiliary clearance of compounds in humans, as well as species-dependent differences in hepatic metabolism and transport, it is very challenging to predict the biliary clearance of drugs and the potential for interactions in biliary clearance with endogenous and exogenous substances in humans (5, 6). This often translates into costly failures of drugs at late stages in development, due to unexpected liver toxicity or drug interactions at the hepatic enzyme and transporter level (7-9).

The anatomy of the human hepatobiliary system, as well as the intermittent and incomplete expulsion of bile from the gallbladder, must be considered when developing an accurate method to quantify biliary clearance of drugs in humans. Recently, we developed a novel clinical methodology to determine the extent of biliary excretion of drugs that improves the recovery of biliary secretions and corrects for incomplete gallbladder contraction (10). After administration of the drug of interest, bile secreted into the duodenum is collected with an oroenteric catheter while temporarily occluding the intestine with an inflatable balloon. Additionally, the degree of gallbladder response to pharmacological

stimulation, and any escape of bile distal to the balloon due to partial occlusion of the intestine, are evaluated by administering an imaging agent that is excreted into bile. In previously published clinical studies, the biliary clearance of two probes (Tc-99m mebrofenin and piperacillin) exhibiting extensive and minimal biliary excretion, respectively, was determined (10, 11). In order to obtain a wide range of biliary clearance values for comparison with *in vitro* determinations, Tc-99m sestamibi was selected for investigation; Tc-99m sestamibi was expected to display an intermediate extent of elimination into bile. Tc-99m sestamibi is a cationic complex of technetium-99m (Tc-99m 2-methoxyisobutylisonitrile) that distributes into the heart in proportion to blood flow and myocardial viability, and is used in nuclear medicine to assess myocardial perfusion (12, 13). A significant portion of the administered dose is excreted into bile (14), with over 27% of the dose recovered in urine and 33% in feces within 48 hours after administration (15).

Biliary excretion of drugs can be investigated *in vitro* using various model systems with different degrees of complexity (5). Primary rat hepatocytes cultured between two layers of gelled collagen in a sandwich configuration have been well characterized. Similarly, sandwich-cultured human hepatocytes repolarize, form canalicular networks, express and properly localize relevant, functional drug transport proteins, and can be used to characterize uptake and efflux of xenobiotics by the liver (16, 17). Using this system, it is possible to determine the biliary excretion of drugs by disrupting the tight junctions via modulation of calcium in the medium (16, 18-20).

In the present study, the predicted biliary clearance values of three probe compounds were estimated from data generated in sandwich-cultured human hepatocytes (SCHH) and these values were compared with *in vivo* biliary clearance values measured in humans in

order to determine how well this *in vitro* model predicted the hepatobiliary clearance of drugs in humans.

RESULTS

Tc-99m sestamibi disposition in healthy volunteers:

Tc-99m sestamibi (2.5 mCi, IV bolus) was administered to seven healthy males, and relevant pharmacokinetic parameters, including renal and biliary clearance, were determined (Table 5.1). The individual Tc-99m sestamibi blood concentration-time profiles are shown in Fig 5.1A. Tc-99m sestamibi quickly distributed out of the blood compartment as demonstrated by a rapid decline in blood concentrations during the 15-min distributional phase. Tc-99m sestamibi disposition was similar in all subjects. A small secondary peak was noticeable in the plasma concentration-time profile of all volunteers at 40 min; this peak accounted for less than 3.4% of the overall exposure to Tc-99m sestamibi. The radioactivity-time profile of Tc-99m sestamibi appearing in duodenal aspirates, after correction of the mass collected in bile post CCK-8 administration for gallbladder ejection fraction (EF), is shown in Fig 5.1B. In subjects 2 and 3, small amounts of radioactivity appeared in the duodenum at early time points, probably due to spontaneous partial emptying of the gallbladder. Six out of the seven volunteers enrolled in this clinical study responded to the pharmacological action of CCK-8 (Table 5.1).

The renal clearance of Tc-99m sestamibi was 4.6±1.2 mL/min/kg; biliary clearance was similar to renal clearance. Correction of biliary clearance ($Cl_{biliary}$) for EF diminished the inter-subject variability in this pharmacokinetic parameter ($Cl_{biliary}$=3.9±2.0 mL/min/kg vs *in vivo* $Cl_{biliary}$=5.5±1.2 mL/min/kg). The gamma scintigraphy images also confirmed that the disposition and elimination of Tc-99m sestamibi were similar in all subjects. Representative images from subject 4 are shown in Fig 5.2. Tc-99m sestamibi quickly accumulated in the gallbladder (12 min) and, at the same time, was excreted extensively into urine (the kidneys

were visible throughout the experiment, and the urinary bladder filled with radioactivity over time; Fig 5.2). Additionally, radioactivity rapidly appeared in the upper and lower regions of the gastrointestinal tract (Fig 5.2, arrow A throughout all time frames). At early time points, Tc-99m sestamibi intestinal secretion was visible more clearly in the lower part of the small intestine (Fig 5.2, arrow A, 12 min). Subsequently, the radioactivity descended along the intestine until it reached the colon where it accumulated, presumably due to fecal compaction. There was no visible discharge of bile and no radioactivity was recovered in duodenal secretions until 120 min post dose when CCK-8 was infused intravenously. These observations suggest that the radioactivity visible in the GI tract was distal to the balloon occlusion and was related to intestinal secretion rather than biliary excretion. At 120 min, CCK-8 was administered, resulting in contraction of the gallbladder and discharge of radioactive bile into the duodenum. Radioactivity was aspirated rapidly and removed via the oroenteric tube; complete intestinal occlusion and aspiration of the duodenal fluids was confirmed by the observation that no additional radioactivity appeared in the lower parts of the GI tract (Fig 5.2, arrow B).

***In vitro* biliary excretion of model probes in SCHH:**

The *in vitro* biliary excretion of Tc-99m mebrofenin, Tc-99m sestamibi and piperacillin was measured in SCHH. As a positive control, taurocholate cellular accumulation and the biliary excretion index (BEI) were evaluated. The BEI of taurocholate ranged from 50% to 66% in the four SCHH preparations; cellular accumulation and biliary excretion were similar among preparations (Fig 5.3). Consistent with the previously reported *in vivo* Tc-99m mebrofenin hepatobiliary disposition data (10), the uptake of this agent into SCHH was very rapid with up to ~ 25% of the dose accumulating in cells+bile over 10 min

(Fig 5.4, Panel A). In addition, biliary excretion of Tc-99m mebrofenin *in vitro* was rapid, as represented by a BEI of 20-54 % at 10 min. In contrast, the hepatic uptake of Tc-99m sestamibi was modest; less than ~2.9% of the administered dose of Tc-99m sestamibi accumulated in the SCHH at 10 min (Fig 5.4, Panel B). The BEI of Tc-99m sestamibi ranged from 23 to 40% at 10 min. The incubation time of SCHH with piperacillin in the *in vitro* experiments was prolonged to 30 min to allow adequate cellular accumulation of piperacillin to detect biliary excretion. The BEI for piperacillin in SCHH after the 30 min incubation ranged from 9-27% (Fig 5.4, Panel C). Less than 0.32% of the piperacillin dose accumulated in SCHH during this time interval; however, in all preparations a detectable amount of piperacillin was excreted into the canalicular networks. The hepatocytes used in these studies were obtained from four different donors; the demographic characteristics of these donors are summarized in Table 5.2. The extent of bile canalicular network formation was donor-dependent and differed widely as evidenced by the microscopic images (Fig 5.5). Sandwich-cultured hepatocytes from Liver 2 exhibited the least canalicular network formation (Fig 5.5A); bile canaliculi were limited in size and did not entirely surround the hepatocytes. In contrast, sandwich-cultured hepatocytes from Liver 4 developed extensive canalicular networks (Fig 5.5B) with bright belt-like structures between hepatocytes. The biliary excretion index of the probes corresponded to the degree of canalicular network development (the BEI for taurocholate, Tc-99m mebrofenin, Tc-99m sestamibi and piperacillin was higher in SCHH from Liver 4 than for Liver 2).

Comparisons of *in vitro-in vivo* biliary clearance:

Intrinsic *in vitro* biliary clearance values (*in vitro* $Cl_{biliary}$) were calculated for the three probes investigated in these studies and for taurocholate (Table 5.3) and scaled to mL/min/kg as

described in the methods. Additionally, the well-stirred model for hepatic disposition was used to estimate a biliary clearance value (predicted $Cl_{biliary}$) from *in vitro* $Cl_{biliary}$ obtained in SCHH. The biliary clearance values determined from the clinical studies were corrected for gallbladder EF to account for variable and incomplete contraction of the gallbladder. This corrected *in vivo* biliary clearance value is a more reliable estimate of biliary clearance in humans and can be considered the true *in vivo* $Cl_{biliary}$. The *in vivo* $Cl_{biliary}$ values for the three probes determined utilizing our clinical methodology were compared to the predicted $Cl_{biliary}$ values from the SCHH data (Table 5.4). The *in vitro* model consistently predicted a lower biliary clearance than the observed value *in vivo*. The relationship between *in vivo* $Cl_{biliary}$ and predicted $Cl_{biliary}$ values is plotted in Fig 5.6. Inspection of Fig 5.6 reveals that the "estimated" value from *in vitro* data was correctly ranked with the "measured" $Cl_{biliary}$ *in vivo* for the three compounds investigated in these studies.

DISCUSSION

The clinical protocol employed in this study to investigate the hepatobiliary disposition of Tc-99m sestamibi yielded numerous pharmacokinetic parameters, including the biliary and renal clearance of this agent. Tc-99m sestamibi is less than 1% bound to plasma proteins (15) and, in this study, the total renal clearance of this agent was determined to be 4.6±1.2 mL/min/kg, which is higher than the glomerular filtration rate (1.7 mL/min/kg), and consistent with the observation that this compound is a substrate for efflux transporters present in the kidney such as P-glycoprotein (P-gp/ABCB1). Interestingly, the radioactivity associated with the presence of Tc-99m sestamibi in the GI tract observed in the images, was distal to the occlusive balloon, suggesting that Tc-99m sestamibi also undergoes intestinal secretion, presumably due to intestinal P-gp activity. P-gp expression is low in the upper part of the intestine, but increases in the lower gastrointestinal tract in humans (21). This may explain why no radioactivity was collected via the catheter in the upper part of the duodenum in the majority of the subjects until after gallbladder contraction was induced by CCK-8. This conclusion also is supported by the gamma images at very early time points depicting radioactivity in the ileum and colon when the gallbladder was slowly filling. The blood activity-time profiles in the seven subjects were comparable to other studies (22); the small secondary peak noticeable in the plasma profiles could be due to some entero-enteric recirculation of this compound. It is unlikely that enterohepatic recirculation could account for this secondary peak since the duodenal occlusive balloon was inflated and no radioactivity was collected until 120 min in 5 out of 7 subjects. Even though Tc-99m sestamibi is a large cationic molecule, a small portion of the dose excreted into the intestine might be reabsorbed along the gastrointestinal tract. It is not possible to differentiate

between intestinal and biliary secretions with this technique. Thus, the radioactivity collected in duodenal aspirates from subjects 2 and 3 prior to administration of CCK-8 (Fig 5.1B) may have been expelled from the gallbladder due to a spontaneous contraction, or may have appeared in the duodenal lumen following intestinal secretion.

From the results of the current study and of the Tc-99m mebrofenin and piperacillin studies it can be concluded that this clinical methodology can be applied to determine biliary clearance of drugs that exhibit high, intermediate and low degrees of excretion into bile. In all cases, the correction for EF reduced the inter-subject variability of the corrected biliary clearance estimate, accounting for incomplete bile and drug expulsion from the gallbladder.

The ability to determine an important parameter such as hepatobiliary clearance *in vivo* allows for comparison of the results obtained with the SCHH model. This *in vitro* system has been employed only recently to investigate the biliary excretion of drugs. The intrinsic biliary clearance of a series of compounds determined in sandwich-cultured rat hepatocytes demonstrated a good correlation between "predicted" and "measured" values obtained in the same animal species (19). Likewise, the results presented here suggest that SCHH can be used to correctly classify the biliary clearance of compounds in humans. The rank order of the biliary clearance values predicted from *in vitro* data corresponded well with biliary clearance values measured *in vivo*. The removal from sinusoidal blood of the model compounds utilized in these studies and elimination into bile is presumably handled by different transport proteins. Thus, it is essential that the *in vitro* system maintains expression and function of hepatic drug transport proteins similar to the *in vivo* situation in order to correctly classify compounds with respect to biliary clearance (low, intermediate or high). The present data provide the first evidence that SCHH are capable of predicting the biliary

clearance of compounds in humans, and enables comparisons of drugs with different chemical structures and diverse mechanisms of hepatic uptake and biliary excretion.

The predicted $Cl_{biliary}$ was consistently lower than the *in vivo* $Cl_{biliary}$ for the probes studied here. These findings could be related to less extensive canalicular network formation in culture compared to liver tissue *in vivo*. In the liver, adjacent hepatocytes form bile canaliculi at each cell-cell contact, and the interconnected canalicular spaces drain bile away from the hepatocytes and into small bile ducts. When cultured in a sandwich configuration, primary human hepatocytes repolarize over time and form bile canaliculi (23); however, the extent of bile canalicular network formation varies from donor to donor, and is not as extensive as observed in the native tissue. If less surface area per hepatocyte is occupied by bile canaliculi, then less drug would be excreted into bile in sandwich-cultured hepatocytes compared to *in vivo*. Ideally, it would be possible to estimate the volume of the canalicular network *in vitro* and *in vivo* and adjust the predicted $Cl_{biliary}$ by this factor. Additionally, the SCHH system is considered mildly cholestatic because the canalicular networks are sealed and cannot drain bile away from the cells. This static system may reduce bile flow and the production of bile acids and, consequently, may influence the biliary excretion of drugs. Despite this, the SCHH system can clearly distinguish between drugs with different extents of hepatic clearance, and is capable of predicting whether a compound would be extensively, moderately or negligibly extracted by the liver and excreted into bile *in vivo* in humans.

Undoubtedly, the ability to determine the biliary clearance of drugs *in vitro* and to predict the extent of hepatic excretion for an uncharacterized compound is important from a pharmacokinetic and toxicological perspective. The application of this *in vitro* model to drug development could provide insight regarding the formation and hepatobiliary disposition of

potentially toxic metabolites, or could predict drug-drug interactions in a more complex system than microsomal incubations. The three probes selected for investigation in the present study displayed almost ideal characteristics (intravenous administration, short half-life, minimal or no metabolism) in order to simplify the execution of these proof-of-concept studies and minimize the length of the intubation time. However, the same approach could be employed, with some modifications, to orally administered, metabolically unstable compounds, or drugs with longer elimination half-lives. Currently, new clinical studies are underway to investigate compounds with more diverse properties and to evaluate *in vivo* drug interactions with this methodology. The work presented here provides the foundation for exploring mechanisms of drug-drug and drug-metabolite interactions in hepatobiliary clearance in humans, both *in vivo* and *in vitro*. The current work, which includes data from both clinical and *in vitro* studies, is the first report comparing predicted values for biliary clearance obtained in SCHH to *in vivo* determinations. The excellent agreement obtained in these studies suggests that SCHH may be a useful model to predict hepatobiliary drug disposition in humans.

METHODS

Clinical Study Conduct: Seven volunteers (7 men, 21-41 years of age) within 20% of their ideal body weight completed the study. All study subjects were non-smokers and in good health as documented by medical history, physical examination, EKG and routine laboratory testing. Subjects were asked to abstain from any medication for 2 weeks prior to the study, and to abstain from caffeine and alcohol during the study. The Clinical Research Advisory Committee and the Committee on the Protection of the Rights of Human Subjects at the University of North Carolina at Chapel Hill School of Medicine approved all procedures. Subjects provided written informed consent prior to participation in the study. Volunteers consumed high-fat meals prior to insertion of the oroenteric tube to avoid overfilling and stimulate gallbladder emptying (10, 11). After an overnight fast, a custom-made oroenteric tube was passed through the mouth and positioned in the upper portion of the duodenum with the aid of dynamic fluoroscopic radiography. The oroenteric tube used in these studies was a silicone multi-lumen extrusion fitted at the distal end with a polyethylene balloon to occlude the intestine during bile collection; this tube has been described in detail previously (10). The extent of biliary excretion of Tc-99m sestamibi (Cardiolite®, Bristol-Myers Squibb, New York, NY) was determined by positioning the subjects under a gamma camera (E-CAM Dual Head Gamma Camera, Siemens), and an IV bolus of ~2.5 mCi Tc-99m sestamibi was administered via an arm vein. The duodenal balloon was inflated with ~ 30 mL of air, and blood and duodenal aspirates were collected at predetermined time points for 180 min. Anterior and posterior gamma scintigraphic images of the abdominal area were acquired at 1-min intervals. Two hours following Tc-99m sestamibi administration, Cholecystokinin-8 (CCK-8, Sincalide, Kinevac®, 0.02 μg/kg) was administered as an IV infusion over 30 min

to facilitate gallbladder contraction. Urine was collected at the conclusion of the sampling period (180 min).

Pharmacokinetic analysis:

The gallbladder EF was calculated from anterior planar scintigraphic images according to the procedure describe previously for Tc-99m mebrofenin using the following formulas:

$$EF = \frac{\left(GB_{120\,\min} - GB_{180\,\min}\right)}{GB_{120\,\min}} \qquad \text{Eq. 1}$$

$$X_{GB} = X_{bile0-120\,\min} + \left(\frac{X_{bile120-180\,\min}}{EF}\right) \qquad \text{Eq. 2}$$

where GB represents the counts over the gallbladder region and the time in all formulas refers to the minutes after Tc-99m sestamibi administration, X_{bile} represents the amount of Tc-99m sestamibi collected in bile, and X_{GB} (excreted dose) represents the amount of Tc-99m sestamibi collected in bile throughout the study corrected by EF to account for the drug that was excreted into bile, but remained in the gallbladder due to incomplete contraction.

The area under the blood concentration-time curve ($AUC_{0-\infty}$) was calculated from the integration of a tri-exponential fit from non-linear least squares regression of the individual plasma profiles using SigmaPlot (SYSTAT Software, Point Richmond, CA), and AUC_{0-180} was calculated with the linear trapezoidal rule using WinNonlin (version 4.2, Pharsight, Mountain View, CA). Total clearance (Cl_{total}) was calculated as the ratio of the administered dose to $AUC_{0-\infty}$, renal clearance (Cl_R) as the ratio of the cumulative amount of drug recovered in urine at the end of the experiment to $AUC_{0-180min}$, biliary clearance ($Cl_{biliary}$) as the ratio of the cumulative amount of drug recovered in bile at the end of the experiment to $AUC_{0-180min,}$ and the corrected biliary clearance (*in vivo* $Cl_{biliary}$) as the ratio of the excreted dose (X_{GB}) and $AUC_{0-180min}$.

Chemicals and Reagents for *In Vitro* Studies:

Insulin/transferrin/selenium (ITS+) was purchased from BD Biosciences (Bedford, MA, USA). Dexamethasone (DEX), piperacillin, sodium taurocholate, Hanks' balanced salt solution (HBSS) and bovine serum albumin were purchased from Sigma Chemical Co. (St. Louis, MO). All other chemicals and reagents were of analytical grade and were available from commercial sources. [^{3}H]Sodium taurocholate (1.19 Ci/mmol purity > 97%) was obtained from Perkin Elmer Life Sciences (Boston, MA, USA), Tc-99m mebrofenin (Choletec®, Bracco Diagnostics, Princeton, NJ) was prepared at the Nuclear Medicine pharmacy, UNC Hospital, and radiochemical purity evaluated by TLC using ITLS-SA (instant thin layer chromatography polysilicic acid) as the stationary phase and 20% sodium chloride as the mobile phase; solutions employed in the experiments had a radiochemical purity ≥ 90% (24). Tc-99m sestamibi (Cardiolite®, Bristol-Myers Squibb, New York, NY) was purchased from Cardinal Healthcare (Research Triangle Park, NC) and the radiochemical purity of each lot was ≥ 95%.

Isolation and Culture of Human Hepatocytes:

Human liver tissue was obtained by qualified medical staff from the University of North Carolina, School of Medicine as waste from surgical resection. Donor consent and IRB approval (Committee on the Protection of the Rights of Human Subjects) were obtained for all studies involving human liver tissue; these studies followed the tenets of the Declaration of Helsinki promulgated in 1964.

Hepatocytes were isolated by a modification of the two-step collagenase digestion method (25). Hepatocytes were cultured according to the methods described by Hoffmaster with modifications (26). Briefly, 1.5×10^{6} hepatocytes/well were seeded on 6-well Biocoat™ pre-

coated culture plates (BD Bioscience) in 1.5 mL of Dulbecco's Modified Eagle's Medium (DMEM, without phenol red) supplemented with 5% fetal bovine serum (FBS), nonessential amino acids (NEAA), L-Glutamine, penicillin/streptomycin and 1 μM dexamethasone (DEX), and allowed to attach for 2–6 h at 37°C in a humidified incubator with 95% air/ 5% CO_2. After cell attachment, culture plates were swirled gently and medium was replaced with DMEM containing 0.1% ITS+, penicillin/streptomycin, NEAA, L-glutamine and 0.1 μM DEX. Cells were overlayed 6-12 hours after seeding, using ice-cold medium containing 0.25 mg/mL Matrigel™ (BD Bioscience). In order to allow for formation of canalicular networks, human hepatocyte cultures were maintained for 6 days prior to experiments; culture medium was replaced every 24 h. Cells were monitored daily for canalicular network development and the biliary excretion index (BEI) of [^{3}H] taurocholate (1 μM, 100 nCi) after 10 min accumulation was determined on day 6 as described below. Only SCHH preparations that yielded a BEI value for [^{3}H] taurocholate ≥50% were employed to study Tc-99m mebrofenin, Tc-99m sestamibi and piperacillin biliary excretion. Additionally, on day 6, canalicular network formation was evaluated with phase contrast microscopy, and digital images were captured with a Zeiss Axiovert 100TV inverted fluorescent microscope (Carl Zeiss Inc., Thornwood, NY).

Accumulation and Efflux studies in SCHH:

Hepatocytes were rinsed twice with 2 mL of standard HBSS (37°C) and pre-incubated in 2 mL of either standard HBSS or Ca^{2+}-free HBSS (in order to open the tight junctions and disrupt the canalicular networks). Hepatocytes were incubated at 37°C in 1 mL HBSS containing the substrate of interest for 10 min ([^{3}H] taurocholate 1 μM, 100 nCi; 0.5 μCi/mL Tc-99m mebrofenin and 0.5-5 μCi/mL sestamibi) or 30 min (300 μM piperacillin) and

subsequently rinsed vigorously four times with 2 mL ice-cold standard HBSS to remove extracellular substrate and determine the accumulation of substrate in cells (with disrupted canalicular network) and cells+bile (with intact bile canaliculi). For determination of accumulation of [^{3}H] taurocholate, Tc-99m mebrofenin and Tc-99m sestamibi, hepatocytes were lysed with 1 mL of ice-cold 0.5% Triton-X 100 and aliquots were analyzed for radioactivity. For piperacillin studies, hepatocytes were lysed with methanol/water 70/30 (v/v) and piperacillin concentrations were determined by LC-MS-MS. Nonspecific binding was accounted for by including a blank plate (Biocoat™ plus Matrigel™ overlay). The accumulation of Tc-99m labeled compounds was corrected for decay (Tc-99m $t_{1/2}$= 6.02 hr). Protein content in cell lysates was quantified with the BCA method (27) using BSA as the standard (0.2-1 mg/mL), and accumulation was normalized for the protein level. Due to incompatibility of the protein assay with methanol, the average protein content for standard HBSS or Ca^{2+}-free HBSS incubations in the same liver preparation was used to normalize piperacillin content.

The biliary excretion index (BEI) and intrinsic *in vitro* biliary clearance (*in vitro* $Cl_{biliary}$) in SCHH were calculated using B-CLEAR® technology (Qualyst, Inc., Research Triangle Park, NC) based on the following equations:

$$BEI = \frac{Accumulation_{cells+bile} - Accumulation_{cells}}{Accumulation_{cells+bile}} \times 100\% \qquad \text{Eq. 3}$$

$$\textit{In vitro}\ Cl_{biliary} = \left[\frac{Accumulation_{cells+bile} - Accumulation_{cells}}{Time_{incubation} \times Concentration_{medium}} \right] \qquad \text{Eq. 4}$$

Medium concentration was defined as the initial substrate concentration in the incubation medium corrected for non-specific binding to the plates for Tc-99m sestamibi and piperacillin, since preliminary experiments established that the drug concentration at the end

of the incubation did not differ by more than 10% from the initial concentration. For Tc-99m mebrofenin, the concentration in the incubation medium was calculated as the average concentration between the beginning and the end of the incubation, to account for non-specific binding to the plates and hepatocytes during the uptake experiment.

Analytical Methods:

Tc-99m mebrofenin and Tc-99m sestamibi were quantified in whole blood and sandwich-cultured hepatocyte lysates by gamma counting (Quantum-8 Multichannel Analyzer, Oak Ridge, TN). Tc-99m sestamibi in bile and urine was analyzed by a CRC-15R dose calibrator (Capintec, Ramsay, NJ) as described previously (10). Taurocholate was analyzed by liquid scintillation spectroscopy (Packard Tricarb, Packard Corp., Meriden, CT, USA). Piperacillin accumulation in SCHH was analyzed by LC-MS-MS; 100 μL of SCHH lysates was spiked with cimetidine (internal standard) at a final concentration of 0.5 μg/mL. The LC-MS-MS method employed was described in detail previously (28).

Calculation of intrinsic biliary clearance:

The *in vitro* intrinsic biliary clearance (μL/min/mg prot) was scaled to kg of body weight assuming the following: 1 mg protein/1.5x10^6cells (the typical value obtained in all preparations), 107x10^6cells/g of human liver tissue (29), and 25.7g of liver tissue per kg of body weight (30). This value was used to obtain the predicted $Cl_{biliary}$, based on the well-stirred model of hepatic disposition, where Q equals blood flow (21 mL/min/kg) for Tc-99m mebrofenin and Tc-99m sestamibi, and plasma flow [blood flow x (1-hematocrit)] for piperacillin, and *in vitro* $Cl_{biliary}$ is the intrinsic *in vitro* $Cl_{biliary}$ calculated as in equation 4 in the absence of protein binding and flow limitations (31-33)

$$\text{Predicted } Cl_{biliary} = \frac{Q \times \text{in vitro } Cl_{biliary}}{(Q + \text{in vitro } Cl_{biliary})} \qquad \text{Eq. 5}$$

Acknowledgments:

This work was supported by National Institutes of Health grant R01 GM41935 and grant RR00046 from the GCRC program of the Division of Research Resources.

The authors are grateful for the technical assistance of Jonathan Simpson, Ann Whitlow and Jennifer Barner with the clinical studies, Drs. H.J. Kim, M. Meyers, Grant Hogeland and Amar Mehta for the procurement of surgical resections, and Drs.Yiwei Rong and Xianbin Tian for hepatocyte isolation. Giulia Ghibellini is an American Foundation for Pharmaceutical Education Predoctoral Fellow. Dr. Lakshmi Vasist is a University of North Carolina/GlaxoSmithKline Pharmacokinetics/Pharmacodynamics fellow. Dr Elaine Leslie is the recipient of a Postdoctoral Fellowship from the Canadian Institutes of Health Research (CIHR).

REFERENCES

1. Obach, RS, Baxter, JG, Liston, TE, Silber, BM, Jones, BC, MacIntyre, F, Rance, DJ, and Wastall, P. 1997. The prediction of human pharmacokinetic parameters from preclinical and in vitro metabolism data. *J Pharmacol Exp Ther* **283**:46-58.

2. Obach, RS, Walsky, RL, Venkatakrishnan, K, Houston, JB, and Tremaine, LM. 2005. In vitro cytochrome P450 inhibition data and the prediction of drug-drug interactions: qualitative relationships, quantitative predictions, and the rank-order approach. *Clin Pharmacol Ther* **78**:582-592.

3. Sasaki, M, Suzuki, H, Aoki, J, Ito, K, Meier, PJ, and Sugiyama, Y. 2004. Prediction of in vivo biliary clearance from the in vitro transcellular transport of organic anions across a double-transfected Madin-Darby canine kidney II monolayer expressing both rat organic anion transporting polypeptide 4 and multidrug resistance associated protein 2. *Mol Pharmacol* **66**:450-459.

4. Endres, CJ, Hsiao, P, Chung, FS, and Unadkat, JD. 2005. The role of transporters in drug interactions. *Eur J Pharm Sci*.

5. Ghibellini, G, Leslie, EM, and Brouwer, KL. Methods to Evaluate Biliary Excretion of Drugs in Humans: an Updated Review. *Mol Pharm*, in press.

6. Lin, JH. 1995. Species similarities and differences in pharmacokinetics. *Drug Metab Dispos* **23**:1008-1021.

7. Lai, Y, Tse, CM, and Unadkat, JD. 2004. Mitochondrial expression of the human equilibrative nucleoside transporter 1 (hENT1) results in enhanced mitochondrial toxicity of antiviral drugs. *J Biol Chem* **279**:4490-4497.

8. Watkins, PB, and Seeff, LB. 2006. Drug-induced liver injury: Summary of a single topic clinical research conference. *Hepatology* **43**:618-631.

9. Scheen, AJ. 2001. Hepatotoxicity with thiazolidinediones: is it a class effect? *Drug Saf* **24**:873-888.

10. Ghibellini, G, Johnson, BM, Kowalsky, RJ, Heizer, WD, and Brouwer, KL. 2004. A novel method for the determination of biliary clearance in humans. *AAPS J* **6**:e33.

11. Ghibellini, G, Vasist, LS, Hill, TE, Bridges, AS, Heizer, WD, and Brouwer, KL. 2005. Determination of Piperacillin Biliary Clearance in Humans and Identification of Its Metabolites in Bile and Urine. *AAPS J* **7**: M1293.

12. Beller, GA, Sinusas, AJ, and Watson, DD. 1990. Assessment of myocardial perfusion and viability with technetium-99m methoxyisobutyl isonitrile. *Trans Am Clin Climatol Assoc* **102**:41-51.

13. Piwnica-Worms, D, Kronauge, JF, and Chiu, ML. 1990. Uptake and retention of hexakis (2-methoxyisobutyl isonitrile) technetium(I) in cultured chick myocardial cells. Mitochondrial and plasma membrane potential dependence. *Circulation* **82**:1826-1838.

14. Gerard, PS, Moallem, A, Wang, WY, and Lehman, H. 1998. Biliary leak demonstrated on delayed scan from Tc-99m sestamibi myocardial imaging. *Clin Nucl Med* **23**:542-543.

15. Cardiolite. Package insert. Bristol-Myers Squibb.

16. Hoffmaster, KA, Turncliff, RZ, LeCluyse, EL, Kim, RB, Meier, PJ, and Brouwer, KL. 2004. P-glycoprotein expression, localization, and function in sandwich-cultured primary rat and human hepatocytes: relevance to the hepatobiliary disposition of a model opioid peptide. *Pharm Res* **21**:1294-1302.

17. Zhang, P, Swift, BD, Tian, X, and Brouwer, KR. 2005. Interspecies variability of transport protein functions in sandwich-cultured (B-ClearTM) rat, dog and human hepatocytes. *Drug Metab Rev* **37**:307-307.

18. Liu, X, LeCluyse, EL, Brouwer, KR, Gan, LS, Lemasters, JJ, Stieger, B, Meier, PJ, and Brouwer, KL. 1999. Biliary excretion in primary rat hepatocytes cultured in a collagen-sandwich configuration. *Am J Physiol* **277**:G12-21.

19. Liu, X, Chism, JP, LeCluyse, EL, Brouwer, KR, and Brouwer, KL. 1999. Correlation of biliary excretion in sandwich-cultured rat hepatocytes and in vivo in rats. *Drug Metab Dispos* **27**:637-644.

20. Liu, X, LeCluyse, EL, Brouwer, KR, Lightfoot, RM, Lee, JI, and Brouwer, KL. 1999. Use of Ca2+ modulation to evaluate biliary excretion in sandwich-cultured rat hepatocytes. *J Pharmacol Exp Ther* **289**:1592-1599.

21. Mouly, S, and Paine, MF. 2003. P-glycoprotein increases from proximal to distal regions of human small intestine. *Pharm Res* **20**:1595-1599.

22. Wackers, FJ, Berman, DS, Maddahi, J, Watson, DD, Beller, GA, Strauss, HW, Boucher, CA, Picard, M, Holman, BL, Fridrich, R, et al. 1989. Technetium-99m hexakis 2-methoxyisobutyl isonitrile: human biodistribution, dosimetry, safety, and preliminary comparison to thallium-201 for myocardial perfusion imaging. *J Nucl Med* **30**:301-311.

23. Zhang, P, Swift, BD, Tian, X, Brouwer, KR, Dasgupta, M, and Huebert, N. 2005. Optimization of transporter expression and function in sandwich-cultured human hepatocytes (B-ClearTM-HU). *Drug Metab Rev* **37**:306-306.

24. Kowalsky, RJ, and Falen, SW. 2004. Radiopharmaceuticals in Nuclear Pharmacy and Nuclear Medicine. Washington, D.C.: American Pharmacists Association.

25. Hamilton, GA, Jolley, SL, Gilbert, D, Coon, DJ, Barros, S, and LeCluyse, EL. 2001. Regulation of cell morphology and cytochrome P450 expression in human hepatocytes by extracellular matrix and cell-cell interactions. *Cell Tissue Res* **306**:85-99.

26. Hoffmaster, KA, Zamek-Gliszczynski, MJ, Pollack, GM, and Brouwer, KL. 2005. Multiple transport systems mediate the hepatic uptake and biliary excretion of the metabolically stable opioid peptide [D-penicillamine2,5]enkephalin. *Drug Metab Dispos* **33**:287-293.

27. Smith, PK, Krohn, RI, Hermanson, GT, Mallia, AK, Gartner, FH, Provenzano, MD, Fujimoto, EK, Goeke, NM, Olson, BJ, and Klenk, DC. 1985. Measurement of protein using bicinchoninic acid. *Anal Biochem* **150**:76-85.

28. Ghibellini, G, Vasist, LS, Hill, TE, Heizer, WD, Kowalsky, RJ, and Brouwer, KL. Determination of The Biliary Excretion of Piperacillin in Humans using a Novel Method. *Br J Clin Pharmacol*. in press.

29. Wilson, ZE, Rostami-Hodjegan, A, Burn, JL, Tooley, A, Boyle, J, Ellis, SW, and Tucker, GT. 2003. Inter-individual variability in levels of human microsomal protein and hepatocellularity per gram of liver. *Br J Clin Pharmacol* **56**:433-440.

30. Davies, B, and Morris, T. 1993. Physiological parameters in laboratory animals and humans. *Pharm Res* **10**:1093-1095.

31. Pang, KS, and Rowland, M. 1977. Hepatic clearance of drugs. III. Additional experimental evidence supporting the "well-stirred" model, using metabolite (MEGX) generated from lidocaine under varying hepatic blood flow rates and linear conditions in the perfused rat liver in situ preparation. *J Pharmacokinet Biopharm* **5**:681-699.

32. Pang, KS, and Rowland, M. 1977. Hepatic clearance of drugs. II. Experimental evidence for acceptance of the "well-stirred" model over the "parallel tube" model using lidocaine in the perfused rat liver in situ preparation. *J Pharmacokinet Biopharm* **5**:655-680.

33. Pang, KS, and Rowland, M. 1977. Hepatic clearance of drugs. I. Theoretical considerations of a "well-stirred" model and a "parallel tube" model. Influence of hepatic blood flow, plasma and blood cell binding, and the hepatocellular enzymatic activity on hepatic drug clearance. *J Pharmacokinet Biopharm* **5**:625-653.

TABLES

Table 5.1: Pharmacokinetic parameters for Tc-99m sestamibi.

Parameter	Subject 1	Subject 2	Subject 3	Subject 4	Subject 5	Subject 6	Subject 7	Mean	SD
Administered Dose (μCi)	2504	3384	3166	3182	3037	3563	3100	**3134**	**331**
Biliary Recovery (% dose)	10.7	15.4	21.6	16.8	4.7	15.8	17.7	**14.7**	**5.5**
Urinary Recovery (% dose)	25.3	7.3	16.3	19.3	22.1	17.4	22.9	**18.7**	**5.9**
[A]Ejection Fraction	0.47	0.63	0.90	0.64	0.16	0.83	0.79	**0.65**	**0.27**
[B]X_{GB} Recovered (% dose)	22.5	23.0	22.1	26.2	16.8	17.8	22.3	**21.5**	**3.2**
Cl_{total} (mL/min/kg)	15.8	20.2	24.2	19.3	17.7	18.2	19.0	**19.2**	**2.6**
Cl_R (mL/min/kg)	4.6	2.0	5.4	4.6	5.5	5.4	5.0	**4.6**	**1.2**
$Cl_{biliary}$ (mL/min/kg)	1.9	4.3	7.1	4.0	1.2	4.9	3.8	**3.9**	**2.0**
In vivo $Cl_{biliary}$ (mL/min/kg)	4.1	6.4	7.3	6.2	4.2	5.5	4.8	**5.5**	**1.2**

[A] EF calculated between 120 and 180 min
[B] X_{GB}= excreted dose as shown in Methods

Table 5.2: Demographics of human liver donors used for the *in vitro* experiments.

All donors had no history of tobacco and alcohol use within the last two years.

Liver Donor Identification	Age (yr)	Gender	Race	Co-medications	Diagnosis
Liver 1	47	Male	Caucasian	Glimepiride	Hepatic Hemangioma
Liver 2	63	Female	Caucasian	Labetalol, Lisinopril, Warfarin	Metastatic Colon cancer
Liver 3	53	Male	Caucasian	Aspirin, Colchicine, Omeprazole	Metastatic Colorectal cancer
Liver 4	68	Male	Caucasian	Lisinopril	Metastatic Colon cancer

Table 5.3: Biliary excretion index and biliary clearance values of taurocholate, Tc-99m mebrofenin, Tc-99m sestamibi and piperacillin. Values were determined in sandwich-cultured human hepatocytes (n=4 livers, in triplicate; Mean ± SD).

Compound	BEI %	*In vitro* $Cl_{biliary}$		*Predicted* $Cl_{biliary}$ (mL/min/kg)
		(µL/min/mg prot)	(mL/min/kg)	
Taurocholate (t=10 min)	56.9 ± 6.7	8.62 ± 2.45	15.8 ± 4.5	N.D.
Tc-99m Mebrofenin (t=10 min)	34.8 ± 14.0	6.36 ± 1.29	11.7 ± 2.4	7.44 ± 0.97
Tc-99m Sestamibi (t=10 min)	33.0 ± 7.7	0.700 ± 0.328	1.28 ± 0.60	1.20 ± 0.53
Piperacillin (t=30 min)	18.8 ± 8.8	0.015 ± 0.011	0.028 ± 0.020	0.028 ± 0.020

Table 5.4: Biliary clearance parameters. The *in vivo* biliary clearance of Tc-99m mebrofenin and piperacillin were determined in previous studies (10, 28).

Compound	$Cl_{biliary}$ (mL/min/kg)	**In vivo* $Cl_{biliary}$ (mL/min/kg)	*Predicted* $Cl_{biliary}$ (mL/min/kg)
Tc-99m Mebrofenin (n=4)	12.5	16.1	7.44
Tc-99m Sestamibi (n=7)	3.90	5.51	1.20
Piperacillin (n=3)	0.012	0.032	0.028

* $Cl_{biliary}$ corrected for EF

Fig 5.1: Tc-99m sestamibi activity-time profiles in seven healthy subjects.

Blood and bile concentration and mass time profiles, respectively are expressed in radioactivity units.

A: Individual blood concentration-time profiles for Tc-99m sestamibi in healthy volunteers.

B: Individual bile mass-time profiles for Tc-99m sestamibi in healthy volunteers. Amounts of Tc-99m mebrofenin are expressed as μCi and were corrected by EF between 120 and 180 min (CCK-8 was administered at 120 min).

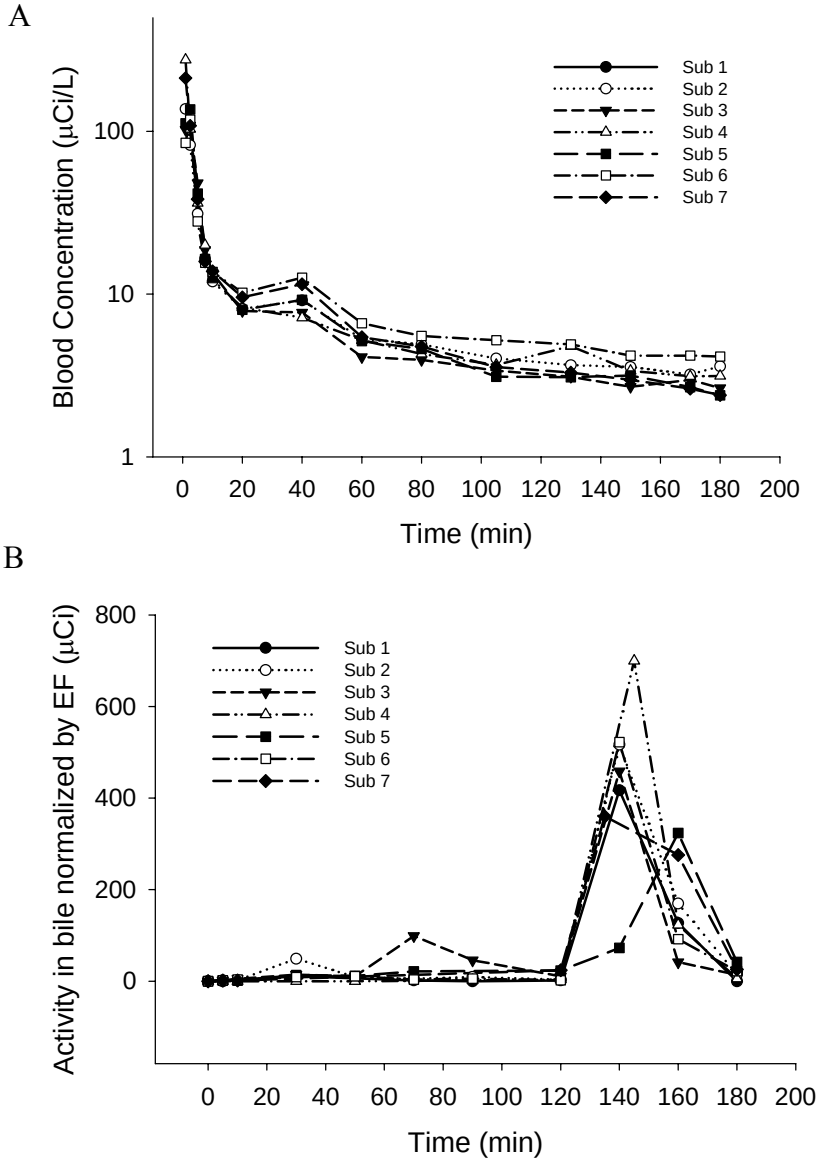

Fig 5.2: Gamma scintigraphic anterior abdominal images of Subject 4 after IV administration of 2.5 mCi Tc-99m sestamibi. In the 5 min frame, the spatial position of all major organs is indicated (HT=heart, SP=spleen, LV=liver, RK and LK=right and left kidney, BL=bladder). The BL was visible only upon filling with radioactive urine (99 min frame). The gallbladder, which started filling with radioactivity at 12 min post dose, overlapped with the RK. A custom-made oro-enteric tube was used to aspirate bile from the duodenum as soon as it was expelled from the common bile duct; inflation of an occlusive balloon in the duodenum facilitated complete bile collection (dotted oval outline indicates the location of the balloon). Intestinal secretion of Tc-99m sestamibi (arrow A) was visible in the lower part of the small intestine at 12 min, and the radioactivity moved down the intestine until it reached the colon (125 min). There was no visible discharge of bile until 120 min when CCK-8 was infused to contract the gallbladder; at this time, radioactive bile was suctioned rapidly from the duodenum via the oro-enteric tube and disappeared (arrow B). No additional radioactivity appeared in the GI tract below the balloon upon gallbladder contraction, indicating successful occlusion of the intestine.

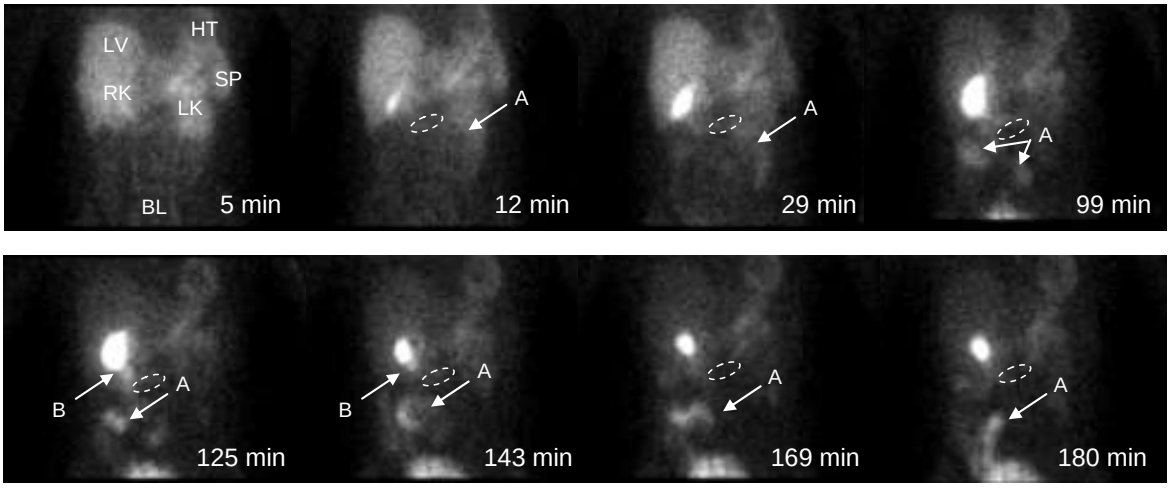

Fig 5.3: Taurocholate accumulation in sandwich-cultured human hepatocytes.

SCHH were incubated with [^{3}H] taurocholate (1 μM, 100 nCi), and cellular accumulation (open bar) and cells+bile accumulation (solid bar) were measured at 10 min (mean ± SD in triplicate, n=4 livers). For each preparation the BEI value is reported.

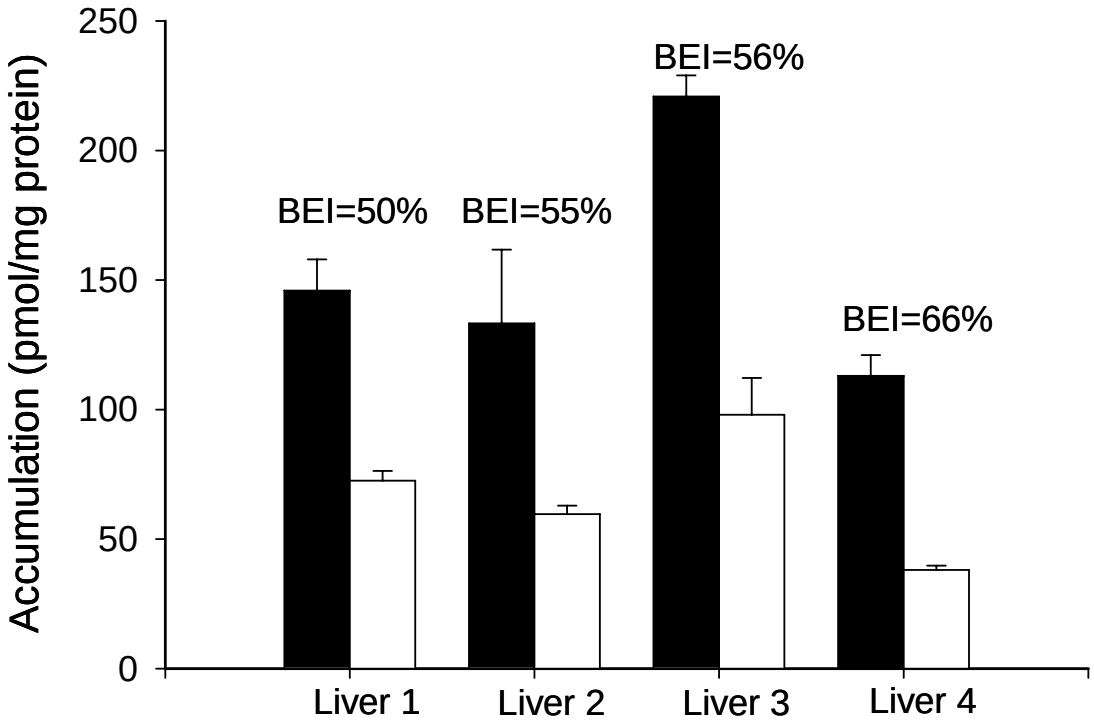

Fig 5.4: Accumulation of Tc-99m mebrofenin, Tc-99m sestamibi and piperacillin in sandwich-cultured human hepatocytes. Bars represent mean ± SD of triplicate determinations in a single liver (n=4 livers). For each preparation the BEI value is reported.

Panel A: SCHH were incubated with Tc-99m mebrofenin (0.5 μCi/mL) and cells (open bar) and cells+ bile accumulation (solid bar) were measured at 10 min.

Panel B: SCHH were incubated with Tc-99m sestamibi (0.5-5 μCi/mL) and cells (open bar) and cells+ bile accumulation (solid bar) were measured at 10 min.

Panel C: SCHH were incubated with piperacillin (300 μM) and cells (open bar) and cells+ bile accumulation (solid bar) were measured at 30 min.

A: Tc-99m Mebrofenin

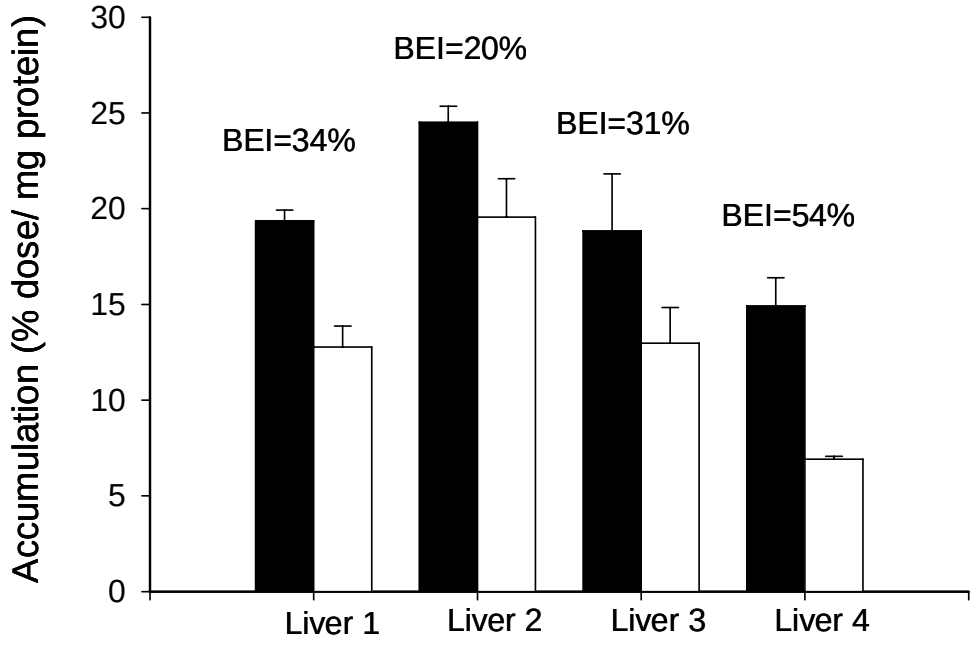

B: Tc-99m Sestamibi

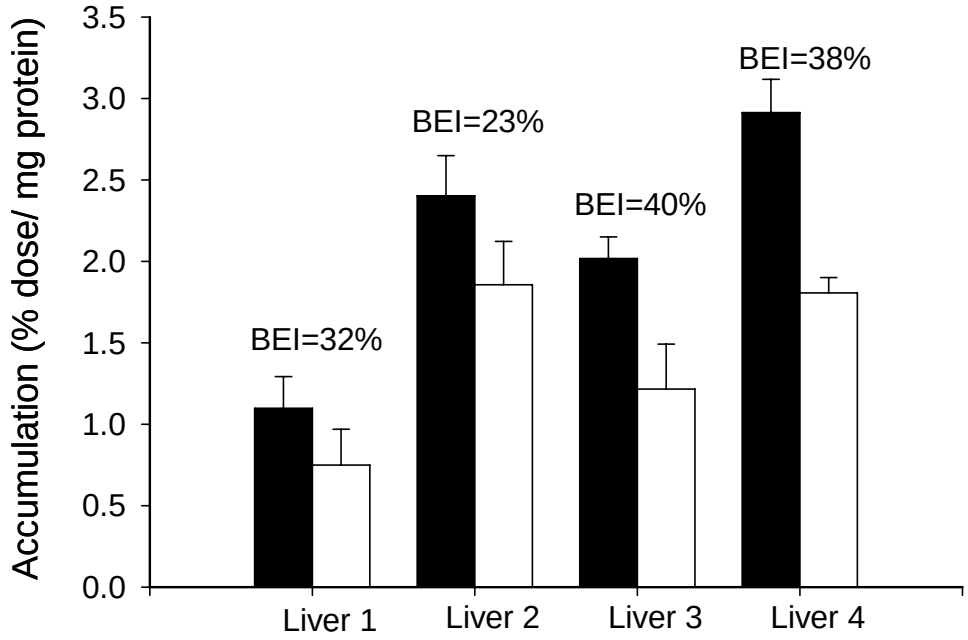

C: Piperacillin

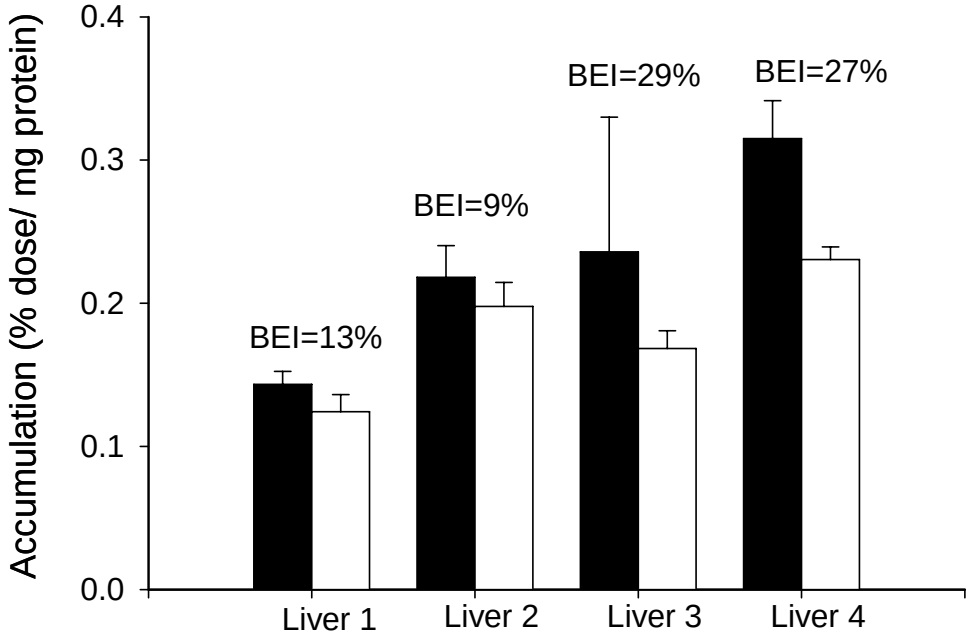

Fig 5.5: Phase contrast images of sandwich-cultured human hepatocytes at day 6 in culture. The bile canalicular network is visible as bright dots or belts between adjacent hepatocytes and is indicated by arrows.

A) human liver #2

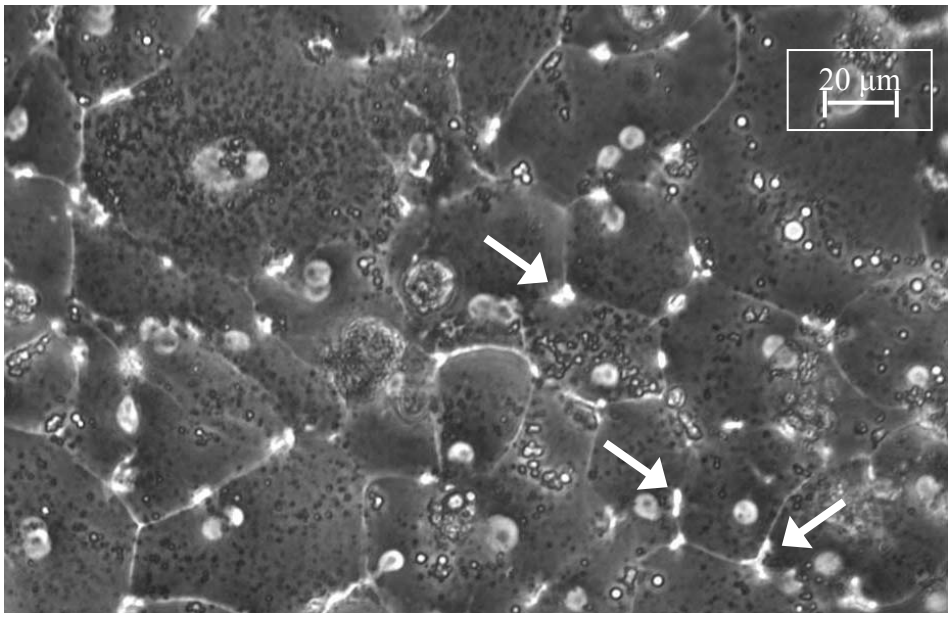

B) human liver #4

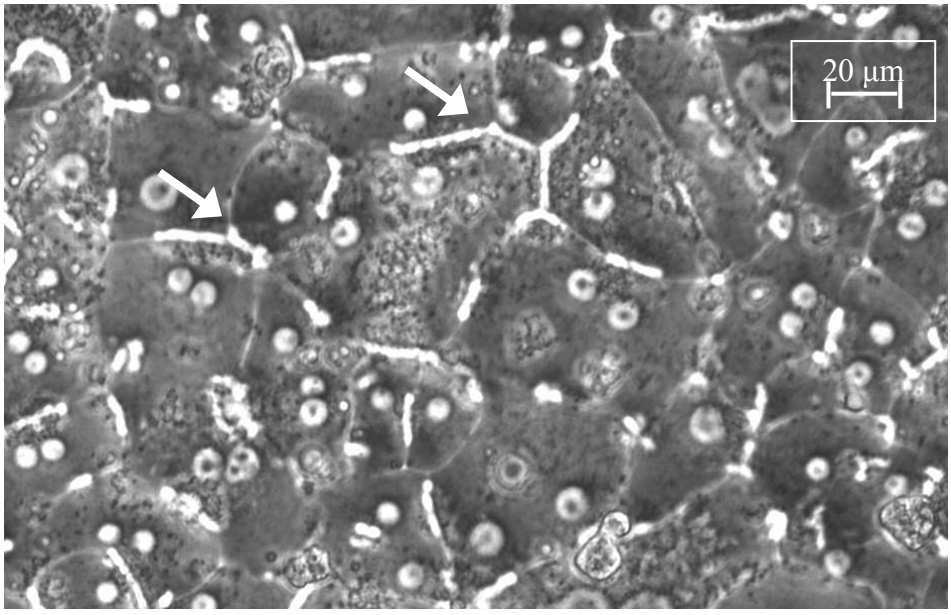

Fig 5.6: Comparison of the *in vitro* and *in vivo* biliary clearance values for the three compounds investigated in these studies.

(solid symbols represent data expressed as mean ± SD).

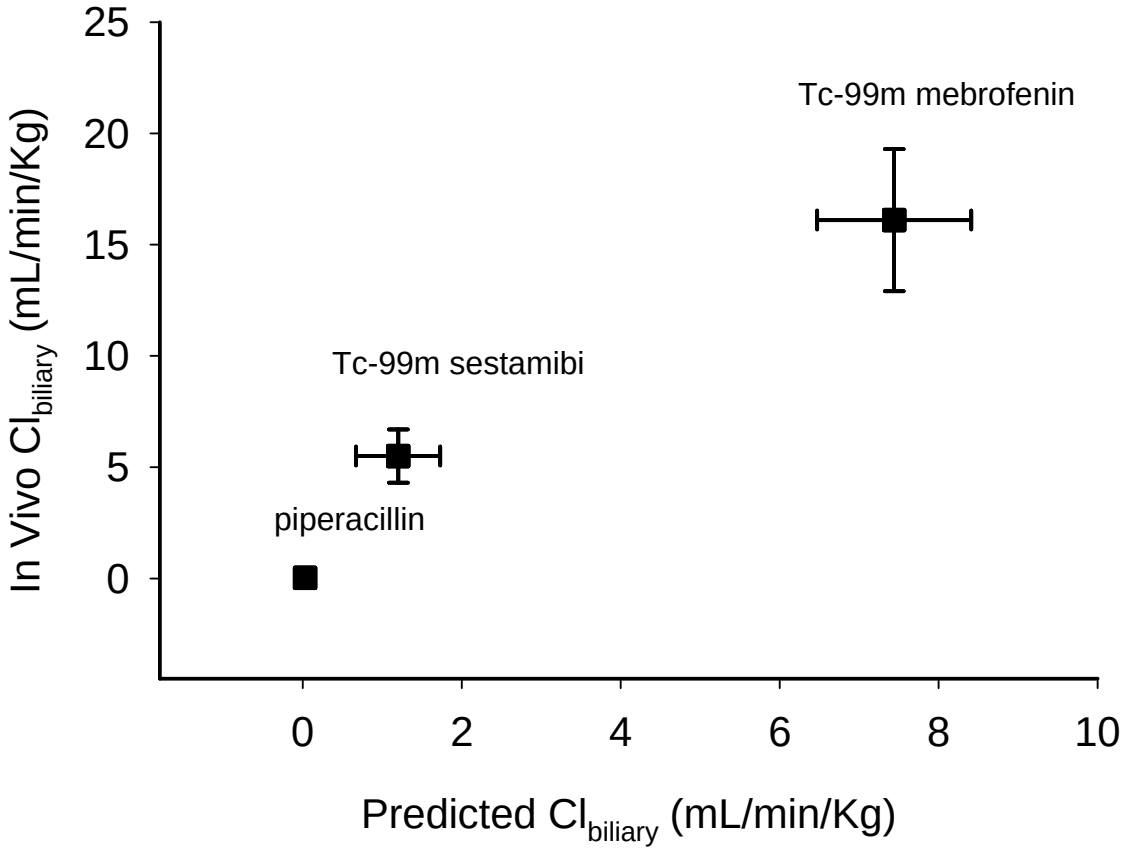

CHAPTER 6

CONCLUSIONS AND FUTURE WORK

The general focus of this dissertation research has been the development of novel *in vivo* and *in vitro* tools to study and characterize biliary clearance of drugs in humans. The contribution of biliary excretion to systemic drug exposure or to intestinal toxicity has been recognized in the literature, at least for drugs like mycophenolic acid and irinotecan metabolites, respectively (1, 2). However, biliary excretion studies are rarely conducted in humans and considerable work is still needed in this field to better elucidate and characterize the processes involved in hepatobiliary drug disposition. This is especially true in light of the significant effects that alterations in hepatobiliary disposition of drugs due to disease states or drug interactions may have on pharmacological efficacy and/or toxicity. The animal models most commonly used to investigate hepatobiliary disposition of drugs are rodents. *In vivo* and *ex vivo* experiments with rats and mice are a very popular way to examine hepatic uptake and efflux mechanisms. An *in vitro* model that may be used for the same purpose is rat hepatocytes cultured in a sandwich configuration. This *in vitro* model has been shown to predict the hepatobiliary disposition of compounds reasonably well compared to results obtained *in vivo* in the same species (3). However, species differences are an insurmountable limitation when performing animal studies. As a result, this research project focused on models that were more relevant to the human species. This dissertation research was designed to provide the basis for the development of an *in vitro-in vivo* correlation in biliary clearance based on data generated in sandwich-cultured human hepatocytes and *in vivo* in humans.

The development of a technique to reliably determine biliary clearance of drugs in humans was the cardinal point of this dissertation. In this study, a technique was developed to collect bile from the duodenum and account for the fraction of secreted bile remaining

within the gallbladder. This has several advantages when compared to similar methods already reported in the literature. Over the past 40 years, many approaches to aspirate pancreatic and biliary secretions have been described; several of these techniques also have been used to estimate the extent of biliary excretion of drugs (Chapter 1). The anatomy of the human gastrointestinal and hepatobiliary tract does not allow easy access to liver or gallbladder bile. In healthy volunteers, bile can be collected in a relatively non-invasive manner only after excretion into the intestine. In all published approaches, a naso- or oroenteric tube has been used to withdraw bile from the duodenum. Complete bile collection has been optimized in various ways by occlusion of the intestinal lumen with an inflatable balloon, to prevent bile flow down the duodenum, and by recovery of a non-absorbable marker perfused at steady-state into the intestinal segment of interest, to correct for incomplete recovery. Perfusion with non-absorbable markers is technically challenging, and also relies on the assumption that the mixing of secretions and perfusate is complete. This may not always be true due to the different density and consistency of these fluids, such a discrepancy could affect the accuracy of this approach. For this reason, and to simplify the execution of the clinical studies, we chose to occlude the duodenum with an inflatable balloon and assess occlusion by monitoring the gamma images of the lower part of the small intestine. Any escape of bile distal to the occlusion would spread radioactivity throughout the intestine after administration of a gamma emitting hepatobiliary imaging agent such as Tc-99m mebrofenin. However, during the clinical study designed to characterize piperacillin biliary excretion, it became apparent that a prolonged intubation, and the presence of the inflated balloon in the duodenum, may have a negative influence on gallbladder responsiveness to pharmacologically induced contraction. In future studies, it would be

advisable to shorten the bile collection period and keep the balloon inflated for no longer than 3-4 hours. If the collection period cannot be shortened, this issue could be overcome by deflating the balloon for cycles of 10-30 min during collection. This only would be possible when any gallbladder contraction and bile discharge into the intestine could be excluded using the gamma images.

An important aspect of the developed method, not previously addressed in the calculation of drug biliary clearance, is the ability to account for variability in the response to CCK-8 by correcting the fraction of dose excreted into bile for the gallbladder ejection fraction. In previous studies, bile was collected over several hours, and typically there was no attempt to expel bile from the gallbladder using a pharmacological approach. However, lack of control over the extent of gallbladder contraction yields highly variable results and unexpectedly low values for biliary clearance. This conclusion is exemplified for digoxin. When measured with the same technique in 3 different studies, digoxin biliary clearance varied widely [72-163, 79-343, 58-142 mL/min (4-7)] and the inter-subject variability was very high. This variability is a major problem when *in vivo* biliary clearance values are compared to *in vitro* biliary clearance values. One explanation for this variability may be that the collection of the digoxin excreted into bile was not complete. In these studies, is was assumed that the gallbladder remained contracted throughout the experiment due to duodenal perfusion with 5% glucose and a mixture of amino acids. If this was true, all the bile containing digoxin would have flowed directly from the liver into the intestine, allowing calculation of digoxin biliary clearance as the rate of excretion divided by the steady-state plasma concentration at the midpoint of the collection interval. It is questionable whether the gallbladder remained contracted for the duration of the entire experiment, or whether there were changes in

intraductal pressure and the state of the sphincter of Oddi. It is quite possible that the rate of digoxin excretion varied greatly during the experiment. Therefore, the reported digoxin biliary clearance values may be grossly underestimated. This could be confirmed by performing a small clinical study (n=4-6 subjects) using the technique developed in this thesis. Digoxin is expected to exhibit an intermediate to low biliary clearance in the SCHH model based on pilot studies conducted at Qualyst, Inc. (Brandon Swift, personal communication). Addition of digoxin to the developing *in vitro in vivo* correlation would be very beneficial.

The model probes selected in the studies presented in this dissertation were administered intravenously and exhibited a short half life (to prevent prolonged intubations). However, the majority of drugs on the market are available only for oral administration. To adapt this technique to a wider range of applications, additional modifications to the oroenteric catheter and optimization of the study design are required. Modifications in the tube design would expand the technique to orally administered drugs. Oral administration of a tablet could potentially contaminate the duodenal contents with residual components from the dissolved tablet. Thus, a solution of drug may be preferable with administration through a new port placed distal to the occluding balloon. Moreover, when drugs with a long half-life are under investigation, the study design should be modified. A parallel design which includes a group of patients intubated for a few hours immediately after drug administration, and other groups intubated at later time intervals would allow sampling over a sufficient period of time to characterize the processes involved in the elimination of the compound under study.

An important finding in one of the clinical studies, presented in this dissertation work, was the identification of desethyl-piperacillin glucuronide in human bile and urine samples. Even though the transformation of piperacillin into desethyl-piperacillin has been reported, a novel finding was the formation of desethyl-piperacillin glucuronide. Clearly, the combination of access to duodenal bile and the application of a very sensitive analytical technique (LC-MS-MS) to the analysis of these biological samples was instrumental in the identification of this new metabolite. Comparing the relative amount of metabolite recovered in urine and bile, it may be concluded that piperacillin was excreted mostly into urine as the parent drug, while biliary excretion was more predominant for the metabolites. The relevance of this novel finding is not expected to be clinically important because metabolism accounts for a very small percentage of piperacillin clearance. However, identification of metabolites for new drugs after human administration could be very desirable. In fact, the combination of this method with the sensitivity of the analytical techniques available today, would offer a new tool to quickly identify metabolites formed in humans that might not be predicted from preclinical studies. The removal of bile containing drug as soon as it appears in the duodenum would preserve metabolites that are unstable in the intestinal environment, or that could be reabsorbed along the intestine.

One additional application of this clinical methodology is in clarifying the relative contribution of enterohepatic versus enteroenteric recirculation in the overall disposition of drugs. In recent years, other groups have attempted to establish the contributions of intestinal secretion and biliary excretion of drugs to overall disposition (8-10). Further characterization of transport protein expression along the gastrointestinal tract has shown clearly that efflux transporters such as P-gp, BCRP and MRP2 could play a role in the removal of drugs from

the bloodstream even after intravenous administration (exemplified by gamma images of intestinal secretion of Tc-99m sestamibi detailed in Fig 5.2, Chapter 5). The relative contributions of enterohepatic and enteroenteric recirculation to the overall disposition of many drugs could be determined by combining the study design developed in this dissertation research to induce and monitor gallbladder contraction, with the technique cited above, which was designed to investigate intestinal metabolism, absorption and secretion,

Other interesting applications of the *in vivo* technique developed here could address the effect of transport protein polymorphisms and/or pharmacological inhibition of transport proteins on the hepatobiliary disposition of model probes, such as Tc-99m mebrofenin. As demonstrated in this research, Tc-99m mebrofenin is an excellent substrate for MRP2 and to a lesser extent for MRP3. A clinical study is ongoing to determine whether ritonavir will inhibit Tc-99m mebrofenin biliary excretion in humans in a manner similar to that shown *in vitro* using inside-out membrane vesicles expressing MRP2 (Appendix C). Tc-99m mebrofenin is a unique probe that may be used to quantify biliary excretion and at the same time detect delays in hepatic uptake due to inhibition of basolateral transport proteins by examining gamma scintigraphy images. Furthermore, gamma scintigraphy is a powerful tool that can be used to differentiate delays in excretion of Tc-99m mebrofenin from the liver into the gallbladder, and from the gallbladder into the duodenum. It is reasonable to expect that polymorphisms in the MRP2 gene could influence either the affinity of this protein (K_m) for Tc-99m mebrofenin, or the overall expression and localization of MRP2 at the canalicular membrane (V_{max}). Alterations in either K_m or V_{max} would be detected by alterations in the biliary clearance of this probe and may provide useful mechanistic information (as exemplified in the mathematical simulations of Tc-99m mebrofenin disposition in Chapter

3). However, most importantly, liver and body exposure could be affected by inhibition of biliary excretion or basolateral uptake and efflux. Many pharmacokinetic studies have been performed to evaluate the effect of drug-drug interactions in the intestine, liver and/or kidney with respect to P-gp inhibition using digoxin as a probe (4-8, 11-14). Tc-99m mebrofenin could be used as an MRP2/MRP3 probe *in vivo* to study drug-drug interactions that affect hepatic uptake or excretion processes, since this probe has virtually no renal elimination and our technique prevents enterohepatic recycling (if any is present).

Most of all, these interactions can be detected and predicted using the SCHH *in vitro* model. An important goal of this research project was to investigate whether the SCHH model accurately predicts hepatobiliary disposition of xenobiotics in the human liver. If so, SCHH could be used to characterize human liver uptake and excretion mechanisms, as well as the effect of interactions between novel compounds and xenobiotics or endogenous molecules. SCHH express relevant transport proteins and qualitatively maintain vectorial transport of substrates such as taurocholate (15, 16). In the current studies, the ability of SCHH to transport numerous probes from the incubation medium into bile was examined (Chapter 5). Human liver tissue typically was obtained from living donors undergoing liver resection. During the surgery, hepatic cancerous tissue was removed together with surrounding normal tissue; human hepatocytes were obtained following collagenase perfusion of only the healthy tissue. These cancer patients are obviously a very different population from the healthy volunteers who participated in our *in vivo* studies, and their liver tissue has been exposed to a variety of medications prior to resection. For ethical reasons, human tissue from healthy subjects is obtained only from cadaver liver not suitable for transplantation. Therefore, ischemic damage to this tissue may be considerable and

hepatocytes obtained from these sources often are not as viable as those obtained from fresh liver resections. Despite the difference in sex, age and previous medication exposure of the four donors (see Table 5.2, Chapter 5), the hepatocyte preparations used in these studies behaved similarly in terms of accumulation and excretion of the four different probes investigated. However, the morphology of the cells during culture and the extent of canalicular network formation varied from preparation to preparation. This affected the overall extent of excretion into canalicular spaces (Appendix D). One approach to account for the differences in canalicular network formation would be to calculate the overall volume occupied by these "cylindrical" structures in each preparation, and to use this number as a correction factor for the amount of drug recovered in bile in the SCHH studies. This correction might be useful when comparing the predicted $Cl_{biliary}$ obtained in this *in vitro* system to the *in vivo* $Cl_{biliary}$ measured in humans in order to minimize the differences in the bile canalicular volume.

In the future, it would be of value to systematically evaluate the expression of relevant transport proteins and metabolizing enzymes after cell isolation and over days in culture in the SCHH. A comparison between freshly isolated human hepatocytes and a time course of human hepatocytes in sandwich-culture using western blot analysis could be useful to understand whether anticancer and other medications that liver donors may have been exposed to and that are known to induce the expression of transport proteins and other metabolizing enzymes through nuclear receptors [i.e. microtubule-stabilizing anticancer agents such as paclitaxel and discodermolide are known to induce PXR-dependent pathways (17)] actually affect protein expression, and whether this induction is lost over time during culture in a sandwich configuration.

In addition, in the present studies, the cellular uptake experiments were performed in the absence of albumin in the incubation medium. Of course, this is not completely representative of the *in vivo* situation for compounds that are highly protein bound. Biliary clearance is defined as the volume of blood (or plasma) cleared of drug that is excreted into bile per unit time. The apparent biliary clearance will represent the rate-limiting step in this process, which can be either clearance across the basolateral or the canalicular membrane. The true biliary clearance process is driven by intracellular unbound drug concentrations. Therefore, when considering protein binding, it may be appropriate to consider cytosolic as well as plasma protein binding. Cytosolic fractions from pooled liver preparations (18) as well as plasma albumin or alpha 1- acid-glyco protein could be used to evaluate the impact of protein in the incubation medium on the *in vitro* biliary clearance.

One characteristic of the SCHH model that makes it a particularly powerful tool is the metabolic capacity in addition to the transport capabilities of the human hepatocytes. In the rat model culture conditions can influence the expression of Phase I and Phase II metabolizing enzymes(3). The optimal culture conditions for drug transport experiments have not been investigated fully with respect to metabolic capacity. In our *in vitro* studies, desethyl-piperacillin was formed in SCHH as early as 30 min post exposure (Appendix D), and in three out of four preparations, a modest degree of biliary excretion of this metabolite was observed, reproducing the clinical findings. However, the Phase II metabolites recovered in human liver microsomal incubations and in the *in vivo* biological samples were below the limit of detection even after SCHH were incubated for 48 hr with the parent drug. The intracellular concentrations of piperacillin in SCHH were lower than in the microsomal incubations, this may explain why the metabolites were not formed at detectable levels.

Although no general conclusion can be drawn from these preliminary experiments, the maintenance of Phase II metabolic activity should be tested using compounds known to be extensively taken up and metabolized by the liver. Even though additional experiments are needed to further define the abilities of this *in vitro* system to biotransform drugs, this feature is extremely desirable in an *in vitro* model that is also capable of transporting the metabolites in a manner similar to what is expected *in vivo* in humans. This would make the SCHH a critical preclinical tool that can form metabolites unique to the human species and is able to handle these products in a physiological manner offering insight into possible mechanisms of hepatoxicity or drug-metabolite interactions otherwise only detectable during clinical studies, when a threat to human health is possible.

Up until now, SCHH have been cultured as a cell monolayer between two layers of extracellular matrix. In order to detect drug excretion into bile, the canalicular networks formed between the cells need to be extensive, and this has posed some challenges to scaling down the culture from 6-well plates to 24- or even 96- well plates in an effort to adapt this model to the requirements for high throughput and automated screening assays. Human hepatocytes are very expensive, and their availability is and will always be limited. Therefore, it would be ideal to increase the number of cell-cell interactions in culture to obtain the largest canalicular network possible per number of cells. This could be achieved, for example, by developing a novel carbohydrate biopolymer gel support to allow culturing of hepatocytes in a 3 dimensional sponge-like scaffold over which the cells would be seeded and allowed to penetrate by gravity. This novel scaffold could provide two major improvements over the current collagen sandwich configuration. It would allow hepatocytes to be cultured in a 3-D configuration in smaller wells (e.g. 24- or 96-well plates), and would

reduce the cost of the raw materials required per experiment. In addition, by tailoring the molecular architecture of the polysaccharide gel, the pore size could be modified to determine whether bile canalicular network development and transport protein expression could be enhanced. Galactose grafted chitosans have been shown to enhance attachment of hepatocytes and allow successful culturing of the cells (19-21). Other biopolymers such as guar and locust bean gum should allow cell adhesion through galactose-cell interactions since they are naturally formed with a linear mannose backbone to which single sugar galactose branches are attached. These polymers can be modified further by addition of other biopolymers such as xanthan, or crosslinked to form a variety of hydrated gels, which can be molded to any shape that is required. Guar and locust bean biopolymers are commercially available at very affordable prices. These polymers could be allowed to gel directly into culture plates (96-well plates) under aseptic conditions; the gels could be lyophilized in advance and only hydrated prior to cell seeding. Another interesting approach to increase the number of cells per unit of well surface area occupying the entire volume of each 96-well plate would be to entrap primary hepatocytes within a double layer of extracellular matrix using electrospinning. Although a thorough description of this technique is beyond the scope of this dissertation, electrospinning has been used extensively in tissue engineering research to obtain nano- and micro-fibers that mimic the composition and architecture of the native extracellular matrix (22). Some blends of collagen and glycosaminoglycan have been successfully electrospun into fibers that are compatible with cell adhesion and proliferation (23, 24). With this technique, it is also possible to entrap living cells within the electrospun fibers. Therefore, it would be very exciting to prove that hepatocytes could be “electrospun” as a chain of cells and entrapped in these filaments. This would create a sandwich within

each strand and the strands could be woven into 3-D balls containing millions of cells, these agglomerates could loosely sit in plastic wells bathed and surrounded by culture or incubation medium. Of course, the most important prerequisite would be that "electrospun" hepatocytes correctly polarize in this environment and form canalicular spaces at each cell-cell contact. A robot could be used for the feeding and accumulation studies; moving these agglomerates into new wells containing fresh medium or HBSS at appropriate times could all be automated.

The sandwich-cultured hepatocyte model can be adapted for co-culturing with other cell types since hepatocytes represent only 60-80% of the entire cell population of the liver (25). *In vivo*, cholangiocytes also play an important role in influencing the composition of bile, once hepatocytes have removed drugs and endogenous substances from the blood and transported them across the canalicular membrane into bile. Recently, the role of cholangiocytes in bile formation has been investigated by several groups (26, 27). These cells express a variety of transport proteins and are thought to play a role in the reabsorption of bile components, modifying the concentration of bile salts and possibly of drugs in bile (28). It would be interesting to develop a co-culture of hepatocytes and cholangiocytes that would more closely mimic hepatic function and biliary excretion.

In conclusion, this project laid the foundation for the development of a correlation between the biliary clearance of drugs measured *in vivo* in humans and biliary clearance values obtained *in vitro* in the SCHH system. The ramifications of this project have implications not only for the determination and prediction of biliary clearance of drugs, but also in understanding alterations in biliary clearance due to drug-drug or metabolite interactions.

REFERENCES

1. M. Horikawa, Y. Kato, C. A. Tyson, and Y. Sugiyama. The potential for an interaction between MRP2 (ABCC2) and various therapeutic agents: probenecid as a candidate inhibitor of the biliary excretion of irinotecan metabolites. *Drug Metab Pharmacokinet* **17**: 23-33 (2002).

2. T. van Gelder, J. Klupp, M. J. Barten, U. Christians, and R. E. Morris. Comparison of the effects of tacrolimus and cyclosporine on the pharmacokinetics of mycophenolic acid. *Ther Drug Monit* **23**: 119-28 (2001).

3. X. Liu, J. P. Chism, E. L. LeCluyse, K. R. Brouwer, and K. L. Brouwer. Correlation of biliary excretion in sandwich-cultured rat hepatocytes and in vivo in rats. *Drug Metab Dispos* **27**: 637-44 (1999).

4. B. Angelin, A. Arvidsson, R. Dahlqvist, A. Hedman, and K. Schenck-Gustafsson. Quinidine reduces biliary clearance of digoxin in man. *Eur J Clin Invest* **17**: 262-5 (1987).

5. A. Hedman, B. Angelin, A. Arvidsson, and R. Dahlqvist. Digoxin-interactions in man: spironolactone reduces renal but not biliary digoxin clearance. *Eur J Clin Pharmacol* **42**: 481-5 (1992).

6. A. Hedman, B. Angelin, A. Arvidsson, and R. Dahlqvist. No effect of probenecid on the renal and biliary clearances of digoxin in man. *Br J Clin Pharmacol* **32**: 63-7 (1991).

7. A. Hedman, B. Angelin, A. Arvidsson, O. Beck, R. Dahlqvist, B. Nilsson, M. Olsson, and K. Schenck-Gustafsson. Digoxin-verapamil interaction: reduction of biliary but not renal digoxin clearance in humans. *Clin Pharmacol Ther* **49**: 256-62 (1991).

8. S. Drescher, H. Glaeser, T. Murdter, M. Hitzl, M. Eichelbaum, and M. F. Fromm. P-glycoprotein-mediated intestinal and biliary digoxin transport in humans. *Clin Pharmacol Ther* **73**: 223-31 (2003).

9. O. von Richter, B. Greiner, M. F. Fromm, R. Fraser, T. Omari, M. L. Barclay, J. Dent, A. A. Somogyi, and M. Eichelbaum. Determination of in vivo absorption, metabolism, and transport of drugs by the human intestinal wall and liver with a novel perfusion technique. *Clin Pharmacol Ther* **70**: 217-27 (2001).

10. H. Glaeser, S. Drescher, U. Hofmann, G. Heinkele, A. A. Somogyi, M. Eichelbaum, and M. F. Fromm. Impact of concentration and rate of intraluminal drug delivery on absorption and gut wall metabolism of verapamil in humans. *Clin Pharmacol Ther* **76**: 230-8 (2004).

11. A. Hedman. Inhibition by basic drugs of digoxin secretion into human bile. *Eur J Clin Pharmacol* **42**: 457-9 (1992).

12. R. Ding, Y. Tayrouz, K. D. Riedel, J. Burhenne, J. Weiss, G. Mikus, and W. E. Haefeli. Substantial pharmacokinetic interaction between digoxin and ritonavir in healthy volunteers. *Clin Pharmacol Ther* **76**: 73-84 (2004).

13. A. Hedman, B. Angelin, A. Arvidsson, R. Dahlqvist, and B. Nilsson. Interactions in the renal and biliary elimination of digoxin: stereoselective difference between quinine and quinidine. *Clin Pharmacol Ther* **47**: 20-6 (1990).

14. A. Johne, J. Brockmoller, S. Bauer, A. Maurer, M. Langheinrich, and I. Roots. Pharmacokinetic interaction of digoxin with an herbal extract from St John's wort (Hypericum perforatum). *Clin Pharmacol Ther* **66**: 338-45 (1999).

15. K. A. Hoffmaster, R. Z. Turncliff, E. L. LeCluyse, R. B. Kim, P. J. Meier, and K. L. Brouwer. P-glycoprotein expression, localization, and function in sandwich-cultured primary rat and human hepatocytes: relevance to the hepatobiliary disposition of a model opioid peptide. *Pharm Res* **21**: 1294-302 (2004).

16. P. Zhang, B. D. Swift, X. Tian, K. R. Brouwer, M. Dasgupta, and N. Huebert. Optimization of transporter expression and function in sandwich-cultured human hepatocytes (B-ClearTM-HU). *Drug Metab Rev* **37**: 306-306 (2005).

17. S. Mani, H. Huang, S. Sundarababu, W. Liu, G. Kalpana, A. B. Smith, and S. B. Horwitz. Activation of the steroid and xenobiotic receptor (human pregnane X receptor) by nontaxane microtubule-stabilizing agents. *Clin Cancer Res* **11**: 6359-69 (2005).

18. S. D. Studenbergand K. L. Brouwer. Hepatic disposition of acetaminophen and metabolites. Pharmacokinetic modeling, protein binding and subcellular distribution. *Biochem Pharmacol* **46**: 739-46 (1993).

19. M. Kawase, N. Michibayashi, Y. Nakashima, N. Kurikawa, K. Yagi, and T. Mizoguchi. Application of glutaraldehyde-crosslinked chitosan as a scaffold for hepatocyte attachment. *Biol Pharm Bull* **20**: 708-710 (1997).

20. Y. M. Elcin, V. Dixit, and G. Gitnick. Hepatocyte attachment on biodegradable modified chitosan membranes: in vitro evaluation for the development of liver organoids. *Artif Organs* **22**: 837-846 (1998).

21. R. A. Quirk, B. Kellam, R. N. Bhandari, M. C. Davies, S. J. B. Tendler, and K. M. Shakesheff. Cell-type-specific adhesion onto polymer surfaces from mixed cell populations. *Biotechnol Bioeng* **81**: 625-628 (2003).

22. W. J. Li, R. Tuli, X. Huang, P. Laquerriere, and R. S. Tuan. Multilineage differentiation of human mesenchymal stem cells in a three-dimensional nanofibrous scaffold. *Biomaterials* **26**: 5158-66 (2005).

23. S. Zhong, W. E. Teo, X. Zhu, R. Beuerman, S. Ramakrishna, and L. Y. Yung. Formation of collagen-glycosaminoglycan blended nanofibrous scaffolds and their biological properties. *Biomacromolecules* **6**: 2998-3004 (2005).

24. J. A. Matthews, G. E. Wnek, D. G. Simpson, and G. L. Bowlin. Electrospinning of collagen nanofibers. *Biomacromolecules* **3**: 232-8 (2002).

25. J. A. Sunman, R. L. Hawke, E. L. LeCluyse, and A. D. Kashuba. Kupffer cell-mediated IL-2 suppression of CYP3A activity in human hepatocytes. *Drug Metab Dispos* **32**: 359-63 (2004).

26. G. Alpini, S. Glaser, L. Baiocchi, H. Francis, X. Xia, and G. Lesage. Secretin activation of the apical Na+-dependent bile acid transporter is associated with cholehepatic shunting in rats. *Hepatology* **41**: 1037-45 (2005).

27. C. Pauli-Magnus, B. Stieger, Y. Meier, G. A. Kullak-Ublick, and P. J. Meier. Enterohepatic transport of bile salts and genetics of cholestasis. *J Hepatol* **43**: 342-57 (2005).

28. K. Tsuboi, S. Tazuma, T. Nishioka, and K. Chayama. Partial characterization of cytoprotective mechanisms of lecithin against bile salt-induced bile duct damage. *J Gastroenterol* **39**: 955-60 (2004).

Appendix A

EXPRESSION OF BASOLATERAL AND CANALICULAR TRANSPORT PROTEINS IN HEPG2 CELLS: EFFECT OF DAYS IN CULTURE AND CULTURE CONFIGURATION

This work was presented in the form of a poster at the AAPS Annual Meeting, Salt Lake City, Utah, 2003

INTRODUCTION

Culturing hepatocytes between two layers of gelled collagen in a sandwich configuration is a well-established technique to maintain liver-specific functions including albumin secretion, cytochrome P-450 expression, as well as bile acid and xenobiotic vectorial transport (1, 2). Sandwich-cultured hepatocytes form extensive bile canalicular networks over time in culture; transport proteins are expressed and functional (3). However, due to the limited availability of freshly isolated human hepatocytes, evaluation of alternative cells is a major focus of current research. HepG2 cells are a human-derived hepatoma cell line frequently used in toxicology studies. Hepatic transport proteins are expressed at lower levels in HepG2 cells relative to human hepatocytes (4). HepG2 cells do not express all of the cytochrome P-450 enzymes at the same levels as human hepatocytes; however, they are capable of synthesizing the majority of liver-specific proteins (5). Previous studies had demonstrated that culturing HepG2 cells between two layers of collagen improved the phenotype, increasing albumin synthesis (6).

The present studies evaluated the influence of culture configuration (polystyrene uncoated petri dishes, polystyrene dishes coated with rat tail type I collagen gel, and collagen gel substratum with collagen overlay or sandwich-cultured) on basolateral and canalicular transport proteins involved in hepatic transport of xenobiotics in HepG2 cells over days in culture. Specifically, expression of the canalicular transport proteins multi-drug resistance associated protein (MRP2; ABCC2), P-glycoprotein (P-gp; ABCB1), breast cancer-resistance protein (BCRP; ABCG2), and the basolateral transport protein MRP3 (ABCC3), as well as the function of MRP2, were examined.

METHODS

Cell Culture

HepG2 cells were seeded at a density of $1x10^5/cm^2$ onto 60-mm polystyrene dishes (uncoated or rat tail type I collagen coated). Dishes coated with collagen (1.5 mg/mL final concentration) were prepared by neutralizing 4 mL rat tail type I collagen, 4 mL deionized water and 1 mL 10x DMEM with 1 mL 0.2 N NaOH (final pH ~7.4). To obtain the sandwich configuration, cells were overlaid with a second rat tail type I collagen layer 48 hr after seeding. Cells were maintained in DMEM-F12 containing 1% insulin/ transferrin/ selenium (ITS+), 50 U/mL penicillin, 50 μg/mL streptomycin, and 0.1 μM DEX. Cells were cultured up to 10 days, and medium was changed daily.

MRP2 Functional Assay

On each day, starting at 72 hr post seeding, MRP2 function was determined. Cells were rinsed 3 times with warm HBSS (Hank's Balanced Salt Solution, pH 7.4), then incubated at 37°C for 10 min in HBSS containing 2 μM 5-(and 6) carboxy-2',7'-dicholorofluorescein (CDF) diacetate, quickly rinsed 4-5 times with warm buffer and light and fluorescence images were captured with a fluorescence microscope (Zeiss, Axiovert) to evaluate the excretion of CDF into apical vacuoles.

Western Blot

Cells were lysed with phosphate buffer (pH 7.4) containing 1% sodium dodecyl sulfate (SDS), Dithriothretol (DTT) and protease inhibitor cocktail (Complete, Roche). Human liver tissue was homogenized and protein was solubilized into Tris-HCl buffer containing protease inhibitor cocktail. Samples were loaded onto a 4-12% Bis-Tris gel (total protein loaded 30-45 μg). Proteins were transferred onto PVDF membranes and probed with specific

antibodies. Anti-MRP2 primary monoclonal antibody (Alexis M2III-6), anti-MRP3 primary monoclonal antibody (Alexis M3II-9), anti-P-gp primary monoclonal antibody (Alexis C494), and anti-BCRP primary monoclonal antibody (Oncogene Ab-1) were incubated with antimouse secondary antibody linked to horseradish peroxidase and detected by Supersignal West Dura chemiluminescence reagent kit. Membranes were stripped and reprobed with mouse anti-actin antibody.

RESULTS

MRP2 and MRP3 Expression

Expression of MRP2 was not influenced by the different culture configurations investigated (Fig A.1). Once normalized for actin content, the slight induction of MRP2 that was observed over time in culture was not significant (< 2-fold). Expression of MRP3 was maintained over days in culture by all three culture configurations (Fig A.2). When MRP3 expression was evaluated over days in culture, the optical density of the MRP3 bands detected by western blot analysis remained constant when normalized for actin.

MRP2 Functional Assay

An apical vacuole was present in HepG2 cells. After passive diffusion of CDF diacetate into the cells and cleavage of the diacetate moiety, the MRP2 substrate CDF was actively pumped by these cells into the apical vacuole. The number of vacuoles increased over days in culture, and was higher in cells cultured on uncoated polystyrene dishes when compared to the other two configurations. After 10 days in culture, some of the vacuoles became enlarged and migrated towards each other only in cells cultured on uncoated dishes (Fig A.3). As evidenced by the light and fluorescent images none of the culture configurations sustained the formation of a functional canalicular network between adjacent cells.

P-gp and BCRP Expression

P-gp and BCRP were expressed in HepG2 cells; expression was not influenced by culture configuration at 3 days after seeding. After actin normalization, the three culture conditions did not differ significantly (< 2-fold increase, Fig A.4).

CONCLUSIONS

MRP2, P-gp, BCRP and MRP3 expression was maintained in HepG2 cells in all the culture conditions investigated in this study. It was interesting to note based on inspection of Western blots that these transport proteins exhibited a slightly different molecular weight in HepG2 cells than in the human liver sample investigated. MRP2 and MRP3 expression was maintained over days in culture, and was not affected by culture configuration. MRP2 function was preserved, as evidenced by CDF excretion into apical vacuoles over days in culture. The apical vacuoles increased in number and size near cell-cell contacts, and were more visible in HepG2 cells cultured on uncoated polystyrene dishes than in any other culture condition.

FIGURES

Fig A.1: Western Blot of MRP2 protein in HepG2 cells cultured in different configurations over time. The band for MRP2 in HepG2 cells showed a slightly higher molecular weight than that of the human liver control. (HL: human liver; Ctrl: uncoated dishes; Coll: collagen coated dishes; SC: collagen sandwich configuration).

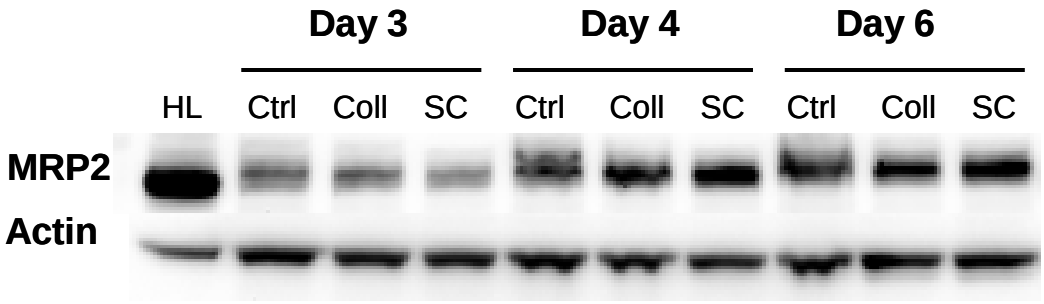

Fig A.2: Western Blot of MRP3 protein in HepG2 cells cultured in different configurations over time. The double band pattern observed for MRP3 in liver was consistent with bands observed in HepG2 cells. In this cell line, the double band was at a lower molecular weight. (HL: human liver; Ctrl: uncoated dishes; Coll: collagen coated dishes; SC: collagen sandwich configuration).

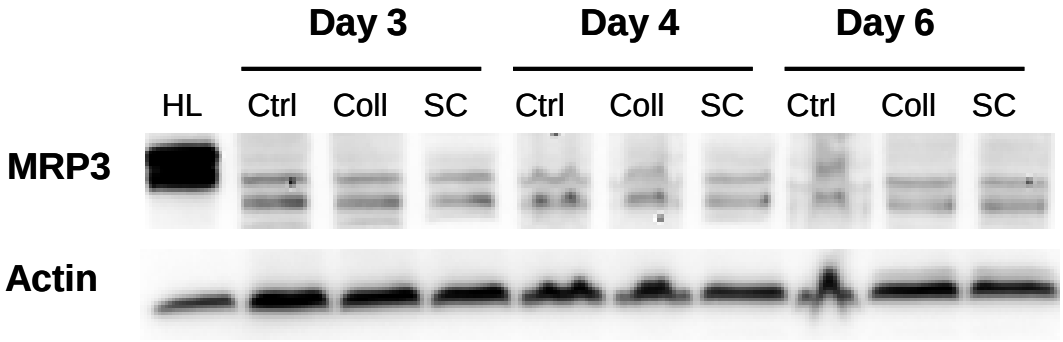

Fig A.3 : CDF fluorescence demonstrating functional activity of MRP2 in HepG2 cells (Days 3, 4, 6 and 10 after seeding) cultured in three different configurations. (Panel A: uncoated polystyrene dishes. Panel B: collagen coated dishes. Panel C: collagen sandwich configuration). Light micrographs are shown to indicate the cell density at each time point. (Magnification 200x).

Panel A:

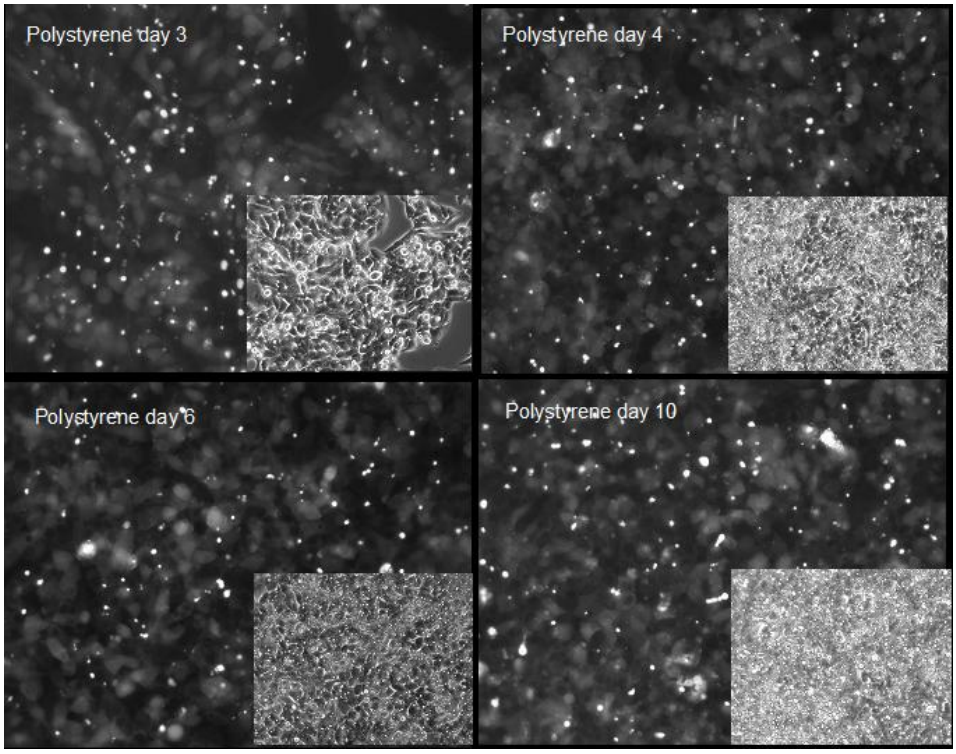

Panel B:

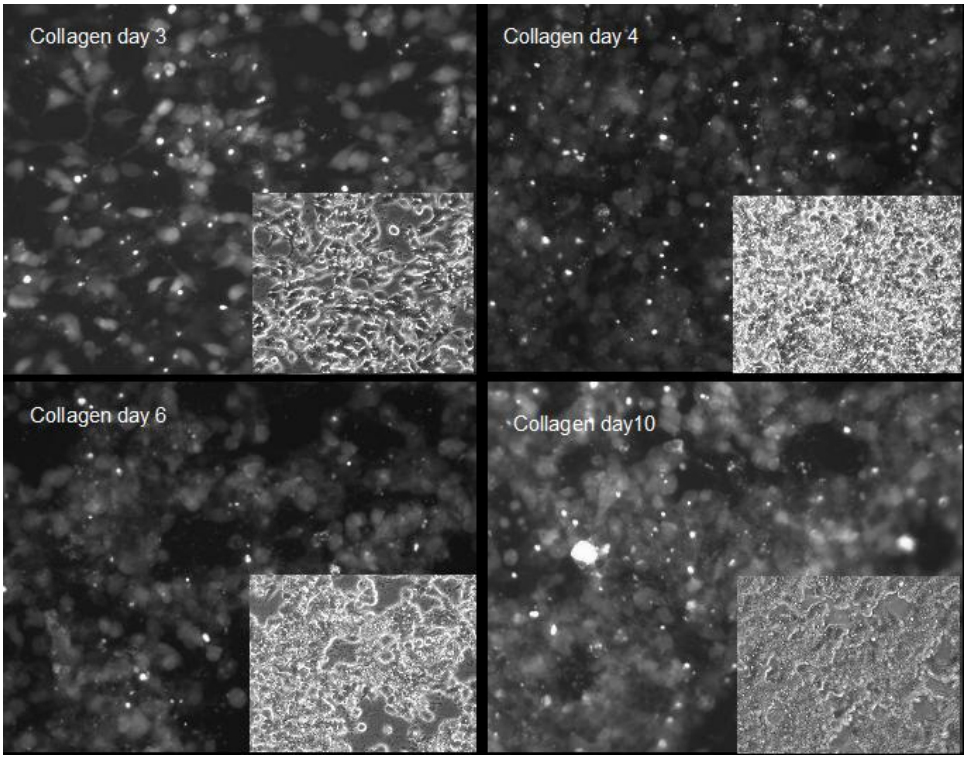

Panel C:

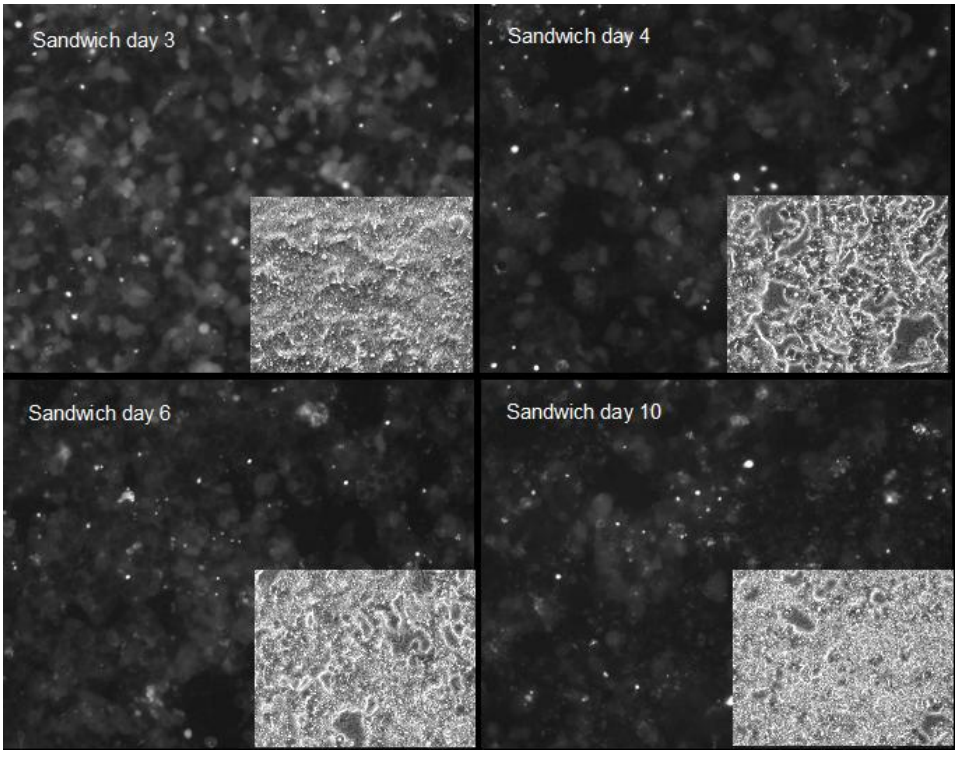

Fig A.4: P-gp and BCRP expression in HepG2 cells in three different culture configurations 3 days after seeding. In both cases, the transport proteins in the HepG2 cells migrated at a higher molecular weight than in the human control liver. (HL: human liver; Ctrl: uncoated dishes; Coll: collagen coated dishes; SC: collagen sandwich configuration).

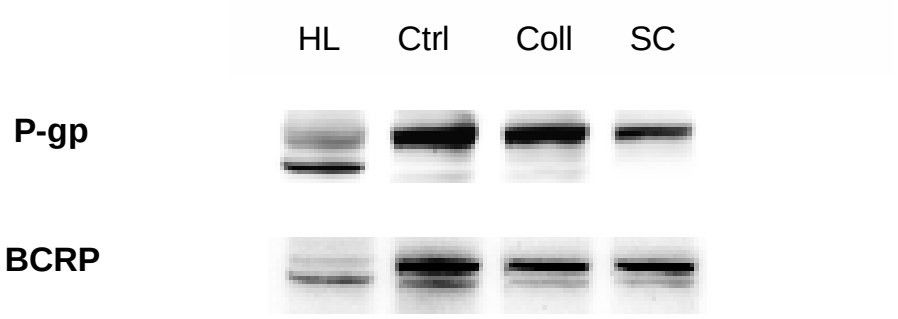

REFERENCES

1. G. A. Hamilton, S. L. Jolley, D. Gilbert, D. J. Coon, S. Barros, and E. L. LeCluyse. Regulation of cell morphology and cytochrome P450 expression in human hepatocytes by extracellular matrix and cell-cell interactions. *Cell Tissue Res* **306**: 85-99 (2001).

2. X. Liu, K. L. R. Brouwer, L. S. L. Gan, K. R. Brouwer, B. Stieger, P. J. Meier, K. L. Audus, and E. L. LeCluyse. Partial maintenance of taurocholate uptake by adult rat hepatocytes cultured in a collagen sandwich configuration. *Pharm Res* **15**: 1533-1539 (1998).

3. X. Liu, E. L. LeCluyse, K. R. Brouwer, L. S. Gan, J. J. Lemasters, B. Stieger, P. J. Meier, and K. L. R. Brouwer. Biliary excretion in primary rat hepatocytes cultured in a collagen- sandwich configuration. *Am J Physiol* **277**: G12-G21. (1999).

4. M. E. Bouma, E. Rogier, N. Verthier, C. Labarre, and G. Feldmann. Further cellular investigation of the human hepatoblastoma-derived cell line HepG2: morphology and immunocytochemical studies of hepatic-secreted proteins. *In Vitro Cell Dev Biol* **25**: 267-275 (1989).

5. Y. Konoand E. A. Roberts. Modulation of the expression of liver-specific functions in novel human hepatocyte lines cultured in a collagen gel sandwich configuration. *Biochem Biophys Res Commun* **220**: 628-32. (1996).

6. T. K. Lee, C. L. Hammond, and N. Ballatori. Intracellular glutathione regulates taurocholate transport in HepG2 cells. *Toxicol Appl Pharmacol* **174**: 207-215 (2001).

Appendix B

Tc-99 MEBROFENIN DISPOSITION IN WILD-TYPE AND TR$^-$ RATS: DEVELOPMENT OF ANALYTICAL TECHNIQUES AND IN VITRO AND IN VIVO INVESTIGATIONS

INTRODUCTION

Tc-99m mebrofenin disposition was investigated in healthy human volunteers in Specific Aim #1. In Specific Aim #2a, a pharmacokinetic model was developed to characterize the processes involved in the elimination of this substrate, and the model was used to simulate the effect of impaired function of the canalicular transport protein MRP2. Ideally, a clinical study designed to investigate the impact of impaired MRP2 function on the hepatobiliary clearance of Tc-99m mebrofenin would have validated the predictions obtained with the simulation. However, it was not possible to recruit a large enough number of patients with Dubin-Johnson syndrome to the UNC Hospitals in a reasonable time frame. A rodent model of the disease is readily available in our laboratory (TR^- rats). Therefore, the disposition of Tc-99m mebrofenin in the wild-type and mutant rat was investigated. Specific Aim #4 proposed to study the disposition of this probe in sandwich-cultured human hepatocytes. The use of day 4 sandwich-cultured hepatocytes from wild-type and Mrp2-deficient rats was proposed as a tool to optimize experimental conditions for the subsequent in vitro studies using sandwich-cultured human hepatocytes. Additionally the pharmacokinetic model developed in Aim #2a was based on a series of assumptions regarding the transport proteins involved in the uptake from sinusoidal blood and efflux into bile of Tc-99m mebrofenin. In vitro tools such as *Xenopus Laevis* oocytes and HEK293 cell membrane vesicles injected/transfected with uptake or efflux transporters, respectively, were proposed to investigate which protein was responsible for Tc-99m mebrofenin disposition in the liver.

In appendixes B.1, B.2 and B.3, the work undertaken to accomplish these goals is described in detail.

Appendix B.1

THE USE OF TECHNETIUM-99 VERSUS TECHNETIUM-99M TO LABEL MEBROFENIN AND SESTAMIBI FOR THE IN VITRO STUDIES

INTRODUCTION

The main goal of this work was to be able to determine the kinetic parameters (V_{max} and K_m) for the transport proteins under investigation as proposed in Specific Aim #2 (*Xenopus laevis* oocytes expressing OATP1B1 and 1B3, and membrane vesicles from MRP2 and MRP3 HEK293 transfected cells). These studies required large amounts of mebrofenin complex, which could pose safety issues if Technetium 99m was used to label mebrofenin, since unacceptably high levels of radioactivity would be associated with the complex. Technetium-99 (Tc-99) is a beta emitter with lower energy and a longer decay half-life than Tc-99m. The use of Tc-99 allows measurement of the actual concentrations of chelate in solution (on the order of μM) when performing *in vitro* studies. Initially, it was assumed that the radiochemical purity of the Tc-99 complex was high (>85-90%); hence, all the beta energy measured during scintillation counting was assumed to be associated with the Tc-99 mebrofenin complex. Tc-99 mebrofenin was used initially as a model for other chelates such as Tc-99 sestamibi, since unlabeled sestamibi is not commercially available.

Tc-99m labeled mebrofenin and sestamibi are technetium-essential compounds in that these complexes have a unique disposition, which is different from either Tc-99m pertechnetate or the ligand alone. The formation of Tc-99m labeled mebrofenin and sestamibi chelates requires technetium to be in a specific oxidation state, which is not necessarily a stable state since the bonds formed with the ligand molecules will stabilize even

particularly unstable oxidation states of Tc. The most stable form of Tc-99m, TcO_4^- (pertechnetate, oxidation state +7), is obtained readily as sodium-pertechnetate. This is the form that is added to radiopharmaceutical kits to obtain the radiopharmaceuticals of interest. All Tc-99m radiopharmaceuticals are provided in a ready-to-label sterile kit to which Tc-99m sodium-pertechnetate is added. These kits are lyophilized powders containing the ligand (mebrofenin or sestamibi) and stannous chloride, which functions as the reducing agent for TcO_4^- , and other adjuvants (1).

METHOD DEVELOPMENT AND RESULTS

Tc-99 mebrofenin Labeling and Counting Protocols

The Choletec™ kit (Bracco Diagnostic) was reconstituted with 5mL of sterile water (water was purged with nitrogen for 30 min to remove oxygen in order to avoid oxidation of stannous ions in the kit). Aliquots (1 mL) of this reconstituted mebrofenin solution were frozen immediately and stored at -80°C until needed. On the day of the experiment, 0.5 mL of a sterile stock solution of Tc-99 sodium pertechnetate (79 mg/L or 0.8mM) was added to 1 mL of reconstituted mebrofenin and the labeling reaction took place at room temperature for 15 minutes. Radiochemical purity of the chelate formed was evaluated with a TLC method using ITLS-SA (instant thin layer chromatography polysilicic acid) as the stationary phase and 20% sodium chloride as the mobile phase; solutions were employed in the experiments only when the radiochemical purity was ≥ 90% (1).

A new counting protocol for scintillation counting of Tc-99 was established and a quench curve was evaluated. Tc-99 has a maximal energy peak at 290 keV. Therefore, a lower window was set between 0 and 400 keV and an upper window was set between 0 and 2000 keV with a counting time of 5 min.

Liquid scintillation detection is a process that converts the energy emitted by radioactive decay into photons of light. It is imperative to control for any factor present in the samples that could cause quenching of the beta emissions. The different matrices used in the in vitro and in vivo experiments could attenuate the photons of light, and this effect could be accounted for once a quench curve for Tc-99 was established. Chloroform is a known chemical quencher that is used to prepare quench curves. The transformed spectral index of the external standard (t-SIE) is a method used to measure the quench of solutions. An

external ^{133}Ba gamma source is positioned under each sample vial and causes a Compton spectrum to be produced in the cocktail solution; the t-SIE parameter is calculated from this spectrum. The t-SIE decreases when the sample is quenched. By comparing the t-SIE parameter associated with experimental samples to those obtained in a quench curve, it is possible to establish whether a sample is quenched, and also to correct the cpm for the actual efficiency and transform the cpm into dpm for any given sample. A quench curve was obtained by adding increasing amounts of chloroform to a known amount of Tc-99. Five milliliters of scintillation cocktail (Biosafe II) was added to 17 μL of saline stock solution of Tc-99 pertechnetate (concentration 79 ng/μL) and the counting efficiency was calculated in the presence/absence of quencher. Blank samples were prepared with scintillation cocktail and chloroform as indicated in Table B.1.1. A quence curve was generated as shown in Fig B1.1 by plotting the percent counting efficiency (cpm/dpm x100) versus the tSIE.

The counting efficiency for Tc-99 is very high as exemplified by the following calculations:

Activity = λ*N

λ = ln 2 / decay $t_{1/2}$

where N = $6.022*10^{23}$ atoms/mole

Tc-99 MW = 99

$t_{1/2}$ = $2.1*10^{5}$ years = $66.23*10^{11}$ sec

Therefore there are $6.096*10^{15}$ atoms/μg of Tc-99. The theoretical activity of 17μL Tc-99 solution (concentration 79 ng/μL) would be:

A= [0.693/($66.23*10^{11}$ sec)] * [1.343μg*($6.096*10^{15}$ atoms/μg)]

A= 857 dps= 51,389 dpm

From Table B.1.1 it can bee seen that the efficiency for an unquenched sample of Tc-99 is 95% Therefore, the cpms approximate the dpms for Tc-99.

FIGURES AND TABLES

Table B.1.1 Quench curve of a sample of Tc-99 sodium pertechnetate (Tc-99) in 5mL of scintillation fluid, and scintillation fluid alone (blank), obtained after adding increasing volumes of chloroform.

	Chlorform μL	cpm	tSIE	Efficiency%
Blank	0	34.8	496	
Tc-99	0	48664.4	478	95
Blank	10	37.2	431	
Tc-99	10	47957.5	432	94
Blank	30	39	362	
Tc-99	30	47654.8	360	93
Blank	60	34.8	290	
Tc-99	60	47234.8	288	93
blank	100	40	230	
Tc-99	100	46510.2	228	91
blank	200	39.4	150	
Tc-99	200	44929.7	154	88
blank	300	31	109	
Tc-99	300	42782.4	114	84
blank	400	38	85.3	
Tc-99	400	41237.4	89.1	81
blank	500	39.2	67.9	
Tc-99	500	39120.8	73.2	77

Figure B.1.1: Efficiency versus tSIE plot. The efficiency was not markedly different over the range of tSIE values observed in the *in vitro* preparations (tSIE=470-350 for SCRH experiments, tSIE=480-320 in rat IPL experiments, tSIE=440 for TLC radiochemical purity assays). Therefore, results were not corrected for quenching and data were expressed as cpm in all experiments.

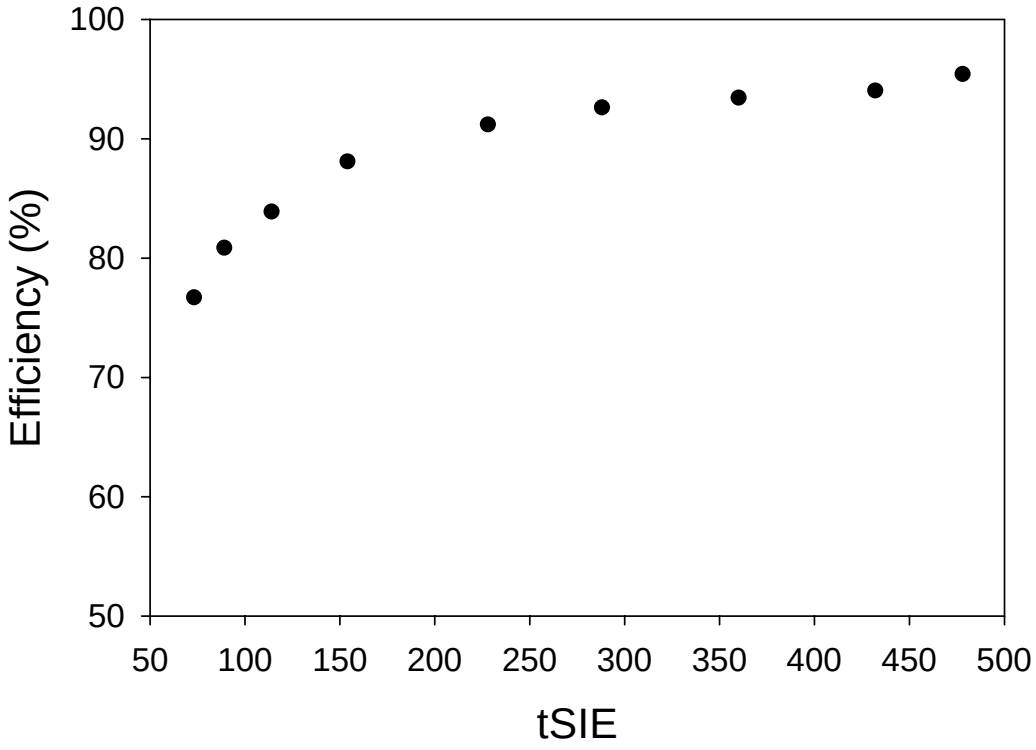

Appendix B.2

Tc-99 MEBROFENIN ACCUMULATION IN SANDWICH-CULTURED RAT HEPATOCYTES

INTRODUCTION

Naturally occurring mutants of the Wistar strain that lack functional Mrp2 are called TR^- rats. A similar phenotype is encountered in humans affected by Dubin-Johnson syndrome. Tc-99m HIDA, an analog of Tc-99m mebrofenin, is transported into bile to a lesser extent in Mrp2-deficient compared to wild-type rats (2).

Evaluation of the effect of this disease state on Tc-99 mebrofenin disposition in TR^- rats can be valuable information to integrate with the predicted modifications in Tc-99m mebrofenin disposition that have been obtained for Dubin-Jonhson syndrome patients using pharmacokinetic simulations (Aim #2.a). In order to accomplish this, *in vitro* experiments to determine Tc-99 mebrofenin BEI and biliary clearance values were performed using primary hepatocytes from Wistar and TR^- rats cultured in a sandwich configuration. Additionally, some *ex vivo* experiments using the recirculating isolated perfused liver technique also were performed in the two rat strains. An additional benefit of the *in vitro* experiments was the optimization of experimental conditions for cellular accumulation of Tc-99 mebrofenin in primary human hepatocytes.

METHODS

Isolation and Culture of Sandwich-Cultured Rat Hepatocytes (SCRH)

Wistar (wild-type or TR^-) male rats were anesthetized prior to portal vein cannulation. Hepatocytes were isolated with a 2-step collagenase perfusion (3). Livers were perfused with Ca^{2+} free Hank's buffer containing glucose (5.5 mM) and EGTA (1 mM) followed by perfusion with buffer containing collagenase type I (150-200 U/mL); 1 min later, 0.5 mmol $CaCl_2$ was added. After collagenase digestion (~10 min), the liver was removed, immersed in ice-cold medium [Dulbecco's modified Eagle's medium (DMEM) with 5% fetal bovine serum (FBS), 50 U/mL penicillin, 50 μg/mL streptomycin, 4 mg/L insulin, 1 μM dexamethasone (DEX)], and the capsule surrounding the liver was torn gently to release hepatocytes, which were filtered through 70-μm mesh and centrifuged (50xg, 2 min, 4°C). The pellet was resuspended in equal parts medium and isotonic Percoll® and centrifuged (70xg, 5 min, 4°C) to separate nonviable cells. The pellet was resuspended in medium and centrifuged (50xg, 2 min, at 4°C). Hepatocytes were counted in a hemocytometer, and viability (>90%) was determined by trypan blue exclusion. Cells were resuspended in medium and diluted to $1x10^6$ cells/mL. Cells were seeded onto 6-well polystyrene dishes (Nalgen Nunc, Rochester, NY) coated with collagen (1.5 mg/mL final concentration) prepared by neutralizing 4 mL rat tail type I collagen, 4 mL deionized water and 1 mL 10x DMEM with 1 mL 0.2 N NaOH (final pH ~7.4). Unattached cells were removed 1-2 hr after plating by replacing the plating medium with DMEM containing 5% FBS, 50 U/mL penicillin, 50 μg/mL streptomycin, 4 mg/L insulin, and 0.1 μM DEX. Medium was aspirated 24 hr after plating, and cells were overlaid with 0.1 mL rat tail collagen type I solution (1.5 mg/mL, pH 7.4) in order to obtain a 'sandwich' configuration. After collagen

overlay, insulin/transferrin/selenium (ITS+) cell culture supplement replaced FBS/insulin in the medium. Medium was changed daily. SCRH were maintained for 4 days before performing experiments.

Accumulation and Efflux Studies in SCRH

Rat hepatocytes were cultured in a collagen-sandwich configuration in 6-well dishes, as described above. Hepatocytes were rinsed twice with 2 mL warm standard Hanks' balanced salt solution (HBSS) and pre-incubated for 10 min in 1.5 mL of either standard HBSS or Ca^{2+} free HBSS (in order to allow the tight junctions that seal the canalicular lumen to open). Subsequently, hepatocytes were incubated in 1.5 mL HBSS containing 15 μM Tc-99 mebrofenin for 30 min and then washed 4 times with 1.5 mL ice-cold standard HBSS to remove extracellular substrate. On one occasion, WT rat SCRH were incubated with 0.5 μCi/mL of Tc-99m mebrofenin. Hepatocytes were lysed with 1 mL of ice cold 0.5% Triton-X 100 by shaking (20 min at room temperature). An aliquot (0.7 mL) of lysate was analyzed for Tc-99 mebrofenin content by scintillation counting, in the case of Tc-99m mebrofenin, 0.5 mL were analyzed by gamma counting and corrected for decay. All values for Tc-99 mebrofenin uptake into cell monolayers were corrected for nonspecific binding to the collagen by subtracting Tc-99 mebrofenin uptake determined in the appropriate control dishes in the absence of cells. Uptake data were normalized to the protein content and expressed as mean ± S.D. from three separate preparations of hepatocytes. The biliary excretion index (BEI) and biliary clearance in SC hepatocytes were calculated as follows:

$$BEI = \frac{Accumulation_{cells+bile} + Accumulation_{cells}}{Accumulation_{cells+bile}} \times 100\%$$

$$\text{in vitro } Cl_{biliary} = \left[\frac{Accumulation_{cells+bile} - Accumulation_{cells}}{Time_{incubation} \times Concentration_{medium}} \right]$$

Cytotoxicity Assay

The commercially available formulation of mebrofenin contains methylparaben and propylparaben as preservatives, and these compounds have been shown to exhibit toxicity when applied to suspended rat hepatocytes. Toxicity experiments were performed using SCRH to establish that the maximum dose (containing preservatives) used in these experiments was non-toxic. (4, 5)

The release of lactate dehydrogenase (LDH) from hepatocytes after toxic insult is proportional to cell damage. The toxicity of methyl- and propyl-paraben preservatives to SCRH was measured using the CytoTox-ONE™ Homogeneous Membrane Integrity Assay Kit (Promega) according to the manufacturer's instructions. Briefly, these compounds were dissolved in DMSO and added to day 3 SCRH in standard HBSS buffer (DMSO≤ 0.1%) to a final concentration of 9.12 mM methyl-paraben and 0.12 mM propyl-paraben (the maximum concentrations used in the accumulation studies with Tc-99m mebrofenin). LDH levels in the medium (100 μL of HBSS) relative to untreated cells were measured after 2 hr exposure to these compounds. HBSS was removed and replaced with DMEM with ITS+. The culture medium was sampled (100 μL) at 3 hr post treatment and assayed for LDH content.

Recirculating Rat Isolated Perfused Liver Experiments

To investigate the disposition of Tc-99 mebrofenin in an *ex-vivo* system, recirculating isolated perfused liver experiments were performed using wild-type Wistar rats (males, 300–350 g; Charles River Laboratories, Inc., Wilmington, MA) and TR^- rats (males, 300–350 g; in-house breeding colony obtained from Dr. Mary Vore, University of Kentucky, Lexington, KY). Male Wistar rats (400 g) were used as blood donors. Animals were maintained on a 12

hr light/dark cycle with ad libitum access to water and chow. The Institutional Animal Care and Use Committee of the University of North Carolina at Chapel Hill approved all procedures, and a mixture of ketamine/xylazine (60/12 mg/kg i.p.) was used to induce deep anesthesia prior to any surgical procedure. Upon cannulation of the bile duct, the liver was perfused through the portal vein with Krebs-Henseleit buffer. Subsequently, the liver was removed from the carcass and placed in a humidified, temperature-controlled chamber, and the perfusion was continued *ex situ* using 80 ml of recirculating Krebs-Henseleit buffer containing 20% (v/v) whole rat blood at a flow rate of 20 mL/min. Perfusate was continually oxygenated with a Hamilton lung and perfusate pH was maintained at 7.4 by addition of sodium bicarbonate. To maintain bile flow, taurocholate (30 μmol/h) was infused into the perfusate reservoir. After initial liver acclimatization (10 min) experiments were initiated by adding a bolus dose of Tc-99 mebrofenin (~5 μM final concentration) to the reservoir. Livers used in these experiments had acceptable viability (portal pressure ≤15 cm of water, initial bile flow > 0.8 and 0.2 μl/min/g liver in wild-type and TR^- rat livers respectively, and normal gross morphology). Perfusate was sampled at 1, 2.5, 5, 7.5, 10, 15, 20, 25, 30, 35, 40, 45, 50, 55, 60, 65, 70, 75, 80, 85 and 90 min, centrifuged and 150 μL of plasma was added with 5mL of scintillation fluid (Biosafe II) and analyzed with a scintillation counter. Bile was collected in toto at 5-min intervals through 90 min, and 5 μL was analyzed by scintillation counting.

Statistical Analysis

Multivariate analysis of variance (MANOVA) was used to compare Tc-99m mebrofenin accumulation in the presence or absence of canalicular spaces, and between the two types of

rats. This analysis accounts for the correlation between the accumulation of Tc-99 mebrofenin with and without Ca^{2+} in the same set of hepatocytes**.**

RESULTS

Cytoxicity of Preservatives

No differences were observed in LDH levels in the culture medium at 3 hr post treatment with methyl- and propyl- paraben preservatives when compared to untreated cells.

Sanwich-Cultured Rat Hepatocyte Experiments

Tc-99 mebrofenin was taken up by SCRH and excreted into bile to a lesser extent than expected from the in vivo observations during the clinical studies. No measurable BEI was observed at 10 min post dose, therefore, the incubation time was increased to 30 min to allow for more intracellular accumulation. The BEI at 30 min calculated in wild-type rats was 16.9%, and there was a significant difference between the mean Tc-99 mebrofenin accumulation in cells compared to accumulation in cells+bile ($p<0.05$). In contrast, there was not a significant difference in mean accumulation in SCRH from TR^- rats; the BEI was only 5.4%. In addition, the mean accumulation of Tc-99 mebrofenin in cells or cells plus bile was not significantly different in SCRH from wild-type (WT) and mutant rats (Fig B.2.1). The *in vitro* biliary clearance determined in SCRH from both WT and TR^- rats was extremely small (Table B.2.1). However, Tc-99 mebrofenin biliary clearance in WT SCRH was more than double the value determined in TR^- SCRH.

When the accumulation of Tc-99 mebrofenin in SCRH was expressed as a percentage of the medium concentration, ~ 15% of the administered dose accumulated in cells and cells+bile. An exception to this was a single experiment performed with WT rat SCRH incubated with Tc-99m mebrofenin (0.5 μCi/mL) for 30 min. In this case, over 38% of the dose accumulated in the cells (Fig B.2.2). However, in this experiment the BEI for Tc-99m mebrofenin after a 30 min incubation was only 10%.

Rat Isolated Perfused Liver Experiments

Livers from WT and one TR^- rat were perfused in these pilot experiments. The disposition of Tc-99 mebrofenin was similar to that observed in SCRH. Over 70% of the administered radioactivity was recovered in bile of the WT rat, while only 30% of the radioactivity was excreted into bile in the TR^- rat (Fig B.2.3). This experiment was repeated at a higher perfusion flow rate (30 mL/min) and the results were similar (data not shown).

FIGURES AND TABLES

Fig B.2.1: Accumulation of Tc-99 mebrofenin in SCRH from wild-type (WT) and Mrp2-deficient (TR^-) rats.

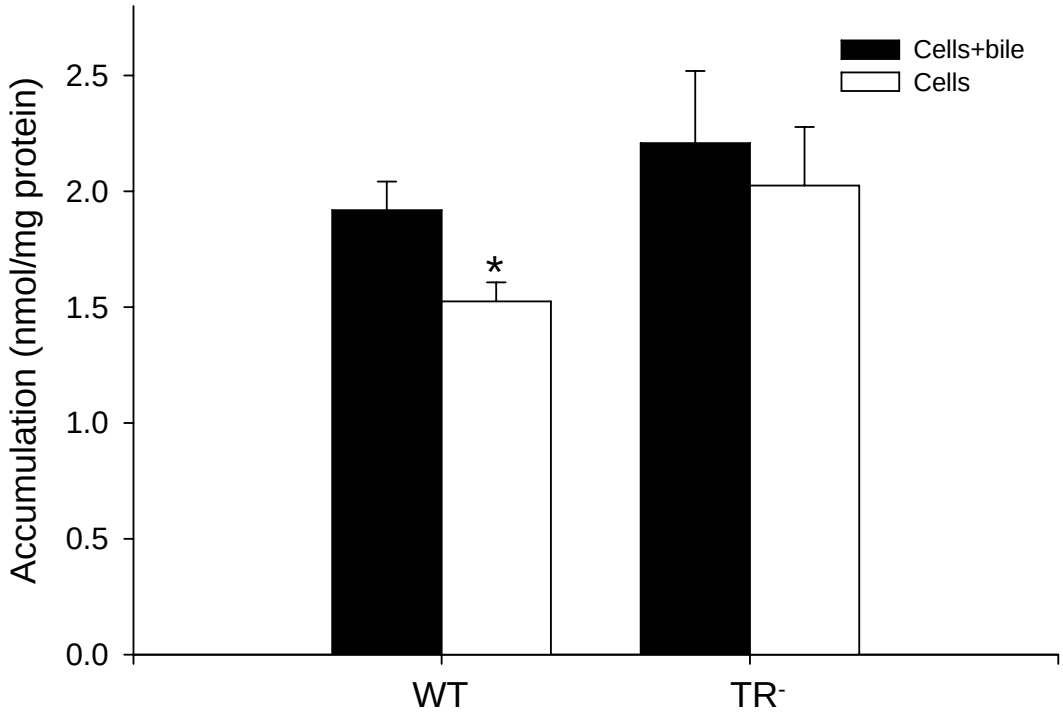

Table B.2.1: BEI and *in vitro* intrinsic biliary clearance values for Tc-99 mebrofenin in SCRH from wild-type (WT) and Mrp2-deficient (TR^-) rats.

	BEI	In vitro $Cl_{biliary}$	
		(ml/min/mg prot)	(ml/min/Kg)
WT rats	16.9	0.000731	5.8
TR^- rats	5.4	0.00026	2.1

Fig B.2.2: Accumulation of Tc-99m mebrofenin in WT SCRH (n=1).

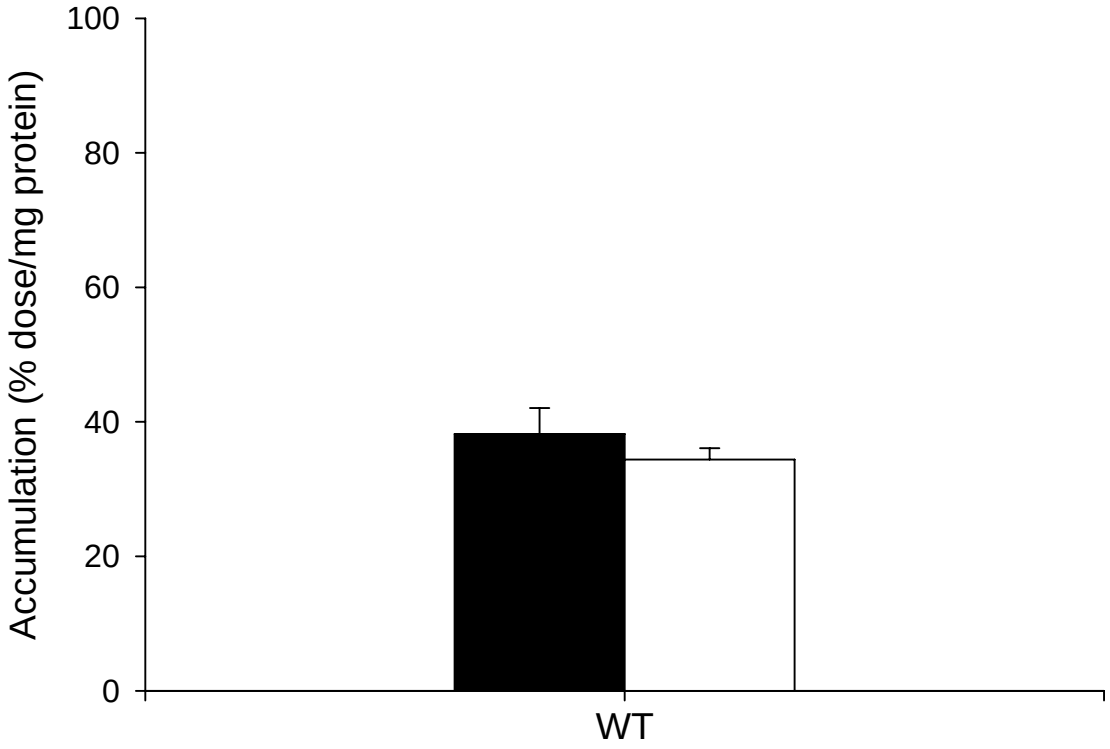

CONCLUSIONS

These experiments demonstrated that Tc-99 mebrofenin is an Mrp2 substrate in rats. It is possible that another residual transport mechanism is present in TR^- rats to explain the significant biliary excretion of Tc-99 mebrofenin in the absence of Mrp2. These findings are consistent with the initial hypothesis that Mrp2 is the primary transport protein responsible for biliary clearance of this compound. It was somewhat troublesome that 20-30% of the total administered radioactivity in the isolated perfused liver experiments remained in the perfusate at the end of the 90-min perfusion experiments. This observation, together with the slower uptake into cells and excretion into bile of Tc-99 mebrofenin into SCRH when compared to the fast and almost complete elimination via the biliary route in the clinical study presented in Chapter 2, may be attributed to species differences between rat and human. Another possible explanation could be that during the labeling of the Tc-99 mebrofenin used for these studies, other radiochemical species were formed, and the complex administered had relatively low radiochemical purity. This latter possibility was investigated further as reported in Appendix B.3, and the findings suggested that this was true, in part. A considerable difference was observed between Tc-99 mebrofenin and Tc-99m mebrofenin accumulation in SCRH. While the BEI for Tc-99m mebrofenin at 30 min in SCRH was only 10%, over 38% of the Tc-99m mebrofenin dose accumulated within the cells. It is possible that in previous experiments with Tc-99 mebrofenin, the higher amounts in solution saturated uptake transporters and prevented cellular accumulation.

Fig B.2.3: Disposition of Tc-99 mebrofenin in plasma and bile of wild-type (WT) and Mrp2-deficient (TR^-) rats after a bolus dose of Tc-99 mebrofenin (5μM) into the perfusate reservoir. Solid symbols refer to plasma and open symbols to bile. Data are expressed as a percentage of the total radioactivity administered (n=1 for both types of rats).

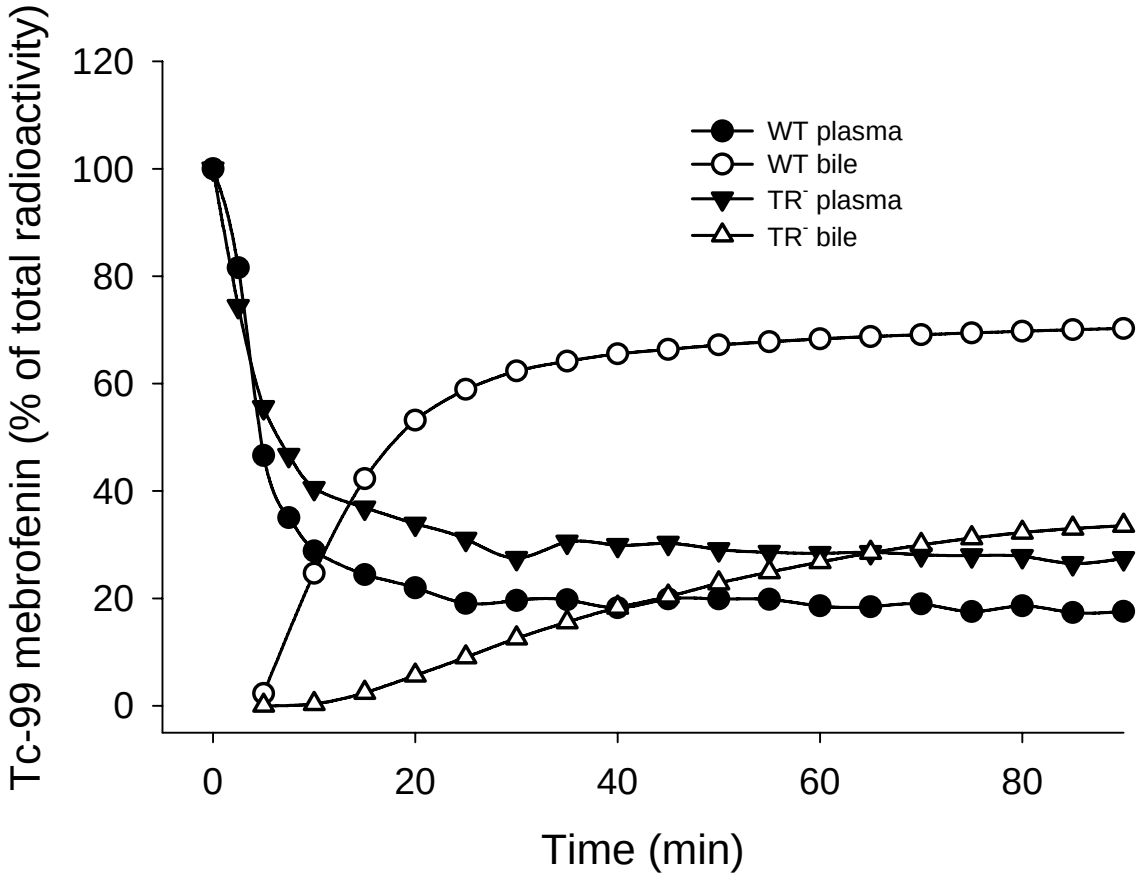

Appendix B.3

DEVELOPMENT OF AN HPLC METHOD TO DETERMINE THE RADIOCHEMICAL PURITY OF TC-99 MEBROFENIN

INTRODUCTION

Results of the SCRH study and two pilot isolated perfused liver experiments in wild type and TR^- rats raised doubts regarding the purity of the Tc-99 mebrofenin complex used in these studies. It did not seem reasonable that a compound that is quickly taken up and excreted into bile *in vivo* in humans would be excreted in SCRH to a much lesser extent, and that 20-30% of the administered radioactivity would still circulate in perfusate from the rat isolated perfused livers after 90 min. To investigate the hypothesis that the administered Tc-99 mebrofenin used in these studies was radiochemically pure, a more sensitive method to determine radiochemical purity needed to be developed to prove that the compound administered was Tc-99 mebrofenin. As pointed out in Appendix B.1, the preparation of radiopharmaceuticals from ready-to-label kits relies upon the presence of reducing agents that will reduce Tc-99 pertechnetate to the desired oxidation state. To obtain Tc-99 labeled mebrofenin for our *in vitro* and *in vivo* studies, the radiochemical labeling procedure was modified in order to use micro-molar concentrations of the complex. Despite the fact that the TLC assay results indicated high radiochemical purity, it is possible that the modifications made to the labeling procedure affected the amount of stannous ions present in solution, and thereby affected the reduction state of TcO_4^-, and/or too much Tc-99 pertechnetate was added causing the stochiometry of the reaction to be incorrect and the yield not quantitative.

HPLC METHOD DEVELOPMENT

Literature on HPLC analysis of Tc-99m mebrofenin is very sparse. A recently published method reported using a C_{18} column and a 30 min linear gradient starting at 10% H_2O (A) with 0.1% trifluoro acetic acid (TFA), and 90% acetonitrile (B) with 0.1%TFA, and ending at 90% A / 10% B (6). When tested with our HPLC system, this method performed poorly with extremely broad peaks. To improve the peak shape, a sharper gradient was employed reducing the run time to 10 min and terminating the run with a 5-min hold at 90% of B. Since mebrofenin has a benzene ring, UV detection was performed at 254 nm; a Phenomenex Luna (C_{18}, particle size 5 μm, 250 x 4.60 mm) column with a flow rate of 1 mL/min was used. A fraction collector was set up in series with the UV detector, and fractions of 0.5 mL were collected every 30 sec for subsequent gamma and beta counting. These fractions were counted immediately with a bench top gamma counter (Tracon Northern TN-1750 multichannel analyzer) and after decay (72 hr) they were analyzed for beta particles (Packard 1600TR liquid scintillation analyzer) when appropriate.

Mebrofenin, already reconstitued in sterile water as described in Appendix B.1, was labeled with only trace amounts of Tc-99m pertechnetate (solution A), Tc-99m and Tc-99 pretechnetate in trace amounts (solution B), and Tc-99 pertechnetate only (solution C) in the same proportion as used in the *in vitro* and *in vivo* experiments.

A solution of Tc-99m pertechnetate in saline (1 μCi/1 μL) was obtained from the nuclear medicine pharmacy at UNC hospitals. This solution was diluted 1:4 in sterile saline. Tc-99m pertechnetate solution (100 μL) was added to 300 μL of mebrofenin stock solution in order to obtain solution A. Solution B was made by adding a mixture of 50 μL of Tc-99m pertechnetate and 50 μL of the Tc-99 pertechnetate stock (0.8 mM) to 300 μL of mebrofenin

aqueous solution. Finally, a beta only labeled complex (solution C) was obtained as previously done for the *in vitro* studies adding 150 μL of the Tc-99 stock (0.8 mM) to 300 μL of mebrofenin aqueous solution (solution C and all the solutions used in the *in vitro* studies developed a pink discoloration upon mixing). The gamma only, gamma/beta and beta only Tc-99m/Tc-99 mebrofenin complexes were allowed to form at room temperature over 15 min and 100 μL of each solution was injected onto the HPLC system. Also Tc-99 pertechnetate stock (100 μL) was injected.

RESULTS AND DISCUSSION

LC-UV detection identified two sharp peaks in the Tc-99m and Tc-99 mebrofenin labeled solutions (solutions A, B and C, Fig B.3.1 panels a and b). Upon gamma and beta counting, no peak was detected at a retention time (RT) of 8.4 min, this suggested that the first peak detected by UV was associated with unlabeled mebrofenin (monomer). In contrast, almost all the radioactivity was associated with the second peak observed in the UV chromatogram (RT in UV 10.2 min), suggesting that this second peak was associated with the radioactive complex Tc-mebrofenin.

The LC-UV analysis of Tc-99m only mebrofenin (solution A) and Tc-99m/Tc-99 mebrofenin (solution B) gave identical results. Therefore, only one chromatogram is shown for both solutions in Fig B.3.1, panel a. The LC-UV analysis of Tc-99 mebrofenin solution C (Fig B.3.1 panel b) also looked very similar to the chromatograms obtained for solutions A and B. The peaks detected by UV had the same shape, height and area in all the samples, regardless of whether they were labeled with traces or a higher amount of Tc-99 sodium pertechnetate.

Injection of the TcO_4^- stock solution demonstrated the presence of an unknown species eluting at 5.5-6 min, which was not detectable in solutions A, B or C (Fig B.3.1, panel c).

Fig B.3.2 panels a, b, c and d refer to plots of relative cpms obtained upon radioactivity detection in the four solutions described. Cpms were determined in each 0.5 mL fraction and then expressed as % of total cpms. The peaks in the radioactivity-time profiles look broader than with UV detection. The Tc-mebrofenin complex eluted at ~11 min in all the solutions tested, and the overall relative cpms associated with this peak were the same in solutions A

and B (when Tc-99m and Tc-99 were added in low amounts to mebrofenin acqueous solutions, Fig B.3.2 panel a, b, c). Addition of the Tc-99m/Tc-99 pertechnetate mixture to a solution of mebrofenin yielded both Tc-99-mebrofenin and Tc-99m mebrofenin complexes, as expected, and as demonstrated by the presence of a single peak both in Fig B.3.2 panel b (gamma cpms) and panel c (beta cpms of the same solution B). The purity calculated as the sum of the % cpms between 8 and 11.5 min, was 96% for solution A and 89% for solution B. A much lower yield of the Tc-99 mebrofenin complex was obtained when higher amounts of Tc-99 pertechnetate (in the same proportion used in the *in vitro* studies) were added to the mebrofenin solution, with a calculated purity equal to 67%. This is in discordance with the TLC radiochemical purity test that was performed on all the solutions used in the in vitro studies, which indicated a purity of 90% or more. In Fig B.3.2 panel d, the beta cpms vs time profile obtained from HPLC fractionation of solution C (Tc-99 mebrofenin prepared as for the *in vitro* studies) and the Tc-99 pertechnetate stock solution are superimposed. The presence of an overlapping peak at ~5.5 min indicates that in solution C, free Tc-99 pertechnetate is present that did not quantitatively react with mebrofenin. Upon further investigation, it became clear that another complex also was formed (RT=8.5 min). It was quite surprising to notice that such a small ion would elute between 5.5-6 min. A peak was detected at the same retention time in the Tc-99 pertechnetate stock solution also using UV detection, consistent with the hypothesis that another complex was present in the original stock solution.

CONCLUSIONS

Upon development of a sensitive HPLC assay for technetium labeled mebrofenin, a discordance was noticed between the results of this method and the TLC method used to evaluate radiochemical purity during the execution of all the *in vitro* and *ex vivo* experiments. Unfortunately, due to the labile nature of the Tc-99 mebrofenin complex, it was not possible to evaluate a posteriori, by using this HPLC method, the purity of the solutions employed in the SCRH and IPL experiments. All the solutions used in the *in vitro* studies exhibited a pink discoloration that only later was associated with an incomplete labeling reaction. For these reasons, it is very difficult to present the data generated in the SCRH and the isolated perfused liver experiments as amounts of Tc-99 mebrofenin accumulated in the cells and canalicular spaces, and remaining in blood or excreted into bile. The incomplete labeling reaction may be due to changes in the chemistry of the radiopharmaceutical kit for mebrofenin. The transport of Tc-99m pertechnetate into bile canaliculi using SCRH also was assessed, and no difference was noticed in accumulation of substrate between cells+bile and cells. It is likely that Tc-99 pertechnetate will behave in the same way. The overall finding that Tc-99 mebrofenin is a Mrp2 substrate still holds true. However, the expression of the data as amounts of Tc-99 mebrofenin complex in bile canaliculi from SCRH, perfusate and bile is not believed to be accurate, considering that other radioactive species probably were present. For these reasons, all the remaining *in vitro* experiments were performed using only Tc-99m mebrofenin reconstituted as suggested by the manufacturer.

FIGURES

Fig B.3.1: LC-UV analysis of Tc-99m mebrofenin (solution A) and Tc-99m/Tc-99 mebrofenin (solution B) and Tc-99 mebrofenin (solution C)

a) Solution A and B chromatograms were identical, as expected (these solutions were labeled with trace amounts of Tc-99m or Tc-99m and Tc-99, respectively)

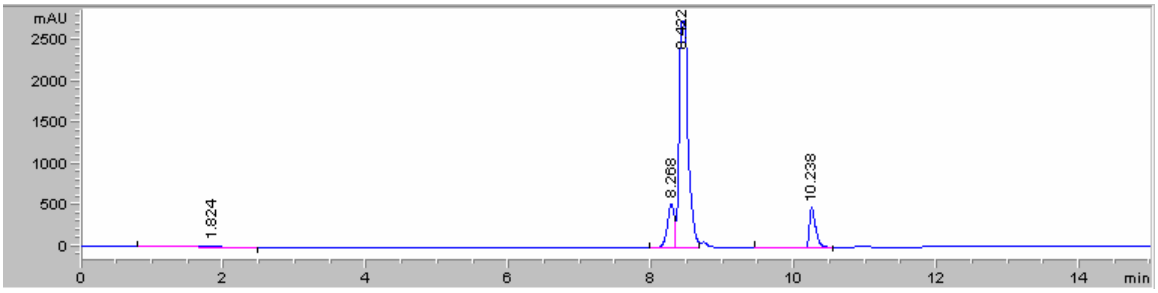

b) Solution C chromatogram (Tc-99 mebrofenin labeled as in the *in vitro* studies) did not show any significant difference from solutions A and B.

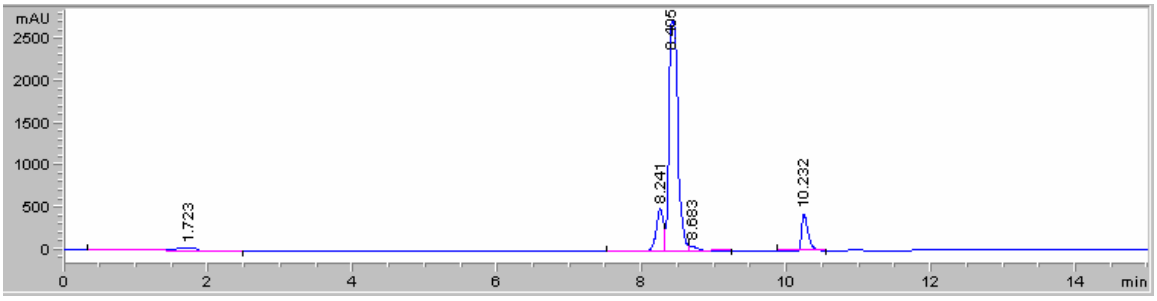

c) Tc-99 pertechnetate stock solution LC-UV chromatogram

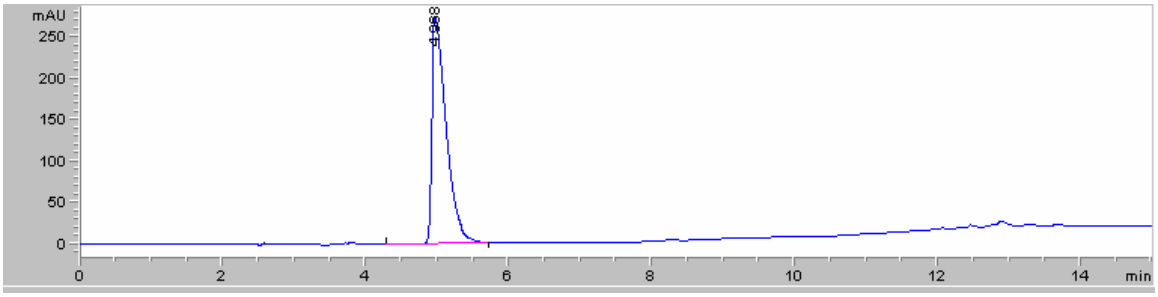

Fig B.3.2: Chromatograms obtained after gamma or beta counting of fractions collected after HPLC analysis of solutions A, B, C and the Tc-99 pertechnetate stock solution.

a) Solution A: Gamma cpm vs time profile expressed as a % of total radioactivity.

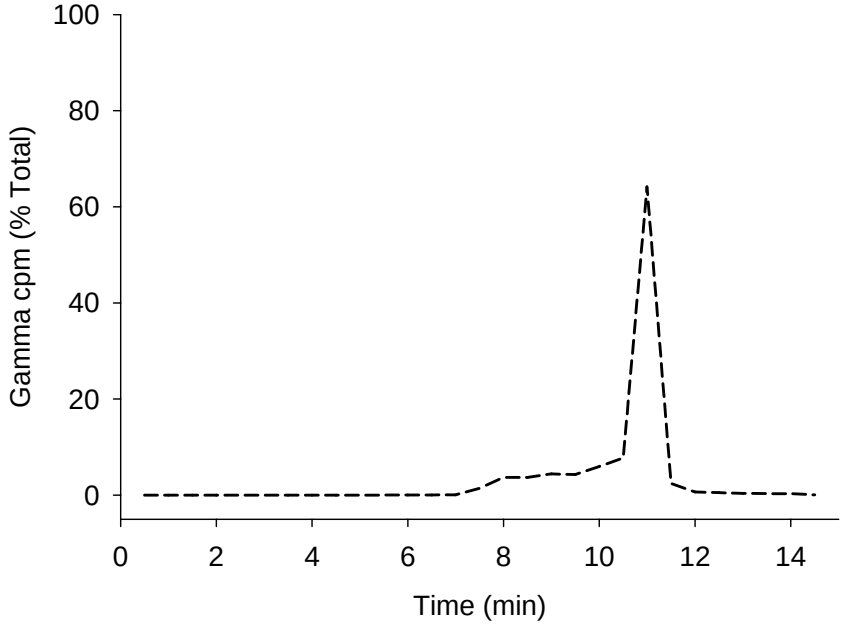

b) Solution B: Gamma cpm vs time profile expressed as % of total radioactivity.

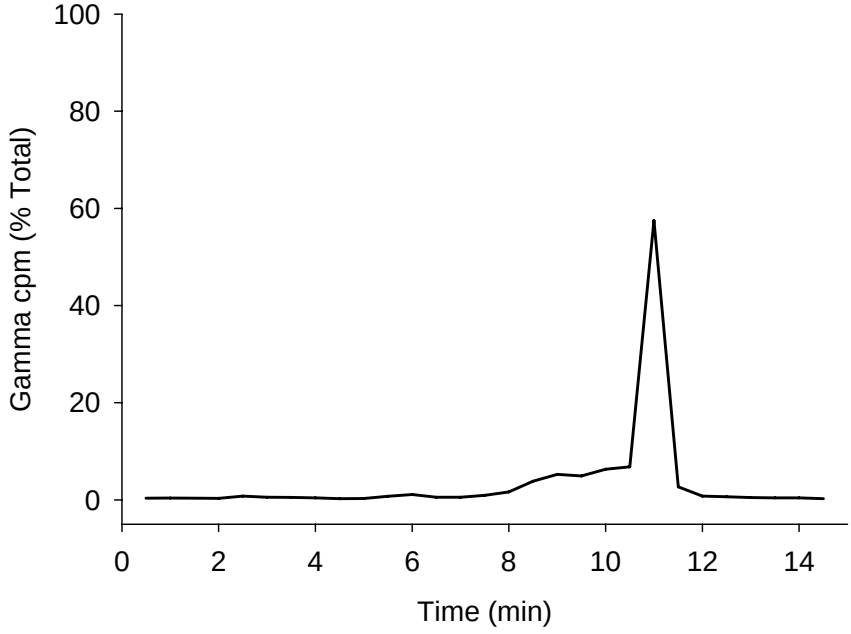

c) Solution B: Beta cpm vs time profile (note the perfect overalap with panel b)

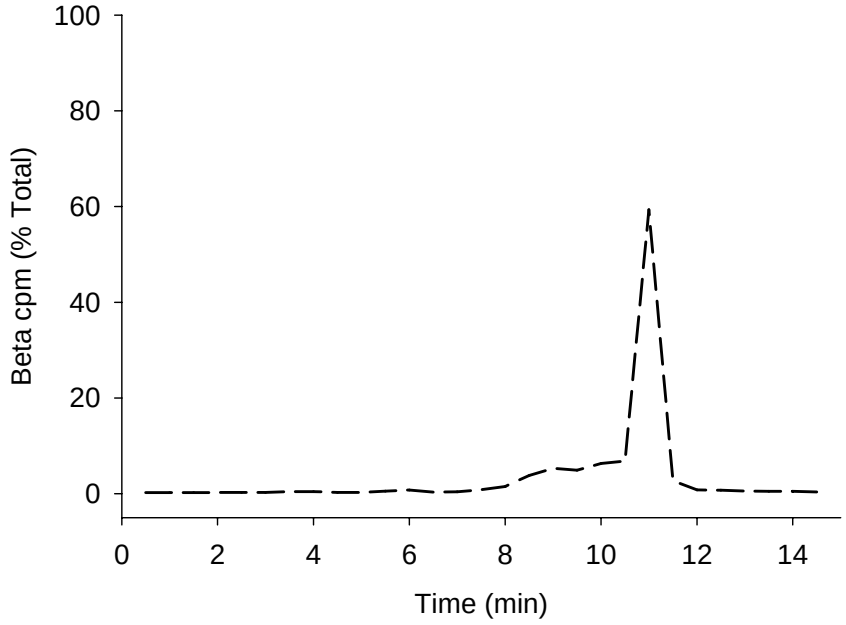

d) Solution C and Tc-99 pertechnetate beta cpm vs time profiles. Solid line refers to solution C, dotted line to Tc-99 pertechnetate stock solution.

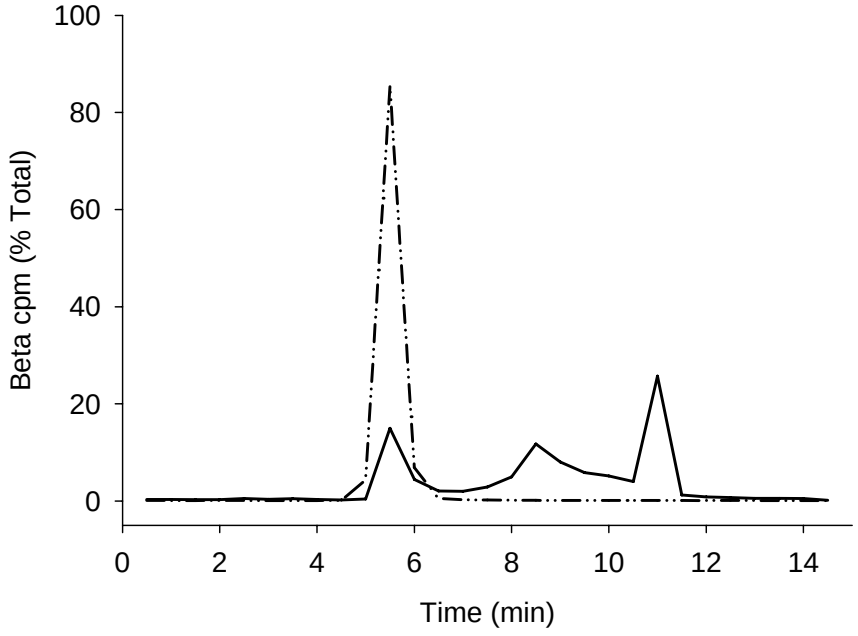

REFERENCES

1. R. J. Kowalsky and S. W. Falen. *Radiopharmaceuticals in Nuclear Pharmacy and Nuclear Medicine*, American Pharmacists Association, Washington, D.C., 2004.

2. N. H. Hendrikse, F. Kuipers, C. Meijer, R. Havinga, C. M. Bijleveld, W. T. van der Graaf, W. Vaalburg, and E. G. de Vries. In vivo imaging of hepatobiliary transport function mediated by multidrug resistance associated protein and P-glycoprotein. *Cancer Chemother Pharmacol* **54**: 131-8 (2004).

3. E. L. LeCluyse, P. L. Bullock, A. Parkinson, and J. H. Hochman. Cultured rat hepatocytes. *Pharm Biotechnol* **8**: 121-159 (1996).

4. Y. Nakagawa and G. Moore. Role of mitochondrial membrane permeability transition in p-hydroxybenzoate ester-induced cytotoxicity in rat hepatocytes. *Biochem Pharmacol* **58**: 811-6 (1999).

5. Y. Nakagawa and P. Moldeus. Mechanism of p-hydroxybenzoate ester-induced mitochondrial dysfunction and cytotoxicity in isolated rat hepatocytes. *Biochem Pharmacol* **55**: 1907-14 (1998).

6. K. Kothari, S. Joshi, M. Venkatesh, N. Ramamoorthy, and M. R. A. Pillai. Synthesis of 99mTc(CO)3-mebrofenin via [99mTc(OH2)3(CO)3]+ precursor and comparative pharmacokinetics studies with 99mTc-mebrofenin. *Journal of Labelled Compounds and Radiopharmaceuticals* **46**: 633-644 (2003).

Appendix C

IN VITRO INHIBITION OF TC-99M MEBROFENIN TRANSPORT BY RITONAVIR

INTRODUCTION

Tc-99m mebrofenin is an imino diacetic acid derivative (HIDA) commonly used in hepatobiliary scintigraphy that displays selective hepatic uptake and fast transit through the liver into bile. (1) This probe was used as described in Aim#1 during a clinical study to develop of a methodology to determine biliary clearance of drugs in humans (2).

In vitro experiments we have demonstrated that hepatic uptake of Tc-99m mebrofenin is mediated, at least in part, by transport proteins belonging to the OATP family. Using inside-out membrane vesicles prepared from HEK293 cells transiently transfected with MRP2 or MRP3, it was also possible to show that Tc-99m mebrofenin egress from the liver into bile involves MRP2 and efflux into sinusoidal blood involves MRP3 (Chapter 3). Additionally, we were able to show that MRP2-dependent transport was inhibited to ~88% of control values by MK571 (50 μM), an LTD_4 receptor antagonist commonly used as an MRP family inhibitor.

Following the successful results obtained in Aim#1, an additional clinical study was designed to investigate the drug-drug interaction between ritonavir and Tc-99m mebrofenin in order to demonstrate that the methodology developed can detect changes in the biliary excretion of drugs. The effects of ritonavir (a known MRP2 inhibitor) on Tc-99m mebrofenin excretion into bile in healthy subjects was proposed. Here, the in vitro study supporting the hypothesis that ritonavir inhibits ATP-dependent transport of Tc-99m mebrofenin at physiologically relevant concentrations is reported.

METHODS

Membrane preparation and transport experiments

In order to evaluate the inhibition of MRP2-mediated transport of Tc-99m mebrofenin, inside-out membrane vesicles prepared from HEK293 cells transfected with MRP2 were used.

HEK293 cells transiently transfected with MRP2 were prepared as reported in Chapter 3.

Transport assays were carried out by a rapid filtration method as described in Chapter 3. Transport in the presence of AMP was subtracted from transport in the presence of ATP, and reported as ATP-dependent Tc-99m mebrofenin transport. The effects of ritonavir inhibition on Tc-99m mebrofenin transport were measured at a single time point of 3 min, using two ritonavir concentrations (5 and 50 μM). These concentrations were chosen to mimic the ritonavir C_{max} in vivo after administration of a 200 mg tablet.

RESULTS

Ritonavir inhibition of Tc-99m mebrofenin MRP2-dependent transport

Inhibition of Tc-99m mebrofenin MRP2-mediated transport by ritonavir (5 and 50 μM) and by MK571 (50 μM) is plotted in Fig C.1. The ATP-dependent MRP2- mediated transport of Tc-99m mebrofenin was inhibited to ~88% of control values by the well-known general MRP inhibitor, MK571 (50 μM). Ritonavir affected MRP2-dependent transport at both concentrations investigated. Tc-99m mebrofenin MRP2-dependent transport was decreased to ~68% and ~40% of control values by ritonavir 5 and 50 μM, respectively.

CONCLUSIONS

Concentrations of unbound ritonavir between 5 and 50 μM are sufficient to significantly inhibit Tc-99m mebrofenin transport by MRP2 in the inside-out membrane vesicle system. It is likely that these concentrations are reached within the hepatocyte after oral administration of 200mg ritonavir. Thus, inhibition of biliary excretion of Tc-99m mebrofenin should be detectable during properly designed *in vivo* studies.

Fig C.1: Tc-99m mebrofenin uptake in inside-out membrane vesicles prepared from HEK293 cells transiently transfected with MRP2 was inhibited in the presence of MK571 (50 μM) and ritonavir (5 and 50 μM). Membrane vesicles were incubated for 3 min with Tc-99m mebrofenin in the presence (open bar) and absence (closed bar) of inhibitor. Results are expressed as a percentage of untreated membrane expressing MRP2. Bars represent mean (± SD) of triplicate incubations in a single experiment.

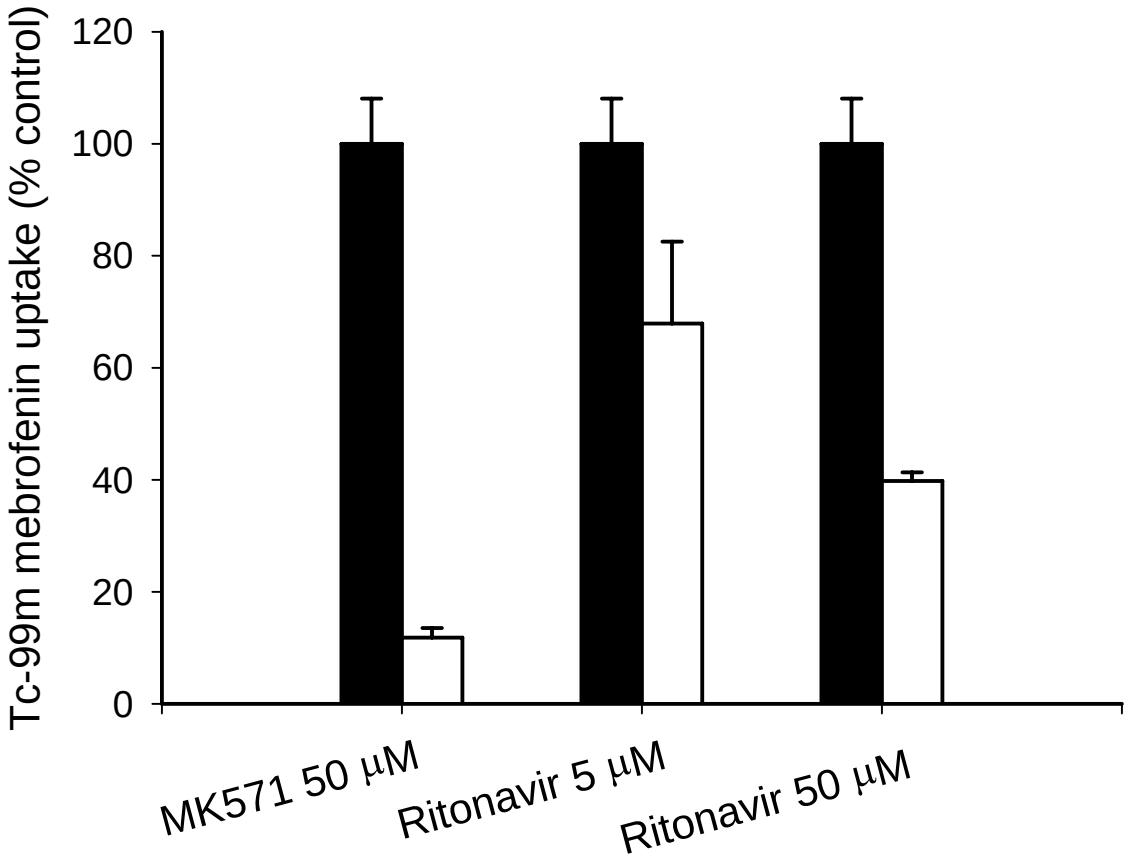

REFERENCES

1. S. Krishnamurthyand G. T. Krishnamurthy. Technetium-99m-iminodiacetic acid organic anions: review of biokinetics and clinical application in hepatology. *Hepatology* **9**: 139-153 (1989).

2. G. Ghibellini, B. M. Johnson, R. J. Kowalsky, W. D. Heizer, and K. L. Brouwer. A novel method for the determination of biliary clearance in humans. *AAPS J* **6**: e33 (2004).

Appendix D

PIPERACILLIN METABOLISM IN SANDWICH-CULTURED HUMAN HEPATOCYTES AND DIFFERENCES IN CANALICULAR NETWORK FORMATION IN DIFFERENT HEPATOCYTE PREPARATIONS

INTRODUCTION

Primary human hepatocytes cultured in a sandwich configuration between a double layer of extracellular matrix have been used to investigate the hepatobiliary disposition of endogenous and exogenous substances and their metabolites as well as the hepatotoxicity of drugs (1-4). However, the maintenance of metabolic capacity of this system has not been systematically investigated. Recently, during a clinical study to quantify biliary clearance of piperacillin in humans, we identified two metabolites of this antibiotic in bile and urine samples. Desethyl-piperacillin is formed by N-dealkylation of the parent drug; while this phase I metabolite had been identified previously in human urine and following incubation of liver homogenates (5, 6), the formation of desethyl-piperacillin glucuronide was not reported previously. The characterization of metabolic pathways that are unique to humans is very important in the drug development process, and often the formation of human-specific metabolites can be predicted using microsomal incubations. Nevertheless, microsomes do not allow for mechanistic studies concerning the excretory route of these metabolites (canalicular vs basolateral excretion). In Chapter 4, we demonstrated that desethyl-piperacillin and its glucuronide were formed in vitro using human liver microsomes upon optimization of the experimental conditions. The goal of this additional study was to investigate whether the SCHH model could be used to investigate the formation as well as the biliary excretion of these metabolites.

The hepatobiliary disposition of taurocholic acid, Tc-99m mebrofenin, Tc-99m sestamibi and piperacillin was investigated in sandwich-cultured human hepatocytes obtained from 4 living donors affected by hepatic cancer (Chapter 5). Despite the difference in sex, age, race and previous medication exposure of these four donors, the hepatocyte preparations used in these

studies behaved in a similar manner with respect to hepatic accumulation of the investigated probes. However, the morphology of the cells over days in culture, and the extent of canalicular network formation, varied from preparation to preparation affecting the extent of excretion of these compounds into canalicular networks. The light micrographs of three of these sandwich-cultured human hepatocytes preparations after 6 days of culture are reported to illustrate these differences.

METHODS

Isolation and Culture of Human Hepatocytes:

Human liver tissue was obtained from liver resections procured through the Department of Surgery, University of North Carolina at Chapel Hill School of Medicine, with donor consent and approval of the UNC Hospitals Ethics Committee. Hepatocytes were isolated by a modification of the two-step collagenase digestion method (7) and cultured according to the methods described previously in the Materials and Methods Section in Chapter 5. In order to allow for formation of bile canalicular networks, SCHH were maintained for 6 days prior to experiments, and culture media was replaced every 24 h. On day 6, canalicular network formation was evaluated with phase contrast microscopy, and digital images were captured with a Zeiss Axiovert 100TV inverted fluorescent microscope (Carl Zeiss Inc., Thornwood, NY, USA).

Piperacillin Metabolism and Metabolite Excretion in SCHH:

Hepatocytes were rinsed twice with 2 mL of standard HBSS (37°C) and pre-incubated for 10 min in 2 mL of either standard HBSS (yielding cells + bile) or Ca^{2+}-free HBSS (yielding cells). After washing, hepatocytes were incubated at 37°C in 1 mL HBSS containing 500 μM piperacillin for 30 minutes and subsequently rinsed vigorously four times with 2 mL ice-cold standard HBSS to remove extracellular substrate. Hepatocytes were lysed with 1 mL of ice-cold methanol/water 70/30 (v/v). Nonspecific binding was accounted for by including a blank plate (Biocoat™ plus Matrigel™ overlay). An aliquot of lysate was analyzed using LC-MS-MS as described below. Due to incompatibility of the protein assay with methanol, the average protein content for standard HBSS or Ca^{2+}-free HBSS incubations in the same

liver preparation was used to normalize piperacillin and metabolite content. Protein content in cellular lysates was quantified with the BCA method (8).

The BEI in SCHH was calculated as follows:

$$BEI = \frac{Accumulation_{cells+bile} - Accumulation_{cells}}{Accumulation_{cells+bile}} \times 100\%$$

Since none of the phase II metabolites were detected after 30 min incubation of Liver 1 SCHH with piperacillin, additional experiments were performed with hepatocytes from Livers 2, 3 and 4. Hepatocytes were incubated for 2 h in HBSS (Livers 2,3 and 4) and for 24 and 48 hr (Liver 4 only) in maintenance medium containing 500 μM piperacillin in the attempt to increase intracellular concentrations of piperacillin and therefore of metabolites.

LC-MS-MS analysis of Piperacillin and metabolites:

Piperacillin and metabolite accumulation in SCHH was analyzed by LC-MS-MS: 100 μL of SCHH lysates were spiked with cimetidine (internal standard final concentration 0.5 μg/mL). To improve the sensitivity of the assay, samples were incubated for 2, 24 and 48h were dried and reconstituted in 1/10 of the original volume prior to analysis.

The LC-MS-MS method employed has been described in detail in Chapter 4. An analytical standard was available only for piperacillin; therefore desethylpiperacillin and desethylpiperacillin glucuronide concentrations were estimated qualitatively and expressed as internal standard peak area ratios per mg of protein.

RESULTS AND DISCUSSION

Desethyl-piperacillin was formed within 30 min in all of the preparations of human hepatocytes used for these experiments. Accumulation in cells and cells+bile is shown in Fig D.1. In SCHH prepared from Livers 1, 3 and 4, more desethyl-piperacillin was detected in cells+bile than in cells alone indicating measurable excretion of this metabolite into bile, in accordance with what was observed in the in vivo study. Unfortunately, actual quantification of this metabolite was not possible due to lack of an analytical standard. For this reason, results are reported as the internal standard area ratio normalized for the protein content.

The levels of desethyl-piperacillin glucuronide and piperacillin glucuronide were undetectable in all preparations after 30 min, 2, 24 or 48 hr incubation in the presence of piperacillin. Although the piperacillin concentration in the medium was similar to the C_{max} obtained in healthy volunteers in the clinical study (Chapter 4), the intracellular concentration of piperacillin in SCHH was very low (Chapter 5), and less than 1% of the dose was taken up by the hepatocytes in 30 min. In microsomal incubations, the formation of the phase II metabolites was detected only after increasing the piperacillin concentration in the incubation mixture to 500 μM. This may explain why no glucuronidation was observed in the SCHH model.

Images of the human hepatocytes cultured in a sandwich configuration from Livers 2, 3 and 4 after 6 days in culture are shown in Fig D.2. Images for Liver 1 were not obtained. Taurocholate BEI values and in vitro $Cl_{biliary}$ were very similar between Livers 2 and 3 liver preparations. However sandwich-cultured hepatocytes from Liver 4 hepatocytes taurocholate as well as all the other probes investigated in Chapter 5 into bile to a greater extent than the livers. This may be attributed to the more developed canalicular networks observed in images

of SCHH from Liver 4 compared to Liver 3 and especially Liver 2. This suggests that extensive formation of bile canaliculi detected by visual inspection of the sandwich-cultured hepatocytes correlates with more extensive excretion into the canalicular spaces. However, since the major determinant of cellular and biliary accumulation is the expression of uptake and efflux transport proteins, visual inspection should be used in conjunction with functional assays, such as taurocholate accumulation and biliary excretion, when assessing the appropriate time in culture to perform accumulation experiments.

CONCLUSIONS

The results of these studies were encouraging, as SCHH were capable of forming desthyl-piperacillin, most likely through a Cytochrome P450-mediated oxidative reaction. In three out of four liver preparations, it was possible to detect metabolite excretion into bile.

The apparent lack of glucuronidation activity towards piperacillin and its metabolite may be due to the very low intracellular concentrations of these substrates. Future studies should focus on the maintenance of phase I and II enzyme activity in SCHH using probe substrates with higher metabolic turnover rates. Light microscopy images of the SCHH preparations on the day of the accumulation studies confirmed the formation of canalicular networks, in most cases, network formation corresponded to greater extent of biliary excretion of the compounds under investigation.

FIGURES

Fig D.1: Accumulation and biliary excretion of desethyl-piperacillin in SCHH. SCHH were incubated with piperacillin (300 μM) and cell (empty bar) and cell+bile (solid bar) accumulation were measured after 30 min. Bars represent mean (±SD) of triplicate determinations in a single experiment; four liver preparations were used in these studies. For each liver the individual BEI value is reported. When cellular accumulation was higher than cell+bile accumulation, the BEI calculation was not possible (NA).

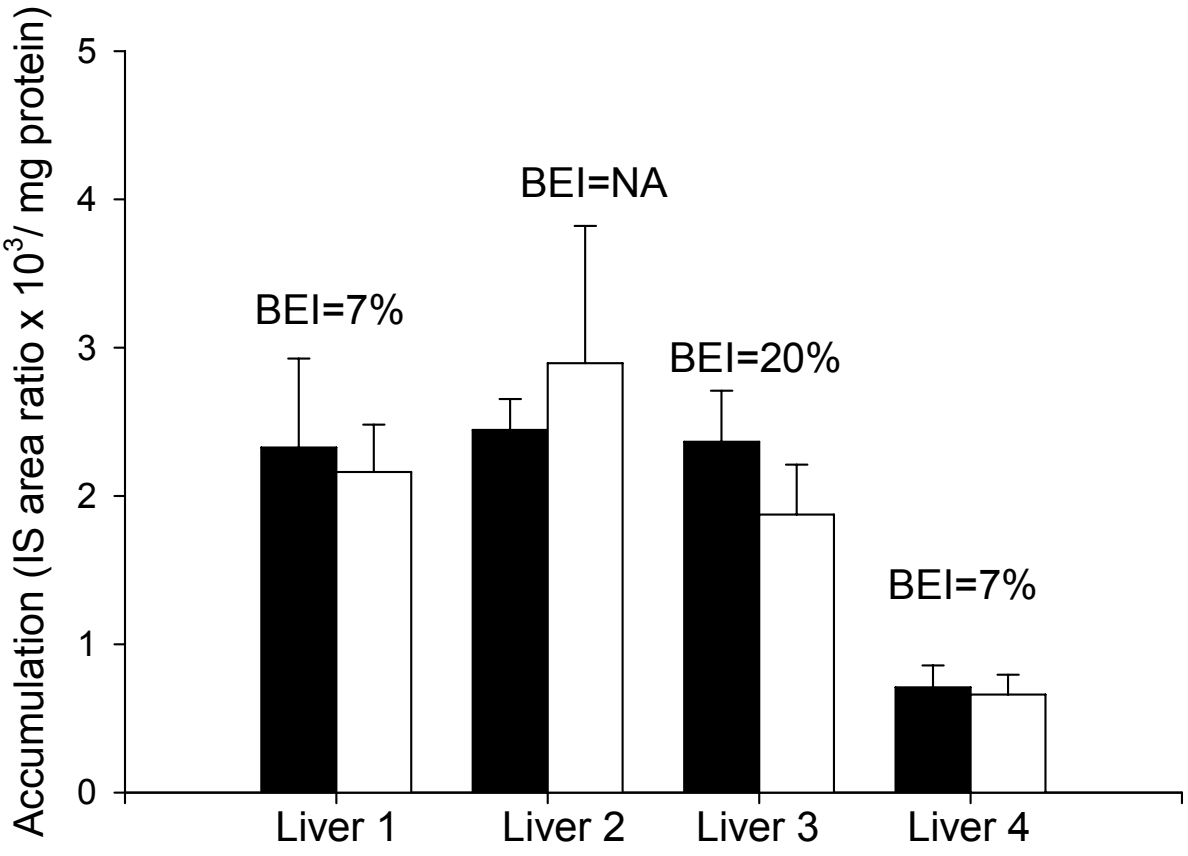

Fig D.2: Phase contrast images of SCHH preparations on day 6 in culture. Bile canalicular networks were visible in all liver preparations, but were more extensive in Liver 4 than in Liver 2 or 3. Images were not available for SCHH from Liver 1. Arrows indicate bile canalicular networks.

UNC2 SCHH day 6

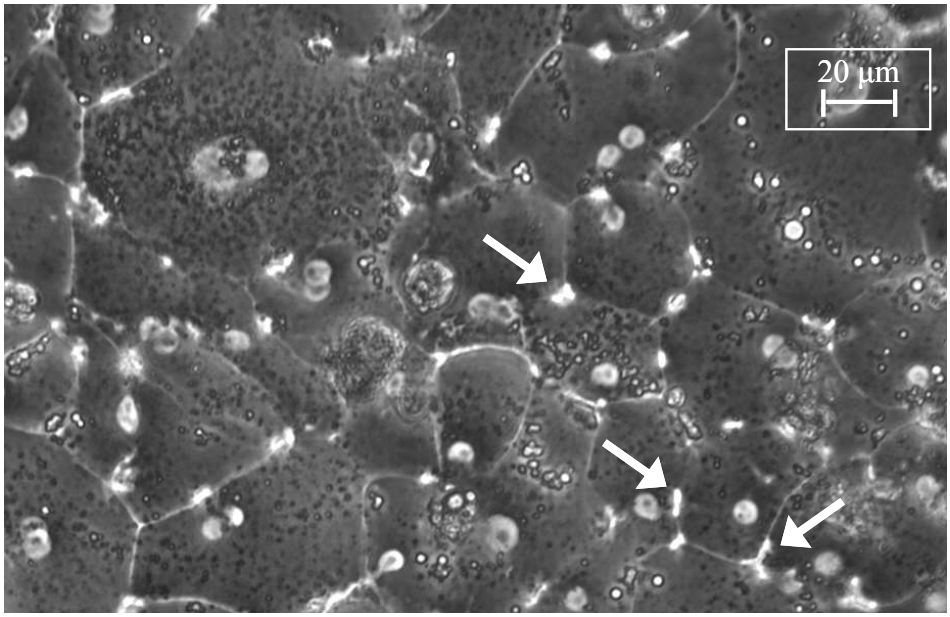

UNC3 SCHH day 6

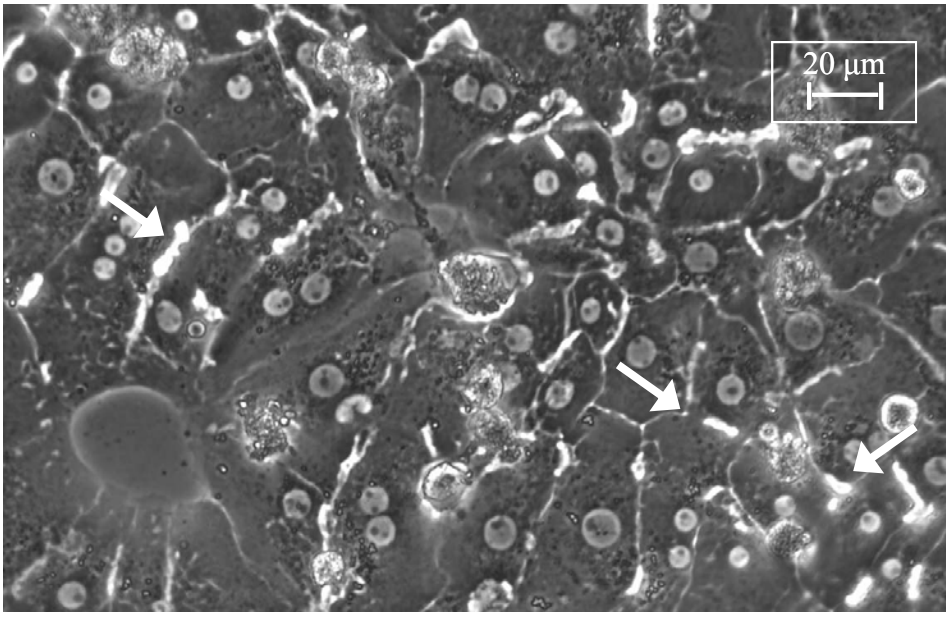

UNC4 SCHH day 6

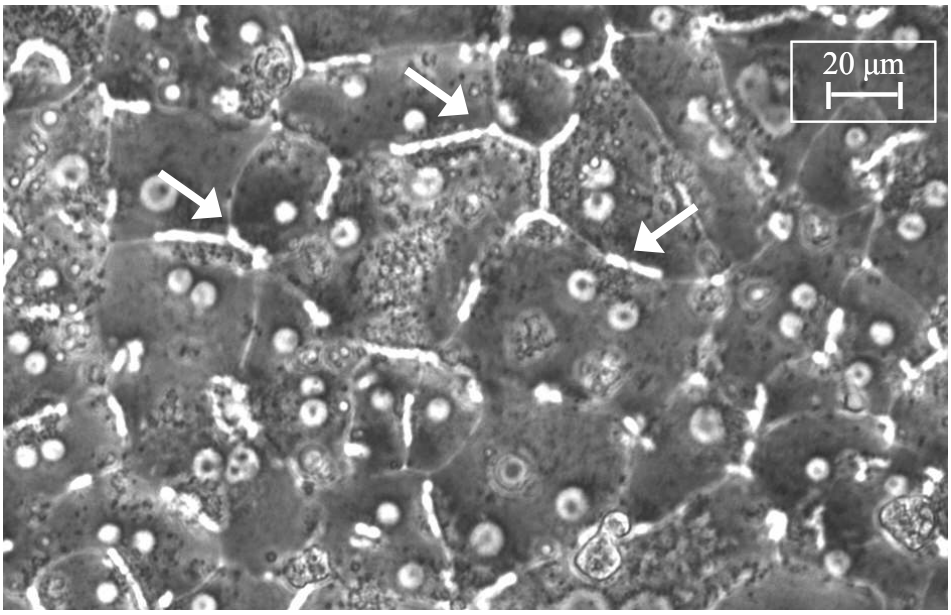

REFERENCES

1. P. Zhang, B. D. Swift, X. Tian, K. R. Brouwer, M. Dasgupta, and N. Huebert. Optimization of transporter expression and function in sandwich-cultured human hepatocytes (B-ClearTM-HU). *Drug Metab Rev* **37**: 306-306 (2005).

2. S. E. Kostrubsky, S. C. Strom, A. S. Kalgutkar, S. Kulkarni, J. Atherton, R. Mireles, R. Kubik, J. Hanson, E. Urda, and A. E. Mutlib. Inhibition of Hepatobiliary Transport as a Predictive Method for Clinical Hepatotoxicity of Nefazodone. *Toxicol Sci* (2006).

3. S. Wilkeningand A. Bader. Influence of culture time on the expression of drug-metabolizing enzymes in primary human hepatocytes and hepatoma cell line HepG2. *J Biochem Mol Toxicol* **17**: 207-13 (2003).

4. G. Lengyel, Z. Veres, P. Szabo, L. Vereczkey, and K. Jemnitz. Canalicular and sinusoidal disposition of bilirubin mono- and diglucuronides in sandwich-cultured human and rat primary hepatocytes. *Drug Metab Dispos* **33**: 1355-60 (2005).

5. M. Komuro, T. Maeda, H. Hayakawa, K. L. Allen, and C. E. Green. The formation of desethyl-piperacillin from piperacillin by human liver S9 in vitro. *Biopharm Drug Dispos* **18**: 185-90 (1997).

6. Y. Minami, M. Komuro, K. Sakawa, N. Ishida, K. Matsumoto, and K. Oishi. Desethyl piperacillin, a new active metabolite of piperacillin in human. *J Antibiot (Tokyo)* **44**: 256-8 (1991).

7. G. A. Hamilton, S. L. Jolley, D. Gilbert, D. J. Coon, S. Barros, and E. L. LeCluyse. Regulation of cell morphology and cytochrome P450 expression in human hepatocytes by extracellular matrix and cell-cell interactions. *Cell Tissue Res* **306**: 85-99 (2001).

8. P. K. Smith, R. I. Krohn, G. T. Hermanson, A. K. Mallia, F. H. Gartner, M. D. Provenzano, E. K. Fujimoto, N. M. Goeke, B. J. Olson, and D. C. Klenk. Measurement of protein using bicinchoninic acid. *Anal Biochem* **150**: 76-85 (1985).

APPENDIX E

RAW DATA FROM THE CLINICAL STUDIES

sub 01
(actual 11)
DOSE
(μCi)
theoretical 2188
Actual N.D.
Gallbladder EF (120-150min)
0.82
BLOOD

time (min)	nCi/ml
0	0
1	0.44
2.5	30.09
5	85.30
7.5	80.72
10	57.35
20	16.29
40	4.96
60	3.38
80	1.86
100	1.33
120	1.02
140	0.87
165	0.78
180	0.76

BILE

time (min)	actual (μCi)	EF corr (μCi)
0	0	0
5	0	0
10	0	0
30	48.83	48.83
50	30.14	30.14
70	29.40	29.40
90	65.71	65.71
110	72.63	72.63
130	57.07	62.00
150	1004.15	1224.58
180	125.53	
Cumulative	1433.47	1533.29

URINE

time (min)	actual (μCi)
0	0
180	14.52

sub 02
(actual 09)

DOSE (μCi)
theoretical 2498
Actual 2072
Gallbladder EF (120-150min)
0.86
BLOOD

time (min)	nCi/ml
0	0
2	87.38
2.75	137.59
5.66	80.73
7.5	55.23
10	38.12
20	17.59
30	10.99
40	4.39
60	2.43
80	1.95
100	1.27
120	1.27
140	0.99
165	0.93
180	1.31

BILE

time (min)	actual (μCi)	EF corr (μCi)
0	0	0
5	0.18	0.18
10	0.55	0.55
30	0.37	0.37
50	0.18	0.18
70	34.88	34.88
90	227.20	227.20
110	111.24	111.24
130	816.80	886.97
150	503.66	585.65
180	51.73	
Cumulative	1746.81	1847.24

URINE

time (min)	actual (μCi)
0	0
180	10.69

sub 03
(actual 12)
DOSE
(µCi)

theoretical 1923
Actual 2282

Gallbladder EF (120-150min)

0.03

BLOOD

time (min)	nCi/ml
0	0
2.166	159.81
5	81.09
7.5	97.93
10	22.31
19	6.98
39.5	2.84
60	1.84
80	1.22
100	0.82
120	0.85
140	0.77
165	1.32

BILE

time (min)	actual (µCi)	EF corr (µCi)
0	0	0
5	0	0
10	0	0
30	174.95	174.95
50	250.24	250.24
70	90.31	90.31
90	2.38	2.38
110	1.47	1.47
130	80.60	80.60
150	44.88	1496.07
180	158.83	
Cumulative	803.66	2096.02

URINE

time (min)	actual (µCi)
0	0
180	15.54

sub 04
(actual 16)

DOSE (µCi)

theoretical 2497
Actual 2476

Gallbladder EF (120-150min)

0.86

BLOOD

time (min)	nCi/ml
0	0
1	166.39
2.5	229.78
5	167.04
7.5	70.94
10	43.53
20	10.00
40	6.03
60	2.68
80	2.51
100	1.84
120	1.51
140	1.57
165	1.35
182	1.64

BILE

time (min)	actual (µCi)	EF corr (µCi)
0	0	0
5	0.16	0.16
10	3.30	3.30
30	132.18	132.18
50	535.33	535.33
70	114.22	114.22
90	117.51	117.51
110	48.62	48.62
130	11.21	11.29
150	979.01	1138.39
180	126.25	
Cumulative	2067.80	2101.00

URINE

time (min)	actual (µCi)
0	0
180	11.67

sub 01 (actual 23)
DOSE (μCi)
Actual 2503

Gallbladder EF (120-180min)
0.47

BLOOD

time (min)	nCi/ml
0	0
1	229.09
2.5	82.24
5	32.42
7.5	20.35
10	15.14
20	9.30
40	8.01
60	4.71
80	4.26
105	3.51
130	3.30
150	2.87
170	2.70
180	2.65

BILE

time (min)	actual (μCi)	EF corr (μCi)
0	0	0
5	1.85	1.85
10	1.86	1.86
30	11.15	11.15
50	0.00	0.00
70	1.86	1.86
90	0.00	0.00
120	1.86	1.86
140	196.08	417.20
160	59.76	127.15
180	0.00	0.00
Cumulative	274.43	562.93

URINE

time (min)	actual (μCi)
0	0
180	634

sub 02 (actual 25)
DOSE (μCi)
Actual 3384

Gallbladder EF (120-180min)
0.63

BLOOD

time (min)	nCi/ml
0	0
1	137.19
2.5	82.18
5	31.17
7.5	16.50
10	11.93
20	8.11
40	9.15
60	5.31
80	4.90
105	4.02
130	3.66
150	3.56
170	3.20
180	3.59

BILE

time (min)	actual (μCi)	EF corr (μCi)
0	0	0
5	0.00	0.00
10	1.82	1.82
30	49.18	49.18
50	9.12	9.12
70	5.49	5.49
90	9.16	9.16
120	3.67	3.67
140	325.50	516.67
160	106.87	169.63
180	9.23	14.65
Cumulative	520.03	779.38

URINE

time (min)	actual (μCi)
0	0
180	246

sub 03 (actual 26)
DOSE (µCi)
Actual 3166

Gallbladder EF (120-180min)
0.9

BLOOD

time (min)	nCi/ml
0	0
1	102.31
2.5	108.74
5	48.13
7.5	18.70
10	13.47
20	7.87
40	7.70
60	4.11
80	3.94
105	3.38
130	3.10
150	2.69
170	2.97
180	2.65

BILE

time (min)	actual (µCi)	EF corr (µCi)
0	0	0
5	1.75	1.75
10	5.26	5.26
30	14.11	14.11
50	10.61	10.61
70	98.63	98.63
90	45.82	45.82
120	10.65	10.65
140	448.44	458.37
160	37.55	41.72
180	12.54	13.93
Cumulative	685.37	700.86

URINE

time (min)	actual (µCi)
0	0
180	518

sub 04 (actual 27)
DOSE (µCi)
Actual 3182

Gallbladder EF (120-180min)
0.64

BLOOD

time (min)	nCi/ml
0	0
1	275.24
2.5	103.28
5	36.29
7.5	20.00
10	12.27
20	8.25
40	7.15
60	5.20
80	4.29
105	3.66
130	4.78
150	3.37
170	3.12
180	3.14

BILE

time (min)	actual (µCi)	EF corr (µCi)
0	0	0
5	0.00	0.00
10	0.00	0.00
30	0.00	0.00
50	0.00	0.00
90	1.80	1.80
120	3.57	3.57
145	447.70	699.54
160	78.83	123.18
180	3.60	5.62
Cumulative	535.502349	833.703431

URINE

time (min)	actual (µCi)
0	0
180	614

sub 05 (actual 28)
DOSE (µCi)
Actual 3037.05818

Gallbladder EF (120-180min)
0.16

BLOOD

time (min)	nCi/ml
0	0
1	111.99
2.5	136.43
5	41.46
7.5	16.42
10	12.76
20	8.01
40	9.22
60	5.14
80	4.60
105	3.10
130	3.09
150	3.16
170	2.68
180	2.39

BILE

time (min)	actual (µCi)	EF corr (µCi)
0		0
5	1.6481727	1.648172703
10	1.6481727	1.648172703
30	13.21	13.21
50	11.57	11.57
70	21.51	21.51
120	23.24	23.24
140	11.63	72.70
160	51.79	323.66
180	6.69	41.78
Cumulative	142.93	510.97

URINE

time (min)	actual (µCi)
0	0
180	671

sub 06 (actual 29)
DOSE (µCi)
Actual 3563

Gallbladder EF (120-180min)
0.83

BLOOD

time (min)	nCi/ml
0	0
1	84.98
2.5	117.99
5	27.96
7.5	15.59
10	13.68
20	10.19
40	12.60
60	6.61
80	5.53
105	5.20
130	4.90
150	4.18
170	4.18
180	4.13

BILE

time (min)	actual (µCi)	EF corr (µCi)
0	0	0
5	1.78329165	1.783291651
10	3.59	3.59
30	8.93	8.93
50	10.73	10.73
70	3.57	3.57
90	5.36	5.36
120	1.79	1.79
140	433.46	522.24
160	76.07	91.65
180	17.94	21.61
Cumulative	563.21	635.50

URINE

time (min)	actual (µCi)
0	0
180	621

sub 07 (actual 30)
DOSE (µCi)
Actual 3100

Gallbladder EF (120-180min)
0.79
BLOOD

time (min)	nCi/ml
0	0
1	212.66
2.5	108.24
5	38.28
7.5	15.85
10	13.80
20	9.55
40	11.50
60	5.43
80	4.76
105	3.56
130	3.30
150	2.97
170	2.62
180	2.39

BILE

time (min)	actual (µCi)	EF corr (µCi)
0	0	0
5	1.69637594	1.696375941
10	1.69963917	1.699639166
120	23.93	23.93
135	284.32	359.90
160	217.86	275.77
180	20.56	26.03
Cumulative	551.768361	690.7228697

URINE

time (min)	actual (µCi)
0	0
180	711

Tc-99m mebrofenin study

sub A (actual 19)

DOSE (mg)

Actual 1700

Gallbladder EF (120-150min)

0.82

BLOOD

time (min)	mg/L
0	0
15	127.96
30	62.61
45	39.99
60	34.62
75	23.00
109	12.36
152	5.33
194	2.96
262	1.43
322	0.97
352	1.34
60	0.65
720	0.54

BILE

time (min)	EF corr (ng)	cumul %
0	0	0
30	0.5	0
60	1701.5	12.9
90	336.1	15.5
120	425.2	18.7
180	562.8	23.0
240	926.2	30.0
270	2073.4	45.8
300	5162.8	85.0
360	1973.4	100.0
cumulative	13162.0	

URINE

time (hr)	actual (mg)
0	0
10	1227.00

sub B (actual 20)

DOSE (mg)

Actual 1764

Gallbladder EF (120-150min)

0.28

BLOOD

time (min)	mg/L
0	0
15	109.02
30	112.09
45	73.00
75	51.81
112	35.25
127	25.40
150	21.13
210	10.32
270	5.93
360	2.77
600	1.46
720	0.33

BILE

time (min)	EF corr (ng)	cumul %
0	0	0
30	157.9	2.8
90	153.2	5.5
120	100.4	7.3
180	5.5	7.4
240	32.1	8.0
270	4058.0	80.1
300	320.5	85.7
360	802.4	100.0
cumulative	5629.9	

URINE

time (hr)	actual (mg)
0	0
10	1499.70

sub C (actual 21)
DOSE
(mg)
Actual 1586

Gallbladder EF (120-150min)
0.07

BLOOD

time (min)	mg/L
0	0
15	118.81
30	68.42
45	36.20
75	36.74
105	14.97
151	7.95
210	3.90
270	1.77
340	0.93
360	0.09
617	1.30
720	0.33

BILE

time (min)	EF corr (ng)	cumul %
0	0	0
30	19.3228973	0.891603168
60	45.8984916	2.117862549
90	12.69855641	0.58594076
120	321.262461	14.82379291
180	183.717926	8.47716998
240	89.7457478	4.141076353
270	219.64517	10.1349361
300	81.26523258	3.749765768
360	1193.651754	55.0778524
cumulative	2167.208236	

URINE

time (hr)	actual (mg)
0	0
10	949.50